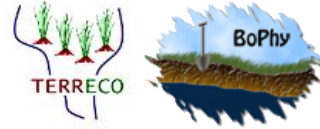




UNIVERSITÄT
BAYREUTH

Department of soil physics



Complex TERRain and ECOlogical Heterogeneity

A cumulative dissertation submitted for the requirement of doctoral degree in
Natural Science (Dr. rer. nat.)

**Integrated watershed modeling of mountainous landscapes:
Assessing the environmental performance of an intensive farming
system in South Korea.**

Submitted to Bayreuth Graduate School of Mathematical and Natural Sciences
(BayNAT)

Submitted by
Ganga Ram Maharjan
born 20 April 1982
in Chapagaun, Lalitpur, Nepal

Bayreuth, August 2015

This doctoral thesis was prepared at the Department of Soil Physics, University of Bayreuth, between April 2012 and August 2015 under supervision of Prof. Dr. Bernd Huwe, Prof. Dr. John Tenhunen, and Prof. Dr. Seong Joon Kim

Date of submission: 26 August 2015

Date of defense: 04 December 2015

Acting director: Prof. Dr. Stephan Kuemmel

Doctoral committee:

- (1) Prof. Dr. Bernd Huwe (1st reviewer)
- (2) Prof. Dr. Martin Volk (2nd reviewer)
- (2) Prof. Dr. Thomas Koellner (chairman)
- (4) Dr. Christina Bogner

Abstract

The agricultural production to secure food for overgrowing world's population and the reduction of associated detrimental effects on the environment are of global concern. Intensive farming systems coupled with a high amounts of fertilizer applied to secure an increasing crop yield have a negative effects on the global environment. The nonpoint source pollution, such as sediments and nutrients from the intensive farming systems and point source pollution from industry are of major threat to the global environment. The point source pollutions from the industries are discernible, which can be fed into wastewater treatment plants before bringing back to the environmental system. Nonpoint source pollutions come from many diffuse sources (surface runoff, atmospheric deposition, precipitation, and seepage) and are more difficult to handle compared to point source pollution. The extent of generation of nonpoint source pollution depends on complex geophysical and environmental conditions in combination with adopted land use and management systems.

The catchments Haean and Jawoon-ri in South Korea are characterized by complex terrain and highly affected by monsoon climate. In addition, mountainous intensive agriculture and application of high amount of fertilizer have produced a considerable amount of sediments and nutrients, which are transported to the downstream reservoir. Furthermore, the catchments are regionally recognized as a "hot spot" of muddy flows and associated contaminants contributing to the downstream Soyang Reservoir. The Soyang Reservoir is a major source of drinking water supply in Seoul, the capital city of South Korea. The reservoir also has problem of yearly siltation, which decreases its water storage capacity. In addition, contaminants sorbed to the sediments are deteriorating the water quality. The regional attention is to improve the water quality while maintaining the agricultural production from the adjoining Haean and Jawoon-ri catchments.

Based on this paradigm, the Complex TERRain and ECOlogical Heterogeneity (TERRECO) project was developed. The studies associated with the TERRECO project included a detailed plot level study of understanding water flow and erosion processes and solute transport under various management practices. The research findings based on plot level studies are important to integrate processes at the catchment level in order to analyze the management impact on agricultural production and export of nonpoint source pollution with an approach of watershed modeling.

Among various watershed modeling tools, we chose the Soil and Water Assessment Tool (SWAT) which can handle various management systems. The SWAT model was adapted to two study sites, the Jawoon-ri and the Haean catchment.

The central focus of the thesis is to identify land use systems and best management practices for permanent reduction of sediments and nutrients export from our study catchments. The first two studies were focused on the technical specifications of the SWAT model, its calibration, validation and associated model sensitivities and uncertainties. The following two studies were related to SWAT

applications to evaluate the impact of different land use systems and agricultural management practices on water quality, crop yield and farm income.

The first study was to test the SWAT model for the prediction potential of discharge from the small agricultural watershed of Jawoon-ri by using hourly rainfall data as rainfall and precipitation are basic and most important input data for runoff estimations in the SWAT model. We found that the use of hourly rainfall data in the SWAT model predicted hourly runoff from the watershed by using the Green and Ampt infiltration approach performed quite well and gave better results than the SCS curve number method with daily data. However, even though the use of sub-daily simulation gave better results, their overall test, and use is restricted by limited availability of input but also measured corresponding output variable like discharge.

After evaluating the performance of the SWAT simulation at the field level of the small agricultural watershed, the model was applied to the higher catchment level of the Haean catchment in the second study. The goal of using the SWAT model at a higher catchment level was to observe the cumulative effect of different agricultural and management practices on the environment of a bigger and more complex environmental situation. We focus on the capability of the SWAT model to predict the spatiotemporal variability in discharge throughout the catchment. The spatial and temporal data gap in precipitation among other meteorological parameters showed considerable impact on modeled plant growth dynamics which effects the overall water balance in the catchment. We developed an algorithm for gap-filling and to interpolate meteorological data in order to consider the convective effects of precipitation variability due to topographic variation in the catchment.

We applied the method of multi-site calibration and validation for discharge which parameterized the variability in flow processes and predicted the respective discharge partitioning within the catchment. The impact on discharge due to engineered structures in relation to drainage and culverts and road network consideration in the SWAT model was evaluated. We observed the drainage and culverts had significant impact on discharge at downstream. Hence, in the second study, we explored the SWAT capability and associated methods to improve the model performance for estimation of discharge.

After the parameterization of discharge modeling in SWAT, which serve as basis for the prediction of other environmental contaminants (sediment and nitrate). Henceforth, the model output variable of sediment and nitrate were calibrated and validated in a similar approach to consider impact due to different land use and management practices, which were further explored in the subsequent two studies.

The model was applied to different land use scenarios. However, the land use system of the study catchment depends on the policy and technological intervention. In the third study, we developed an extreme land use scenario by expanding major dryland crops of Haean catchment: cabbage, potato, radish, and soybean. We present a simplistic and transparent approach to identify scenario-based

optimal land use systems for a) minimum discharge, b) minimum sediment, c) maximum crop yield and d) maximum income. The implemented optimal land use system and associated trade-offs were analyzed. We found that the implementation of the land use system which was optimal for minimum discharge and minimum sediment had the trade-offs of producing minimum crop yields and minimum income. On the other hand, the optimal land use systems for maximum income and maximum crop yield produced more discharge and sediment export. This methodological approach to develop optimal land use systems and the analyses of associated trade-offs are of major importance for policy makers and farmers to select a particular land use system which is sustainable for both ecology and economy.

The final application of the SWAT model was for the implementation of best management practices (BMPs). Based on recommendations of previous studies and considering the catchment agricultural practices, the BMPs scenarios of cover crop and split fertilizer application were implemented. The applications of BMPs were aimed at better environmental performance by reducing nonpoint source pollution while increasing the crop yields. The BMPs of cover crop and split fertilizer application were assessed for effectiveness in sediment and unproductive nitrate reduction. We found that cover crop has a considerable effects on reducing both sediment and nitrate losses, and at the same time increased crop yields. The BMP with the split fertilizer application showed supportive effects in reducing nitrate but not reduce erosion and did not increase crop yields. The simultaneous application of BMPs with cover crop and split fertilizer application exhibited even greater impacts on environmental performance in reducing sediment and nitrate losses and increased crop yield.

Summing up, in this study we used integrated watershed modeling to identify the environmental performance of study catchments. In general, the land use system that was identified to produce a minimum sediment loss and the application of combining BMPs (cover crop and split fertilizer) would have positive environmental effects regarding sediment and nutrient losses from the intensive farming systems of similar mountainous agricultural landscapes in South Korea. The approach that we apply in this study to assess the environmental performance of intensive farming system could be applicable to similarly structured agricultural area in South Korea. However, a policy to compensate associated income losses needs additionally to be considered for effective implementation of the recommended land use systems and BMPs made by this study.

Zusammenfassung

Die Steigerung der landwirtschaftlichen Produktion zur Sicherung der Nahrungsgrundlage für eine wachsende Weltbevölkerung bei gleichzeitiger Reduzierung der damit verbundenen nachteiligen Auswirkungen auf die Umwelt stellt weltweit eine große Herausforderung dar. Sedimentfrachten, Nährstoffe und andere Agrochemikalien wie z.B. Pestizide aus der intensiven Landwirtschaft wirken hierbei als diffuse Eintragspfade ins Grundwasser und sind, etwa im Vergleich zu Punktquellen aus kommunalen Leckagen und industriellen Unfällen, oft schwierig zu handhaben und durch ein geeignetes Umweltmanagement zu regulieren. Hierbei greifen Topographie, Geologie, Geophysik, Klima, ökologische Rahmenbedingungen, Landnutzung und Landnutzungsänderungen eng ineinander und sind im Rahmen eines nachhaltigen Umweltmanagements adäquat zu berücksichtigen.

Im Rahmen der hier vorliegenden Arbeit wurden zwei Einzugsgebiete intensiv untersucht: das Haean-Einzugsgebiet und das Jawoon-ri-Einzugsgebiet. Beide liegen im Norden Südkoreas und sind durch Topographie, Geologie und Nutzungsverhältnisse komplex strukturiert. Die intensive Landwirtschaft in der Region ist durch den Einsatz hoher Düngermengen und Mobilisierung einer beachtlichen Sedimentfracht charakterisiert, die zu stromabwärts gelegenen Reservoirs transportiert werden. Insbesondere werden die beiden Einzugsgebiete regional als wesentliche Quellen für die Verunreinigung der Gewässer durch Schlämme und Umweltchemikalien angesehen, die letztlich im Soyang Reservoir akkumuliert werden. Da das Soyang Reservoir eine wichtige Quelle für die Trinkwasserversorgung in Seoul, der Hauptstadt Südkoreas, darstellt, ist diese Thematik außerordentlich brisant. Die Sedimente reduzieren die Speicherkapazität des Reservoirs, die gleichzeitig eingetragenen Schadstoffe verschlechtern die Wasserqualität. Das regionale Management zielt tendenziell darauf ab, die Wasserqualität zu verbessern und gleichzeitig die landwirtschaftliche Produktion in den stromaufwärts liegenden Einzugsgebieten Haean und Jawoon-ri auf hohem Niveau sicherzustellen.

Vor diesem Hintergrund wurde das DFG-geförderte binationale Projekt TERRECO (Complex TERRain and ECOlogical Heterogeneity) ins Leben gerufen. Die in TERRECO durchgeführten Studien auf Plot- und Einzugsgebietsebene sollen ein detailliertes Verständnis über Wasserflüsse, Erosionsfrachten und Stofftransport unter verschiedenen Nutzungsszenarios und Managementstrategien ermöglichen. In Plotstudien werden die Auswirkungen des Managements auf die landwirtschaftliche Produktion und Umweltbelastung durch diffuse Quellen analysiert. Auf der Einzugsgebietsebene wird das SWAT-Modellpaket (Soil and Water Assessment Tool) verwendet, das es erlaubt, prozessbasiert verschiedenen Managementsysteme quantitativ auszuwerten. Das SWAT-Modell wurde an die Untersuchungsgebiete der Jawoon-ri - und Haean - Einzugsgebiete mit komplexem Gelände angepasst. Hierbei wurden Erkenntnisse aus Publikationen zu verschiedenen SWAT-Anwendungen in Südkorea berücksichtigt.

Hauptziel der Arbeit war es, das Landnutzungssystem und die besten Managementstrategien für eine dauerhafte Reduzierung von Sedimenten und Nährstoffen aus den Modellgebieten zu identifizieren. Unsere ersten beiden Studien befassten sich mit wichtigen technischen Details des SWAT-Modells, der Kalibrierung und Validierung und der zugehörigen Modellsensitivität, sowie der Unsicherheit der Ergebnisse. Thematik der folgenden zwei Studien war die SWAT-basierte Bewertung der Auswirkung verschiedener Landnutzungssysteme und landwirtschaftlicher Bewirtschaftungsstrategien auf die Wasserqualität, den Ertrag und die Betriebseinkommen.

In der ersten Studie wurde das SWAT-Modell hinsichtlich der Vorhersage der Wasserflüsse aus dem kleinen landwirtschaftlichen Einzugsgebiet Jawoon-ri mit Hilfe stündlicher Niederschlagsdaten bewertet (im Vergleich zu gröberen und feineren Datenaggregationen), da Niederschlagsdaten zu den wichtigsten Eingangsdaten für Abflussschätzung im SWAT-Modell gehören. Wir fanden heraus, dass die Verwendung von stündlichen Niederschlagsdaten (in Verbindung mit dem Infiltrationsmodell von Green und Ampt), die gemessenen Gebietsabflüsse besser reproduzieren konnten als bei Verwendung von täglichen Niederschlagsdaten und des SCS-curve-number-Verfahrens. Allerdings sind stündliche Eingabedaten und deren korrespondierenden Abflussdaten oft nicht ausreichend verfügbar.

Im Anschluss daran wurde das Modell auf das größere und komplexere Haeon-Einzugsgebiet ausgedehnt. Ziel war hierbei die Anwendung des SWAT-Modells zur Analyse der kumulativen Auswirkungen verschiedener Praktiken des Agrarmanagements auf die Umwelt auf der Einzugsgebietsebene. Wir konzentrierten uns zunächst auf die Fähigkeit des SWAT-Modells, um die räumliche und zeitliche Variabilität des Abflusses im gesamten Einzugsgebiet vorherzusagen. Räumliche und zeitliche Datenlücken im Niederschlag haben erhebliche Auswirkungen auf modellierte Ergebnisse zum Pflanzenwachstums, was den errechneten Gesamtwasserhaushalt im Einzugsgebiet empfindlich beeinflusst. Wir entwickelten daher einen Algorithmus, der die fehlenden meteorologische Daten interpoliert, hauptsächlich um die Wirkung der höhenabhängigen Niederschlagsvariabilität im Einzugsgebiet zu berücksichtigen. Zur Kalibrierung und Validierung des Modells im Hinblick auf die Gebietsabflüsse verwendeten wir eine speziell entwickelte, sequentielle Multi-Site-Methodik zur Berücksichtigung der räumlichen Gliederung des Einzugsgebiets in Teileinzugsgebiete. Die Auswirkungen ingenieurtechnischer Anlagen zur Abführung von Oberflächenwasser wurden über die Abflussanalysen ausgewertet. Wir beobachteten, dass diese Kanalisationen erhebliche Auswirkungen auf den Abfluss hatten. Daher untersuchten wir in der zweiten Studie, inwieweit durch die Berücksichtigung dieser Konstruktionen in SWAT die Modellperformance zur Abschätzung des Abflusses verbessert werden kann.

Im Anschluss an die Parameterisierung der Abflussmodellierung von SWAT, als Basis für die Prognose anderer umweltrelevanter Stoffe, wurden dann Sedimentfrachten und Nitratexport separat kalibriert und validiert, um die Auswirkungen hinsichtlich unterschiedlicher Landnutzungs- und Management-Praktiken analysieren und bewerten zu können.

Die Landnutzung des untersuchten Einzugsgebiets wird jedoch stark von Eingriffen der Politik und von technologischen Aspekten geprägt wird, wodurch der Anbau von Kohl, Kartoffeln, Rettich und Soja stark favorisiert wurde. Daher hatten wir in der dritten Studie zunächst extreme Landnutzungsformen implementiert, indem wir den exklusiven Anbau je einer der großer Trockenfeldpflanzen des Haean Einzugsgebiets (Kohl, Kartoffeln, Rettich oder Sojabohnen) im Modell repräsentierten. Dies entspricht einem vereinfachenden, aber effizienten und transparenten Ansatz, um eine optimale Landnutzung für a) minimalen Abfluss, b) minimale Sedimentfracht, c) maximalen Ernteertrag und d) maximales Einkommen zu identifizieren. Die Umsetzung in ein optimales Landnutzungssystem und die damit verbundenen Kompromisse (trade-offs) wurden analysiert. Wir beobachteten, dass die Realisierung eines Landnutzungssystems, das optimal ist für minimalen Abfluss und minimalen Sedimentexport, zu minimalen Ernteerträgen und minimalem Einkommen der landwirtschaftlichen Bevölkerung führte. Andererseits führte ein optimiertes System für maximales Einkommen und maximale Ernteerträge zu höheren Gebietsabflüssen und Erosion. Die hier beschriebene Methodik zur Entwicklung eines optimalen Landnutzungssystems hat möglicherweise ein hohes Potential zur Unterstützung der politischen Entscheidungsträger und der Landwirte bei der Etablierung eines nachhaltigen, wirtschaftlichen und umweltverträglichen Agrarmanagements.

Die abschließende Anwendung des SWAT Modell zielte auf die Umsetzung des Konzepts der “Best Management Practices” (BMPs), basierend auf Empfehlungen früherer Studien für landwirtschaftliche Praxis im Einzugsgebiet. In dieser Studie wurden speziell die BMP-Szenarien der Gründüngung und der zeitlich aufgeteilten Düngergaben implementiert und bewertet. Durch die Anwendungen dieser BMPs werden bessere Umweltleistungen durch Reduzierung diffuser Umweltbelastungen bei gleichzeitiger Erhöhung der Ernteerträge angestrebt. Es zeigte sich, dass Gründüngung deutliche, positive Auswirkungen auf die Belastung der Umwelt hat, sowohl durch die Verringerung der Sedimentfracht als auch durch die Reduzierung unproduktiver Nitratverluste, was wiederum eine Erhöhung der Ernteerträge zur Folge hatte. Die BMP-Szenarien zur zeitlich aufgeteilten Düngung hatten ebenfalls einen deutlichen Einfluss auf die Reduzierung von Nitratverlusten, aber keine vergleichbaren Wirkungen hinsichtlich der Sedimentfracht und der Ernteerträge. Die gleichzeitige Anwendung von Gründüngung und zeitlich aufgeteilter Düngergabe wiederum hat einen noch größeren Einfluss auf die Umweltleistung bezüglich der Verringerung der Sedimentfracht und der Nitratverluste.

Insgesamt werden in der hier vorgelegten kumulativen Dissertation mit einer integrierten Einzugsgebiets-Modellierung für ein komplexes Terrain Landnutzungsszenarien analysiert, die es erlauben, die Umweltleistung der Modellgebiete zu identifizieren und zu quantifizieren. Das hier ermittelte optimale Landnutzungs-System ermöglicht eine Minimierung der Erosion und damit einen minimalen Sedimentexport, sowie durch die Anwendung von Deckfruchtanbau und geteilten

Düngergaben eine Reduzierung unproduktiver Nährstoffverluste bei gleichzeitig positiven Auswirkungen auf Erträge bzw. Ertragssicherheit. Im Prinzip sollte das Konzept auch auf ähnlich strukturierte landwirtschaftliche Gebiete in Südkorea übertragbar sein. Allerdings sind hier zu einem hohen Maße auch flankierende politische Maßnahmen erforderlich, z.B. um eventuelle Einkommensverluste zu kompensieren.

Acknowledgements

In general, I would like to thank all the people who have helped directly and indirectly to complete this study.

My sincere gratitude goes to Prof. Dr. Bernd Huwe for giving me an opportunity to conduct my doctoral research work at the Department of Soil Physics. In addition, I am very much thankful to Prof. Dr. Bernd Huwe for being my supervisor who has always time for advising my research activity and constructive suggestion to improve my PhD work was highly valuable. My sincere thanks also go to my co-advisors, Prof. Dr. John Tenhunen for an opportunity to associate my doctoral research work in "TERRECO" project and Prof. Dr. Seong-Joon Kim for his valuable suggestions.

My special thanks to Dr. Christopher. L Shope for his guidance to setup my modeling work and highly appreciated his technical support and editing the compiled manuscripts. Many thanks also go to Dr. Sebastian Arnhold for R coding and fruitful discussion and critical comments and editing the individual manuscripts of this thesis. His brief description about different location of my study catchment during the field visit is highly appreciated. I also wish to thank Prof. Dr. Thomas Koellner, Dr. Trung Thanh Nguyen, and Dr. Marianne Ruidisch for their valuable comments and suggestions during preparation of the manuscript.

The lab members: Jong Yoon Park, Rim Ha and Sora Ahn and Prof. Seong-Joon Kim from the Department of Civil and Environmental System Engineering, Kunkuk University, Seoul are highly thanked for their all kind of help during my stay in their lab. I would like to thank Prof. Kyoung Jae Lim, from Kangwon National University for his useful suggestion to my work. The automation of R code from Kwanghun Choi during my modeling work is highly appreciated. I also like to thank all "TERRECO" members for wonderful social events.

My special thanks to department of soil physics group for providing wonderful working place and my thanks also go to Sandra Thomas, Gabriele Wittke, and Dr. Bärbel Heindl-Tenhunen for official coordination during my PhD study.

I would like to appreciate my brother Sagar Maharjan for taking care of my parents and belongings, which made it possible to accomplish my study abroad.

Finally, I would like to extend my invaluable gratitude to my parents and my wife, Rasmila Kawan for supporting me along this incredible journey.

Table of contents

Abstract	i
Zusammenfassung	v
Acknowledgements	ix
List of figures	xiv
List of tables	xvii
List of summary boxes	xix
List of abbreviations	xx
List of SWAT variables.....	xxii
List of symbols	xxiv
Chapter 1 Synopsis	1
1.1 Introduction	1
1.1.1 Watershed, natural resources and ecosystem services.....	1
1.1.2 Watershed modeling and choice of model	3
1.1.3 Research rationale and objectives.....	4
1.2 Methodological approach	7
1.2.1 Conceptual framework	7
1.2.2 Study area	8
1.2.3 Soil and Water Assessment Tool: SWAT model	10
1.2.4 Model calibration, validation and uncertainty analysis	12
1.2.5 Evaluation of SWAT model for sub-daily runoff estimation	17
1.2.6 Hydraulic process description and partitioning in Haeon Catchment, South Korea	18
1.2.7 Identifying optimal land use systems and trade-offs between farm income and environment.....	20
1.2.8 Assessing the effectiveness BMP of split fertilizer and cover crop cultivation	21
1.3 Results and discussion.....	22
1.3.1 Evaluation of SWAT to estimate hourly runoff	22
1.3.2 SWAT application to improve process description and hydrologic partitioning in South Korea.....	24
1.3.3 Determination of optimal land use systems and quantification of associated trade-offs between farm income and environment	28
1.3.4 Application of BMP and assessing their effectiveness for different crop and catchment level.....	33
1.4 Conclusions and recommendations	36
1.5 List of manuscripts and specification of individual contributions	41
1.6 References	43

Chapter 2 Evaluation of SWAT sub-daily runoff estimation at small agricultural watershed in Korea	46
Abstract	46
2.1 Introduction	47
2.2 Methodology	48
2.2.1 Study area	48
2.2.2 General rainfall and temperature at the watershed	49
2.2.3 Modification of digital elevation model (DEM).....	50
2.2.4 Land uses, soil, and weather data at the study watershed.....	51
2.2.5 Analysis of hourly precipitation	52
2.2.6 Modification in SWAT input files for sub-daily simulation	53
2.2.7 Calibration and validation of estimated flow	53
2.3 Results and discussion.....	54
2.3.1 SWAT hourly simulation	54
2.3.2 SWAT daily simulation.....	57
2.4 Conclusions	58
2.5 Acknowledgements	59
2.6 References	60
Chapter 3 Using the SWAT model to improve process descriptions and define hydrologic partitioning in South Korea	62
Abstract	62
3.1 Introduction	63
3.2 Catchment characteristics.....	65
3.3 Methods and model Construction.....	67
3.3.1 Model description.....	67
3.3.2 Model inputs.....	67
3.3.2.1 Climate data.....	67
3.3.2.2 Discharge and evapotranspiration estimates.....	69
3.3.3 Spatial data	70
3.3.3.1 DEM	70
3.3.3.2 Soils	71
3.3.3.3 Land use and land cover (LULC).....	72
3.3.4 Management inputs and crop parameterization.....	72
3.3.4.1 Management parameter estimation.....	72
3.3.4.2 Biomass sampling, analysis, and plant growth.....	73

3.3.4.3 Rice paddies, potholes, and water abstraction	76
3.4 Results and discussion	76
3.4.1 Meteorological drivers and the effects of interpolation.....	76
3.4.2 Model calibration, validation, and uncertainty assessment	77
3.4.2.1 Sensitivity and model parameterization	77
3.4.2.2 Metrics of model performance for calibration procedures	81
3.4.2.3 Manual and automated model calibration	81
3.4.3 Spatiotemporal flow partitioning with respect to river discharge	83
3.4.4 Agricultural management and production	86
3.4.5 Influence of engineered landscape structure	88
3.5 Conclusions	89
3.6 Acknowledgements.	91
3.7 References	92
Chapter 4 Identifying scenario-based optimal land use systems and assessing trade-offs between farm income and environment: Haean catchment, South Korea.....	96
Abstract	96
4.1 Introduction	97
4.2 Methodology	98
4.2.1 Study area	98
4.2.2 Data collection and model setup.....	100
4.2.3 The SWAT model.....	101
4.2.4 Model parameterization, calibration, and validation	102
4.2.5 Determination of crop allocation.....	109
4.2.6 Cost benefit analysis.....	110
4.3 Results	111
4.3.1 SWAT simulation for monoculture land use system.....	111
4.3.2 SWAT simulation for the optimal land use system	113
4.3.3 Trade-off analysis	117
4.4 Discussion	119
4.5 Conclusions	122
4.6 Acknowledgements	123
4.7 Appendix (4A–4G).....	124
4.8 References	131

Chapter 5 Assessing effectiveness of split fertilization and cover crop cultivation to conserve soil and water resources and improve crop productivity	134
Abstract	134
5.1 Introduction	135
5.2 Materials and methods.....	137
5.2.1 Study area	137
5.2.2 Model application.....	138
5.2.3 Model parameterization.....	138
5.2.4 Model calibration and validation.....	139
5.2.5 BMP scenarios.....	140
5.3 Results	141
5.3.1 SWAT model performance.....	141
5.3.2 BMP impact on sediments.....	142
5.3.3 BMP impact on nitrate.....	144
5.3.4 BMP impact on crop yield.....	147
5.3.5 BMP impact on water quality at catchment outlet	149
5.4 Discussion	151
5.5 Conclusions	153
5.6 Acknowledgements	154
5.7 Supplementary material (Supplementary Table: ST 5.1-ST 5.6 & Figures SPF1-SPF6).....	155
5.8 References	166
Declaration / Erklärung	171

List of figures

Figure 1.1 Conceptual framework for assessing sustainable intensive farming system.....	8
Figure 1.2 The study sites of Jawoon-ri catchment (a) and the Haeon catchment (b) are major nonpoint source pollution to Soyang reservoir.	9
Figure 1.3 Line diagram of hydraulic cycle presented in SWAT model (White et al., 2012).....	11
Figure 1.4 The line diagram to represent different processes of nitrogen assimilation considering different source nitrogen in nitrogen cycle (White et al., 2012)	12
Figure 1.5 The subbasins and HRUs (not shown) within subbasin considered for parameterization during multi-site calibration conducted one at a time	17
Figure 1.6 Land use discretization for the base line scenario and each of the four monoculture system scenarios. For the monoculture systems, HRUs representing agricultural crops were adjusted to the individual monoculture crop type throughout the entire catchment	29
Figure 1.7 Optimal land use systems derived by comparing individual HRUs to obtain A. Minimum surface runoff (SR), B. Minimum sediment, C. Maximum yield, and D. Maximum income. Note: “New” refers to the percent area corresponding to the optimal land use and “Base line” refers to the percent area in the base line scenario	30
Figure 2.1 Location of study area with drain channel	49
Figure 2.2 Temperature and precipitation for 2007(a) and 2008(b).....	50
Figure 2.3 Sub-watershed boundaries with manual delineation after automatic delineation. (a) automatic delineation; (b) manual delineation.....	51
Figure 2.4 Hourly precipitation variation for events of 2007(a) and 2008(b) at the study watershed	53
Figure 2.5 Comparison of simulated and measured runoff for calibration: (a) simulated and measured runoff in calibration; (b) comparison of simulated and measured runoff for calibrated events	57
Figure 2.6 Comparison of simulated and measured runoff for validation: (a) simulated and measured runoff in validation; (b) comparison of simulated and measured runoff for validated events	57
Figure 2.7 Comparison of daily simulated and measured runoff for events of 2007 and 2008 : (a) daily simulated and measured runoff for events of 2007 and 2008; (b) comparison of daily simulated and measured runoff at similar condition of SWAT sub-daily	58
Figure 3.1 Haeon study area within the Lake Soyang watershed is located in northeastern South Korea along the demilitarized zone (DMZ) border with North Korea. The regional KMA weather station and local meteorological stations are denoted with white circles and (WS). River discharge monitoring locations are denoted by (S) and the yellow squares	66
Figure 3.2 Multiple river system and infrastructure model configurations within the Haeon catchment which, contribute to surface discharge accumulation and flow routing. The panels display the configuration for (A) solely the Haeon river network; (B) the river network and engineered culvert drainage system; and (C) the river network, the culvert system, and the road infrastructure	71
Figure 3.3 Meteorologic variability and average daily value of each variable throughout the Haeon catchment for 2010. (A) describes the daily precipitation and temperature variability, (B) is the range in solar radiation and the average value between all of the locations, (C) is the wind speed variability, and (D) is the relative humidity range.....	77

Figure 3.4 SWAT simulated parameter sensitivity (p value) and model significance (t test) for the Haean catchment for monitoring locations S1, S4, S5, S6, and S7 along the elevation transect.....	78
Figure 3.5 Calibrated and validated daily comparison of drainage area normalized observed and simulated river discharge along the elevation transect of monitoring locations S1, S4, S5, S6, and the catchment outlet S7. Included on each panel are the objective function and optimization statistics	84
Figure 3.6 Daily heat sum estimate between 1998 and 2010 for the S1forest boundary monitoring location within the Haean watershed (Figure 3.1)	87
Figure 3.7 Comparison of simulated versus observed leaf area index (LAI) for five of the primary crops grown in Haean and the deciduous forest.....	88
Figure 4.1 Location of the study area on the Korean peninsula and within the Soyang Lake watershed. In addition, the land use distribution of the Haean catchment is depicted. Land use abbreviations are provided in Table 4.1. The Haean catchment is a hot spot for sediment and nutrients transport to the Soyang Reservoir.....	99
Figure 4.2 Average monthly temperature and precipitation in the Haean catchment for the period of 1999 - 2011 from all weather stations (Figure 4.1) throughout the entire catchment.....	99
Figure 4.3 Observed and simulated discharge for the calibration (2009-2010) (a) and validation (2011) (b) periods at each of the different monitoring locations. The inverted secondary y-axis represents precipitation	105
Figure 4.4 Observed and simulated sediment for the calibration (2009-2010) (a) and validation (2011) (b) at each of the different monitoring locations. The inverted secondary y-axis represents precipitation.....	106
Figure 4.5 Observed (black dash line) and simulated mean leaf area index (LAI) (black solid line) during each growing season for 7 of the major agricultural crops (a-g: cabbage, potato, radish, soybean, rice, corn and orchard) and (h) deciduous forest in the Haean catchment. Gray shaded band: maximum and minimum LAI simulated from respective land use type HRUs. In addition, the mean simulated biomass production (red solid line) and range (pink shaded band: maximum and minimum biomass simulated from respective land use type HRUs) are depicted. For comparative purposes, the estimated evapotranspiration time series is included by blue lines.....	108
Figure 4.6 Hierarchical line diagram of the conceptual development of individual SWAT scenarios under different land use systems and crop reallocation to derive the optimal land use and associated trade-offs	110
Figure 4.7 Land use discretization for the base line scenario and each of the four monoculture system scenarios. For the monoculture systems, HRUs representing agricultural crops were adjusted to the individual monoculture crop type throughout the entire catchment.....	113
Figure 4.8 Optimal Land Use /Land Classification (LULC) systems derived by comparing individual HRUs to obtain A. Minimum surface runoff (SR), B. Minimum sediment, C. Maximum yield, and D. Maximum income. Note: “New” refers to the percent area corresponding to the optimal land use and “Base line” refers to the percent area in the base line scenario.....	114
Figure 4.9 Spider plot showing the outputs from the different optimal land use and base line scenarios. Detailed spatial representation of the optimized land use systems (A, B, C and D) and " base line" scenarios are provided in Figure 4.8 and Figure 4.7. The four axes represent different scales for respective output variables. The numerical pairs at the four corners represent minimum (at crossing of the axes) and maximum (at the end point of the corner) for respective output variables	119

Figure 5.1 Location and land use distribution of the Haean catchment including sub-basins, weather stations, and stream monitoring points used for this study. The Haean catchment is one of the hotspots for sediment and nutrients transport into the Soyang reservoir	138
Figure 5.2 Variation of sediment loss from the respective crop HRUs simulated for the different scenarios. Small letters "a" and "b" are used to indicate statistical significance between the scenarios. Presence of same letter indicates no significance while different letter indicates significant differences between scenarios.....	143
Figure 5.3 Total sediment loss from four major dryland crops estimated for different BMP scenarios	144
Figure 5.4 Variation of total nitrate from the respective crop HRUs simulated in different scenarios	146
Figure 5.5 Total nitrate loss from four major dryland crops estimated for different BMP scenarios	147
Figure 5.6 Variation of crop yield from the respective crops HRUs simulated for different scenarios	148
Figure 5.7 Total crop yield from four major dryland crops estimated for different BMP scenarios.	149
Figure 5.8 Simulated daily nitrate concentration (A) and cumulative daily total nitrate load (B) at the catchment outlet for different scenarios.....	150
Figure 5.9 Simulated sediment concentration (A) and cumulative total sediment load (B) at catchment outlet for different scenarios.....	151

List of tables

Table 2.1 Soil properties at different soil horizon at the watershed	51
Table 2.2 Precipitation data format in SWAT sub-daily run	52
Table 2.3 Hourly flow results in calibration and validation for each storm events	55
Table 2.4 Parameter range of variables derived from sensitivity analysis.....	55
Table 2.5 Corresponding parameters values at 10 % lower and higher.....	56
Table 2.6 Outflow response at 10 % change in sensitive parameters	56
Table 2.7 Simulation result at different time resolution of precipitation records	57
Table 3.1 Principle input data sets for the construction of the Haean catchment SWAT model.....	69
Table 3.2 Percentage of Haean catchment associated with the individual aggregated land use, soil, and slope classifications. The slope classification generally defines the difference between forest, dryland farming, and rice paddy systems throughout Haean	71
Table 3.3 Agricultural crop management schedule including planting and harvest dates, fertilization dates, amounts, and type of fertilizer, tilling dates and method, SCS curve number for each crop, and the heat units required to reach maturity	73
Table 3.4 Example SWAT model crop parameter database variations in the Haean model	75
Table 3.5 SWAT parameter sensitivity and significance between discharge parameters throughout the Haean catchment (Figure 3.4). Calibrated SWAT parameters for the Haean catchment, including the individual ranking along the elevation-based transect, the minimum and maximum parameter values for all subbasins accounted for by each monitoring location, and the average calibrated parameter value. Because of the distributed nature of the Haean model, individual parameters varied depending on crop type, elevation, aspect and therefore, a specific parameter value is not available	79
Table 3.6 Calibration and validation statistics for each of the monitoring locations throughout the Haean Catchment. The data includes the subbasin demarcation of the monitoring locations, the total number of observations, the observed and simulated water balance, the NSE, R ² , and PBIAS statistics, and the percent baseflow contribution.....	81
Table 3.7 Biomass production and crop yield statistics for South Korea and specifically, for the Haean catchment.....	86
Table 4.1 Land use distribution in the Haean catchment.....	100
Table 4.2 Sources and scale of each of the input data sets for the SWAT model construction and daily meteorological inputs.....	100
Table 4.3 Soil type distribution throughout the Haean catchment.....	101
Table 4.4 Statistical performance of the model during calibration and validation	104
Table 4.5 Total production cost estimates for potato, cabbage, radish, and soybean in the Haean catchment.....	111
Table 4.6 Catchment level model output for the monoculture system and base line scenarios.....	112
Table 4.7 Land use distribution as a percentage of the catchment for the different derived optimal land use systems and the base line scenario.	115
Table 4.8 Model output at the catchment level for derived optimal land use system and base line land use system.....	117
Table 5.1 Input data set for SWAT model of the Haean catchment	139

Table 5.2 Management schedules for the cultivation of the four major dryland crops in the Haean catchment.....	139
Table 5.3 Model performance for different output variables at different stream sites	141
Table 5.4 Scenario impact on sediment loss from different crop types: ton ha ⁻¹ (% difference compared to BL scenario).....	144
Table 5.5 Scenario impact for total nitrate loss for the different crops: kg ha ⁻¹ (% difference from BL scenario).....	147
Table 5.6 Scenario impact on crop yield for the different crops: ton ha ⁻¹ (% difference from BL scenario).....	149

List of summary boxes

Box1 result summary: Hourly runoff estimation using SWAT (Manuscript 1).....	24
Box2 result summary: Hydrologic process modeling and discharge partitioning (Manuscript 2).....	27
Box3 result summary: Drive optimal land use and trade-offs quantification (Manuscript 3).....	32
Box4 result summary: Modeling of split fertilization and cover crop cultivation (Manuscript 4).....	35

List of abbreviations

a.s.l	average sea level
ARS	Agricultural Research Services
BL	base line scenario
BMPs	best management practices
CC	cover crop cultivation scenario
CMS	cubic meter per second
DEM	digital elevation model
DMZ	Demilitarized Zone
ESWAT	Enhance Soil and Water Assessment Tool
ET	evapotranspiration
FAO	Food and Agriculture Organization
FRSD	deciduous forest
FRSE	coniferous forest
GADM	Global Administrative Areas
GIS	geographic information system
GPS	geographic positioning system
HRUs	hydrologic response units
IDW	Inverse Distance Weighted
IRTG	International Research Training Group
KMA	Korean Meteorological Agency
LAI	leaf area index
LULC	land use land cover
MSL	Mean Sea Level
MUSLE	Modified Universal Soil Loss Equation
NGII	National Geographic Information Institute
NO ₃ ⁻	Nitrate
ORCD	orchard
PET	potential evapotranspiration
PIXGRO	Plant Physiology Model
RDA	Rural Development Administration
RICE	rice
RIG	Research Institute of Gangwon
SCS	Soil conservation service
SF	split fertilization scenario
SFCC	split fertilization and cover crop cultivation scenario
SPF	supplementary figure (<i>chapter 5</i>)

ST	supplementary table (<i>chapter 5</i>)
SUFI 2	Sequential Uncertainty Fitting Algorithm
SWAT	Soil and Water Assessment Tool
TERRECO	Complex TERRain and ECOlogical Heterogeneity
U.S.D.A	United States Department of Agriculture
URBN	residential area
USA	United Atate of America
USLE	Universal Soil Loss Equation
WATR	inland water
WWTPs	waste water treatment plants
YCO	Yanguu County Office

List of SWAT variables

Variables	Description	Units
ALPHA_BF	baseflow alpha factor	[-]
ALPHA_BNK	baseflow alpha factor for bank storage	[days]
ANION_EXCL	fraction of porosity from which anions are excluded	[-]
BLAI	potential maximum leaf area index for the plant	[-]
CANMX	maximum canopy storage	[mm]
CH_COV1	channel erodibility factor	[-]
CH_COV2	channel cover factor	[-]
CH_EROD	channel erodibility factor	[-]
CH_K2	effective hydraulic conductivity in main channel alluvium	[mm hr ⁻¹]
CH_N2	mannings "n" value for the main channel	[-]
CMN	rate factor for humus mineralization of active organic nutrients	[-]
CN2	SCS curve number for moisture condition II	[-]
DLAI	fraction of growing season at which senescence becomes the dominant growth process	[-]
ESCO	soil evaporation compensation factor	[-]
FRGRW1	fraction of the growing season corresponding to the 1 st point on the optimal leaf area development curve	[-]
FRGRW2	fraction of the growing season corresponding to the 2 nd point on the optimal leaf area development curve	[-]
GW_DELAY	ground water delay time	[day]
GWQMN	a threshold minimum depth of water in the shallow aquifer required for return flow to occur	[mm]
HRU_SLP	average slope steepness (m/m)	[-]
IDT	length of time step $\Delta t = \text{IDT}/60$	[min]
IEVENT	rainfall, runoff, routing option	[-]
LAIMX1	fraction of the maximum plant leaf area index corresponding to the 1 st point on the optimal leaf area development curve	[-]
LAIMX2	fraction of the maximum plant leaf area index corresponding to the 2 nd point on the optimal leaf area development curve	[-]
LAT_SED	sediment concentration in lateral flow and groundwater flow	[mg l ⁻¹]
LAT_TIME	lateral flow travel time	[day]
N_UPDIS	nitrogen uptake distribution parameter	[-]
NPENCO	nitrogen percolation coefficient	[-]
OV_N	mannings "n" value for overland flow	[-]
PHU	potential heat unit for plant growing at beginning of simulation	[deg]

	(heat units)	
PRF	peak rate adjustment factor for sediment routing in the main channel	[-]
REVAPMIN	minimum depth of water in shallow aquifer for re-evaporation to occur	[mm]
RUE	radiation use efficiency	[(kg/ha) (MJ/m ²) ⁻¹]
SLSUBBSN	average slope length	[m]
SOL_AWC	available water capacity of the soil layer (mm H ₂ O/mm soil)	[-]
SOL_CBN	Organic carbon content (% soil weight)	[-]
SOL_DB	Moist bulk density	[g cm ⁻³]
Sol_K	saturated hydraulic conductivity of first layer	[mm hr ⁻¹]
SPCON	linear parameter for calculating the maximum amount of sediment that can be reentrained during channel sediment routing	[-]
SPEXP	exponent parameter for calculating sediment reentrained in channel sediment routing	[-]
USLE_K	soil erosivity	[0.013 metric ton m ² hr (m ³ metric ton cm) ⁻¹]

List of symbols

$area_{hru}$	area of the HRU	[ha]
$CFRG$	coarse fragment factor	[-]
C_{USLE}	USLE cover factor	[-]
E_a	amount of evapotranspiration	[mm]
E_{NS}	Nash–Sutcliffe efficiency (<i>chapter 2</i>)	[-]
FI	Farm Income	[won ha ⁻¹]
H_{phosyn}	amount of intercepted photosynthetically active radiation	MJ m ⁻²
HUSC	Percentage of total heat unit	[-]
K_{USLE}	USLE soil erodibility factor	[0.013 metric ton m ² hr (m ³ metric ton cm) ⁻¹]
LS_{USLE}	USLE topographic factor	[-]
NSE	Nash–Sutcliffe efficiency	[-]
p - factor	Indicator for simulated results within 95% confidence interval to include the observational data	[-]
PBIAS	Percentage bias	[-]
P_e	estimated precipitation	[mm]
P_o	observed precipitation	[mm]
P_r	price per kg crops	[won ha ⁻¹]
P_{USLE}	USLE support practice factor	[-]
Q_{GW}	amount of return flow	[mm]
q_{peak}	peak runoff rate	[m ³ s ⁻¹]
Q_{surf}	amount of surface runoff	[mm]
r - factor	uncertainty bad	[-]
R^2	Coefficient of determination	[-]
R^2	Coefficient of determination (<i>chapter 3 and 5</i>)	[-]
R_{day}	amount of precipitation in a day	[mm]
RUE	radiation-use efficiency of the plant	[(kg/ ha). (MJ/m ²) ⁻¹]
sed	sediment yield	[metric tons]
SW_0	initial soil water content	[mm]
SW_t	final soil water content	[mm]
TCP_{crop}	total cost of production	[won ha ⁻¹]

W_{seep}	percolation and bypass flow exiting the bottom of the soil profile	[mm]
Y_{crop}	crop yield	[ton ha ⁻¹]
Z	elevation	[m]
Δbio	the potential increase in total biomass	[kg ha ⁻¹]
v	total number of observational meteorological stations	[-]
φ	observation point aspect	[deg]
ω	weighting factor	[-]

Chapter 1 Synopsis

1.1 Introduction

1.1.1 Watershed, natural resources and ecosystem services

A watershed is an area of land that drains rain water or snow into one location such as a stream, lake or wetland (Brooks et al., 2013). Watersheds include various natural resources of forest, water, and arable land which provide various ecosystem services like; supporting services (nutrient cycling, soil formation, and retention), provisioning services (production of crop yield and fresh water), regulating services (climate, flood and disease regulation and water purification) and cultural services (recreational, aesthetic, and educational) which are important for human well beings (Daily, 1997).

Watershed in particular, mountainous landscapes represents one-quarter of the earth's land surface and are important source of fresh water to downstream residents. Mountainous landscape includes 10 % of the world's population (Brooks et al., 2013). The increase of global world population has put more stress on watersheds (natural resources) and has changed global ecosystems to support food production along with economic development (Millennium Ecosystem Assessment, 2005). Security of food supply for the growing population has lead to intensive farming system in the watersheds. Intensive farming coupled with high-yield crop varieties, excessive use of tillage, fertilizer, irrigation, and pesticides have contributed a lot to increased food production over last 50 years (Matson et al., 1997). Agricultural ecosystems including intensive farming systems and their management are mainly in the focus to satisfy human needs (Poppenborg, 2014). The management of intensive farming systems along with deforestation and infrastructure development (culverts and road networks) leads to land use changes, affecting the spatiotemporal variations on stream discharge and water quality. Thus, the intensive farming has negative environmental effects due to transport of sediment and associated contaminants to water bodies (Tilman et al., 2002).

Soil erosion and sediment loss from intensive farming with excess tillage reduces soil fertility because of organic matter and nutrient loss. Sediments deposited to stream channels raise the bed level potentially causing flooding to adjacent land. Furthermore, sediment with attached nutrients transported to lakes and reservoirs have detrimental effects by reducing water quality and storage volume that decreasing reservoir's lifetime (Pimentel et al., 1995). The substantial use of chemical fertilizers and pesticides further harm the environment by polluting and poisoning soil and water. The global use of nitrogen fertilizer has increased by 8.5 times from 12 to 110 million tons yr⁻¹ between 1961 and 2010 (FAO, 2011a cited in Pradhan, (2015)). Only 30-50 % of the applied nitrogen fertilizer is taken up by crops and remaining amount of applied nitrogen are lost from the agricultural fields (Tilman et al., 2002). As a result, agricultural activity is the major diffuse pollution source (nonpoint source pollution) to aquatic ecosystems. The excessive presence of nutrients i.e., nitrates and phosphorous can produce eutrophication that deteriorates the water quality and further impair the use of water (Carpenter et al., 1998). The threshold level of nutrients like NO₃-N in drinking water is 10

mg l⁻¹. Excess nitrate can affect the human health and can be fatal for newly born babies due to blue baby disease. According to Environmental Protection Agency, United States have stipulated in 1976 the allowable limit of NO₃-N concentration in drinking water at 10 mg l⁻¹ (Brooks et al., 2013). Water from lakes and reservoirs contaminated with such nutrients experience algal blooms, which is expensive to purify for drinking or industrial use. Excess fertilizer in intensive agricultural production for food security has to bear on-site and off-site damage due to deterioration of water quality.

The global concern is to secure the food through intensive farming while controlling point and nonpoint source pollution both in local and global levels. Meanwhile, the worldwide degradation of productive farmland was recognized. The UN Convention to Combat Desertification (Stavi and Lal, 2015; UNCCD, 2012) has postulated to achieve global zero net land degradation until 2030. Increasingly social concerns to control pollution are considered by the implementation of various environment control legislation in many parts of the world. Legislations focused on the control of both point and nonpoint source pollution by the implementation of different management practices. Point source pollution can be better controlled than nonpoint source pollutions, as point source pollutions can be fed into the treatment plant before they are released into natural water systems. Nonpoint source pollutions originate mostly from intensive agricultural fields and pollute surface and ground water of the watershed. Nonpoint source pollutions are spatially distributed throughout the watershed. The variability of nonpoint source pollution from the different farm fields are dependent on management practices and associated variability in climate, topography, soil, and hydraulic characteristics of the particular field.

Different control measures have been adopted to control the pollution level to secure improved water quality from the watershed. The improved water quality from the watershed can be secured by changes in land use policy from intensive annual farming system to perennial crops. The land use policy and the resultant land use system for improving environment (good water) quality has to tolerate losses in economic production (lower crop yield). A land use system targeting at one ecosystem service may bring the trade-offs for other ecosystem services (Seppelt et al., 2013). The analysis of trade-offs and synergies are important before a decision is made for implementation of any land use policy or land use scenario. The analysis of trade-offs assists on determination of optimal land use system for sustainable production.

In addition to favourable land use policy, the best management practices (BMPs) are designed in order to be implemented in agricultural landscapes to mitigate the transport of sediment, nutrient, pesticides and other pollutants into stream network. The BMPs are structural (engineering) measures which include sediment basins and traps, terraces, drainage channels, check dams, and weirs among others. Non structural measures include: land use conversion, mulching, vegetative filter strips, no tillage, contour tillage, and cover crop plantation (Choi et al., 2010). The control measures through BMPs (like cover crop) implementation are motivated by increasing the land coverage that develops surface

roughness and reduces surface runoff which has positive impacts on retaining sediment and nutrients transport while increasing infiltration and ground water recharge. The BMPs in relation to reduce nutrient losses to ground water resource are reduced fertilizer application, split fertilizer application and relevant crop rotation practices (Cestti et al., 2003).

The measure and effectiveness of BMPs to reduce nonpoint source pollution depends on specific site condition. Therefore, the effectiveness of one specific BMP to a site cannot be guaranteed for another site unless the BMP is modified and reflects site-specific characteristics. A wide range of plot experiments has been conducted to assess the effectiveness of BMPs in different agricultural systems. Watershed include different land use and agricultural systems. The establishment of experiment plots to every field in the watershed is not possible and also requires increased time and money for data generation (Morgan, 2005). However, the analysis of effectiveness of BMPs which are implemented in watershed can be accessed through application of suitable watershed modeling. Watershed modeling is one of the promising approaches to study the impact of different management practices on sediment, nutrients, pesticides, and crop growth.

1.1.2 Watershed modeling and choice of model

The natural resources and different ecosystem services from the watersheds are due to complex interactions among land resources and land use and management practices that correspond to climate and topographic features of the watersheds. Watershed models are a representations of these complex system interactions and processes through different mathematical equations. The models are constrained by the inability of mathematical representation of complex watershed processes of hydrology, biological and physical functions and hydrologic response to various climatic inputs. They use sets of different parameters to reflect the watershed characteristics of real fields. Depending on the study purpose, various watershed models are used in a lumped to spatially distributed approach with a combination of empirical to process based, single event to continuous simulation and statistical to stochastic response. Parameters used in the lumped watershed models are not spatially variable while parameters used in distributed models are vary in space. In spatially distributed models, the users are able to consider the occurrence of spatial variability of soil and vegetation along with temperature and precipitation and other climatic variables. In addition, water flow related processes in watershed like interception, infiltration and change in soil moisture content are considered in spatially distributed watershed model (Brooks et al., 2013).

The use of geographical information system (GIS) data in watershed models has improved the realization of spatial variability of land use and soil in distributed watershed models. The intention of this study is to improve the water quality (reduced sediment and nutrients) via implementation of different land use and best management practice in the watershed. Hence, the primary importance for this study is the spatial representation of individual fields, associated bio-physical variability (topography and climate) and a continuous record of flow and solute transport form the watershed.

Based on this presumption, the study utilized the Soil and Water Assessment Tool (SWAT) model. The SWAT model is a comprehensive tool to represent the characteristics of individual fields and to simulate the continuous flow of discharge and solute (sediment, nutrients, pesticides, and chemical) resulted from various land use and management implemented in the watershed. The SWAT model is a product of the Agricultural Research Service (ARS) of the US Department of Agriculture. It is freely available software and source code, provides links to GIS database. The SWAT model has been continuously used in USA to simulate all type of watersheds for more than a decade. The historic development and world wide application of SWAT model has been documented in Gassman et al., (2007). There have been almost 2009 peer review journal research articles related to applications of SWAT modeling (April 2015, https://www.card.iastate.edu/swat_articles/).

1.1.3 Research rationale and objectives

The agricultural land use of South Korea is about 22 % of the total area (Ruidisch et al., 2013a) and 70 % of its land is covered by mountains (Jung, 2013). The limited land resource for agriculture in South Korea has led to mountainous agriculture mainly for production of vegetables (cabbage, potato, radish, and soybean). The intensive mechanization during tillage operation and excessive use of fertilizer and pesticides to increase crop yield are prevalent agricultural practices in mountainous landscapes throughout South Korea. Such agricultural practices in combination with high intensity rainfall due to east monsoon (Park et al., 2010) export large amount of sediments and nutrients to the rivers and streams. The major rivers and streams originate from mountainous landscapes and are the water resources to the downstream reservoirs, which are the major source of drinking water supply for the people living in urban areas. The nutrients in the water cause eutrophication problems and the reservoirs fed by polluted streams and rivers face a degraded water quality. Pollutants from urban and industrial areas (point source pollution) in South Korea are strictly regulated by governmental policies (Park et al., 2014). However, the pollutant loads due to upstream mountainous agriculture are still not controlled. The improvement of ecosystem services related to good downstream water quality largely depends on the upstream land use systems and agricultural practices of mountainous landscapes. There exist different types of BMPs adopted worldwide to ameliorate the detrimental effect of mountainous agriculture. Therefore, agricultural activities with appropriate BMPs are particularly important in decreasing environmental degradation while improving crop yields and water quality status in downstream reservoirs.

Based on this rationale, the central objective of this thesis was to recommend land use systems and best management practices that would promote the sustainable intensive farming system for higher crop yields and income coupled with production of improved water quality from the study catchment. In order to achieve our central objective, we present four studies with individual objectives, which are related to the overarching of this thesis. All four of the studies used the SWAT model to quantify ecosystem services from the study catchment.

Study 1: Initially the SWAT model was setup to evaluate hourly runoff estimation from a field size-agricultural watershed. As runoff from the watershed is the most important driving force to transport sediments and nutrients from agricultural field, the SWAT model was evaluated for reliable estimation of runoff using rainfall data recorded for various time steps. Hence, the only single objective of this study was to:

1. Evaluate the SWAT model applicability for hourly runoff estimation.

The use of hourly rainfall for the reliable prediction of hourly runoff in the SWAT model was optimal. However the hourly simulation is limited by unavailability of measured water quality data (sediments and nutrients) in hourly time step for model calibration and validation which was the case for further studies (Chapter 3-5). The computational time and requirement of high storage volume may also constrain the applicability of hourly simulation.

Study 2: In this study, the applicability of the SWAT model had been adopted to bigger catchment with a higher structural complexity. We present the technique of a data gap-filling algorithm and interpolation method for the climatology, mainly the precipitation variability during convective storm events in the topographic feature of the bowl-shaped catchment. The importance of reliable discharge and its variability within the catchment was proved by a multi-site calibration approach. The multi-site calibration and distributed parameterization approach adopted in this study had improved the process-based estimates of catchment-wise hydrologic partitioning. The impact of culverts and road networks on discharge estimate was also explored in this study. The objectives of this study were to:

1. Assess the potential of a spatiotemporal algorithm to estimate the spatial variability of precipitation from limited, temporally variable, monitored precipitation gauges (weather stations).
2. Characterize and parameterize the catchment from multiple locations for the spatiotemporal variability in the discharge pattern.
3. Test the capability of the SWAT model to capture daily monsoonal rainfall-runoff in complex mountainous terrain.
4. Quantify the impact of engineered structures (culverts and road networks) on discharge estimations by the model.

In study 2, the reliability and variability of the stream discharge has been explored by application of SWAT model for the study catchment. The real world SWAT model application for scenario analysis for different land use systems (Chapter 4) and best management practice (Chapter 5) were considered in two more studies.

Study 3: In this study, the SWAT model was setup to quantify discharge, sediment, and crop yield from baseline land use systems attributed in land use map of 2010. The farm income from cultivation

of different crops adopted for specific land use systems is not implicitly embedded into the SWAT model. Therefore, we developed an R-script for post-processing of the SWAT model runs to estimate the farm income as a function of crop yield (model output), crop price and associated production cost. The implementations of different land use systems were analyzed in order to quantify the impact on production of surface runoff, sediment and crop yield and associated farm income. We implemented monoculture land use systems for four major crops (cabbage, potato, radish, and soybean) cultivated in the study catchment. The impacts of implementations of baseline and monoculture land use systems on surface runoff, sediment, crop yield and farm income were analyzed to derive different optimal land use systems. The objectives of this study were to:

1. Quantify the impact of baseline land use systems on surface runoff, sediment, crop yield, and farm income.
2. Assess the impact of baseline and monoculture land use systems on model output and derive four optimal land use systems that were attributed to generate a) minimum surface runoff, b) minimum sediment c) maximum crop yield and d) maximum income.
3. Quantify the trade-offs associated due to implementation of derived optimal land use systems.

The quantified trade-offs due to application of optimal land use systems would be of valuable information to stakeholders and decision makers in order to decide or recommend for implementations of the particular land use systems for environmental and economical benefit.

Study 4: In this study, the SWAT model was applied to assess the effectiveness of best management practices (BMPs) to controls sediment and nitrate from the study catchment. The application of the SWAT model by using land use systems for 2010 was considered as baseline (BL) scenario and was calibrated and validated for discharge, sediment, nitrate, and crop yield. The major dominant dryland agricultural crops in the catchment are cabbage, potato, radish, and soybean, which are also major contributors to nonpoint source pollution to the downstream water bodies. We applied BMP scenarios of split fertilization (SF), cover crop plantation (CC) and combinations of both as SFCC scenarios to these major crops. The BMP scenarios were compared with BL scenario to quantify the effectiveness of implemented BMP scenario to control generation of sediment, nitrate, and its impact on crop yield. The objectives of this study were to:

1. Estimate crop yields from the dominant dryland agricultural crops including cabbage, potato, radish, and soybean under current management practices.
2. Quantify sediment and nitrate loss from the area of these specific dryland agricultural crops as well as for the entire catchment area under current management practices.

3. Estimate crop yields and quantify sediment and nitrate loss for the individual crop types and the whole catchment when applying BMPs.
4. Provide useful recommendations for farmers and policy makers, those who could redesign agriculture management in order to meet both higher crop yields and thus higher farm income as well as environmental benefits by conservation of soil and water resources.

From this study, the quantified effectiveness of BMPs helps the policy makers to choose particular BMPs for the control of nonpoint source pollution to downstream water bodies. The integration of all these four studies has provided a modeling framework for the assessment of intensive farming systems adopted in the study catchment. The recommendations proposed for particular land use systems and the BMPs may be of relevance for practical applications and could contribute to improvements and sustainable agricultural production for ecological and economical benefit.

1.2 Methodological approach

1.2.1 Conceptual framework

The main practical goal of this thesis was to contribute to retaining sediments and nutrients from the study catchment. The current land use systems and associated cultivation practices in the study catchment produce considerable amounts of sediments and nutrients to the stream network. The analysis of different land use systems and best management practices are important for the recommendation of appropriate land use and management practices to retain sediments and nutrients. We used the SWAT model as primary tool for the evaluation of different land use systems and management practices and its capability to reduce environmental effect and their impact on crop production. Initially the model was designed to characterize the site-specific characteristics of land use distribution, topography, soil type including other hydrological properties (Koch and Grünwald, 2009). The scenario application for different land use and management practices decisions which are made by stakeholders or government can be implemented into such a comprehensive watershed model. It is also possible to perform “what if?”- scenarios. However, the careful analysis of model outputs are of great importance for involved stakeholders to make up decisions. The conceptual framework that presents inter linkage of watershed model input and scenario implementation is presented in Figure 1.1.

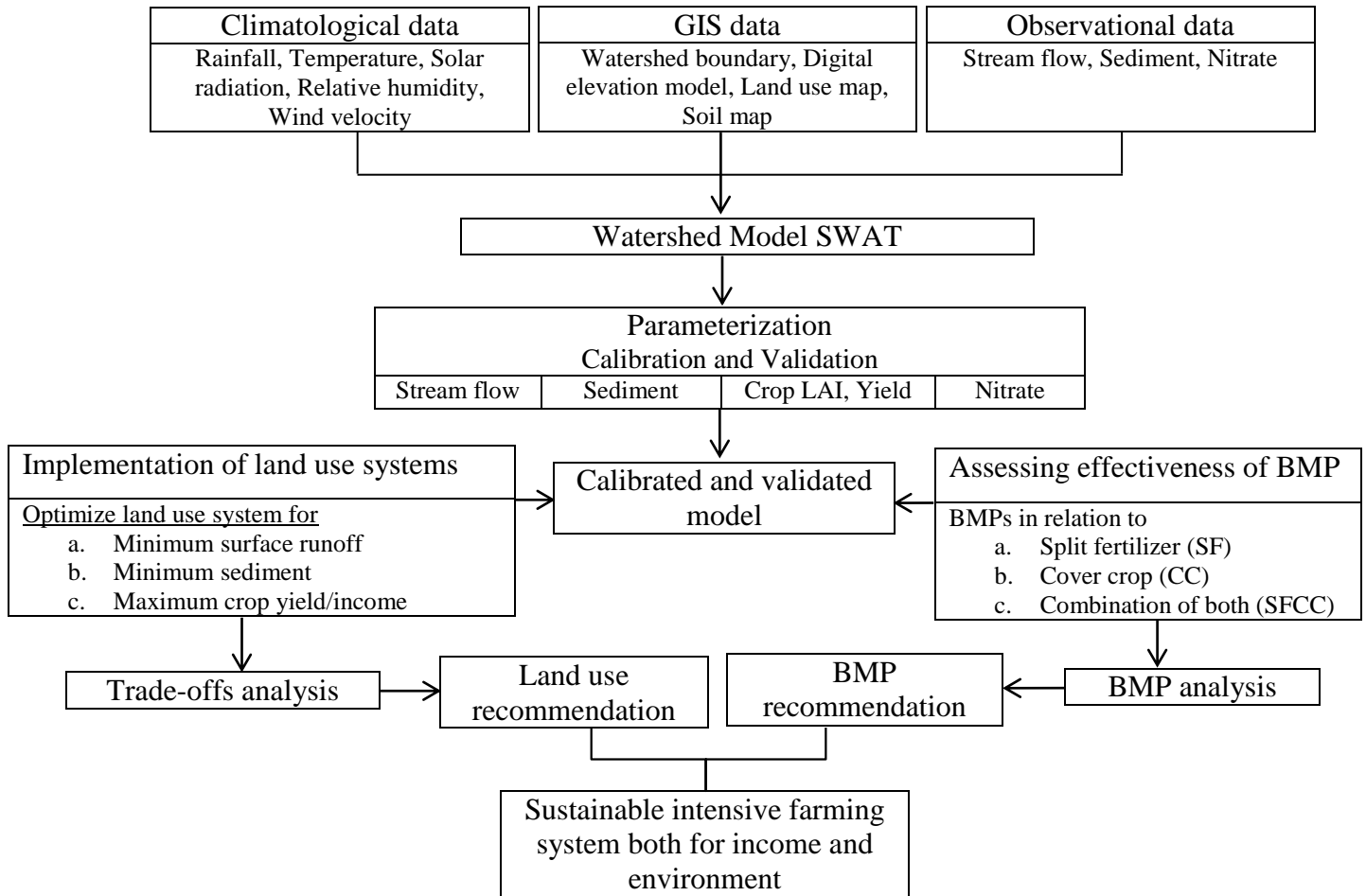


Figure 1.1 Conceptual framework for assessing sustainable intensive farming system

1.2.2 Study area

The first part of this study (Chapter 2) was conducted in Jawoon-ri catchment which is northern part of the South Korea and situated at 37° 52' N and 127° 43' E. The catchment is with about 0.8 ha, a small field-sized watershed and has an elevation ranging from 650 to 700 m. Concrete channels at the edge of the field (Figure 1.2a) transport the runoff and sediment towards the watershed outlet. The average maximum temperature in the study was about 30°C in August and average minimum was below 5°C January based on monthly temperature record in 2007 and 2008. The average annual precipitation was 1163 mm, 75 % of annual precipitation occurred during the summer (June to September).

The remaining part of this study from chapter 3-5 was conducted in Haeon catchment (128°5' to 128°11'E, 38°13' to 38°20'N) which is also located in the northern part of South Korea near the Demilitarized Zone (DMZ) between South and North Korea (Figure 1.2b). In Soyang watershed, the typical land use systems and farm management practices, especially both of the study catchments Jawoon-ri and Haeon export large amounts of nutrients due to excess fertilization and sediments during monsoon rains. The area of Haeon catchment is about 62.7 km². The elevation of the Haeon catchment ranges from 340 to 1320 m with an average slope of 28 % and a maximum slope of 84 %.

The catchment is bowl-shaped valley with high mountains surrounding the valley in lower level. The surrounding mountains are approximately 56.7 % covered with deciduous and coniferous forest, mostly in elevated parts of the catchment. The land use distribution is based on intensive field based surveys (Seo et al., 2014) for each of the years from 2009 to 2011. The study used a digitized map of 2010 in shape file format. The map attributed individual land patches under 60 different land use types, which were spatially distributed within the study catchment. The land use type were reduced into 9 different land use type categories (Figure 1.2b). The main dryland crops cultivated in Haeon catchment were annual cash crops, primarily cabbage, potato, radish and soybean (7.8 %) spatially distributed mostly on hill slopes near the forest edges. Other land use includes perennial crops such as orchards and ginseng (8.3 %), and maize, pepper, rye, and sunflowers (4.1 % of the total catchment included as other dryland crop). The valley bottom mostly at the center part of the catchment was dominated by rice paddies (8.2 %). The non agricultural area covered by field margins, residential, and fallow lands were about 14.9 % of the catchment area. The yearly maximum and minimum average temperatures were 12.5 and 2.5°C respectively, and the annual precipitation was 1658 mm, based on 13 years weather station records in the Haeon catchment (1999-2011). Almost 70 % of the annual precipitation was concentrated in the monsoon season between June and September.

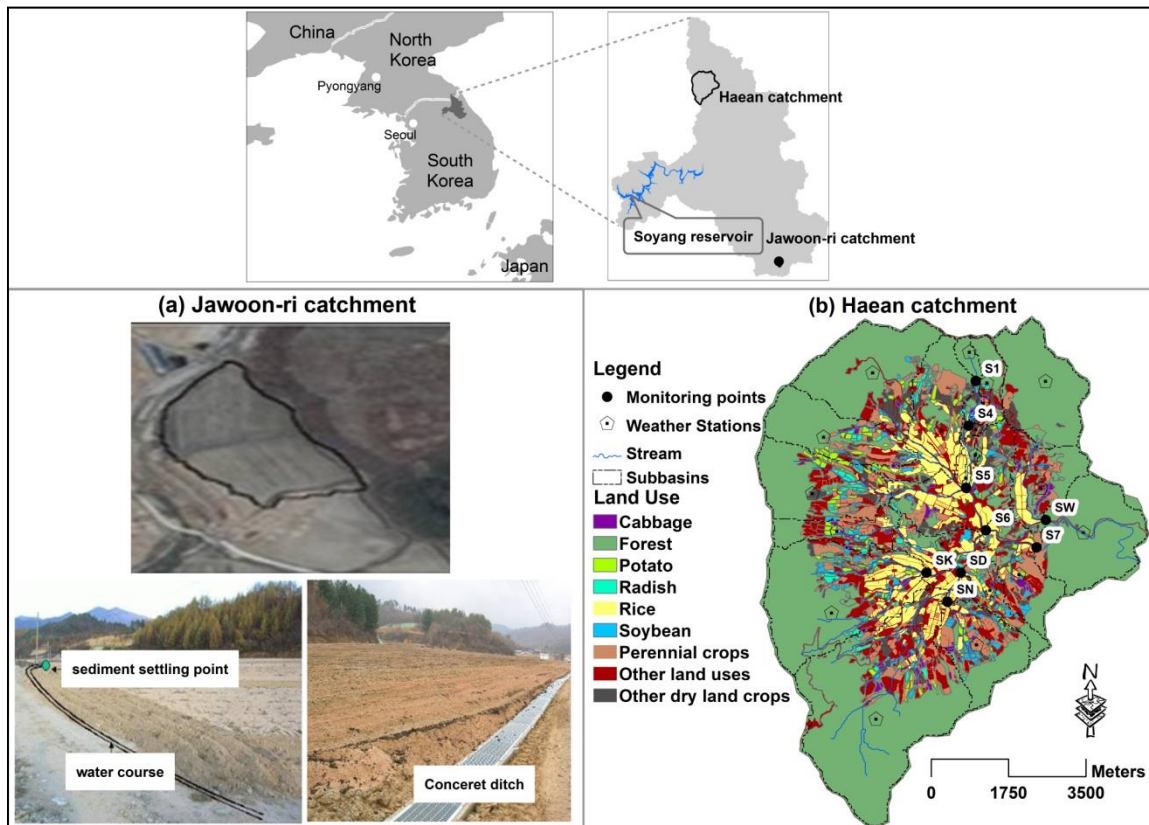


Figure 1.2 The study sites of Jawoon-ri catchment (a) and the Haeon catchment (b) are major nonpoint source pollution to Soyang reservoir.

1.2.3 Soil and Water Assessment Tool: SWAT model

The SWAT model was developed through the USDA Agricultural Research Service (ARS) with instantaneous improvements in last two decades. SWAT was used as an integral part of primary tools throughout all studies (Chapter: 2-5) in this thesis. SWAT is an effective tool to predict the impact of land management practices on discharge, sediment loss, nutrients, and agrochemicals originating from the watershed with varying soils, land use and management conditions over long time period. The application of SWAT to the study catchment hydrology starts with delineation of subbasins which are further subdivided into hydraulic response units (HRUs). Every HRU in the catchment represents the spatial distribution of land use, soil, and topographic feature. Further HRUs are lumped land areas as a unique combination of land cover, soil and management conditions within the subbasin. The interaction of weather, soil properties, topography, vegetation, and land management that exist in the watershed are modeled in SWAT to quantify output variables of discharge, sediment, nutrients, and other water quality parameters.

The hydrological components (surface runoff and discharge) in the watershed are the main component to understand the physical processes related to infiltration, evapotranspiration, and percolation for water yield, sediment and nutrients losses, and crop growth in the SWAT model. Crop growth depends on the state of soil moisture and nutrient residuals under different climatic and management condition. The hydraulic processes in the watershed are simulated for land and routing phases. The land phase of hydraulic simulation quantifies the amount of water, sediment, nutrients and pesticides from every HRU in the watershed. The simulated output variables (water, sediment, nutrients, and pesticides) are summed from all the HRUs to subbasin level. Hence, the land phase quantifies the loading to channel/stream in subbasin level. The routing phase determines the transport of loadings through the stream network of the watershed to the catchment outlet. The model outputs: discharge, sediment, nitrate, and crop yield were analyzed under different perspective of model application in the studies accumulated in this thesis.

The land phase of hydraulic cycle for the estimation of surface runoff considered in the SWAT model is based on the following water balance equation.

$$SW_t = SW_0 + \sum_{i=1}^t \left[(R_{day})_i - (Q_{surf})_i - (E_a)_i - (W_{seep})_i - (Q_{GW})_i \right] \quad (1.1)$$

where, SW_t is the final soil water content ($\text{mm H}_2\text{O day}^{-1}$), SW_0 is the initial soil water content on day i ($\text{mmH}_2\text{O day}^{-1}$), R_{day} is the amount of precipitation on day i ($\text{mmH}_2\text{O day}^{-1}$), Q_{surf} is the amount of surface runoff on day i ($\text{mmH}_2\text{O day}^{-1}$), E_a is the amount of evapotranspiration on day i ($\text{mmH}_2\text{O day}^{-1}$), W_{seep} is the amount of percolation and bypass flow exiting the bottom of the soil profile on day i ($\text{mmH}_2\text{O day}^{-1}$), and Q_{GW} is the amount of return flow on day i ($\text{mmH}_2\text{O day}^{-1}$). The principle of hydraulic cycle considered in the model is presented in Figure 1.3.

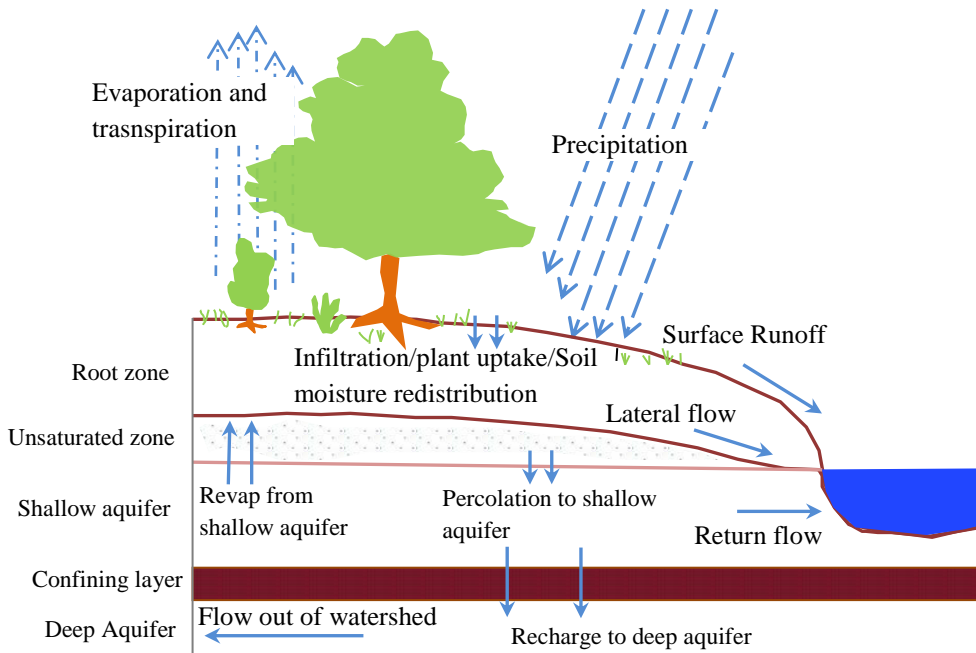


Figure 1.3 Line diagram of hydraulic cycle presented in SWAT model (White et al., 2012)

The sediment generation due to erosion in land phase depends on impact of raindrops to detach the soil particle and surface flow of water under various condition of land surface. The SWAT model estimates the sediment yield based on the Modified Universal Soil Loss Equation (MUSLE), which contains several parameters related to topography, soil properties, rainfall, as well as the crop and management practices applied throughout the catchment. Sediment loss is calculated as

$$sed = 11.8 \cdot (Q_{surf} \cdot q_{peak} \cdot area_{hru})^{0.56} \cdot K_{USLE} \cdot C_{USLE} \cdot P_{USLE} \cdot LS_{USLE} \cdot CFRG \quad (1.2)$$

where, sed is the sediment yield on a given day (metric tons), Q_{surf} is the surface runoff volume ($\text{mm H}_2\text{O ha}^{-1}$), q_{peak} is the peak runoff rate ($\text{m}^3 \text{s}^{-1}$), $area_{hru}$ is the area of the HRU (ha), K_{USLE} is the USLE soil erodibility factor ($0.013 \text{ metric ton m}^2 \text{ hr} (\text{m}^3 \text{ metric ton cm})^{-1}$), C_{USLE} is the USLE cover and management factor, P_{USLE} is the USLE support practice factor, LS_{USLE} is the USLE topographic factor, and CFRG is the coarse fragment factor.

Several soil nutrients are attached or sorbed to the eroded soil. Nitrogen is one of the essential nutrients for the plant growth. The mineral nitrogen available to plant is associated with different sources. The nitrogen nutrients in excess of plant uptake is available for leaching or export to stream via different path way of water flow and sediment transport. The nitrogen cycle along with related processes considered in the SWAT model is depicted in Figure 1.4.

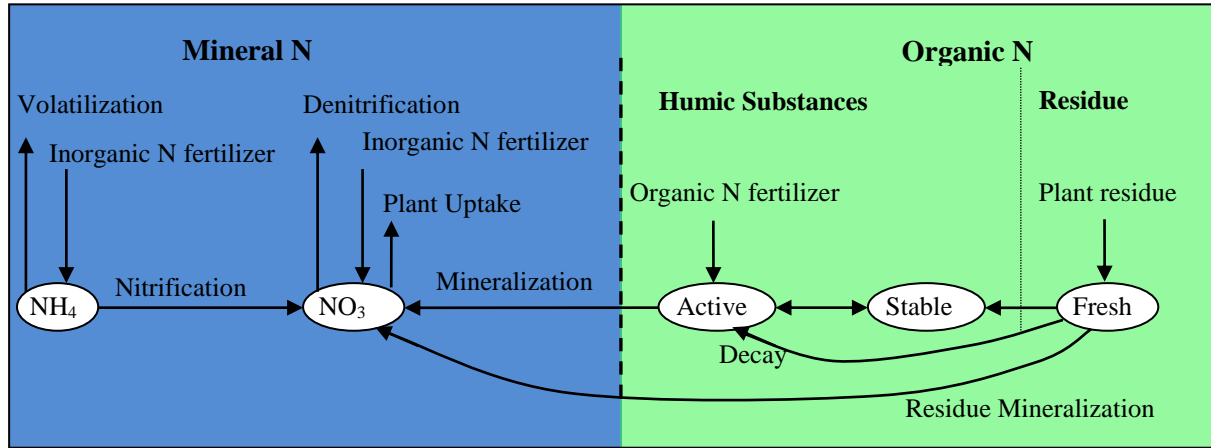


Figure 1.4 The line diagram to represent different processes of nitrogen assimilation considering different source nitrogen in nitrogen cycle (White et al., 2012)

The plant growth in the SWAT model is considered based on the accumulation of potential heat units required to reach maturity. The potential heat unit for a particular crop is calculated as the daily sum of degree temperature that exceeds the base temperature during its growing period. The actual plant growth in the model is effected by stresses due to temperature, water, nitrogen, or phosphorus. The plant biomass and yield for the plant is simulated by following relation.

$$\Delta bio = RUE \cdot H_{phosyn} \quad (1.3)$$

where, Δbio is the potential increase in total biomass on a given day (kg ha^{-1}), RUE is the radiation-use efficiency of the plant ($\text{kg ha}^{-1} \cdot (\text{MJ (m}^2\text{)}^{-1})^{-1}$ or 0.1g MJ^{-1}). H_{phosyn} is the amount of intercepted photosynthetically active radiation on a given day (MJ m^{-2}). Further details on the respective output variables of the model component are provided in the SWAT Theoretical documentation (Neitsch et al., 2011).

1.2.4 Model calibration, validation and uncertainty analysis

The model calibration and validation are the most important part of the watershed modeling for further consideration of scenario analysis. After completion of model set up, the model was calibrated and validated for various model outputs considered in the respective studies (Chapter 2-5). The model performance was evaluated by statistical measure of coefficient of determination (R^2), Nash–Sutcliffe efficiency (NSE), and percent bias (PBIAS) which are mostly use for watershed model evaluation.

The coefficient of determination (R^2) (equation 1.4, (Zambrano-Bigiarini, 2014)) is the degree of correlation between observed and simulated data and represents the proportion of the variation in observed data that explained by the model. The R^2 values range from 0 to 1 with higher R^2 values indicating that the simulated values are closely follow the trend of the measured values.

$$R^2 = \left(\frac{1}{n-1} \sum_{i=1}^n \frac{(O_i - O_{mean})(S_i - S_{mean})}{\sigma_o \sigma_s} \right)^2 \quad (1.4)$$

where, O_i is the i^{th} observation for the constituent being evaluated, O_{mean} is the mean of observed data for the constituent being evaluated, n is the total number of observation, S_i is the i^{th} simulated value for the constituent being evaluated and S_{mean} is the mean of simulated data for the constituent being evaluate, σ_o and σ_s represents the standard deviation of the observed and simulated data set respectively.

Nash–Sutcliffe efficiency (NSE) (*equation 1.5*, (Zambrano-Bigiarini, 2014)) measures the extent of predicting the observed data of the constituent and indicates the fitness plot between observed versus simulated data in 1:1 line. The NSE values range from negative $-\infty$ to 1, where 1 is the optimal value for perfect fit, values between 0 and 1 are indicated as acceptable performance of model simulation and negative values indicates that the mean observed value is a better predictor than the simulated value which is indicated as unacceptable performance.

$$NSE = 1 - \frac{\sum_{i=1}^n (O_i - S_i)^2}{\sum_{i=1}^n (O_i - O_{mean})^2} \quad (1.5)$$

where O_i is the i^{th} observation for the constituent being evaluated, S_i is the i^{th} simulated value for the constituent being evaluated, O_{mean} represent the mean of observed data for the constituent being evaluated, n is the total number of observation.

The magnitude of percent bias (*PBIAS*) represents the average tendency of simulated values to be larger or smaller than the observed values for the constituent being evaluate. The optimal value for *PBIAS* is 0 and the *PBIAS* with low magnitudes are preferred. The positive *PBIAS* values indicated overestimation bias, whereas negative values indicate model underestimation bias (R-package "hydroGOF", *equation 1.6*, (Zambrano-Bigiarini, 2014)).

$$PBIAS = \frac{\sum_{i=1}^n (S_i - O_i) \times 100}{\sum_{i=1}^n (O_i)} \quad (1.6)$$

The calibration was performed both using manual and automatic calibration. In manual calibration the model parameters values were changed iteratively and the model simulated output for the considered variable was compared with the measured data. The performance statistics for model evaluation during calibration and validation were based on the several statistical measure defined by *equation 1.4* to *1.6*. The automatic calibration for the constituents was based on SWAT-CUP algorithm (Abbaspour et al., 2004). The brief descriptions for the steps involved in automatic calibration and prediction uncertainty of the interested constituent by using Sequential Uncertainty Fitting (SUFI-2) approach in SWAT-CUP are presented as follows.

Step 1. An objective function is defined. The objective function of NSE was chosen for the constituent being evaluated.

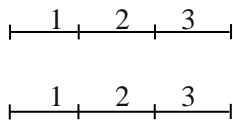
Step 2. Meaningful absolute minimum and maximum ranges $[b_{absmin}, b_{absmax}]$ for the parameters being optimized are defined based on knowledge of expertise.

Step 3. After being fixed with absolute parameter range in step 2, the parameter range within the absolute range is defined as $[b_{min}, b_{max}]$ such that $b_{min} \geq b_{absmin}$ and $b_{max} \leq b_{absmax}$. where, b_{min} and b_{max} are the minimum and maximum parameter values.

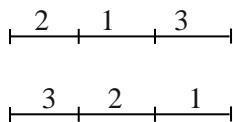
Latin hypercube sampling is carried out for all the parameters ranges defined in this step. The line diagram for the Latin hypercube sampling of two parameters in order to run model for 3 simulations is presented below. The sampled b_j is such that $b_j: [b_{j,min} \leq b_j \leq b_{j,max}]$ and $j=1 \dots m$

where b_j is the j -th parameter and m is the number of parameters to be optimized.

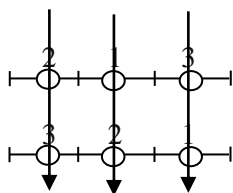
step 3.1 Two parameters ranges are divided into the 3 identical number of simulation



step 3.2 The segments of the parameter are randomized



step 3.3 The parameter value is taken at the middle of every segment



The vertical combination of the parameter values are then a parameter set used as input to the model for the consecutive simulations (line diagram modified from Abbaspour, (2015)).

Step 4. Parameters sets equal to an assigned number for n simulation are produced (as based on steps 3.1 to 3.3). The model then runs for n times for the simulation output of the considered constituent (i.e., discharge, sediment, or nitrate) and is saved together with corresponding observed data. The objective function defined in step 1 is evaluated for every simulation, and the sensitivity matrix J and the parameter covariance matrix C are calculated according to

$$J_{ij} = \frac{\Delta g_i}{\Delta b_j}, \quad i=1, \dots, c_2^n, j=1, \dots, m, \quad (1.7)$$

where, \mathbf{c}_2^n is the number of rows in the sensitivity matrix (equal to all possible combinations of two simulations), and j is the number of columns (number of parameters).

$$\mathbf{C} = S_g^2 (\mathbf{J}^T \mathbf{J})^{-1} \quad (1.8)$$

where, S_g^2 is the variance of the objective function values resulted from the model run of n times.

The estimated standard deviation and 95 % confidence interval of a parameter b_j is calculated from the diagonal elements of \mathbf{C} as follows.

$$b_{j,lower} = b_j^* - t_{v,0.025} \sqrt{C_{jj}}, \quad b_{j,upper} = b_j^* + t_{v,0.025} \sqrt{C_{jj}} \quad (1.9)$$

where standard deviation of a parameter is $\sqrt{C_{jj}}$, b_j^* is the parameter b_j for best estimates, v is the degree of freedom ($n-m$).

step 5. The model uncertainty for the prediction of the corresponding constituent is determined by assuming 95 percent prediction uncertainties (95PPU). The 95PPU is estimated at 2.5th (X_L) and 97.5th (X_U) percentiles of the cumulative distribution of simulated output for respective time step (e.g., daily simulation).

$$\bar{d}_x = \frac{1}{k} \sum_{l=1}^k (X_U - X_L)_l \quad (1.10)$$

$$R\text{—factor} = \frac{\bar{d}_x}{\sigma_x} \quad (1.11)$$

where k is the number of observed data points, \bar{d}_x is the average distance between the upper and lower 95PPU, X_U and X_L represent the upper and lower boundaries of the 95PPU, and σ_x is the standard deviation of the measured data.

Hence the goodness of fit is calculated from the percentage of measured data bracketed by the 95PPU band which is assessed by the closeness of the P—factor to 100 % (i.e., all observations falling inside the prediction uncertainty band) while having the narrowest band (R—factor \rightarrow 0). P—factor is estimated as the ratio of number of measured data points bracketed by 95PPU to the total number of measured data points used in the calibration.

$$P\text{—factor} = \frac{\text{Observed data points within 95PPU}}{\text{total nuber of observed points}} \quad (1.12)$$

step 6. If the P—factor and R—factor are check for its satisfactory level otherwise, $[b_{\min}, b_{\max}]$ i.e., parameter ranges are updated as follows for next iteration to increase P—factor while conserving R—factor. The updated parameters values for minimum and maximum are as follows.

$$b'_{j,min} = b_{j,lower} - \max\left(\frac{b_{j,lower}-b_{j,min}}{2}, \frac{b_{j,max}-b_{j,upper}}{2}\right), b'_{j,max} = b_{j,upper} - \max\left(\frac{b_{j,lower}-b_{j,min}}{2}, \frac{b_{j,max}-b_{j,upper}}{2}\right) \quad (1.13)$$

Parameter sensitivities were calculated by calculating the following multiple regression system, which regresses the Latin hypercube generated parameters against the objective function values:

$$g = \alpha + \sum_{i=1}^m \beta_i b_i \quad (1.14)$$

where, g is the objective function, α is the intercept, β_i slope of regression line due to scatter plot for parameter and objective function, b_i the value for i^{th} Latin hypercube parameter, m is the total number of parameter used for optimization.

A t-test is then used to identify the relative significance of each parameter b_i . The sensitivities given by *equation 1.14* are estimates of the average changes in the objective function resulting due to changes in each parameter, while all other parameters are changing. Therefore, *equation 1.14* gives relative sensitivities based on linear approximations and, hence, only provides partial information about the sensitivity of the objective function to model parameters (Abbaspour et al., 2004). The t-stat provides a measure of sensitivity (larger in absolute values are more sensitive) p-values determined the significance of the sensitivity. A value close to zero has more significance.

Based on this SUFI 2 procedure, once the iteration of several simulation is completed, there is a best fit parameter set for highest objective function among other simulation. When the objective function and the associated uncertainties are not satisfied, the next iteration could be performed with new suggested parameter range (setp 6). When the objective function and the model uncertainties are satisfied the best fit parameter sets values are transferred to the model as baseline calibrated model. The model validation is performed with same calibrated parameter values to compare the simulated and measured data of different time periods.

In multi-site calibration approach, the calibration was conducted for each outlet starting primarily for catchment outlet at S7 (downstream outlet) and subsequently calibrated for other outlets from top to bottom approach (i.e., S1 through S6) (Figure 1.5). All the studies (Chapter 2-5) presented in this thesis have a similar modeling approach by using the SWAT model while having different perspectives of the model application. The respective methodologies applied to individual studies are briefly presented in subsequent sections.

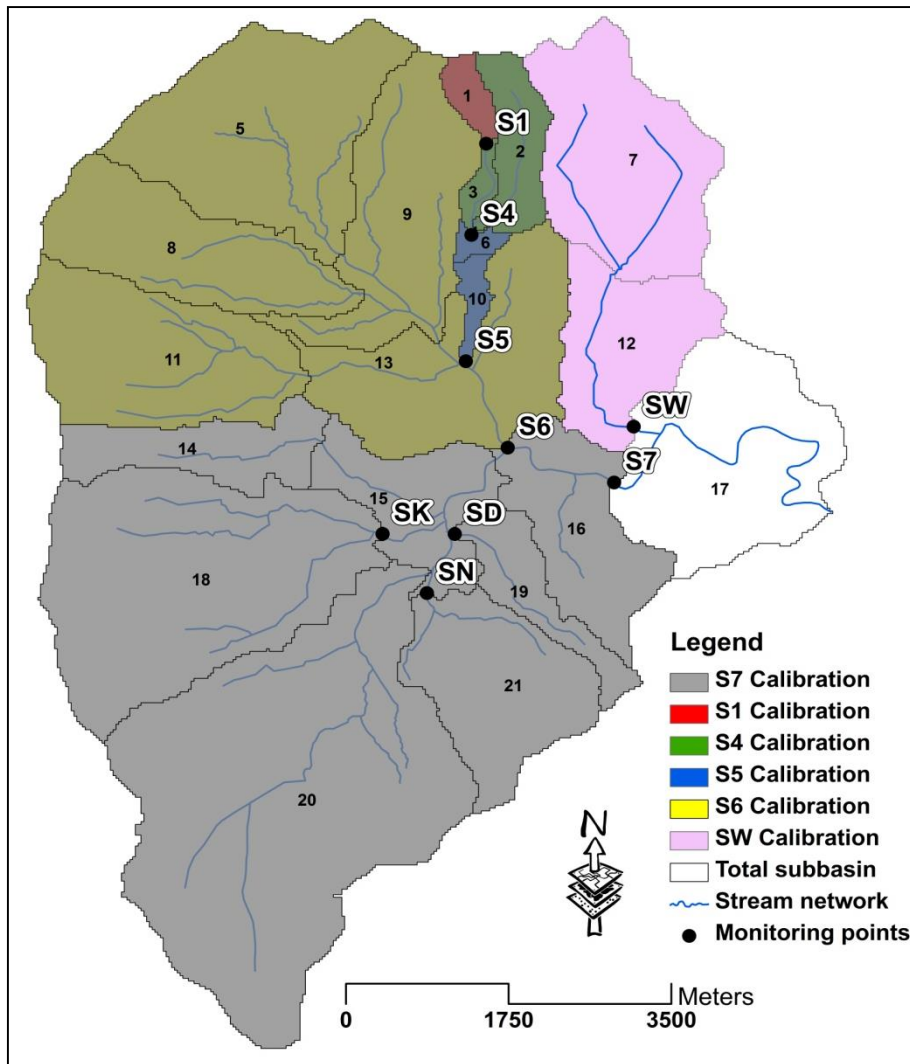


Figure 1.5 The subbasins and HRUs (not shown) within subbasin considered for parameterization during multi-site calibration conducted one at a time

1.2.5 Evaluation of SWAT model for sub-daily runoff estimation

Jawoon-ri is the field size agricultural watershed of 0.8 ha in South Korea. The watershed was selected to evaluate the SWAT model for sub-daily runoff estimation. The runoff generated in the watershed is channel down towards main outlet of the watershed with the instrumental setup to measure the amount of runoff. The study area is of agricultural field dominated by silt loam with 21.00 % clay, 52.74 % silt, and 26.26 % sand. All the meteorological data sets: temperature, humidity, precipitation, solar radiation, and wind speed were obtained from closest weather station. The digital elevation model (DEM) for the study watershed is important to delineate the watershed into sub-watersheds (subbasin) and characterize the respective topographical feature (elevation, slope, and slope length) of the subbasin. The contours of 5 m were only available for the study site which had limitation to route runoff generated at each field (subbasin) to the main outlet of the study area. The linear interpolation of 5 m DEM was used to produce finer cell size DEM. Based on the visual inspection of overland flow paths in the field, the subbasins were manually delineated to reflect the fields (subbasins) of the

watershed. The SWAT model was used in conjunction with Arc View geographic information system (GIS) as the AVSWAT model was setup for 5 subbasins corresponding to one HRU in each subbasin. The DEM used in the SWAT model delineates the subbasins in which the slope length estimated for each subbasin is based on the relationship between average slope and average field slope length. However, the used DEM in the model estimates average slope for HRUs, which was not representative to field measurement. The detailed field measurement of slope length and field slopes were used for each HRU in each subbasin. The average slope of 5.5 % and slope length of 59.5, 70.0, 79.7, 64.4, and 50.8 m were used for the respective HRUs.

The AVSWAT model is not embedded with the necessary adjustment in the model setup for hourly runoff estimation. The hourly runoff simulation by the Green and Ampt infiltration approach in AVSWAT model is an optional tool which can be activated by modifications in SWAT input files. The files in the SWAT model that needed modification are *file.cio*, **.bsn*, *fig.fig*, and *pcp.pcp*. The detail sub-daily configuration for hourly simulation are presented in chapter 2 in section 2.2.6.

After the model setup based on input data and the modification in SWAT input files for hourly runoff estimation, the model was calibrated and validated and the model performance was evaluated. In addition the sensitivity of the parameters for this study was performed by using sensitivity analysis tool incorporated within the SWAT model as explain in sensitive guidelines by Van Liew and Veith (Unpublished). The most sensitive parameters for hydrological component such as CN2 (curve number), LAT_TIME (lateral flow travel time), ESCO (soil evaporation compensation factor) GWQMN (a threshold minimum depth of water in the shallow aquifer required for return flow to occur) , GW_DELAY (ground water delay time), ALPHA_BF (base flow alpha factor) and REVAPMIN (minimum depth of water in shallow aquifer for re-evaporation to occur) were selected during calibration and validation for hourly runoff simulation. We did manual calibration to parameterize the selected hydrological parameters. The 10 rainfall events of 2007 and 8 rainfall events of 2008, altogether 18 rainfall event of which 9 rainfall events and corresponding runoff were used for calibration and the remaining 9 rainfall events for validation. The hourly simulated runoff that was aggregated to corresponding rainfall event and measured daily runoff at the watershed outlet were compared during calibration and validation for the corresponding rain event. The statistic performance of R^2 and NSE were applied to evaluate the model performance in estimation of hourly runoff. The model performance of hourly simulation and daily simulation were compared to observe the impacts of sub-daily precipitation on runoff estimation by using Green and Amp method.

1.2.6 Hydraulic process description and partitioning in Haean Catchment, South Korea

In this study, the SWAT model was implemented for Haean Catchment, South Korea to define hydraulic process and hydrologic partitioning in the catchment. Several HRUs were developed within the subbasin of the Haran catchment. The HRUs within the respective subbasin represent spatial heterogeneity of land use distribution, soil type, and topographical variability in the catchment. The

topographical variability of the catchment was incorporated into the SWAT model by using 30 m resolution DEM of Soyang watershed that was clipped to the extent of the catchment boundaries. The natural stream network, engineering structure related to drainage and culvert and the road network in the Haean catchment have significant effects on flow routing and discharge accumulation. Three different model setups were considered with 1) stream network, 2) stream network, drainage and culverts, and 3) stream network, drainage and culvert and road network to observe their respective impact on flow partitioning in the catchment. The respective drainage and culverts and road network were considered in the SWAT model as impervious with no transmission losses which were imbedded into the stream network of the catchment. The clear delineation of each network in the catchment uses the burn-in option for accurate perdition of the respective stream network during the SWAT model setup.

The distribution of the land use and land cover map was based on 2009 and used in the model for their spatial representation for the study. The intensive soil profiles survey (Arnhold, 2013) up to 1.2 m depth were coupled with regional soil database (Rural Development Administration, 1:25000) and agricultural land use in order to determine spatial distribution of various soil types within the catchment. Different soil types that are distributed in the Haean catchment and corresponding soil texture, hydraulic conductivity, and soil hydraulic group were incorporated in soil database of the SWAT model.

The main climatological data required for model simulation are: relative humidity, temperature, solar radiation, wind speed, and precipitation. The data were collected from several regional stations of the Korean Meteorological Agency (KMA) and 15 micro-meteorological stations distributed throughout the catchment. After refinement of raw data, gap-filling of missing data was accomplished by using an algorithm defined as a function of elevation, station proximity, and aspect. The meteorological variability in the catchment considered in the SWAT model is based on assigning the nearby weather station from the centroid of delineated subbasin to the respective subbasin (Neitsch et al., 2011). We developed the virtual weather stations to all delineated subbasins by inverse distance weighted (IDW) interpolation method from the real 15 micro-meterological stations. The virtual weather station to each subbasin is expected to capture the climatological (precipitation) variability due to elevation variation in the catchment.

The agricultural management practices such as: tillage operation, crop plantation, fertilizer application, irrigation, and harvest operation were specific to various crops which were identified based on interviews with 300 stakeholders and farmers (Nguyen et al., 2012; Tenhunen et al., 2011). The database in relation to the management schedule, different type of equipment used for tillage and the amount of fertilizer used for specific crops was prepared to simulate the crop growth in the model. The various agricultural management practices were assigned to every single HRU developed in the catchment. The simulation of management practices in the SWAT model is based on presenting

management schedule either by month and day or as fraction of base zero potential heat units. For the study we adopt the fraction of potential heat unit for the considered management operation (i.e., tillage, fertilizer, planting, irrigation, harvesting). Several plot scale experiment was conducted for assessing the LAI and biomass (Lindner et al., 2015) development for different crops in the Haean catchment which were used in the crop database of the SWAT model. In particular to simulate the rice crop as depressions/potholes, it is important to create a single rice paddy HRU in the subbasins which contains a rice crop. During the formation of HRUs, a 51 % soil type threshold was prescribed to form a single rice paddy HRU in each sub basin containing rice crop.

There were altogether 14 discharge measurement locations throughout the catchment and discharge locations (S1, S4, S5 and S6) (Bartsch, 2013) routed to the catchment outlet (S7) (downstream outlet) (By the Department of Environmental Science laboratory, Kangwon National University, Chuncheon, South Korea) were used for calibration and validation of the SWAT model. The multi-site calibration for the discharge was intended to parameterize the hydraulic characteristics of the catchment and better represent the spatial variability in hydrologic partitioning. The model calibration was performed by both manual and automated calibration. Basically the manual calibration helps to understand the system processes defined by various parameters (system behavior i.e., discharge varied by change in CN) and the knowledge from the manual calibration assists to define the sensitive parameters range for automatic calibration which finally determined the model uncertainty. The SWAT model was daily simulated from 2006 to 2011 with 3 years of warm up period to exclude the effect of initial parameters values. The discharge calibration was performed for 2010 and the validation period for 2009. The automatic calibration was performed by using the Sequential Uncertainty Fitting Algorithm (SUFI-2) in SWAT-Cup (section 1.2.4) to optimize the model performance statistics (section 1.2.4).

1.2.7 Identifying optimal land use systems and trade-offs between farm income and environment

In this study, a detailed land use map of the Haean catchment for 2010 was used to setup the SWAT model (Figure 4.1). The model was calibrated and validated based on the methodological approach as adopted in previous section 1.2.6. The model was calibrated and validated for discharge and sediment for multi-site locations along the elevation transect (S1 to S7, Figure 4.1) in the catchment. The calibrated and validated model was considered as the baseline study. The economic activity of the Haean catchment is based on dryland agriculture. The dryland agriculture mainly cabbage, potato, radish and soybean are considered as major vegetables crops both in Haean catchment and South Korea. Due to this reason, the major crops are more likely to be allocated at the expense of other minor crops. Based on this presumption, we developed the explicit monoculture land use system for cabbage, potato, radish, and soybean. The monoculture land use system for each major crop was implemented in the calibrated model. The crop yield from the SWAT model links to an econometric equation as a function of crop yield, crop price, and production cost (chapter 4, *equation 4.4*) which was encoded as an R-script for post-processing of the SWAT model to estimate the farm income associated with

certain land use systems. The crop price and production cost were based on the interview data from farmers and stakeholders conducted through 2009-2010 (Nguyen et al., 2012). The SWAT model output related to surface runoff, sediment, crop yield and the farm income from all monoculture land use systems including the baseline land use system were analyzed. The reallocation of different land uses were performed in order to determine the optimal land use systems which are explicitly attributed for generation of minimum surface runoff, minimum sediment, maximum crop yield and maximum farm income.

The optimal land use systems which were derived were implemented in the SWAT model to determine the status of non-optimal attributes. The analysis of optimal land use systems helps to quantify the associated trade-offs between different output variables. For example, the optimal land use system that was derived for maximum income could have trade-offs with producing high level of sediment and surface runoff. The land use system defined as deciduous forest (FRSD), coniferous forest (FRSE), residential area (URBN), rice (RICE), inland water (WATR), and orchard (ORCD) were not changed during analysis of entire monoculture and optimal land use system.

1.2.8 Assessing the effectiveness BMP of split fertilizer and cover crop cultivation

The SWAT model in this study was prescribed the Haeon catchment land use for 2010 (Figure 5.1). In addition to discharge and sediment, nitrate was also calibrated and validated as similar methodological approach as implemented in section 1.2.6. The crop yield from the model was compared with field measurement data by manual calibration of crop growth parameters. The application of best management practices have been implemented worldwide to control sediments and nutrients generation and its transport to downstream water bodies. Based on previous field level studies Ruidisch et al. (2013b) and Arnhold et al. (2014) have recommended the implementation of split fertilizer to reduce nitrate leaching and cover crop to reduce sediment export to the stream network of the study catchment. We considered the calibrated and validated model as a baseline (BL) scenario to compare the model output due to implementation of BMPs. The total BMPs considered for comparison with BL scenario and assessing their effectiveness to control soil and water resource while improving crop yield were split fertilizer application as SF scenario, cover crop cultivation as CC scenario and combination of split fertilizer and cover crop cultivation as SFCC scenario.

The effectiveness of BPM comparing to baseline scenario was estimated as follows

$$\text{Effectiveness of BMPs} = \left(\frac{\text{BL}_{\text{output variable}} - \text{BMP}_{\text{output variable}}}{\text{BL}_{\text{output variable}}} \right) \cdot 100\%$$

where, BL is baseline scenario, BMP is best management scenarios: SF, CC and SFCC, output variable is one of the SWAT output variables: sediment loss, nitrate loss, and crop yield. The model output considered for effective estimation were sediment, nitrate and crop yields from HRU level to overall catchment level.

The BL scenario was prescribed with conventional management practices using single fertilizer application before planting of the crop. In the split fertilizer application (SF scenario) the single fertilizer application was split into several applications. We select rye grass as cover crop which was implemented as CC scenario. The rye grass has a low base temperature which can be grown well in cold season with high ground cover. The detail management schedule for all BMPs including baseline scenario is shown in the supplementary Table ST 5.3 (Chapter 5)

1.3 Results and discussion

1.3.1 Evaluation of SWAT to estimate hourly runoff

With the necessary modifications in SWAT input files (Chapter 2, section 2.2.6) we explored the possibility for hourly runoff estimation. Hourly runoff estimations are important hydrological data for water resource management, especially for flood and erosion control. Hence the precise estimation of runoff with higher time resolution (hourly runoff) from the watershed has practical consequence for precise estimates of water quality parameters (sediments and nutrients) and in the end for the simulation of agricultural management practices and its effectiveness.

The SWAT model has been widely use to estimate water balances and associated sediment and contaminants due to various management practices in different time steps (daily, monthly and yearly) (Cotter, 2002; Kannan et al., 2007; Tripathi et al., 2003). However the model has ability to simulate sub-daily simulation for runoff estimation by using Green-Ampt infiltration method which has not been widely studied for runoff prediction (King et al., 1999; Rawls et al., 1993). The studied by Di Luzio and Arnold (2004) and Debele et al (2009) have implemented the investigation of sub-daily simulation for stream flow prediction by using gridded precipitation (NEXRAD) data and disaggregated daily precipitation data into hourly data. The reliable prediction of runoff from the watershed needs the model calibration. During the calibration process for hourly runoff estimates, the hydrological parameters of the SWAT model was manually modified to 90 for CN2 (curve number), 0.5 day for LAT_TIME (lateral flow travel time), 0.98 for ESCO (soil evaporation compensation factor), 50 mm for GWQMN (a threshold minimum depth of water in the shallow aquifer required for return flow to occur), 10 day for GW_DELAY (ground water delay time), 1.048 for ALPHA_BF (baseflow alpha factor) and 1 mm for REVAPMN (minimum depth of water in shallow aquifer for re-evaporation to occur). The highest parameter sensitive for the hourly runoff estimation was CN2 followed consequently by ESCO, GW_DELAY, ALPHA_BF and remaining three parameters (GWQMN, REVAPMN and LAT_TIME) were least sensitive and all ranked by 5th position. The detailed sensitivity statistics for the parameters are presented in Table 2.4 (Chapter 2). The CN2 as the highest sensitivity for the runoff estimates in this watershed, which might be due to the field management practice of plastic mulch and tractor compaction than other ground water parameters (GWQMN, REVAPMN and LAT_TIME). The manually calibrated values were allowed to change by $\pm 10\%$ to observe their impact on flow estimation deviated from calibrated simulation. It was observed

to have increased by 70.5 % in the discharge amount when the calibrated parameters were increased by 10 % and decreased by 23.2 % when the calibrated parameters decreased by 10 %. Hence the parameter values were observed more sensitive towards increasing parameter values than lowering the values from calibrated parameters.

The continuous hourly measured flow data were not available to compare hourly simulated data for the study watershed. It is worthwhile to mention that the hourly simulated flow data were aggregated to daily flow data and compared with the daily measured flow data for the 18 rainfall events in 2007-2008 during calibration (9 rainfall events) and validation (9 rainfall events). The coefficient of determinant (R^2) and the Nash–Sutcliffe efficiency (NSE) based on the comparison of simulated and measured flow data were both equal to 0.88. The R^2 and NSE during validation are observed to be 0.91 and 0.84 respectively. To evaluate the effect of measured rainfall at different time interval on runoff simulation, we used rainfall data recorded for 1 hourly, 2 hourly, 6 hourly and 12 hourly to simulate respective runoff and compared with measured data. We observed that R^2 and NSE values from runoff comparisons decrease with increasing time interval. This indicated that the use of rainfall measured in smaller intervals performs better to estimate the runoff with SWAT sub-daily configuration. We further used 15 minute interval for rainfall data and found that the use of hourly data to estimate runoff was optimal regarding R^2 and NSE (0.874 and 0.898). Further, the evaluation of sub-daily simulation of SWAT was compared with daily simulation for 2007-2008. The R^2 and NSE value were 0.79 and -0.01 respectively for SWAT daily simulation. It turned out that daily runoff estimations by using SCS CN method was overestimated. The SWAT daily runoff estimation was based on the rainfall data which were aggregated into daily data with higher amount of accumulated rainfall that impact on overestimation of runoff than measured flow. We observed, the use of hourly rainfall data was optimal to estimate runoff from the watershed. The model applicability for the hourly simulation is always limited by measured flow and water quality data in hourly time steps. Due to this reason, the applications of the SWAT model for consequent studies accumulated in this thesis were considered for daily simulation.

Box1 result summary: Hourly runoff estimation using SWAT

(Manuscript 1)

- The SWAT model performance to predict hourly runoff using hourly rainfall data in combination with Green and Ampt infiltration was better than daily simulation using daily rainfall with SCS CN method.
- The performance statistic measures indicated by coefficient of determinant (R^2) and Nash–Sutcliffe efficiency (NSE) for hourly simulation were respectively 0.874 and 0.898 whereas for daily simulation were 0.79 and -0.01 respectively.
- Daily runoff simulations overestimate due to aggregated effect of hourly rainfall.
- The model performance for hourly runoff estimation was observed optimal which was confirmed by comparing the result with 15 min, 2 hourly, 6 hourly and 12 hourly runoff.

1.3.2 SWAT application to improve process description and hydrologic partitioning in South Korea

In the second study, the SWAT model has been setup for Haeon catchment to capture the interlinked processes associated to produce discharge and sediment export and attached nutrients. Land use systems and management practices pertaining to climatic and topographical variability in the catchment are highly linked to hydrological process. Hydrological processes being key processes for export of various pollutants due to implementation of different land use systems in the catchment. Quantification of hydrological processes are of paramount importance for the associated processes of sediments and nutrients transport to the catchment stream network. The SWAT model is one of the watershed models that can couple hydrology and crop production to simulate the interconnection between catchment physical characteristics, agricultural practices, and weather effect on discharge.

The study has successfully adopted the SWAT model into Haeon catchment to represent variability in topography and climate. The discharge variability within the catchment was successfully simulated by defining the spatial variability of the process based parameters. Out of numerous model input parameters, the precipitation is one of the main factor to generate the stream discharge. The catchment is characterized by high variability in topography which effects on local variability on precipitation, soil moisture and plant growth. The algorithm related to data gap-filling and different interpolation methods (inverse distance weighted (IDW), spline, nearest neighbor, and kriging) from measured stations were used to capture the precipitation and climatic difference induced by altitudinal variability of the catchment. The variability of river discharge due to different interpolation at the downstream outlet S7 (Figure 3.1) was less than 0.1 % and with negligible variation in other upstream outlets (S1, S4, S5, and S6) (Figure 3.1). However the IDW interpolation technique for the precipitation had resulted for improved simulation of crop growth response for the selected crops and locations than other methods. Due to this reason the IDW interpolation method for precipitation was adopted to produce the climate and precipitation variability in the catchment.

The SWAT model for Haeon catchment was topographically discretized into 142 subbasins and 2532 HRUs within the catchment. As stated earlier, the simulations were carried out from 2006 through 2011 excluding the results analysis from 2006-2008 as model warmup period. Generally the warmup period in the modeling studies are common to reduce the impact of the initial values considered in the model. The model was calibrated for 2010 and validated for 2009. Measured discharge (Bartsch, 2013) from several monitoring locations along the elevation transect from upstream to downstream of the catchment were used to calibrate the model. Only discharge related parameters were used to calibrate the model. Primarily we adopt the manual calibration to each monitoring location and determined 8-11 out of 15 discharge-related parameters were sensitive to catchment-wide flow partitioning Figure 3.4 (Chapter 3). Further automated calibration was completed by using SWAT-CUP. We observed that the semi-distributed (vary parameter value by crop types and subbasins) and fully distributed (vary parameter value by HRU) have a similar improved model predictability (discharge) compared to the model using lumped parameterization (vary parameter by crop type for entire catchment). In order to improve the model predictability and reduce computational time, the semi-distributed approach was considered as optimal in this study. During auto-calibration by SWAT-CUP, at least 300 simulations were assigned to calibrate each monitoring location. The sensitivity of the parameters for each monitoring location were quantified by "t-stat" as sensitive parameter and "p-value" as the significance of the corresponding sensitive parameters. The higher absolute t-stat which corresponds to higher sensitive parameter and the higher significance measured by the p-value that approaches to zero (Abbaspour et al., 2004). We observed the parameters in relation to the surface runoff and routing were more sensitive at higher elevation (S1) and the groundwater and infiltration parameters were highly sensitive in lower elevation (S6 and S7) (Figure 3.1). The mid-elevations monitoring points (S4 and S5) have higher sensitivity to surface runoff and routing parameters. The catchment with higher elevation has shallow soil depth with highly permeable soil over bedrock (Arnhold et al., 2013) which can have high infiltration rates to contribute to increased baseflow and streamflow. The soils in mid to low elevation locations were highly disturbed by agricultural management practices that lead to runoff and less infiltration. The parameters sensitivity of the model for different locations from upstream to downstream are presented in Figure 3.4 (Chapter 3).

The model performance during calibration and validation at each location were presented by coefficient of determination (R^2), Nash–Sutcliffe efficiency (NSE), and percentage bias (PBIAS). However, the model performance statistic could be improved without realistic representation of plant growth simulation. To avoid this possibility, this study also crosschecks plant growth simulation with measured plant growth indicator like Leaf area index (LAI) (Figure 3.7, Chapter 3). Several discharge related parameters were adjusted to optimize the model performance statistics. The SWAT parameters that control the baseflow processes in the Haeon catchment were observed to be GW_REVAP (groundwater "revap" coefficient) i.e., the rate movement of water from the shallow aquifer to the root zone, GWQMN (a threshold minimum depth of water in the shallow aquifer required for return flow

to occur), GW_DELAY (ground water delay time), ALPHA_BF (baseflow alpha factor), and ESCO (soil evaporation compensation factor). The surface runoff in the catchment is mainly controlled by CN2 (curve number) and SOL_AWC (available water capacity of the soil layer) parameters of the model. The semi-distributed parameterization approach in the model has to the benefit of assigning different parameters values to respective crop types throughout subbasins in the catchment. This has improved the model predictability of the constituent variable and quantifies contribution from subbasins to the catchment outlet. The multi-site calibration of SWAT model adopted in this study had improved the flow process for reliable prediction of the discharge variability through the catchment. The reliable prediction of the constituent variable of the model has important implication of scenario analysis for comprehensive recommendation to solve different environmental problems (Chapter 4-5).

The overall NSE values measured for model performance through S1 and S7 ranged between 0.64 and 0.95 with an average score of 0.76 for the 2010 calibration period and between 0.40 and 0.98 for the validation period (Figure 3.5, Chapter 3). According to Moriasi et al. (2007), the NSE value > 0.5 is considered as acceptable performance of the model prediction for the constituent being evaluated. We observed the NSE values for all the monitoring points i.e., 14 locations within the Haean catchment during discharge calibration were evaluated over 0.5 and the values for 12 monitoring points of 14 were in the acceptable value of NSE during validation period. The average value of R^2 during calibration period was 0.81 that ranges from 0.70 to 0.96 depending on monitoring location and the R^2 values for validation period were between 0.71 and 0.97 (Figure 3.5, Chapter 3). The PBIAS measure in this study was adopted from Gupta et al. (1999) based on which the optimal value is 0 and positive value indicates underestimation and negative as overestimate indicating a converse convention in signs from the PBIAS explained in section 1.2.4 (R-package "hydroGOF"). We observed the PBIAS in high and mid-elevation monitoring locations (S1 to S5) (Figure 3.1, Chapter 3) to range from 1.3 to 9.6 % during calibration and -9.1 to 18 % during validation. The difference of simulated and observed discharge at lower elevation locations (S6 to S7) are respectively 41 and 29 % during calibration (Figure 3.5 in chapter 3). This difference could be explained due to rapid and large flow contribution from high elevation area and routed down to lower elevation through impermeable engineered structures like drainage and culverts and the road network. The drainage and culverts and road network of the catchment were realized into the existing stream network (Figure 3.2B and C, Chapter 3). The impact on discharge simulation due to such anthropogenic structure was further analyzed mainly at lower elevation monitoring locations. We observed the inclusion of drainage and culverts to stream network (Figure 3.2B, Chapter3) has reduced the difference between the simulated and observed discharge at S6 and S7 as explained by the PBIAS decreases from 41 to 8 % and 29 to 9 % respectively. However the inclusion of road network to drainage and culverts and stream network as in Figure 3.2C in chapter 3 has not improved the difference between observed and simulated discharge for respective locations (S6 and S7). The prevalent conditions of existing drainage and culverts and

impervious road next to the fields have significant effect on exporting applied fertilizer rapidly to the river network which causes water quality problem.

The model uncertainty during calibration and validation were explained by P—factor and R—factor as described in section 1.2.4. The P—factor for all monitoring location during calibration varies from 0.54 to 0.69 with an average value of 0.64 and the R—factor range from 0.10 to 0.38 with average value of 0.21. The average P—factor during validation is 0.74 in the range from 0.64 to 0.79 for corresponding location and average value for R—factor is about 0.14 that range from 0.10 to 0.21 (Figure 3.5, Chapter 3). Hence the majority of simulation results have included the observed discharge within the 95 % confidence interval (P-value) of cumulative distribution of simulated output (discharge) during calibration and validation of the SWAT model within the minimum uncertainty band as defined by the R—factor. In addition the crop growth dynamics in the model were also simulated and compared with measured LAI while improving model performance by calibration and validation. As the proper simulation of crop growth has a significant impact on overall hydrological balance in the catchment as the plant growth is directly linked to evapotranspiration. We observed the R^2 due to comparison of measured and simulated LAI ranges from 0.51 to 0.76 for selected crop types in the study catchment (Figure 3.7, Chapter 3). The crop growth simulation in the model has contributed to a realistic prediction of discharge throughout the catchment.

Box2 result summary: Hydrologic process modeling and discharge partitioning (Manuscript 2)

- The SWAT model was successfully applied to the complex terrain catchment to predict reliable discharge.
- The multi-site calibration approach used in this study has parameterized the discharge related parameter to capture the discharge variability within the catchment.
- The surface runoff parameters (CN: curve number, SOI_AWC: Soil available water) and routing (CH_K2: effective hydraulic conductivity of channel, CH_N2: Manning's value for the main channel) more sensitive in higher elevation and the ground water (GWQMN: Threshold water level in shallow aquifer for baseflow) and infiltration parameter (SOL_K: Saturated hydraulic conductivity of first soil layer) in the lower elevation.
- The both performance statistics (R^2 and NSE) of the SWAT model for discharge prediction at different monitoring locations within the catchment were higher than 0.5 for both calibration and validation period.
- The engineering structures related to drainage and culverts and road network were model as additional stream network to observe the discharge prediction variability.
- The inclusion of drainage and culverts reduced the difference between simulated and observed discharge at downstream outlet.

1.3.3 Determination of optimal land use systems and quantification of associated trade-offs between farm income and environment

The SWAT model was setup up in order to assess the impact of different land use systems adopted in the Haean catchment in South Korea. The model has been delineated for 21 subbasins and 792 HRUs. The land use in the Haean catchment during model setup was typically based on 2010 (Seo et al., 2014). The cultivation of these major dryland crops and their respective proportion are changing depending on the farmer's willingness to cope with changing market price and subsidy policy. Due to the complexity of determining the inter-connection between market equilibrium and subsidy policy to predict potential land use system had not been considered in this study. The development of monoculture systems in the model are flexible to convert to respective monoculture crop in expense of any other dryland corps. The HRUs in relation to land use/crop type of forest (FRSD), coniferous forest (FRSE), residential area (URBN), water bodies (WATR), and rice (RICE) were not modified to develop the extreme monoculture systems. The numbers of HRUs of 505 out of total 792 HRUs were linked to major dry land crops and other minor crops which were modified to respective crop for the development of monoculture system. However the extreme monoculture scenario does not generally exist in real field situations and was mostly intended to provide the most extreme effect on surface runoff, sediment, crop yield and farm income.

Based on this regulation we had developed a monoculture land use system for cabbage, potato, radish, and soybean. The calibrated and validated model for discharge and sediment was implemented for extreme scenarios of individual monoculture systems of the major dryland crops. The model was simulated for the period of 2007-2011 and a warmup period of 2 year was not considered for the analysis of model outputs. The average annual SWAT model output of surface runoff, sediment, and crop yield were analyzed for the implemented monoculture land use systems. The average annual farm income was indirectly computed as function of crop yield and respective crop price and production cost. We observed the highest average annual surface runoff and sediment of 565.49 mm and 19 tons ha^{-1} respectively. The lowest surface runoff was due to implementation of radish monoculture system (546.40 mm). The lowest sediment yield was about 10.19 tons ha^{-1} from the baseline land use system consisting of multiple crops throughout the catchment. The highest farm income (67.40 Million won ha^{-1}) was estimated due to the implementation of a soybean monoculture system. The crop price during the analyzed period (2009-2011) was average to highest (Table 4.5, Chapter 4) for soybean that results for highest income generation despite the lowest crop yield (1.6 tons ha^{-1}). In contrast the maximum farm income due to the soybean monoculture system was associated with the production of relatively high sediment yield (14.94 tons ha^{-1}). The highest crop yield (4.8 tons ha^{-1}) was observed due to a potato monoculture system which also produced the minimum income (43.00 million won ha^{-1}) and highest sediment (15.00 tons ha^{-1}). The detailed spatial distributions for each monoculture land use are presented in Figure 1.6. The possibilities of extreme effects on different model outputs was also explored due to extreme monoculture system.

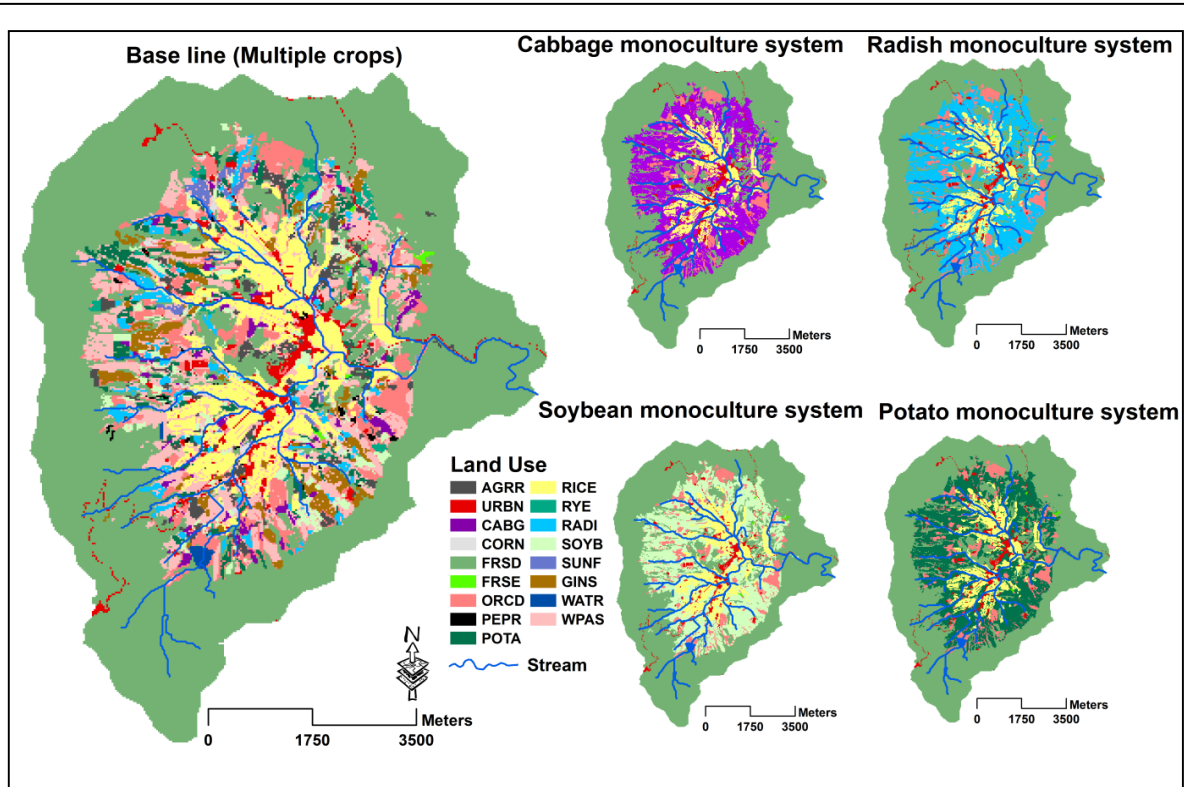


Figure 1.6 Land use discretization for the base line scenario and each of the four monoculture system scenarios. For the monoculture systems, HRUs representing agricultural crops were adjusted to the individual monoculture crop type throughout the entire catchment

Based on this extreme database of monoculture systems and baseline land use system, their respective model output were individually analyzed. Every single HRUs of agricultural crops were analyzed to derive an optimal land use system with the objective of producing minimum surface runoff, minimum sediment, maximum crop yield and maximum income. For example, to derive an optimal land use system that has the capacity to produce the minimum sediment, the solution was based on analyzing sediment generated from individual HRUs of monoculture land use systems and the baseline land use system. We re-allocate the corresponding land use that produced the minimum sediment among the datasets (monoculture land use system and baseline land use system). At the end, the set of 505 HRUs which produce the minimum sediment and their corresponding land use were allocated to derive the optimal land use that attributes to produce the minimum sediment. Likewise we derived other three other optimal land use systems that have capacity to produce minimum surface runoff, maximum crop yield and maximum income. The spatial land use distributions for all optimal land use systems are presented in Figure 1.7.

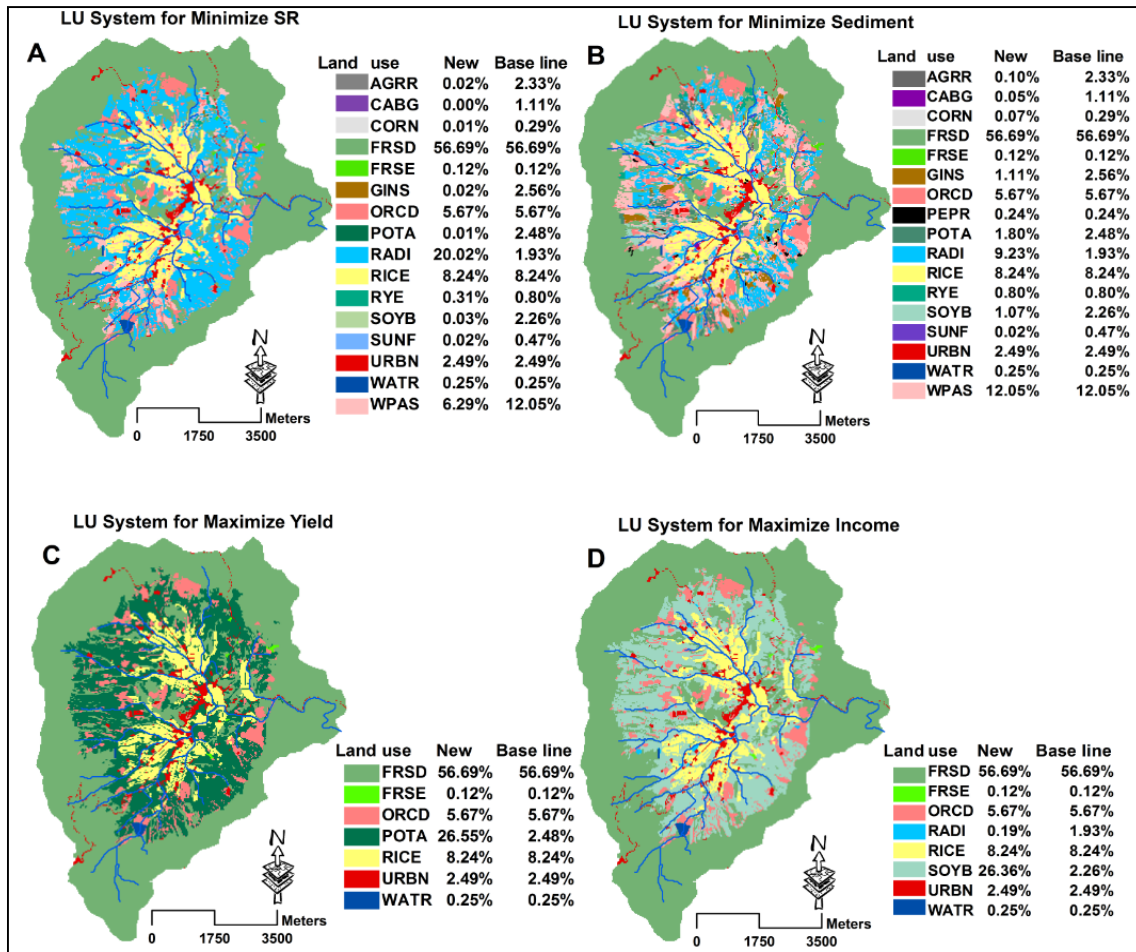


Figure 1.7 Optimal land use systems derived by comparing individual HRUs to obtain A. Minimum surface runoff (SR), B. Minimum sediment, C. Maximum yield, and D. Maximum income. Note: “New” refers to the percent area corresponding to the optimal land use and “Base line” refers to the percent area in the base line scenario

After identifying the optimal land use systems, the SWAT model was applied to those optimal land use systems to quantify the impact on non-optimal variable. For example the optimal land use system derived to produce the minimum sediment was implemented in the SWAT model to quantify the trade-offs between optimal and non-optimal output variables (i.e., surface runoff, crop yield, and farm income). The other three optimal land use system were also implemented to quantify the associated trade-offs that need to bear for the benefit of the respective optimal land use system. The variation of surface runoff due to different optimal land use systems varies from 545.15 to 563.11 mm, sediment varies from 10.19 to 14.94 tons ha⁻¹, crop yield from 1.6 to 4.8 tons ha⁻¹ and farm income from 43 to 67 million won ha⁻¹. However there is the possibility to produce a synergic effect due to the implementation of the optimal land use system. The land use system that has the capacity to generate maximum income could have the possibility to generate minimum sediment as a synergistic effect of optimal land use for maximum income. We did not observe such synergic effect in our study by implementation of the derived optimal land use systems. We observed that the implementation of optimal land use for maximum income had deteriorative impacts on the environment due to production

of higher sediment loss. The optimal land use system for maximum income was benefited by producing maximum farm income of 67 million won ha⁻¹ which was about 13 %, 19 % and 56 % higher farm income than what would have been produced by respective optimal land use systems for minimum surface runoff, minimum sediment and maximum crop yield. On the other hand, the optimal land use system for maximum income had trade-offs to produce a higher sediment yield of 14.87 tons ha⁻¹ which was about 46 % higher than what would have been produced by the optimal land use derived for minimum sediment loss (10.19 tons ha⁻¹). The other two output variables due to optimal land use system for maximum income produces crop yield of 1.6 tons ha⁻¹ and surface runoff of 563.11 mm which were 67 % lower crop yield than crop yield that could be produced by optimal land use system for maximum crop yield and 3 % more surface runoff than the surface runoff that could be produced by optimal land use system for minimum surface runoff. Similar trade-offs analyses were assessed for the remaining three optimal land use systems. From the detailed trade-offs analysis, we observed the implementation of a land use system for minimum sediment has to bear an income loss by 16 % what would have been gained by implementation of optimal land use system derived for maximum income (67.4 million won ha⁻¹). Hence the policy to recover the lost farm income and crop yield due to implementation of an optimal land use system for minimum sediment would encourage the stakeholder in decisions to implement the optimal land use system that would improve the water quality.

The analysis of the SWAT model output (discharge, sediment, and crop yield) for different land use systems implemented in Haean catchment were entirely based on the calibrated and validated model. The discharge and sediment were compared with measured flow data and sediment loss at various monitoring location within the Haean catchment. The simulated crop growth dynamics (LAI and biomass) for main dryland crops considered in this study were compared with respective crop growth measured in the plot based experiment by Lindner et al. (2015). The SWAT model outputs intrinsically depend on the feature of HRUs characteristics defined by topography, climate, and management practice of related crops. The calibrated and validated SWAT model was parameterized to reflect those characteristics in the model and to rely on the model predictability for different scenarios. The calibrated and validated model was considered as a baseline scenario. The model outputs such as average annual sediment loss from the dryland crop (cabbage, potato, radish and soybean) was 48 tons ha⁻¹. The previous studied by Arnhold et al. (2014) from the erosion experiment of similar crops estimate sediment loss from 30.6 to 54.8 ton ha⁻¹ yr⁻¹ which were consistent with the model simulation. The model predictability was reasonable by measures of statistical performance (NS, R² and PBIAS) and field experimental data. If the model predictability is not secured, further scenario analyses and recommendation based on the model output could mislead the interpretation.

The methodological approach to derive different optimal land use systems was dependent on individual HRU analysis for particular objective function of minimum surface runoff, minimum

sediment, maximum crop yield, or maximum income. The re-allocation of several crop types to individual HRUs was based on an empirical data set from a series of SWAT model simulations of the baseline scenario with an existing land use distribution and simulated monoculture land use systems of potato, cabbage, radish, and soybean. There have been several methodological approaches to re-allocate the best management practices applied to particular land uses for multiple economic and environmental objectives. One of the popular methods to re-allocate crop and management practices for multi-objective is based on a genetic algorithm which has been successfully implemented by Arabi et al. (2006) and later by Maringanti et al. (2011, 2009) for placement of best management practice in an economically efficient manner. Besides the necessity of large computational infrastructure and complexity in developing an algorithms for multi-optimization, the genetic algorithm methods the procedure cannot assure the optimal solution (Lautenbach et al., 2013). The multi-optimization approaches by global programming define weighting factors or assigning equal weighing factors which would bias the optimal solution (Darradi et al., 2012). The methodology we develop for a single objective optimization approach is simple and transparent, avoiding large computational time and defining complex algorithm and consideration of weighting factor. Hence the optimal land use system derived for a single objective function and quantified trade-offs would provide important information for stakeholders and decision makers to decide on specific land use systems.

Box3 result summary: Drive optimal land use and trade-offs quantification

(Manuscript 3)

- The SWAT model was used to assess the impact of different monoculture land use systems on discharge, sediment loss, crop yield and farm income.
- The model output from monoculture land use systems and baseline land use system were analyzed to derive four independent optimal land use systems i.e., which has respective capability to produce
 - a. Minimum surface runoff
 - b. Minimum sediment
 - c. Maximum crop yield
 - d. Maximum income
- The derived four optimal land use systems were implement into SWAT model in order to assess the trade-offs associated with non optimal variable.
- We found the implementation of optimal land use system for (a) minimum surface runoff and (b) minimum sediment have to bear less crop yield and less income in comparison to the crop yield and income generated by land use systems of (c) Maximum crop yield and (d) Maximum Income .
- The implementation of land use systems for (c) Maximum crop yield and (d) Maximum income have negative impact on environment by producing higher amount of surface runoff and sediment as compared to surface runoff and sediment loss generated by optimal land use system of (a) Minimum surface runoff and (b) Minimum sediment.

1.3.4 Application of BMP and assessing their effectiveness for different crop and catchment level

We developed BMP scenarios for split fertilizer application (SF), cover crop plantation (CC) and a combination of split fertilizer and cover crop plantation (SFCC). The considered BMPs were implemented in the SWAT model to assess their effectiveness to control sediment and nitrate and their impact on specific crop yield. The SWAT model was calibrated and validated for discharge, sediment, and nitrate was considered the model as the baseline (BL) model scenario.

The average sediment loss from major dryland crops in BL scenario were between 35 and 53 tons ha⁻¹. The highest average sediment loss was observed from potato HRUs (53 tons ha⁻¹) and followed by radish HRUs was 52 tons ha⁻¹ and 48 tons ha⁻¹ from cabbage HRUs. The least sediment loss was observed from soybean HRUs which was about 35 tons ha⁻¹. The variation of sediment loss simulated from different crop HRUs are due to spatial heterogeneity in topography and soil properties in the catchment. The four major crops were observed to produce higher sediment and nutrients losses due to current crop management practices of fallow land in winter and intensive fertilizer application. Because of this reason the BMPs scenarios were implemented for those four crop HRUs. The BMP scenarios of CC and SFCC was applied to all four major crops which had significantly reduced the sediment loss from the respective crop HRUs. The importance of cover crop plantation has been highlighted due to its effectiveness of reduction on sediment loss as compared to BL scenario. The cover crop is planted after harvest of the main crop and to work as a protective layer to reduce rainfall impacts during the winter period. The cover crop has the positive impact on reducing erosivity by reducing rainfall impact which further helps to reduce the soil erosion (Morgan, 2005). The root growth of the cover crop and the incorporation of a cover crop into soil before plantation of the main crop improve the soil aggregates and supports to protect soil erosion protection (Morgan, 2005). In the SWAT model the cover crop is considered by modifying the C factor to a lower value (cover factor in the MUSLE equation), which has a direct impact on reduction of sediment losses.

The application of the SF scenario does not have an impact on the reduction of sediment losses. As the SF scenario is expected to increase crop biomass which may impact on decreasing the C factor that helps reduction in sediment loss. We did not observe the increase of crop growth biomass by SF scenario due to which the reduction of sediment loss was not realized. The effectiveness of CC and SFCC scenarios were almost equal in comparison to BL scenarios. The highest reduction of sediment losses by CC and SFCC were found in cabbage HRUs where we found a reduction of 81 and 80 % respectively. The least sediment reduction capability by CC and SFCC scenario were observed in soybean only by 20 % for both scenarios. The reduction of sediment losses from potato and radish due to CC and SFCC applied to respective crop were 64 and 52 % from its BL scenarios.

The total sediment losses in BL from the four major crops were 23000 tons which was sufficiently reduced to 10607 tons and 10704 tons after the application of respective CC and SFCC scenarios. However the CC and SFCC application were not significantly different on reduction capability of

sediment loss, SFCC had 1 % less effectiveness in reduction of sediment loss than compared to CC scenario. The sediment loss in the BL scenario due to all land use types in the catchment was 63973 tons which contains 36 % generated by four major dryland crops. The CC and SFCC applied to four major crops reduced 19 % of the sediment loss at the catchment level.

The application of fertilizer in excess of crop requirements is a general practice in the Haean catchment to reduce the risk of crop yield (Kettering et al., 2012). The access of mineral fertilizer, primarily as nitrogen, is the main source of nitrate in different flow pathway of the catchment. The CC, SF, and SFCC scenario were applied to major crop land uses to reduce the nitrate in different pathways (nitrate: surface runoff, lateral flow, and leaching). The total nitrate loss for different crops in the BL scenario was between 95 kg ha⁻¹ in soybean and 315 kg ha⁻¹ from radish. The SF scenario application reduces the total nitrate from 8 % to 13 % as compared to BL scenario for cabbage and radish. The SF had a higher impact on reducing the nitrate in surface runoff and later flow. It was observed to reduce nitrate in surface runoff by 45 % and 6 % reduction in nitrate in lateral flow due to SF application in radish crop while no effect in nitrate leaching reduction. Similar effectiveness for different crops was assessed due to application of CC and SFCC. In general we found the SF scenario had a higher capability to reduce nitrate in surface runoff. The fertilizer application data coincide with rainfall events could have a significant loss of nitrate via surface runoff (Sanchez and Blackmer, 1988) which is mostly prevalent in the BL scenario. As the Haean catchment is highly affected by a monsoon climate, so the date for the application of split fertilizer is comprehensively planned to avoid rainfall date and to synchronize with plant uptake (Kettering et al., 2012; Ruidisch et al., 2013b). Because of this reason the SF scenario was observed to be the most effective in reducing nitrate from surface runoff. We observed that the CC scenario reduced the nitrate thorough leaching. The cover crop plantation in the CC scenario helps to utilize the residual nitrogen and would leave a small amount of nitrate in the soil for leaching (Saleh et al., 2007). The application of SFCC had positive effects on reducing nitrate in all pathways (see supplementary Tables ST4-ST6, Chapter 5) for all type of crops.

The overall total nitrate observed due to the four major crops yield 97835 kg nitrate in the BL scenario, the largest part of which was contributed from radish (38129 kg), followed by potato (30041 kg), cabbage (16218 kg), and soybean (13447 kg). The total nitrate due to the cumulative effect of major crops was reduced by 9, 18, and 28 % due to the respective BMP of SF, CC, and SFCC scenarios. The total nitrate from all land use types in the catchment in BL scenario was 245993 kg from which 40 % was contributed by four major crops. The implementation of BMPs of SF, CC, and SFCC in the four major crops reduces the total nitrate by 4, 7, and 11 % respectively in the catchment level.

The impact of crop yield due to the application of SF, CC, and SFCC were assessed for cabbage, potato, radish, and soybean in the Haean catchment. SF did not show the impact on crop yield to all of the crop types. The CC and SFCC scenarios had shown significant effect on crop yield. But soybean

did not show any change in crop yield due to the applied BMP. The potato yield was highly increased by 39 % due to SFCC scenario as compared to the BL scenario and also significantly increased the crop yield for cabbage and radish by 17 and 27 % respectively.

The BMP applications for different crops in the catchment and their impact at the main catchment outlet are equally important to assess the effectiveness to control off-site impacts to downstream water bodies. The cumulative total nitrate loss in the BL scenario at the catchment outlet was about 181977 kg which could be reduced by 3, 12, and 15 % due to the respective BMP of SF, CC and SFCC scenarios. The cumulative total sediment load estimated at the catchment outlet in BL was 61546 tons per year which was reduced by the BMP application of CC and SFCC scenarios with equal effectiveness by 18 %.

Overall the effectiveness of BMPs was assessed at different levels from different crop types to catchment level. We observed the effectiveness assessed for different crops was higher than that assessed at the catchment level. The reduction capability of BMPs were observed to be less effective at catchment level as BMP applications were implemented into small portions of the catchment, similar to results by Arabi et al. (2006). This finding has emphasized the effectiveness of BMP is limited, when not applied to all possible land uses, including hotspots throughout the catchment. The quantified BMP effectiveness has the practical consequence of recommendation of particular BMP application to all the possible crop types in the study catchment. The application of BMPs to the study catchment can maintain the ecosystem services. The regulating services of erosion and nutrient loss are retained in the system and improve the provisioning services by sustainable production of improved water quality and increased crop yield.

Box4 result summary: Modeling of split fertilization and cover crop cultivation

(Manuscript 4)

- In this study we have quantified the effectiveness of best management practices (BMPs) scenarios of split fertilizer application and cover crop applied to major crops: cabbage, potato, radish, and soybean.
- The effectiveness was measured by evaluating the comparative difference of model output due to application of BMP and without BMP as baseline scenario.
- The application of BMP related to split fertilizer has considerable effect to reduce total nitrate loss produced from major crops whereas sediment loss and crop yield did not have any effect in comparison to baseline scenario.
- The application of cover crop as BMP to major crops has reduced both sediment and nitrate loss while improving the crop yield as compared to baseline scenario.
- The combination of both BMPs (split fertilizer and cover crop plantation) showed highest level of reducing nitrate and sediment loss from the respective crop field.
- The BMPs applied only to major crops have shown limited reduction of sediment and nitrate losses at the catchment outlet.

1.4 Conclusions and recommendations

Potential of SWAT model to solve the environmental problem in northern part of South Korea

In this study, we consider the two study sites the Jawoon-ri and the Haeon catchments within the Soyang watershed in the northern part of South Korea. Both the study catchments are associated with intensive mountainous agriculture. The practices of intensive mountainous agriculture have generated large amount of sediments and nutrients as nonpoint source pollution contributing to downstream Soyang reservoir. The Soyang reservoir is the source of drinking water supply to the Seoul, capital city of South Korea. One of the environmental problems associated with intensive mountainous agriculture in the northern part of South Korea is export of sediments and nutrients as nonpoint source pollution deteriorating the water quality of downstream waterbodies.

We have conducted four subsequent studies. The common methodological approaches for those four studies were to apply SWAT as a primary tool for watershed modeling. Different issues and the aspects of SWAT modeling in the individual studies are overarching to assess environmental performance of intensive farming system in order to recommend the potential solution to reduce the associated environmental problems. The first two studies presented the details of model setup and relevant technical detail in methodological approach for calibration, validation, and uncertainties in order to access reliable prediction of model output. The next subsequent two studies were to adopt the developed methodological setup to quantify different ecosystem services, importantly regulating services (sediment and nutrient loss) and provisioning services (water quality and crop yield/farm income). The subsequent sections briefly summarize the conclusion and recommendation made by respective studies.

Study1: Evaluation of SWAT model for hourly runoff simulation

In our first study, we setup the SWAT model to small field size agricultural watershed of 0.8 ha in Jawoon-ri watershed. We evaluated the SWAT model performance for reliable prediction of runoff by using hourly rainfall data with Green and Ampt method. We observed statistical performance of R^2 and NSE equivalent to 0.874 and 0.898 for hourly runoff simulation. The use of daily rainfall data to simulate daily runoff resulted 0.79 and -0.01 for respective R^2 and NSE values. Hence we found that SWAT sub-daily simulation by using hourly rainfall data for reliable estimate of runoff at field sized watershed with higher accuracies than daily simulation.

The reliable prediction of runoff can secure further estimate of sediments and nutrients losses. The practical consequence of SWAT hourly simulation for reliable prediction of different output variables by using daily rainfall data could be use to evaluate precise effectiveness of different best management practices (BMPs) in the watershed. However the data availability is always limited in modeling studies due to large computational time and high storage volume of model output. The lack of an hourly time step field measurement data for many water quality parameters could also limit the application of the hourly simulation.

Study2: Improving flow process and hydrologic partitioning

In this study, we apply SWAT model to higher catchment as compared to previous study 1. The applicability of SWAT model was explored in the Haeon catchment of complex terrain and extreme environments of East Asian monsoon climate for flow processes and hydrologic partitioning. The complexity of the study catchment that exists in overall landscapes is highly motivated to capture in this watershed modeling by using SWAT. The fundamental data sets (Tenhunen et al., 2010) to represent topographical variability, soil variability, spatiotemporal climatological variability, land use distribution and associated management practices are respectively represented by digital elevation model (DEM), soil map (Arnhold, 2013), weather station data, and land use map (Seo et al., 2014) of the Haeon catchment.

In Haeon catchment the measurements of climatic and meteorological data from different weather stations were limited and data gaps were prevalent. We developed an algorithm to fill the data gaps and adopt an interpolation method (IDW) to capture the meteorological variability that exists due altitudinal variability throughout the catchment. This has improved the modeled plant growth dynamic of different crops effecting evapotranspiration and overall waterbalance of the catchment.

The variability of discharge prediction by the model was assess by assigning variability in flow related parameters values during both semi and fully distributed parameterization of the model. The novelty of this study was to adopt a multi-location calibration and validation approach to define flow processes and discharge partitioning. We identified location wise discharge related sensitive parameters along the elevation transect (S1 to S7). However there exists general approximation (knowledge of understanding) to parameter variable of the model due to unavailability of measured data to parameterize each and every spatial point. We adopt stochastic simulation by using SUFI-2 algorithm in SWAT CUP (Abaspour et al., 2007) in order to quantify the uncertainty of the model prediction. In addition to the field level studies (Arnhold 2013, Ruidisch 2013) in this particular catchment, we have captured the complexity of the landscapes and distributed parameterization approach during multi-site calibration and validation has improved the reliable and acceptable estimate of discharge variability within the landscapes.

Hence, this study presented a methodological approach to consider the difficulties associated with climatic variability through meteorological data gap-filling and interpolation. The result of diversified measures (R^2 , NSE, PBIAS, baseflow and plant growth) of evaluating the model performance during multi-site calibration and validation has proven the reliable estimate of discharge partitioning throughout the catchment. The reliability in the use of SWAT model based on the methods adopted in this study could be transferable to the watershed of similar characteristic (mountainous region, climatological variability) for assessing different output variable (e.g., nutrient loading and contaminant transport). The precise estimate of discharge variability in spatiotemporal pattern

presented in this study has importance during analysis of different scenario studies (Chapter 4-5) to improve water quality and other ecosystem services.

Study 3.Scenario-based optimal land use systems and trade-offs between farm income and environment

In this study, we used SWAT model to represent the inherent characteristic of biophysical process of the Haeon catchment. The ability of SWAT model to incorporate different land use scenarios and quantifying their impact on environmental and economical aspects were investigated in this 3rd study. However, development of land use scenarios are implicitly related to complex interactions of crop price, governmental policy, availability of knowledge and technology and socio-economic status of the involved stake holder. We developed the extreme land use scenarios considering four different monoculture land use systems for cabbage, potato, radish, and soybean respectively in order to experience the possible extreme values of different model output variable from individual crop HRUs (fields). The HRUs of each monoculture land use system and baseline land use system were analyzed for the individual objectives of a) minimum surface runoff, b) minimum sediment, c) maximum crop yield and d) maximum income one at a time. Re-allocating a corresponding land use/crop type for each HRU satisfying each objective (a-d) to determine the optimal land use for respective objectives. We had derived four optimal land use systems relating to the individual objectives of a) minimum surface runoff b) minimum sediment loss c) maximum crop yield and d) maximum income.

The implementation of optimal land use in the model was used to determine the trade-offs associated with non optimal output variables. For example, we observed the application of an optimal land use for maximum income had to bear environmental degradation by exporting higher amounts of surface runoff and sediment loss. The similar exercise could be performed to estimate the included trade-offs between optimal and non-optimal output variable for every optimal land use systems (a-d). In a detailed analysis of trade-offs, we observed that the implementation of environmentally optimal land use system which was attributed for minimum sediment loss had to bear an economic loss by loss of 16 % farm income that could benefit from the application of an optimal land use system for maximum income. The policy could be developed to compensate (scheme: payment for ecosystem service) for economic loss due to which the farmers could be encouraged to adopt land use system that produced less sediment. Hence the quantification of associated trade-offs due to the implementation of optimal land use systems has a practical implication to plan for compensating the effect of trade-offs for mutual benefits (environment and economic).

The simulation of dynamic land use systems considering soci-economic variables and application of such land use systems into SWAT model in order to assess the associated trade-offs would be real world application of presented method. The determination of different land use system simulated by considering soci-economic variable in multi-agent based modeling could be one of the potential input data source to elucidate the trade-offs between environmental and economical aspect. In parallel to this

study, a research was initiated to derive multi-agent based land use system for Soyang watershed (Ilkwon kim, personal communication). In further study, the outcome from his study applied to Haeon catchment (part of Soyang watershed) would generate different land use systems which could be an important input data source to the SWAT for the analysis of trade-offs. The immediate response of trade-offs due to implementation of different land use systems helps the stake holders and farmers to make the decision of particular land use system to implement into real field.

Study 4. Assessing the BMP effectiveness in relation to split fertilizer application and cover crop cultivation.

In this study, we assess the effective of best management practices (BMPs) in relation to split fertilizer application and cover crop plantation by using SWAT model. The choice of BMPs in Haeon catchment were due to prevalent management practice of excess use of fertilizer and the fallow land after harvest of main crops to major dryland crops (cabbage, potato, radish, and soybean). The application of best management practice (BMP) scenarios in relation to split fertilizer application (SF) and cover crop plantation (CC) and combination of BMPs as SFCC were hypothesized to reduce sediment and nutrients loss to the stream network. BL is the baseline scenario that refers to the current practice of leaving fields as fallow land after harvest of dryland crops.

The split fertilization (SF scenario) to the dryland crops was effective in controlling the nitrate loss, in contrast we did not observe an increased crop yield that can be expected due to synchronizing the effect of split application and plant uptake. The implementation of a CC scenario showed a considerable effect in reducing sediment in comparison to BL scenario. The CC scenario also indicated the mutual benefit of reducing nitrate loss in addition to the reduction of sediment loss, which might be due to the use of residual nitrogen after excessive fertilization of dryland crops. We observed the combination of BMP scenarios through the SFCC scenario had shown a synergistic effect on reducing sediment and nitrate loss while increasing the crop yield.

The real application of recommended BMPs mainly the cover crop plantation to the field might not be as effective to increase crop yield as it assess in model due to production of harmful chemical (allelopathy corn field due to ray cover crop). The SWAT model does not consider the effect of harmful chemical in reducing the crop yield. The reduction of crop yield in the model is only considered by stress induced by heat, water, and nutrients (nitrogen and phosphorus).

However the BMP scenarios that we considered in this study have been considered as effective BMP application in many other studies. We had quantified their effectiveness based on different crop types and their cumulative effect at the catchment level. We observed the effectiveness of BMPs varied between the various crops. We found that the effectiveness of the BMP depends on site specific topology and the crop type, which had been observed to soybean crops showing less effectiveness compared to other crops. Based on this finding we could suggest, additional BMPs to increase the

effectiveness of pollutant retention. The effectiveness of BMPs observed at the catchment level (nitrate at catchment outlet) was not as effective as those observed for different crops. The reason for this might be slow release of nitrate to the stream and higher denitrification process from the field. The impact of slow release of the pollutant like nitrate can be taken into account by simulating the SWAT model for more than several decades (if climatological data is provided). In addition, the use of static land use map for 2010 can be updated with historical archive for every land parcel to consider yearly land use change. Based on this consideration, in the further study, it is important to consider the BMPs to other minor crop and land use types in catchment-wise management plan which can considerably impact the ability of reducing the pollutant load to improve water quality.

The consequent studies accumulated in this thesis have analyzed intensive farming in mountainous landscapes. The recommendation made on third study in associated to particular land use system and the BMP recommendation on fourth study in combination could be of sustainable intensive farming system in mountainous landscape for both farm income and environment.

1.5 List of manuscripts and specification of individual contributions

This thesis is a cumulative of published and submitted manuscripts. Manuscripts 1 and 2 have published in respective journal of *Frontiers of Environmental Science & Engineering* and *Hydrology and Earth System Science*. Manuscript 3 and 4 are in review under *Agricultural system* and *Agricultural water Management*. The manuscripts details and authors contributions are presented below.

Manuscript 1

Title	Evaluation of SWAT sub-daily runoff estimation at small agricultural watershed in Korea		
Authors	Ganga Ram Maharjan, Youn Shik Park, Nam Won Kim, Dong Seok Shin, Jae Wan Choi, Geun Woo Hyun, Ji-Hong Jeon, Yong Sik Ok, Kyoung Jae Lim		
Status	Published in <i>Frontiers of Environmental Science & Engineering</i> . 2013, 7(1): 109–119		
Contributions	Ganga Ram Maharjan	82 %	idea, method, data analysis, modelling, manuscript writing, figures, discussion, manuscript editing
	Youn Shik Park	5 %	idea, discussion, manuscript editing
	Nam Won Kim	1 %	discussion
	Dong Seok Shin	1 %	discussion
	Jae Won Choi	2 %	data collection, discussion
	Geun Woo Hyun	1 %	discussion
	Ji-Hong Jeon	1 %	discussion
	Yong Sik Ok	1 %	discussion
	Kyoung Jae Lim	6 %	idea, manuscript editing, corresponding author

Manuscript 2

Title	Using the SWAT model to improve process descriptions and define hydrologic partitioning in South Korea		
Authors	Christopher L. Shope, Ganga Ram Maharjan, John Tenhunen, Bumsuk Seo, Kiyong Kim, Jeanne Riley, Sebastian Arnhold, Thomas Koellner, Yong Sik Ok, Stefan Peiffer, Bomchul Kim, Ji-Hyung Park, and Bernd Huwe		
Contributions	Christopher L. Shope	55 %	idea, method, data analysis, modeling, manuscript writing, figures, discussion, manuscript editing, corresponding author
	Ganga Ram Maharjan	32 %	idea, method, modeling, discussion, manuscript editing
	John Tenhunen	2 %	idea, discussion, manuscript editing
	Bumsuk Seo	1 %	data collection
	Kiyong Kim	1 %	data collection
	Jeanne Riley	1 %	manuscript editing
	Sebastian Arnhold	1 %	manuscript editing
	Thomas Koellner	1 %	manuscript editing

Chapter 1-Synopsis

	Yong Sik Ok	1 %	manuscript editing
	Stefan Peiffer	1 %	manuscript editing
	Bomchul Kim	1 %	data collection
	Ji-Hyung Park	1 %	manuscript editing
	Bern Huwe	3 %	idea, discussion, manuscript editing
Status	Published in <i>Hydrology and Earth System Science</i> . 2014, 18, 539–557		
Manuscript 3			
Title	Identifying scenario-based optimal land use systems and assessing tradeoffs between farm income and environment: Haeon catchment, South Korea.		
Authors	Ganga Ram Maharjan, Christopher L. Shope, Trung Thanh Nguyen, Thomas Koellner, Bernd Huwe, Seong Joon Kim, John Tenhunen, Sebastian Arnhold		
Status	in review in <i>Agricultural System</i> . 2015		
Contributions	Ganga Ram Maharjan	80 %	idea, method, data analysis, modelling, manuscript writing, figures, discussion, editing corresponding author
	Christopher L. Shope	3 %	manuscript editing
	Trung Thanh Nguyen	4 %	idea, manuscript editing
	Thomas Koellner	1 %	discussion
	Bernd Huwe	5 %	idea, discussion, manuscript editing
	Seong Joon Kim	1 %	discussion
	John Tenhunen	1 %	discussion
	Sebastian Arnhold	5 %	idea, discussion, manuscript editing
Manuscript 4			
Title	Assessing effectiveness of split fertilization and cover crop cultivation to conserve soil and water resources and improve crop productivity		
Authors	Ganga Ram Maharjan, Marianne Ruidisch, Christopher L. Shope, Kwanghun Choi, Bernd Huwe, Seong Joon Kim, John Tenhunen, Sebastian Arnhold		
Contributions	Ganga Ram Maharjan	78 %	idea, method, data analysis, modelling, manuscript writing, figures, discussion, manuscript editing, corresponding author
	Marianne Ruidisch	5 %	idea, discussion, manuscript editing
	Christopher L. Shope	1 %	manuscript editing
	Kwanghun Choi	4 %	r-coding, manuscript editing
	Bernd Huwe	5 %	idea, discussion, manuscript editing
	Seong Joon Kim	1 %	discussion
	John Tenhunen	1 %	discussion, manuscript editing
	S. Arnhold	5 %	idea, discussion, manuscript editing
Status	in review <i>Agricultural Water Management</i> . 2015		

1.6 References

- Abbaspour, K.C., C.A. Johnson, M.T. van Genuchten, 2004 Estimating uncertain flow and transport parameters using a sequential uncertainty fitting procedure. *Vadose Zone Journal* **3**: 1340-1352.
- Abbaspour, K.C., 2015 SWAT-CUP:SWAT calibration and uncertainty programs-A user manual. Eawag: Swiss Federal Institute of Aquatic Science and Technology.
- Arabi, M., R.S. Govindaraju, M.M. Hantush, 2006 Cost-effective allocation of watershed management practices using a genetic algorithm. *Water Resources Research*. **42**: W10429.
- Arnhold, S., S. Lindner, B. Lee, E. Martin, J. Kettering, T.T. Nguyen, T. Koellner, Y.S. Ok, B. Huwe, 2014 Conventional and organic farming: soil erosion and conservation potential for row crop cultivation. *Geoderma*. **219-220**: 89-105.
- Arnhold, S., M. Ruidisch, S. Bartsch, C.L. Shope, B. Huwe, 2013 Simulation of runoff patterns and soil erosion on mountainous farmland with and without plastic-covered ridge-furrow cultivation in South Korea. *Trans. ASABE*. **56**: 667-679.
- Bartsch, S., 2013 Monsoonal affected dynamics of nitrate and dissolved organic carbon in a mountainous catchment under intensive land-use. Ph.d, Thesis, University of Bayreuth, Germany.
- Brooks, K.N., P.F. Ffolliott, J.A. Magner, 2013b Hydrology and the management of watersheds. John Wiley & Sons, Inc. **fourth ed.**
- Carpenter, S.R., N.F. Caraco, D.L. Correll, R.W. Howarth, A.N. Sharpley, V.H. Smith, 1998 Nonpoint pollution of surface waters with phosphorus and nitrogen. *Ecological Applications*. **8**: 559-568.
- Cestti, R., J. Srivastava, S. Jung, 2003 Agriculture non-point source pollution control good management practices: chesapeake bay experience. Environmentally & Socially Development Unit. Europe and Central Asia, The World Bank, Washington, D.C.
- Choi, J.D., H.J. Lee, S.Y. Park, C.H. Won, Y.H. Choi, K.J. Lim, 2010 Sediment control practices in sloping highland fields in Korea. 19th World Congress of Soil Science, Soil Solutions for a Changing World. Brisbane, Australia
- Cotter, A., 2002 Critical Evaluation of TMDL data requirements for agricultural watersheds. Dissertation Master degree.
- Daily, G.C., 1997 Introduction: what are ecosystem services? in: Daily, G. C. (Ed.), *Nature's services. Societal dependence on natural ecosystems*. Island Press, Washington D.C.: pp. 1-10.
- Darradi, Y.s., E. Saur, R. Laplana, J.-M. Lescot, V. Kuentz, B.C. Meyer, 2012 Optimizing the environmental performance of agricultural activities: A case study in La Boulouze watershed. *Ecological Indicators*. **22**: 27-37.
- Debele, B., R. Srinivasan, J.Y. Parlange, 2009 Hourly analyses of hydrological and water quality simulations using the ESWAT Model. *Water Resources Management*. **23**: 303-324.
- Di Luzio, M., J.G. Arnold, 2004 Formulation of a hybrid calibration approach for a physically based distributed model with NEXRAD data input. *Journal of Hydrology*. **293**: 136-154.
- Gassman, P.W., M.R. Reyes, C.H. Green, J.G. Arnold, 2007 The Soil and Water Assessment Tool: historical development, applications, and future directions. *Transactions ASABE*. **50**: 1211-1250.
- Gupta, H., S. Sorooshian, P. Yapo, 1999 Status of automatic calibration for hydrologic models: comparison with multilevel expert calibration. *Journal of Hydrologic Engineering*. **4**: 135-143.
- Jung, E., 2013 Quantifying water use by temperate deciduous forests in South Korea: roles of species diversity, canopy structure, and complex terrain. Ph.d, Thesis, University of Bayreuth, Germany.

- Kannan, N., S.M. White, F. Worrall, M.J. Whelan, 2007 Hydrological modelling of a small catchment using SWAT-2000 Ensuring correct flow partitioning for contaminant modelling. *Journal of Hydrology*. **334**: 64-72.
- Kettering, J., J.-H. Park, S. Lindner, B. Lee, J. Tenhunen, Y. Kuzyakov, 2012 N fluxes in an agricultural catchment under monsoon climate: a budget approach at different scales. *Agriculture, Ecosystems & Environment*. **161**: 101-111.
- King, K.W., J.G. Arnold, R.L. Bingner, 1999 Comparison of Green–Ampt and Curve Number methods on Goodwin Creek Watershed using SWAT. *Transactions of the ASAE*. **42**: 919-925.
- Koch, H., U. Grünewald, 2009 A comparison of modelling systems for the development and revision of water resources management plans. *Water Resources Management*. **23**: 1403-1422.
- Lautenbach, S., M. Volk, M. Strauch, G. Whittaker, R. Seppelt, 2013 Optimization-based trade-off analysis of biodiesel crop production for managing an agricultural catchment. *Environmental Modelling & Software*. **48**: 98-112.
- Lindner, S., D. Otieno, B. Lee, W. Xue, S. Arnhold, H. Kwon, B. Huwe, J. Tenhunen, 2015 Carbon dioxide exchange and its regulation in the main agro-ecosystems of Haean catchment in South Korea. *Agriculture, Ecosystems & Environment*. **199**: 132-145.
- Maringanti, C., I. Chaubey, M. Arabi, B. Engel, 2011 Application of a multi-objective optimization method to provide least cost alternatives for NPS pollution control. *Environmental Management*. **48**: 448-461.
- Maringanti, C., I. Chaubey, J. Popp, 2009 Development of a multiobjective optimization tool for the selection and placement of best management practices for nonpoint source pollution control. *Water Resources Research*. **45**: W06406.
- Matson, P.A., W.J. Parton, A.G. Power, M.J. Swift, 1997 Agricultural intensification and ecosystem properties. *Science*. **277**: 504-509.
- Millennium Ecosystem Assessment, 2005 Ecosystems and human well-being. Synthesis. Island Press, Washington D.C.
- Morgan, R.P.C., 2005 Soil Erosion and Conservation. Third ed. Blackwell, Malden. Natural Resources Conservation Service (NRCS), 2007. Conservation Practice Standards. United States Department of Agriculture.
- Moriassi, D.N., J.G. Arnold, M.W.V. Liew, R.L. Bingner, R.D. Harmel, T.L. Veith, 2007 Model Evaluation Guidelines for Systematic Quantification of Accuracy in Watershed Simulations. *Trans. ASABE*. **50**: 885–900.
- Neitsch, S.L., J.G. Arnold, J.R. Kiniry, J.R. Williams, 2011 Soil and Water Assessment Tool Theoretical Documentation Version 2009. Texas Water Resources Institute Technical Report No. 406.
- Nguyen, T.T., V.-N. Hoang, B. Seo, 2012 Cost and environmental efficiency of rice farms in South Korea. *Agricultural Economics*. **43**: 369-378.
- Park, J.-H., L. Duan, B. Kim, M.J. Mitchell, H. Shibata, 2010 Potential effects of climate change and variability on watershed biogeochemical processes and water quality in Northeast Asia. *Environment International*. **36**: 212-225.
- Park, J.-Y., Y.-S. Yu, S.-J. Hwang, C. Kim, S.-J. Kim, 2014 SWAT modeling of best management practices for Chungju dam watershed in South Korea under future climate change scenarios. *Paddy and Water Environment*. **12**: 65-75.
- Pimentel, D., C. Harvey, P. Resosudarmo, K. Sinclair, D. Kurz, M. McNair, S. Crist, L. Shpritz, L. Fitton, R. Saffouri, R. Blair, 1995 Environmental and Economic Costs of Soil Erosion and Conservation Benefits. *Science*. **267**: 1117-1123.

- Poppenborg, P., 2014 The impact of socio-economic land use decisions on the provision of ecosystem services. Ph.D thesis, University of Bayreuth, Germany.
- Pradhan, P., 2015 Food demand and supply under global change. Ph.D thesis, University of Potsdam, Germany.
- Rawls, W.J., L.R. Ahuja, D.L. Brakensiek, A. Shirmohammadi, 1993 Infiltration and soil water movement. In: Maidment D R, editor, New York: Mc Graw-hill.
- Ruidisch, M., S. Arnhold, B. Huwe, C. Bogner, 2013a Is Ridge cultivation sustainable? A case study from the Haean Catchment, South Korea. *Applied and Environmental Soil Science*. Article ID 679467. **2013**.
- Ruidisch, M., S. Bartsch, J. Kettering, B. Huwe, S. Frei, 2013b The effect of fertilizer best management practices on nitrate leaching in a plastic mulched ridge cultivation system. *Agriculture, Ecosystems & Environment*. **169**: 21-32.
- Saleh, A., E. Osei, D.B. Jaynes, B. Du, J.G. Arnold, 2007 economic and environmental impacts of lsnt and cover crops for nitrate-nitrogen reduction in walnut creek watershed, iowa, using fem and enhanced swat models. *Transactions of the ASABE*. **50**: 1251-1259.
- Sanchez, C.A., A.M. Blackmer, 1988 Recovery of Anhydrous Ammonia-Derived Nitrogen-15 During Three Years of Corn Production in Iowa. *Agronomy Journal*. **80**: 102-108.
- Seo, B., C. Bogner, P. Poppenborg, E. Martin, M. Hoffmeister, M. Jun, T. Koellner, B. Reineking, C.L. Shope, J. Tenhunen, 2014 Deriving a per-field land use and land cover map in an agricultural mosaic catchment. *Earth Syst. Sci. Data*. **6**: 339-352.
- Seppelt, R., S. Lautenbach, M. Volk, 2013 Identifying trade-offs between ecosystem services, land use, and biodiversity: a plea for combining scenario analysis and optimization on different spatial scales. *Current Opinion in Environmental Sustainability*. **5**: 458-463.
- Stavi, I., R. Lal, 2015 Achieving zero net land degradation: Challenges and opportunities. *Journal of Arid Environments*. **112, Part A**: 44-51.
- Tenhunen, J., B. Seo, B. Lee, 2011 Spatial setting of the TERRECO project in the Haean catchment of Yanggu-gun and the Soyang watershed in Gangwan-do. *AsiaFlux Training Course on Flux Monitoring: From Theory to Application*, Seoul, South Korea.
- Tilman, D., K.G. Cassman, P.A. Matson, R. Naylor, S. Polasky, 2002 Agricultural sustainability and intensive production practices. *Nature*. **418**: 671-677.
- Tripathi, M.P., R.K. Panda, N.S. Raghuvanshi, 2003 Identification and prioritization of critical subwatershed for soil conservation management using the SWAT model. *Biosystems Engineering*. **85**: 365-379.
- UNCCD, 2012 Zero net land degradation. A Sustainable Development Goal for Rio+20, UNCCD Secretariat policy brief.
- Van Liew, M.W., T.L. Veith, Unpublished Guidelines for using the sensitivity analysis and auto-calibration tools for multi-gage or multi-step calibration in SWAT. Manual.
- White, M.J., R.D. Harmel, J.G. Arnold, J.R. Williams, 2012 SWAT Check: A screening tool to assist users in the identification of potential model application problems. *J. Environ. Qual.* **43**: 208-214.
- Zambrano-Bigiarini, M., 2014 hydroGOF: Goodness-of-fit functions for comparison of simulated and observed hydrological time series. R package version 0.3-8. <http://CRAN.R-project.org/package=hydroGOF>.

Chapter 2 Evaluation of SWAT sub-daily runoff estimation at small agricultural watershed in Korea

Ganga Ram Maharjan¹, Youn Shik Park², Nam Won Kim³, Dong Seok Shin⁴,

Jae Wan Choi⁴, Geun Woo Hyun⁵, Ji-Hong Jeon⁶, Yong Sik Ok⁷, Kyoung Jae Lim¹

¹GIS Environmental System Lab., Department of Regional Infrastructure Engineering, Kangwon National University, Chuncheon 200-701, R. O. Korea

²Department of Agricultural and Biological Engineering, Purdue University, West Lafayette, IN 47907, USA

³Water Resource Research Department, Korea Institute of Construction Technology, Goyang 411-712, R. O. Korea

⁴National Institute of Environmental Research, Incheon 404-708, R. O. Korea

⁵Department of Water Research Division, Gangwon Institute of Health and Environment, Chuncheon 200-822, R. O. Korea

⁶Department of Environmental Engineering, Andong National University, Andong 760-380, R. O. Korea

⁷Department of Biological Environment, Kangwon National University, Chuncheon 700-71, R. O. Korea

Abstract

A study was undertaken for the prediction of runoff flow from 0.8 ha field-sized agricultural watershed in South Korea using SWAT (Soil and Water Assessment Tool) sub-daily. The SWAT model with sub-daily configuration predicted flow from the watershed within the range of acceptable accuracy. The SWAT sub-daily simulations were carried out for a total of 18 rainfall events, 9 each for calibration and validation. Overall trend and extent of matching simulated flow for the rainfall events in 2007—2008 with measured data during the calibration process were coefficient of determination (R^2) value of 0.88 and Nash and Sutcliffe Efficiency (E_{NS}) value of 0.88. For validation, R^2 and E_{NS} values were 0.9 and 0.84, respectively. Whereas R^2 and E_{NS} values for simulation results using daily rainfall data were 0.79 and -0.01 , respectively that were observed to be out of acceptable limits for the model simulation. The importance of higher time resolution (hourly) precipitation records for flow simulation were evaluated by comparing R^2 and E_{NS} with 15 min, 2 h, 6 h and 12 h precipitation data, which resulted in lower statistics with increases in time resolution of precipitation data. The SWAT sub-daily sensitivity analysis was performed with the consideration of hydraulic parameter and was found as in the rank order of CN2 (curve number), ESCO (soil evaporation compensation factor), GW_DELAY (ground water delay time), ALPHA_BF (base flow alpha factor), GWQMN (a threshold minimum depth of water in the shallow aquifer required for return flow to occur), REVAPMN (minimum depth of water in shallow aquifer for re-evaporation to occur), LAT_TIME (lateral flow travel time) respectively. These sensitive parameters were evaluated at 10% higher and lower values of the parameters, corresponding to 70.5% higher and 23.2% lower in simulated flow out from the SWAT model. From the results obtained in this study, hourly precipitation record for SWAT sub-daily with Green-Ampt infiltration method was proven to be efficient for runoff estimation at field sized watershed with higher accuracies that could be efficiently used to develop site-specific Best Management Practices (BMPs) considering rainfall intensity, rather than simply using daily rainfall data.

Keywords: *Soil and Water Assessment Tool (SWAT), sub – daily simulation, runoff, rainfall*

2.1 Introduction

A watershed is one of the potential natural resources like forest resources, arable land, water, etc. to mankind. As the earth's population is growing rapidly and more stress has been put on watershed resources to support the increased population. This stress leads to agricultural intensification and deforestation resulting in serious qualitative and quantitative harms to water resource both on regional and global scale. Watershed management to secure water resource is always research objective with accurate prediction of runoff and pollutant contaminants. Watershed modeling with Geographic Information System (GIS) application has been widely used to mimic real processes (topography, soil, land use, land cover, etc.) occurring at the watershed. Furthermore, watershed models are considered as holistic approach in terms of cost and time for the assessment of pollutant loads and simulation of watershed processes under various management practices (Shrestha et al., 2006). Numerous watershed models have been developed to assist in understanding hydrologic systems and pollutant loadings. These models range from simple screening and planning models, such as USLE (Wischmeier and Smith, 1978), to complex hydrological assessment models, such as CREAMS, ANSWERS, SPNM, EPIC, SWRB, GLEAMS, NAPRA WWW, WEPP, AGNPS, and PESTFADE, HSPF, SWAT (Arnold and Allen, 1996; Beasley et al., 1980; Clemente et al., 1993; Donigan et al., 1995; Knisel, 1980; Lane and Nearing, 1989; Leonard et al., 1987; Lim and Engel, 2003; Williams et al., 1985; Williams, 1980; Williams et al., 1982; Young et al., 1994).

Among complex hydrological assessment models, the Soil and Water Assessment tool (SWAT) with ArcView GIS or ArcGIS interface is a promising model with numerous calibrations and validations (within permissible range for various time steps) tested for many watersheds worldwide (Shepherd et al., 1999). Shepherd et al. (1999) evaluated 14 models and found SWAT to be the most suitable for estimating phosphorus loss from a lowland watershed in the UK. The SWAT divides given watershed into sub-watersheds and further to Hydrologic Response Units (HRUs, unique combination of land use and soil, or slope) within the sub-watershed (Kannan et al., 2007). SWAT is used for estimating water balances with associated sediment and pollutant from HRUs and flow routed through the channel network of the watershed. In the previously research papers by Cotter et al. (2002) and Tripathi et al. (2003) SWAT was applied in monthly basis for total flow simulation. The R^2 and E_{NS} values were of 0.76 and 0.77 for calibration in Cotter's study (Cotter, 2002), and 0.98 and 0.97 for Tripathi's (Tripathi et al., 2003) calibration in their studies. However, SWAT simulation on high temporal resolution (with sub-daily time step, sub-hourly time steps) is not widely used despite its availability in SWAT model on this time resolution with combination of sub-daily rainfall data and Green - Ampt infiltration method (King et al., 1999; Rawls et al., 1993). In Di Luzio and Arnold (2004) study, the SWAT was used to simulate hourly stream flow prediction with the input data of gridded precipitation (NEXRAD) and then compared results for 24 events with measured flow, giving promising $E_{NS} > 0.79$, except a couple of events. In case of unavailability of precipitation data at required temporal resolution, ESWAT (Enhance soil and water assessment tool) model, developed by Debele et al.

(2009) successfully disaggregate daily rainfall data (along with other climatic parameters) into hourly data sets for simulation of hydrological and water quality with sub-daily time steps with R^2 and E_{NS} values of 0.6 and 0.65, respectively.

The SWAT sub-daily simulation using measured hourly rainfall data set, considering rainfall intensity, is assumed to be real response of the watershed in generating runoff and sediment at the instant time than SWAT simulation with daily time setup. Thus, predicted runoff is assumed to be precise information to the watershed planners and decision makers, implementing project of flood mitigation and other management practice for maintaining a healthy watershed in sustainable manner. The hourly simulation in previous studies was applied for bigger watersheds with disaggregated or gridded precipitation, not for field scale watersheds with measured sub-daily rainfall data. Simulated flow at bigger watershed outlet with SWAT hourly simulation could match measured flow data reasonably well without validation of flow from fields within the watershed because of complex watershed behaviors to rainfall-runoff processes. Hence, with proper validation of SWAT predicted runoff from field-sized watershed with SWAT sub-daily run, the accuracy for bigger watershed can be secured.

Therefore, the objective of this study was to set up SWAT sub-daily simulation using measured sub-daily rainfall data modifying SWAT configuration along with calibration and validation for hydrology component using measured flow data and measured sub-daily rainfall data at the watershed under study.

2.2 Methodology

2.2.1 Study area

The study area, Jawoon-ri watershed (Figure 2.1), falls in the northern part of the South Korea and situated at $37^{\circ} 52' N$ and $127^{\circ} 43' E$. The area of the watershed is about 0.8 ha with the elevation ranging from 650 to 700 m MSL (mean sea level). Runoff generated at the study area was transported to the main outlet through concrete channels network constructed at the edge of the field. Its hourly flow variation was monitored with precipitation from the experimental setup at main outlet of sediment settling point (Figure 2.1). Measured precipitation data and runoff were used for calibration and validation of the SWAT sub-daily flow prediction.

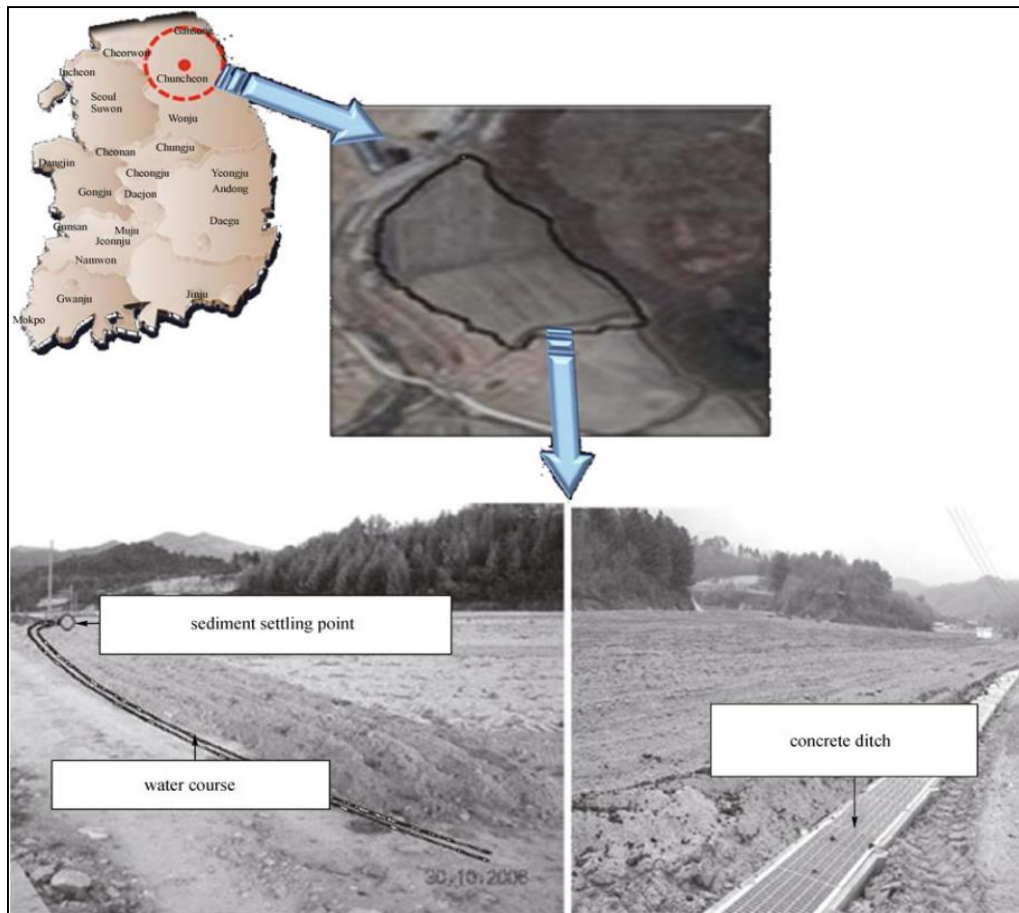


Figure 2.1 Location of study area with drain channel

2.2.2 General rainfall and temperature at the watershed

General rainfall and temperature data are described to provide a brief idea of rainfall and temperature patterns in the study area. Monthly variations in precipitation and average maximum air temperature for the year 2007 and 2008 in the study area are portrayed in Figures 2.2(a) and 2.2(b). The highest amount of precipitation was above 400 mm received in the month of August, 2007 and June, 2008. Average annual precipitation is 1,163 mm, of which more than 75 % occurs during summer (June to September). The average maximum temperature is 30 °C in the month of August and average minimum is below 5 °C in the month of January.

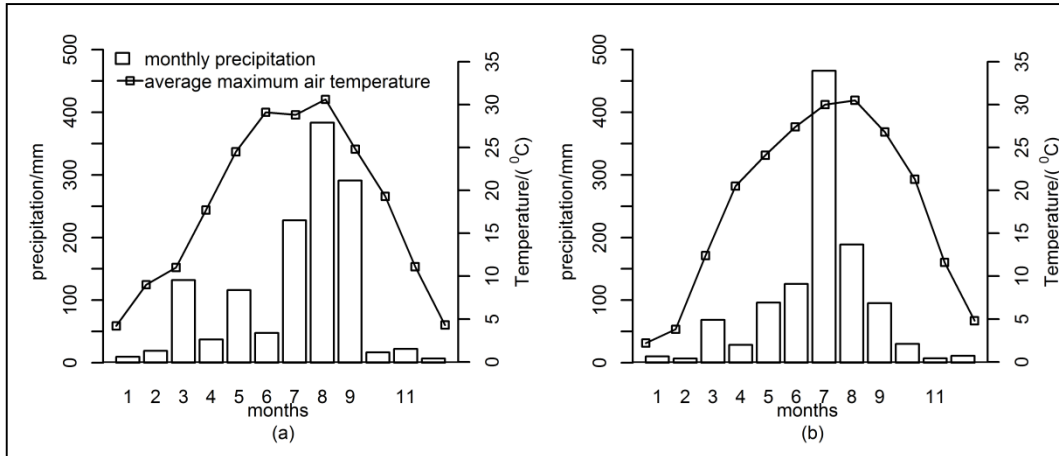


Figure 2.2 Temperature and precipitation for 2007(a) and 2008(b)

2.2.3 Modification of digital elevation model (DEM)

The DEM in SWAT is crucial to divide watershed into several sub-watersheds (sub-basin) for simulation of hydrology and water quality through the channel networks within the watershed. Thus spatial resolution of DEM is important in defining channel networks and sub-watershed boundaries. However, only contours of 5 m is available for the study area, which is not detail enough to route flow generated at each field (sub-basin) to the desired outlet (main outlet) of the study area. In this study, AVSWT 2005 (Di Luzio et al., 2005) was used to delineate sub-watershed boundaries. With 5 m DEM, it was not possible to delineate sub-watershed boundaries as expected. Thus, sub-watershed boundaries were delineated with visual inspection of overland flow paths in the real field after linear interpolation of the 5 m DEM to finer cell size DEM. However, sub divisions of watershed with automatic delineation did not mask the whole watershed as shown in Figure 2.3(a). Thus, manual delineation of sub-watersheds was performed to reflect the study area at the field (Figure 2.3(b)).

The SWAT model estimates field slope length in each sub-basin based on the relationship between average slope and average field slope length (Kim et al., 2009; Neitsch et al., 2002). Average slope values of HRUs were exaggerated with coarse DEM resolution. Thus, measured field slopes and slope lengths were used for each HRU in each sub-basin at the study area. The field slope lengths of 59.5, 70.0, 79.7, 64.4, 50.8 m were used for HRUs in combination with an average slope of 5.5 %, for all with some modifications.

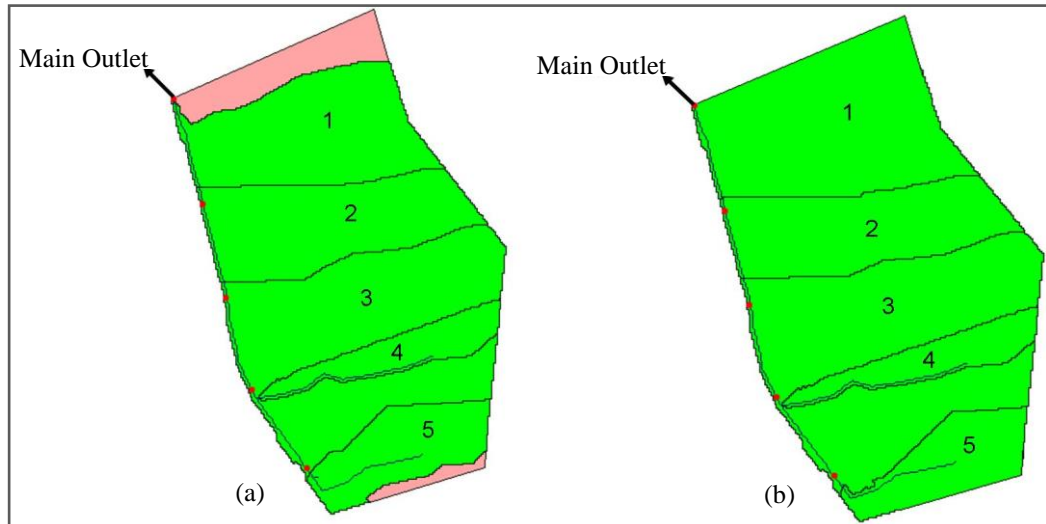


Figure 2.3 Sub-watershed boundaries with manual delineation after automatic delineation. (a) automatic delineation; (b) manual delineation

2.2.4 Land uses, soil, and weather data at the study watershed

The study area consists of agricultural fields with silt loam (21.00 % clay, 52.74 % silt and 26.26 % sand) classified as AnB type. As a common practice in Korea, the field was reconditioned with a layer of 250 mm soil for suitable agricultural production. The farmers recondition their agricultural fields every 2—3 years to compensate soil loss and to provide enough root zone for cash-crops. However, due to heavy cultural operation over the years, saturated conductivity for first two soil layers defined in SWAT has lowered than default values (as set by attribute of soil map) as shown in the study by Heo et al. (2008). With these modifications, the SWAT simulated flow matches the measured flow data well. Table 2.1 shows soil properties that resemble the real field data.

Table 2.1 Soil properties at different soil horizon at the watershed

soil class/AnB	five soil layers from surface				
	Z1	Z2	Z3	Z4	Z5
depth/mm	250	453.2	631	1215.2	1901
bulk density moist/(g·mL ⁻¹)	1.4	10.25	1.35	1.85	1.8
saturated hydraulic conductivity Ksat./ (mm·h ⁻¹)	20	10	20	20	20
organic carbon /(weight %)	2.91	0.97	0.97	0.32	0.11
clay/(weight %)	21	14	14	20	20
silt /(weight %)	52.74	55.62	55.62	7.83	37.83
sand/(weight %)	26.26	30.38	30.38	42.17	42.17

The remaining climatic data required to run SWAT was obtained from the nearest weather station. Sub-daily precipitation data was calculated using Green and Ampt infiltration method for hourly runoff simulation in the study area. The SWAT is capable to locate start date in the data file thereby save time on the user's part. Unlike daily precipitation data, SWAT verifies that the date is correct on all lines. The number of lines of precipitation data per day is determined by the minute that was assigned to IDT variable in file.cio and was set 60 for hourly rainfall data. Sequential lines are assigned to each hour of a rainy day with their corresponding precipitation datum recorded. For non-

rainy days, only one line is required without further lines for every hour in the day indicating year, Julian day and hours with blank delimiter. Table 2.2 shows the file format for sub-daily precipitation in a rainy day. Other climatic data files required for SWAT sub-daily were not changed in daily SWAT run data sets.

Table 2.2 Precipitation data format in SWAT sub-daily run

year	Julian days	hour	PCP/mm
2008	170	00:00	0
2008	170	01:00	0
2008	170	02:00	0
2008	170	03:00	0.5
2008	170	04:00	2
2008	170	05:00	4
2008	170	06:00	3.5
2008	170	07:00	3.5
2008	170	08:00	2.5
2008	170	09:00	2.5
2008	170	10:00	3.5
2008	170	11:00	3.5
2008	170	12:00	1
2008	170	13:00	17
2008	170	14:00	0
2008	170	15:00	0
2008	170	16:00	0
2008	170	17:00	0
2008	170	18:00	0
2008	170	19:00	0
2008	170	20:00	0
2008	170	21:00	0
2008	170	22:00	0
2008	170	23:00	0

2.2.5 Analysis of hourly precipitation

Variations in precipitation during different events for the year 2007 and 2008 are shown in following Figures 2.4(a) and 2.4 (b). The events in 2007 are greater than those in 2008. In recent years, the rainfall pattern changes due to climate changes. The highest precipitation recorded on the 221st day at 15:00 h in 2007 is about 112 mm. The amount of precipitation observed at 13:00, 4:00 and 16:00 h on 220th, 258th and 216th days are 36, 33.5 and 32.5 mm, respectively. The precipitation on the storm event days of 221st, 220th, 247—258th and 216—217th are about 136.5, 71, 92 and 92.3 mm, respectively. The scenario for the year 2008 can be described similarly. The amount of total rainfall that produced runoff was 1474.8 mm during the year 2007, whereas 1140.4 mm during 2008. The crucial analysis of the hourly precipitation data set is important for precise runoff prediction in the SWAT sub-daily runs.

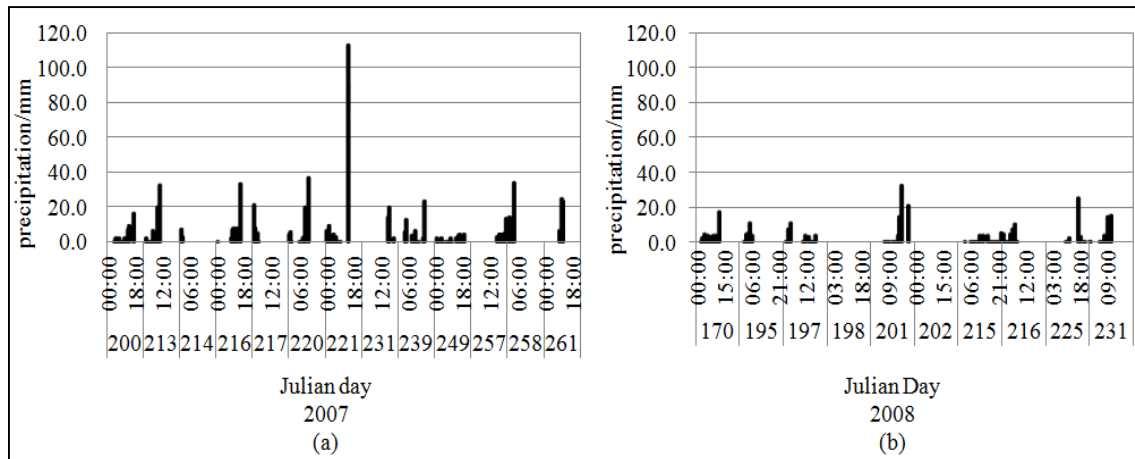


Figure 2.4 Hourly precipitation variation for events of 2007(a) and 2008(b) at the study watershed

2.2.6 Modification in SWAT input files for sub-daily simulation

The SWAT model provides numerous options for prediction of different watershed management practices. The hourly simulation of SWAT in existing shape is not a widely used option among many researchers but it can be a good tool if manual modification in SWAT input files is made. The file *.cio*, **.bsn*, *fig.fig* and *pcp.pcp* are the files that need some modification to their variable in supporting SWAT sub-daily simulation option. The *file.cio* contains the information related to variable for modeling option and climatic input according to the number assigned to the respective variables for the calculation of climatic parameters and others. Basin input file in the SWAT model refers to heterogeneous characteristic of watershed through different variables. The variables IDT and IEVENT in *file.cio* and **.BSN* should be 60 and 3, respectively, for rainfall data file recorded for every 60 min and simulation of runoff using the Green and Ampt infiltration method. The ‘Savecon’ command was added to the existing *fig.fig* file to obtain the hourly simulated result in a separate file. The next important thing for sub-daily run is *pcp.pcp* file, which should be in sub-daily format as shown in Table 2.2. This is a prerequisite according to the modifications made in *.cio*, **.bsn* and *fig.fig* files. In addition to these modifications, the options that were used in this simulation were Priestley-Taylor for Potential Evapotranspiration (PET) and Variable Storage routing method for hourly stream routing. More detailed information for sub-daily run can be found in ‘*input.std*’ file.

2.2.7 Calibration and validation of estimated flow

Calibration and validation of the model are important aspects prior to its application to real world problem. These processes were conducted for reasonable prediction that co-relates the measured value to greater extent. Calibration of a hydrologic component was carried out in accordance with the SWAT user manual and other published literature by SWAT users (Lenhart et al., 2002; Moriasi et al., 2007; Santhi et al., 2001). The most sensitive factors in hydrologic component that had been selected for calibration and validation processes were CN2 (curve number), LAT_TTIME (lateral flow travel time), ESCO (soil evaporation compensation factor), GWQMN (a threshold minimum depth of water in the shallow aquifer required for return flow to occur), GW_DELAY (ground water delay time),

ALPHA_BF (base flow alpha factor) and REVAPMIN (minimum depth of water in shallow aquifer for re-evaporation to occur). Coefficient of determination (R^2) and Nash and Sutcliffe Efficiency (E_{NS}) were used to evaluate SWAT sub-daily performance. The SWAT sub-daily was calibrated with measured sub-daily precipitation data and flow data in the year 2007 and 2008. Total events of 18 events (10 events from 2007 and 8 events from 2008) were considered (9 events for calibration and another 9 events for validation). The hourly simulated values corresponding to considered events were averaged from hourly result to the events due to unavailability of measured hourly flow data from the study watershed for evaluation of SWAT sub-daily simulation. The SWAT daily simulation was also performed in the study with the same input parameter set, which were used in SWAT sub-daily calibration and validation. Comparison of estimated flow using SWAT sub-daily and daily simulations were made to explore impacts of sub-daily precipitation on flow estimation although we can expect different simulated results when calibrating the SWAT with daily option.

2.3 Results and discussion

2.3.1 SWAT hourly simulation

After modification in the input files and sub-daily data, the hourly simulation was done for the study watershed. Hourly-based flow results are summarized for rainfall event days of 2007 and 2008. The summary results are tabulated as shown in Table 2.3. In calibration process, the simulated flow values were compared with the measured values by adjusting values of the sensitive parameters (CN2, LAT_TIME, ESCO, GWQMN, GW_DELAY, ALPHA_BF, REVAPMN). The corresponding values adjusted for the these sensitive parameters during calibration were 80, 0.5 d, 0.98, 50 mm, 10 d, 1.048 and 1 mm, respectively. Also, sensitivity of the SWAT model to various hydrological parameters was analyzed using SWAT models under the same condition of delineated watershed and HRUs. The sensitivity ranking for the parameters is shown in the following Table 2.4 and the sensitivity analysis of CN2, ESCO, GW_DELAY, ALPHA_BF, GWQMN, REVAPMN, LAT_TIME was performed. The plastic mulching and tractor compaction in the study area was significantly observed which cause CN2 with the highest sensitivity ranking than other ground water hydrological parameters.

Table 2.3 Hourly flow results in calibration and validation for each storm events

years	measured precipitation/mm	Julian days (Events)	hourly simulation cubic meter per sec /(CMS)	measured cubic meter per sec /(CMS)	remarks
2007	41.5	200	3.46E-04	1.50E-04	calibrated events
	73	213-214	1.84E-03	1.90E-03	
	92.3	216-217	1.80E-03	1.94E-03	
	71	220	2.44E-03	1.63E-03	
	136.5	221	5.65E-03	6.90E-03	
	35.5	231	1.11E-03	6.02E-04	
	52	239	1.21E-03	1.77E-03	
	25	249	6.53E-04	4.32E-04	
	92	257-258	1.56E-03	3.07E-03	
	53	261	1.88E-03	2.03E-03	
2008	41.5	170	5.16E-05	2.43E-04	validated events
	23	195	1.10E-05	1.62E-04	
	29	197-198	1.88E-05	3.47E-04	
	75	201-202	1.25E-03	1.02E-03	
	24	215	4.73E-05	1.85E-04	
	27	216	2.80E-04	6.71E-04	
	31	225	3.02E-04	3.70E-04	
	39.5	231	9.60E-04	7.75E-04	

Table 2.4 Parameter range of variables derived from sensitivity analysis

parameter	description	range	rank	mean	maximum	variance
ALPHA_BF	base flow alpha factor	0.00 to 2	4	3.51E-03	3.51E-02	3.51E-03
CN2	curve number	-25 to 90	1	6.25E-02	0.20441	6.25E-02
ESCO	soil evaporation compensation factor	0.00 to 1.00	2	1.70E-02	5.62E-02	1.70E-02
GW_DELAY	ground water delay time	-10 to 10	3	1.21E-02	3.07E-02	1.21E-02
GWQMN	a threshold minimum depth of water in the shallow evaporation coefficient	0.00 to 1000	5	0.00E + 00	0.00E + 00	0.00E + 00
REVAPMN	minimum depth of water in shallow aquifer for re-evaporation to occur	-100 to 100	5	0.00E + 00	0.00E + 00	0.00E + 00
LAT_TIME	lateral flow travel time	0.000 to 50.00	5	0.00E + 00	0.00E + 00	0.00E + 00

The corresponding sensitive parameters values were both increased and decreased by 10 % to evaluate its impact on flow estimation. When the sensitive parameters were increased by 10 % (Table 2.5), the simulated flow increased by 70.5 %, while when decreased by 10 % (Table 2.5) the simulated flow decreased by 23.20 %. When the parameters were deviated from fixed values by 10 %, the parameters were observed to be more sensitive toward by increasing than lowering the parameter values. Table 2.6 below shows respective outflow at deviated values of 10 % in the considered parameters.

Table 2.5 Corresponding parameters values at 10 % lower and higher

parameters	values of parameters fixed at calibration and validation	10 % higher	10 % lower
CN2	80	88	72
ESCO	0.98	1.078	0.882
GW_DELAY	10	11	9
ALPHA_BF	1.048	1.1528	0.9432
GWQMN	50	55	45
REVAPMN	1	1.1	0.9
LAT_TIME	0.5	0.55	0.45

Table 2.6 Outflow response at 10 % change in sensitive parameters

measured (CMS)	flow values at fixed parameters hourly	out flow at 10 % higher parameters from fixed	out flow at 10 % lower parameters from fixed	change in flow by 10 % higher parameters values	change in flow by 10 % lower parameters values
1.50E-04	3.46E-04	4.28E-04	2.33E-04	2.36E + 01	3.28E + 01
1.90E-03	1.84E-03	0.001895	1.69E-03	2.99E + 00	8.26087
1.94E-03	1.80E-03	0.001901	0.001723	5.61E + 00	4.277778
1.63E-03	2.44E-03	5.75E-03	2.38E-03	1.36E + 02	2.30E + 00
6.90E-03	5.65E-03	6.02E-03	5.46E-03	6.58E + 00	3.39823
6.02E-04	1.11E-03	1.04E-03	1.14E-03	-6.13E + 00	-2.43E + 00
1.77E-03	1.21E-03	1.30E-03	1.04E-03	7.52E + 00	13.96694
4.32E-04	6.53E-04	5.97E-04	6.40E-04	-8.58E + 00	2.01E + 00
3.07E-03	1.56E-03	0.001692	0.001122	8.43E + 00	28.0641
2.03E-03	1.88E-03	1.95E-03	1.72E-03	3.67E + 00	8.56383
2.43E-04	5.16E-05	2.34E-04	3.93E-05	3.53E + 02	2.38E + 01
1.62E-04	1.10E-05	5.79E-06	5.74E-06	-4.74E + 01	47.81818
3.47E-04	1.88E-05	0.000157	1.36E-05	7.36E + 02	27.71809
1.02E-03	1.25E-03	0.001513	0.000502	2.11E + 01	59.828
1.85E-04	4.73E-05	4.45E-05	2.91E-05	-5.96E + 00	38.52008
6.71E-04	2.80E-04	4.24E-04	1.76E-04	5.16E + 01	37.17857
3.70E-04	3.02E-04	2.72E-04	1.55E-04	-9.80E + 00	48.74172
7.75E-04	9.60E-04	8.69E-04	6.46E-04	-9.50E + 00	32.67708
			total % change	70.5	23.2

Figure 2.5(a) shows flow results during calibration of SWAT sub-daily for the first 9 rainfall events. Overall trend extent of matching simulated flow values with measured during calibration are shown in Figure 2.5(b) with the $R^2 = 0.88$ and $E_{NS} = 0.88$. Rainfall amount and antecedent moisture condition during simulation affect estimated flow data. Hourly simulation results for remaining 9 events during validation (2007—2008) are shown in Figure 2.6(a) and Figure 2.6(b). The R^2 and E_{NS} value for validation are observed to be 0.91 and 0.84. To evaluate the effect of precipitation (measured at interval of 15 min, 1 h, 2 h, 6 h and 12 h) on simulated results, flow out from the study watershed was compared with measured data. The respective R^2 and E_{NS} at these times resolutions are shown in Table 2.7. R^2 and E_{NS} decreases with the increase of time interval considered in measuring precipitation data which depicts that the simulated flow out due to precipitation data recorded at lower interval is better in SWAT sub-daily configuration. With the acceptable values of R^2 and E_{NS} for both calibration and validation in SWAT sub-daily simulation (hourly) for runoff estimation, the SWAT model with sub-daily configuration can be applicable for further scenario analysis at different condition of management practice.

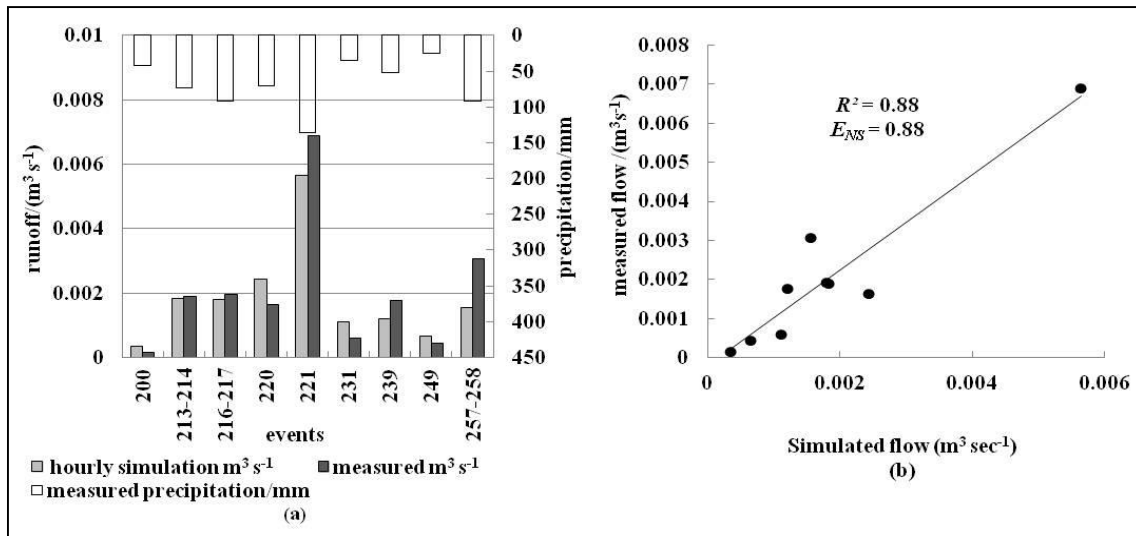


Figure 2.5 Comparison of simulated and measured runoff for calibration: (a) simulated and measured runoff in calibration; (b) comparison of simulated and measured runoff for calibrated events

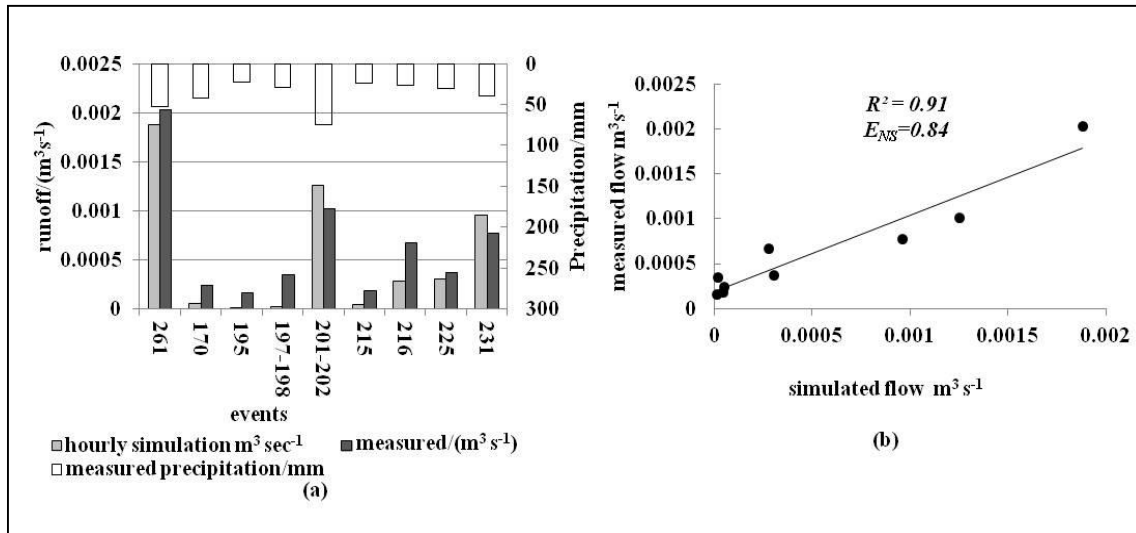


Figure 2.6 Comparison of simulated and measured runoff for validation: (a) simulated and measured runoff in validation; (b) comparison of simulated and measured runoff for validated events

Table 2.7 Simulation result at different time resolution of precipitation records

time resolution of precipitation	15 minute	hourly	2 hourly	6 hourly	12 hourly
ENS	0.804	0.874	0.853	0.83	0.462
R ²	0.817	0.898	0.875	0.855	0.662

2.3.2 SWAT daily simulation

The SWAT sub-daily calibration and validation provides higher R^2 and E_{NS} values, indicating the SWAT sub-daily should be used for exact simulation of runoff generation from field sized watershed. In this study, SWAT daily simulation results were also compared with measured flow data collected at the study area (Figure 2.7(a) and 2.7(b)).

The daily simulation over-estimates for all the events considered during 2007-2008 except for only one event 257—258 is under estimated. The maximum flows during these events occurred in 2007 on the Julian day of 201 and followed by events on Julian day of 220, 216—217 in the same year. In daily SWAT application, the precipitation for corresponding Julian day were summed up daily from the hourly precipitation data which contribute to occur greater amount of flow than measured using SCS CN method in SWAT. The trend and extend of simulated values with measured for flow were found to be R^2 (0.79) and E_{NS} (-0.01) as shown in Figure 2.7(b). The SWAT sub-daily run uses hourly time step precipitation and Green and Ampt infiltration for runoff calculation. The sub-daily SWAT has shown greater accuracy in prediction of runoff closely with higher R^2 and E_{NS} values than SWAT daily simulation considering cumulative rainfall during each hours of the day with SWAT SCS CN method. Hence, with the higher values of R^2 and E_{NS} in SWAT sub-daily simulation in the study, it is realistic to use Green and Ampt option for runoff prediction.

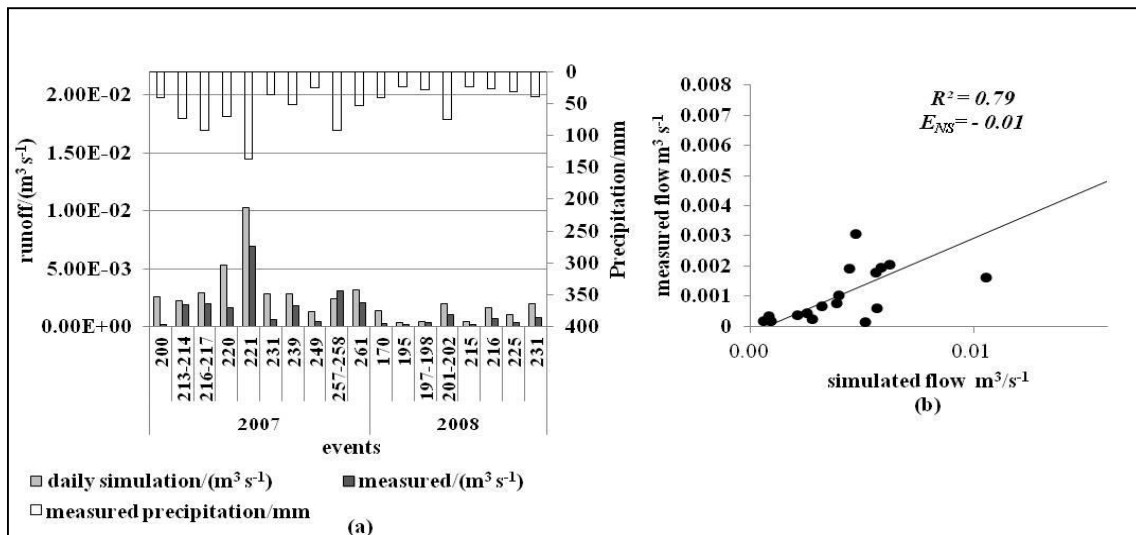


Figure 2.7 Comparison of daily simulated and measured runoff for events of 2007 and 2008 : (a) daily simulated and measured runoff for events of 2007 and 2008; (b) comparison of daily simulated and measured runoff at similar condition of SWAT sub-daily

2.4 Conclusions

In many watersheds, total flow at the watershed outlet is assumed to be the crucial hydrological component which is a driving force of sediment load and other nonpoint source pollution simulation from the watershed. The exact quantification of the flow in combination of sediment and pollutant has always been rationale behind development and application of various hydrologic and water quality model.

In this study, SWAT sub-daily was evaluated for hourly runoff prediction at field-sized study watershed. The evaluation index R^2 and E_{NS} values for predicted runoff from SWAT sub-daily were within acceptable range > 0.80 during calibration and validation in the study. The sensitivity analysis focusing on the hydrological parameters were ranked in sub-daily SWAT configuration wherein CN2

was observed with the highest sensitivity followed by ESCO, GW_DELAY, ALPHA_BF, GWQMN, REVAPMN, LAT_TIME reflecting the field management system of plastic mulching and tractor compaction during cultural operation in the study area. However the model sensitivity was further evaluated in the response of flow from the study area at 10 % change (higher and lower) in sensitivity parameters, resulting in 70.5 % higher and 23.20 % lower in simulated outflow.

The study also comparatively evaluates its results with SWAT daily results for performance evaluation of the SWAT sub-daily, which showed better performance than the daily simulation. The effect of precipitation at different temporal resolution in simulation of flow showed significantly higher values of E_{NS} and R^2 for hourly precipitation than other time resolution (2 h, 6 h and 12 h time resolution) of precipitation. Hence it was found that the SWAT sub-daily with Green-Ampt infiltration method was proven to be efficient for runoff estimation at field sized watershed with higher accuracies and the results can be efficiently used to develop site-specific Best Management Practices (BMPs) considering rainfall intensity, rather than simply daily rainfall data. With the result of the study, it is advisable to use SWAT sub-daily simulation for critical analysis of field scale watershed in runoff estimation. The SWAT sub-daily with higher accuracies in flow estimation could be used to evaluate the various BMPs, such as Vegetated Filter Strip (VFS) using sub-daily time step VFSSMOD modeling system because the SWAT VFS module uses very simple regression equation to evaluate the VFS.

Although promising result was obtained from SWAT sub-daily flow estimation, more in-depth researches are needed for accurate simulation of sediment and nonpoint pollutant loading estimation using SWAT sub-daily.

2.5 Acknowledgements

This research was supported by Nancy Sammons at Texas A&M University, USA for her technical support in initial stage of SWAT sub-daily run for the study watershed. This research was supported by the Eco-Star Project (code: EW32-07-10) in Korea.

2.6 References

- Arnold, J.G., P.M. Allen, 1996 Estimating hydrologic budgets for three Illinois watersheds. *Journal of Hydrology*. **176**: 57-77.
- Beasley, D.B., L.F. Huggins, E.J. Monke, 1980 ANSWERS: A model for watershed planning. *Transactions of the ASAE. American Society of Agricultural Engineers*. **23**: 938-944.
- Clemente, R.S., S.O. Prasher, S.F. Barrington, 1993 PESTFADE, a new pesticide fate and transport model: model development and verification. *Transactions of the ASAE. American Society of Agricultural Engineers*. **36**: 357–367.
- Cotter, A., 2002 Critical Evaluation of TMDL data requirements for agricultural watersheds. Dissertation Master degree.
- Debele, B., R. Srinivasan, J.Y. Parlange, 2009 Hourly analyses of hydrological and water quality simulations using the ESWAT Model. *Water Resources Management*. **23**: 303-324.
- Di Luzio, M., G. Mitchell, Sammons N, 2005 N. AVSWAT-X short tutorial Watershed Modeling using SWAT 2003. In: *Proceedings of Third Conference on Watershed Management to Meet Water Quality Standards and Emerging TMDL*. Georgia: Sheraton Atlanta.: 5-9.
- Di Luzio, M., J.G. Arnold, 2004 Formulation of a hybrid calibration approach for a physically based distributed model with NEXRAD data input. *Journal of Hydrology*. **293**: 136-154.
- Donigian, A.S., B.R. Bicknell, J.C. Imhoff, 1995 Hydrological simulation program Fortran (HSPF). In: Singh, V.P. *Computer Models of Watershed Hydrology*. Colorado: WRP, Highlands Ranch: 395–442.
- Heo, S., M.S. Jun, S. Park, K.S. Kim, S.K. Kang, Y.S. Ok, K.J. Lim, 2008 Analysis of soil erosion reduction ratio with changes in soil reconditioning amount for highland agricultural crops. *Journal of Korean Society on Water Quality*. **24**: 185–194.
- Kannan, N., S.M. White, F. Worrall, M.J. Whelan, 2007 Hydrological modelling of a small catchment using SWAT-2000 Ensuring correct flow partitioning for contaminant modelling. *Journal of Hydrology*. **334**: 64-72.
- Kim, J.-G., Y. Park, D. Yoo, N.-W. Kim, B.A. Engel, S.-j. Kim, K.-S. Kim, K.J. Lim, 2009 Development of a SWAT patch for better estimation of sediment yield in steep sloping watersheds. *JAWRA Journal of the American Water Resources Association*. **45**: 963-972.
- King, K.W., J.G. Arnold, R.L. Bingner, 1999 Comparison of Green–Ampt and Curve Number Methods on Goodwin Creek Watershed Using SWAT. *Transactions of the ASAE*. **42**: 919-925.
- Knisel, W.G., 1980 CREAMS, A field scale model for chemical, runoff and erosion from agricultural management systems. Conservation Report.
- Lane, L.J., M.A. Nearing, 1989 USDA - Water erosion prediction project: Hillslope profile model documentation. . NSERL Report.
- Lenhart, T., K. Eckhardt, N. Fohrer, H.G. Frede, 2002 Comparison of two different approaches of sensitivity analysis. *Physics and Chemistry of the Earth*. **27**: 645-654.
- Leonard, R.A., W.G. Knisel, D.A. Still, 1987 GLEAMS: groundwater loading effects of agricultural management systems. *Transactions of the ASAE. American Society of Agricultural Engineers*. **30** 1403–1418.
- Lim, K.J., B.A. Engel, 2003 Extension and enhancement of national agricultural pesticide risk analysis (NAPRA) WWW decision support system to include nutrients. *Computers and Electronics in Agriculture*. **38**: 227-236.

- Moriasi, D.N., J.G. Arnold, M.W. Van Liew, R.L. Binger, R.D. Harmel, T.L. Veith, 2007 Model evaluation guidelines for systematic quantification of accuracy in watershed simulations. *Transactions ASABE*. **50**: 885-900.
- Neitsch, S.L., J.G. Arnold, J.R. Kiniry, R. Srinivasan, J.R. Williams, 2002 Soil and water assessment tool user's manual version 2000. Water Resources Institute, College Station, Texas TWRI Report, TR-192.
- Rawls, W.J., L.R. Ahuja, D.L. Brakensiek, A. Shirmohammadi, 1993 Infiltration and Soil Water Movement. In: Maidment D R, editor, New York: Mc Graw-hill.
- Santhi, C., J.G. Arnold, J.R. Williams, W.A. Dugas, R. Srinivasan, L.M. Hauck, 2001 Validation of the swat model on a large Rwer Basin with point and nonpoint sources. *JAWRA Journal of the American Water Resources Association*. **37**: 1169-1188.
- Shepherd, B., D. Harper, A. Millington, 1999 Modelling catchment-scale nutrient transport to watercourses in the U.K. *Hydrobiologia*. **395-396**: 227-238.
- Shrestha, S., M.S. Babel, A.D. Gupta, F. Kazama, 2006 Evaluation of annualized agricultural nonpoint source model for a watershed in the Siwalik Hills of Nepal. *Environmental Modelling & Software*. **21**: 961-975.
- Tripathi, M.P., R.K. Panda, N.S. Raghuwanshi, 2003 Identification and prioritization of critical subwatershed for soil conservation management using the SWAT model. *Biosystems Engineering*. **85**: 365-379.
- Williams, J., A. Nicks, J. Arnold, 1985 SWRRB: Simulator for Water Resources in Rural Basins. *Journal of Hydraulic Engineering*. **111**: 970-986.
- Williams, J.R., 1980 SPNM, a model for predicting sediment, phosphorus, and nitrogen yields from agricultural basins. *Water Resources Bulletin*. **16**: 843-848.
- Williams, J.R., P.T. Dyke, C.A. Jones, 1982 EPIC—A model for assessing the effects of erosion and soil productivity. In: *Proceedings of the Third International Conference on State-of-the Art in Ecological Modeling*.: 156–158.
- Wischmeir, W.H., D.D. Smith, 1978 Predicting rainfall erosion losses. *Agricultural Handbook*.
- Young, R.A., C.A. Onstad, D.D. Bosch, W.P. Anderson, 1994 Agricultural non-point source pollution model. *AGNPS User's Guide, USDAARS, Version 4.03*.

Chapter 3 Using the SWAT model to improve process descriptions and define hydrologic partitioning in South Korea

Christopher L. Shope^{1,*}, Ganga Ram Maharjan², John Tenhunen², Bumsuk Seo², Kiyong Kim², Jeanne Riley², Sebastian Arnhold³, Thomas Koellner⁴, Yong Sik Ok^{5,6}, Stefan Peiffer¹, Bomchul Kim⁷, Ji-Hyung Park⁸, and Bernd Huwe³

¹University of Bayreuth, Dept. of Hydrology, Universitatstrasse 30, 95440 Bayreuth, Germany

²University of Bayreuth, Dept. of Plant Ecology, Universitatstrasse 30, 95440 Bayreuth, Germany

³University of Bayreuth, Dept. of Soil Physics, Universitatstrasse 30, 95440 Bayreuth, Germany

⁴University of Bayreuth, Professorship of Ecosystem Services, Universitatstrasse 30, 95440 Bayreuth, Germany

⁵Kangwon National University, Dept. of Biological Environment, 192-1 Hyoja-Dong, Gwangwon-do, Chuncheon 200-701, Republic of Korea

⁶University of Alberta, Dept. of Renewable Resources, Alberta, Canada

⁷Kangwon National University, Dept. of Env. Science, 192-1 Hyoja-Dong, Gwangwon-do, Chuncheon, 200-701, Republic of Korea

⁸EWHA Womans University, Dept. of Environmental Science and Engineering, Seoul 120-750, Republic of Korea

*now at: US Geological Survey, 2329 Orton Circle, Salt Lake City, UT, USA

Abstract

Watershed-scale modeling can be a valuable tool to aid in quantification of water quality and yield; however, several challenges remain. In many watersheds, it is difficult to adequately quantify hydrologic partitioning. Data scarcity is prevalent, accuracy of spatially distributed meteorology is difficult to quantify, forest encroachment and land use issues are common, and surface water and groundwater abstractions substantially modify watershed-based processes. Our objective is to assess the capability of the Soil and Water Assessment Tool (SWAT) model to capture event based and long-term monsoonal rainfall–runoff processes in complex mountainous terrain. To accomplish this, we developed a unique quality-control, gap-filling algorithm for interpolation of high-frequency meteorological data. We used a novel multi-location, multi-optimization calibration technique to improve estimations of catchment-wide hydrologic partitioning. The interdisciplinary model was calibrated to a unique combination of statistical, hydrologic, and plant growth metrics. Our results indicate scale-dependent sensitivity of hydrologic partitioning and substantial influence of engineered features. The addition of hydrologic and plant growth objective functions identified the importance of culverts in catchment-wide flow distribution. While this study shows the challenges of applying the SWAT model to complex terrain and extreme environments; by incorporating anthropogenic features into modeling scenarios, we can enhance our understanding of the hydroecological impact.

Keywords: *Agricultural soils, Dye tracers, Preferential flow, Flow patterns, Ridge cultivation, Tillage management*

3.1 Introduction

Land use and land cover (LULC) distribution can have a substantial influence on catchment water balance due to localized precipitation, evaporation, transpiration, soil moisture redistribution, and crop associated temporal variations in surface runoff. The effects of land use change, including deforestation (Forti et al., 1995), agricultural intensification (Berka et al., 2001), yearly variations in agricultural land use (Tilman et al., 2002), and construction of roads, culverts, and sediment detention ponds (Strauch et al., 2014) on stream discharge and water quality occur at many spatial and temporal scales. Deforestation significantly affects streamflow characteristics (Calder, 1992) by increasing erosion and decreasing soil moisture and soil nutrient concentrations. Agricultural intensification influences surface runoff by altering infiltration, evaporation, and timing of runoff. As agricultural land use increases, the need for water resources management increases, particularly in complex topography driven by extreme events.

The water resources of the Haean catchment in South Korea are important to quantify because the catchment represents an important contributor to the Han River and the Soyang Lake watershed, which is a major drinking water source for major metropolitan areas including the city of Seoul (Jo and Park, 2010). The catchment is also a significant source of sediment and nutrients due to the high agricultural activity and forest encroachment (Jung et al., 2012; Lee et al., 2014). Small-scale agriculture is the largest economic activity within the basin, engaging 85 % of the population and up to 44 % of the available land area within the catchment. Increasing agricultural encroachment into the forest region imposes a significant risk to water yield and quality with a reduction in forested area by 37 % over the past 20 yr (Kim et al., 2011). Furthermore, routing and flow management in Haean has significantly increased the erosive power and decreased infiltration during individual events (Arnhold et al., 2013). Previous studies have suggested an appreciable decline in aquatic species, attributed in large part to an increase in fine grain sediment erosion and nutrient concentrations (B. Kim, personal observation, 2010; Jun, 2009). Since the end of the Korean War in 1953, a variety of amelioration measures such as river regulation, installation of catchment drainage systems, and waste water treatment plants (WWTPs) have been implemented in order to enlarge communities and increase local agricultural production. These measures have led to a change in the catchment-wide water balance, spatiotemporal nutrient dynamics, and floodplain ecology (Jun, 2009). Several conservation projects have been implemented within the Haean catchment and throughout South Korea to limit and effectively manage soil erosion including retention pond construction, modification of riparian channel widths, and channel reinforcement. Consequently, the landscape has been intensively altered, creating a mosaic of ecohydrologic landscape patterns. Surface water and groundwater abstractions, dam and reservoir operations, and engineered hydraulic structures (culverts, sediment ponds, and roads) have disrupted the natural hydrology of the catchment. In higher elevations, surface water flow has been observed to be entirely depleted over extended stretches due to domestic and irrigation abstractions for dryland farms (Shope et al., 2013). Previous research has indicated that seasonal precipitation, as well

as individual events, influences the hydrologic flushing of organic materials from the land surface (Jung et al., 2012; Lee et al., 2014). The longterm interdisciplinary research group TERRECO (Tenhunen et al., 2011), has collected spatiotemporal terrestrial surface runoff measurements to calculate sediment yield (Arnhold et al., 2013), conduct dye tracer experiments to estimate soil structure and variably saturated flow and transport processes (Ruidisch et al., 2013), and examine groundwater and surface water exchange on spatiotemporal fluxes and nearstream biogeochemistry (Bartsch et al., 2014). To quantify overland runoff, sediment transport, and soil loss from individual crops under specific management practices, it is critical to understand sustainable resource allocation and scenario implications in this agriculturally productive, complex terrain.

Coupled hydrological and crop production watershed-scale models are a useful tool to simulate the interactions of catchment physical characteristics, agricultural practices, and weather inputs on the water yield and to evaluate conservation practices in locations with limited observational data (Cho et al., 2012). Model scenarios can be helpful in identifying reasonable measures for assessing environmental ecological status (Lam et al., 2012; Volk et al., 2009). Gassman et al. (2007) found that the distributed Soil and Water Assessment Tool (SWAT) model was a promising model for predominately agricultural watersheds located throughout the world when compared to several other integrated watershed models. SWAT has also been successfully applied in a wide variety of data-limited studies, particularly in South Korea (Lee et al., 2012, 2011; Stehr et al., 2008; Mekonnen et al., 2009). We use the SWAT model because it is a well documented, efficient model that couples long-term climate, land use, and management practices to evaluate catchment-wide hydrology.

This study builds upon multiple research investigations distributed throughout the Soyang Lake watershed by implementing the SWAT ecohydrologic model within the Haeon catchment to quantify hydrologic processes and catchment-wide flow partitioning. Our objectives are to (1) assess the potential of a spatiotemporal algorithm to improve discretization of monitored precipitation, (2) characterize the spatiotemporal river discharge patterns at multiple locations throughout the monsoon driven catchment through multiobjective optimization, (3) determine the capability of the SWAT model to capture daily monsoonal rainfall–runoff processes in complex mountainous terrain, and (4) quantify the significance of engineered structures (roads, culverts, sedimentation ponds) on flow partitioning. To accomplish these objectives, we utilized robust and comprehensive, spatiotemporal river discharge estimates at 14 locations throughout the Haeon catchment to quantify flow partitioning. We discuss the construction of the ecohydrologic SWAT model for the Haeon catchment, the selection and sensitivity of model parameters, and the calibration and validation of the model. Finally, we evaluate three different river routing systems including (1) the surface water drainages; (2) a combination of the rivers and engineered culverts; and (3) the rivers, culverts, and road network, to identify flow partitioning throughout the catchment.

3.2 Catchment characteristics

The Haean catchment study area (38.239–38.329° N, 128.083–128.173° E) is located in the Gangwon Province of the northeastern portion of South Korea along the demilitarized zone (DMZ) between South and North Korea (Figure 3.1). The 62.7 km² catchment has a unique bowl-shaped physiographic characteristic with elevation ranging between 339 to 1321 m a.s.l., which drastically alters the local meteorological conditions. The catchment drainage is the Mandae River with a maximum length of 8.6 km. Limited historical observations are available, although this is typical for most areas outside of Europe and North America. The average catchment discharge at the outlet is 4.32 m³ s⁻¹ (1.20–379 m³ s⁻¹) while the average discharge at the S1 headwater monitoring location is 0.03 m³ s⁻¹ (1.4 × 10⁻⁴–10.0 m³ s⁻¹). The catchment hydrology is further described in Shope et al. (2013). The catchment is 56 % forested and 44 % agricultural LULC.

Geologically, the basin is composed of a Precambrian gneiss complex at the higher elevation mountain ridges and a highly weathered Jurassic biotite granite intrusion that was subsequently eroded throughout the central portion of the catchment (Kwon et al., 1990). Alluvium generally extends up to 2 m in depth and bedrock is typically observed between 20 and 45 m below land surface in the catchment interior. Surficial soil texture is typically saprolitic sand and sandy loam with high infiltration capacity (Arnhold et al., 2013; Jo and Park, 2010).

The climate in South Korea is humid continental to humid subtropical, influenced by the East Asian summer monsoon and early autumn typhoons. The monsoon season extends from the end of June through the end of July, followed by scattered events through early September, with up to 70 % of the total annual precipitation between the months of June and August. The average annual rainfall over the most recent 12 yr of record is 1514 mm (930 to 2299 mm yr⁻¹) with a maximum precipitation as high as 48.6 mm h⁻¹ or up to 223.2 mm d⁻¹. The average annual temperature is 8.65 ± 0.35 °C ranging between -26.9 °C in January to 33.4 °C in August. Choi et al. (2010) found that the temperature lapse rate within the Haean catchment ranged between -0.56 °C 100 m⁻¹ throughout the spring to +1 °C 100 m⁻¹ during early morning inversions after many consecutive sunny days.

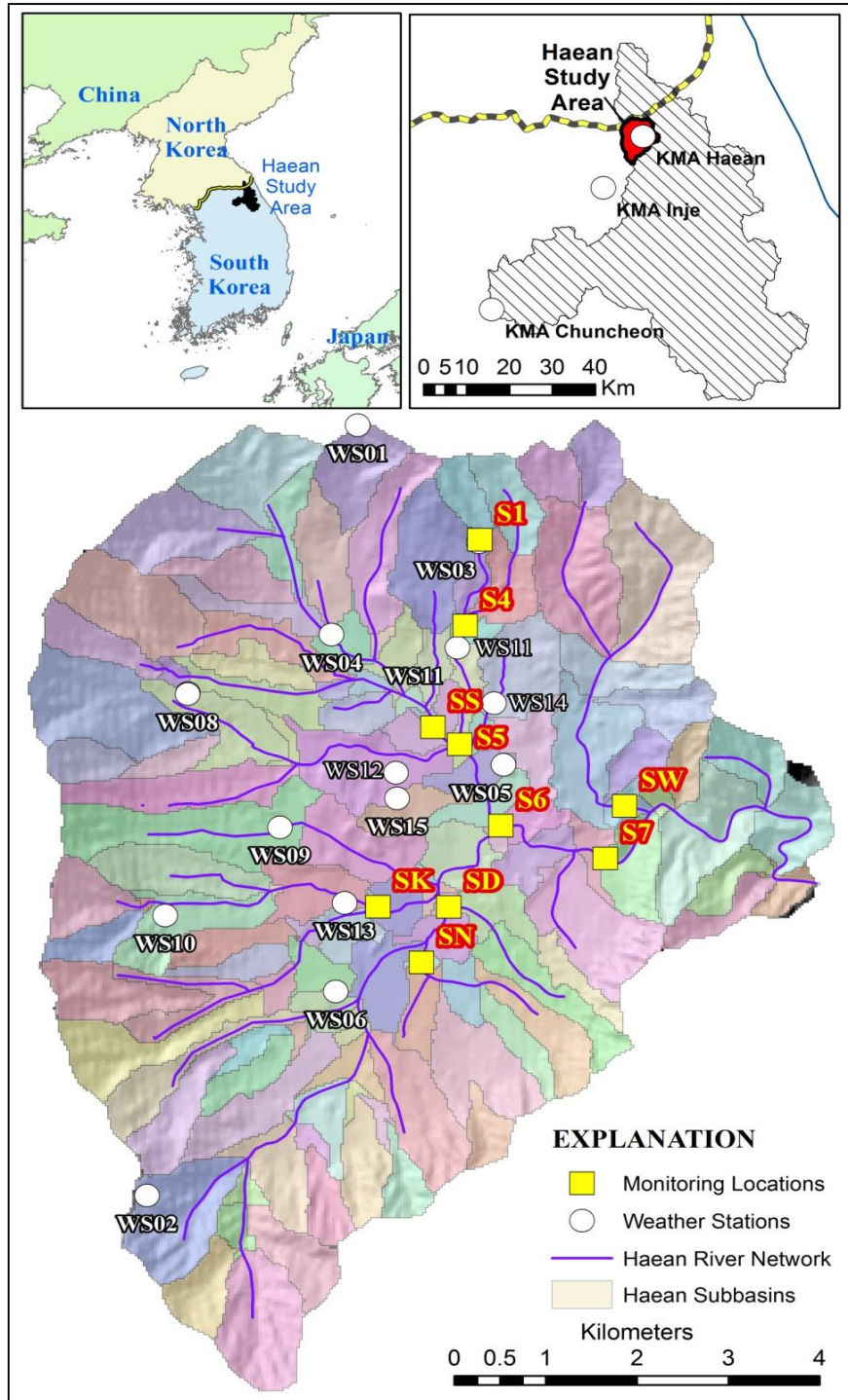


Figure 3.1 Haeon study area within the Lake Soyang watershed is located in northeastern South Korea along the demilitarized zone (DMZ) border with North Korea. The regional KMA weather station and local meteorological stations are denoted with white circles and (WS). River discharge monitoring locations are denoted by (S) and the yellow squares

3.3 Methods and model Construction

3.3.1 Model description

The SWAT model is a continuous, physically based, distributed model originally developed to predict the long-term impact of climate and land use management practices on hydrologic, sediment, and agricultural chemical yields in large, complex basins (Arnold et al., 1998). Essentially, SWAT uses the water balance approach to simulate watershed hydrologic partitioning as described by Neitsch et al. (2010). Catchments are divided, typically on a topographic basis, into spatially linked subbasins and the subbasins are segregated into unique hydrological response units (HRUs) by integrating the combination of LULC, soil type, and slope to describe the system physical heterogeneity. The modeled hydrological components include surface runoff, percolation, lateral flow, groundwater flow, evapotranspiration (ET), and transmission losses. The simulation of watershed hydrology with SWAT is split into the land phase and the channel or routing phase of the hydrologic cycle, which controls the amount of water, sediment, and nutrients into the main channel in each subbasin and through the channel network to the watershed outlet (Neitsch et al., 2011). Incoming precipitation is partitioned into canopy storage, infiltration, and surface runoff through either the SCS (Soil Conservation Service) curve number (CN) method (U.S.D.A., 1972) or the Green–Ampt (Green and Ampt, 1912) method. Daily runoff volume from the SCS retention parameter can be calculated through the shallow soil water content or through accumulated plant ET. The SCS curve number method with calculated plant evapotranspiration was selected for the Haean catchment simulations. The hydrologic condition of the vegetation is important in determining CN for individual HRUs (U.S.D.A., 1972). Therefore, the distributed CN was further modified within individual HRUs through time-variable LULC characterization and crop growth. The model uses the modified Rational Method to estimate peak flow (Neitsch et al., 2011). Runoff in SWAT is aggregated from the HRU level into the subbasin level and then routed through the stream network. The Manning equation is used to estimate the flow rate and velocity through the channels. Flow routing is based on either the variable storage or the Muskingum routing method; and for this study, we chose the variable storage method (Neitsch et al., 2011).

3.3.2 Model inputs

3.3.2.1 Climate data

Hourly climate data for the period from 1998 to 2011 were measured and collected from several regional stations of the Korean Meteorological Agency (KMA) (Figure 3.1). Precipitation and minimum/maximum temperature were obtained from the Haean KMA station (38.287° N, 128.148° E). Relative humidity, temperature, and wind speed were obtained from the Inje KMA station in the adjacent Yanggu County (38.207° N, 128.017° E). Solar radiation was collected from the Chuncheon KMA station (37.904° N, 127.749° E). Distributed climate data were also collected from 15 micrometeorological stations (Delta-T Devices, Ltd.) throughout the catchment (Figure 3.1) between 2009 and 2011. Sub-hourly data was aggregated into hourly precipitation (± 0.2 mm), minimum/maximum air temperature ($\pm 0.2^\circ$ C), wind speed (± 0.1 m s⁻¹), solar radiation (± 5 Wm⁻²), and

relative humidity ($\pm 2\%$). Each parameter was quality controlled by removing erroneous data and then gap filling from a similar station using a weighted algorithm based on elevation, station proximity, and aspect. The algorithm, as formulated for precipitation, is presented as

$$P_e(z, d, \varphi) = \left\{ \begin{array}{l} [_{i=1}^{\alpha}(p_o[\text{minimize}_{i=1}^{\nu}(\varphi_e - \varphi_o)])\omega_3] + \dots \\ \left[\left([_{i=1}^{\alpha} \left[\left(\frac{d_x}{d_x + d_y} \right) \cdot |p_x - p_y| \right] + p_x \right) \omega_2 \right] + \dots \right. \\ \left. [_{i=1}^{\alpha}(p_o[\text{minimize}_{i=1}^{\nu}(z_e - z_o)])\omega_1] \right\} \quad 3.1$$

The variable P_e is the estimated precipitation (mm), z is the elevation (m), d is the distance to the observation point (m), φ is the observation point aspect (deg.), i is the time step, α is the total number of consecutive missing data, P_o is the observed precipitation (mm), ν is the total number of observational meteorological stations, j is the cumulative number of stations, the “e” and “o” subscripts are the estimated and observed location values, ω is the weighting factor, and x and y subscripts are the first and second most proximal locations to the estimation location, respectively. Locally based relative humidity was modified by accounting for the temperature dependent local dew point. The SWAT model does not explicitly interpolate spatial meteorological conditions but instead, prescribes the nearest weather station parameters to the centroid of each subbasin (Neitsch et al., 2011). Due to the large variation in topographical complexity throughout the catchment, precipitation volume, soil moisture, and plant growth were impacted when SWAT assigned the meteorological data to each subbasin. We tested several interpolation methods to grid the measured meteorology results throughout the catchment (inverse distance weighted (IDW), spline, nearest neighbor, and kriging). The IDW method performed optimally and was used to grid the measured meteorological results throughout the catchment and the virtual weather corresponding to each subbasin centroid was prescribed. Principle data sources used for the Haeon catchment ecohydrologic model are provided in Table 3.1. Choi et al. (2010) found highly variable temperature lapse rates, implying that stagnant East Asian monsoon high pressure systems can significantly vary climatic conditions on a local scale. A temperature lapse rate of $-0.52^{\circ}\text{C } 100 \text{ m}^{-1}$ was incorporated into the continuous spatial interpolation for temperature.

Table 3.1 Principle input data sets for the construction of the Haean catchment SWAT model

Data set	Agency	Data set type	Scale
(a) Spatial data sets			
General boundaries	GADM ^a	Bathymetry, coastline, roads, lakes, rivers, counties, watersheds	1 : 10 000
Watershed DEM	NGII ^b	Clipped DEM from Soyang Lake contour map	1 : 25 000
Stream channels	TERRECO ^c	Hydrologically corrected high-density flow network	1: 10 000
Soils	RDA ^d	Clipped from Soyang Lake surficial soils map	1 : 25 000
Soils	TERRECO ^e	From 2009–2011 field based shallow soil (1.2) m observations	1 : 10 000
Land cover	TERRECO ^f	Agriculture and Forest field validated LULC	1 : 5000
(b) Temporal data sets			
Precipitation, temperature	KMA ^g	Haean Cooperative Network weather station (1998–2009)	Point
Relative humidity, wind speed	KMA ^g	Yanguu Cooperative Network weather station (1998–2009)	Point
Solar radiation	KMA ^g	Chuncheon Cooperative Network weather station (1998–2009)	Point
Local meteorology	TERRECO ^h	TERRECO stations, 15 in catchment (2009–2011)	Point
WWTP point sources	YCO ⁱ	Wastewater treatment statistics at 5 plants (2002–2010)	Point
Discharge and loads	TERRECO ^j	Field-based, discharge measurements (2003–2011)	Point
Agricultural management data	TERRECO ^k	Farmer, county, administrative interviews and field-based plots	

^a GADM – Global Administrative Areas. ^b NGII – National Geographic Information Institute. ^c TERRECO – Field-based TERRECO IRTG observations, GPS surveyed perennial and ephemeral stream channels. ^d RDA – Rural Development Administration. ^e TERRECO – Field-base ^d TERRECO IRTG observations, 2009–2011 test pits, soil samples, soil characterization. ^f TERRECO – Field-based TERRECO IRTG observations, 2009 (36 classes), 2010 (114 classes), 2011 (100 classes). ^g KMA – Korean Meteorological Weather Station Network. ^h TERRECO – Field-based TERRECO IRTG observations, 2009–2011 (precipitation, temperature, relative humidity, wind speed, solar radiation). ⁱ YCO – Yanguu County Office, wastewater treatment statistics 2003–2010. ^j TERRECO – Field-based, spatially distributed, discharge measurements as described in Shope et al. (2013). ^k TERRECO – Field-based, spatially distributed plots of example management and interviews with multiple stakeholders.

3.3.2.2 Discharge and evapotranspiration estimates

Event-based and baseflow surface water discharge measurements were collected at up to 14 locations throughout the catchment between 2003 and 2011 (Figure 3.1) through multiple methods as described by Shope et al. (2013). Observed streamflow at interior locations within the catchment (S1, S4, S5, and S6) and the catchment outlet (S7) were utilized for daily and monthly model calibration to better parameterize spatial variability in hydrologic partitioning. These monitoring locations are distributed throughout the catchment along an elevation gradient with increasing drainage area and provide regional representation of model parameterization. In addition, the unique punchbowl shape enabled the calibration parameters to be correlated to other ungauged subcatchments with similar slope, elevation, and aspect.

Spatiotemporal aquifer contributions were investigated by quantifying the relative baseflow from the hydrograph using several baseflow separation techniques including differential discharge measurements and recession analysis (Shope et al., 2013). For estimate consistency between each of the monitoring locations, we applied a recursive digital filter to separate the low-frequency baseflow signal from the high-frequency runoff in the formulation described by Eckhardt (2005). The calculated baseflow was subsequently compared to the SWAT modeled baseflow contribution.

The SWAT model also includes several methods to calculate potential evapotranspiration (PET) (Hargreaves and Samani, 1985; Monteith, 1965; Penman, 1948; Priestley and Taylor, 1972) depending

on the observational meteorological data available. Because of the robust and highfrequency spatially variable micrometeorologic data available through the TERRECO project, we simulated daily PET using the Penman–Monteith method (Penman, 1948). As described in Ruidisch et al. (2013) and Shope et al. (2013), the weather conditions throughout the catchment are heterogeneous and therefore, the physically based Penman–Monteith estimates were preferred over the alternative methods. Soil evaporation and crop transpiration were estimated using the FAO Penman–Monteith equation as described in Allen et al. (1988).

3.3.3 Spatial data

3.3.3.1 DEM

The Soyang watershed 30 m resolution digital elevation model (DEM) obtained from the National Geographic Information Institute (NGII) was clipped to the extent of the Haeon catchment boundaries (Figure 3.1). The Haeon catchment was divided into three slope classes representing steep forested high elevation (10° to 90°), moderately sloped dry land agriculture (2° to 10°), and mildly sloping rice paddies in the central portion of the catchment (0° to 2°) (Table 3.2). The observed river network was geo-referenced and explicitly incorporated into the DEM because modification of stream channels in highly managed catchments is prevalent and inclusion of stream delineation improves hydrologic segmentation and boundary delineation. In addition, extensive ground-based surveys of engineered channels, diversions, culverts, drainage features, sediment retention ponds, and roads throughout the Haeon catchment were completed. To investigate the role that engineered structures have in channel routing, three channel classifications were constructed for (1) the river network; (2) the river network and engineered culverts; and (3) the river network, culvert system, and existing roads (Figure 3.2). We implemented the engineered structures in SWAT by sequentially adding them to the prescribed river network and we superimpose the modified networks onto the DEM. The roads and culverts were then prescribed as impervious channels with no transmission loss on the river network. Therefore, we had three complete model constructs from the beginning to the end with different hydrographic segmentation and subbasin boundary delineation.

Table 3.2 Percentage of Haeon catchment associated with the individual aggregated land use, soil, and slope classifications. The slope classification generally defines the difference between forest, dryland farming, and rice paddy systems throughout Haeon

Category	Area (km ²)	Percent watershed	Category	Area (km ²)	Percent watershed
Landuse			Soils		
Barren soil	5.92	9.43 %	Flat dry soil	8.07	12.87 %
General beans	1.63	2.60 %	Forest soil	19.74	31.46 %
Rice	8.53	13.59 %	Moderately steep dry soil	8.33	13.28 %
General cabbage	3.21	5.12 %	Rice paddy soil	13.78	21.96 %
Coniferous forest	0.04	0.06 %	Sealed ground	12.47	19.87 %
Deciduous forest	35.29	56.25 %	Very steep forest soil	0.35	0.55 %
Ginseng	0.81	1.29 %	Slope		
Inland water	0.03	0.04 %	Low slope rice paddy	8.02	12.79 %
Residential land use	1.05	1.67 %	Moderate slope dryland	17.43	27.78 %
Maize	0.52	0.83 %	Steep slope forest uplands	37.28	59.43 %
General orchards	0.86	1.36 %			
Potato	2.47	3.93 %			
Radish	2.12	3.38 %			
Codonopsis	0.28	0.44 %			

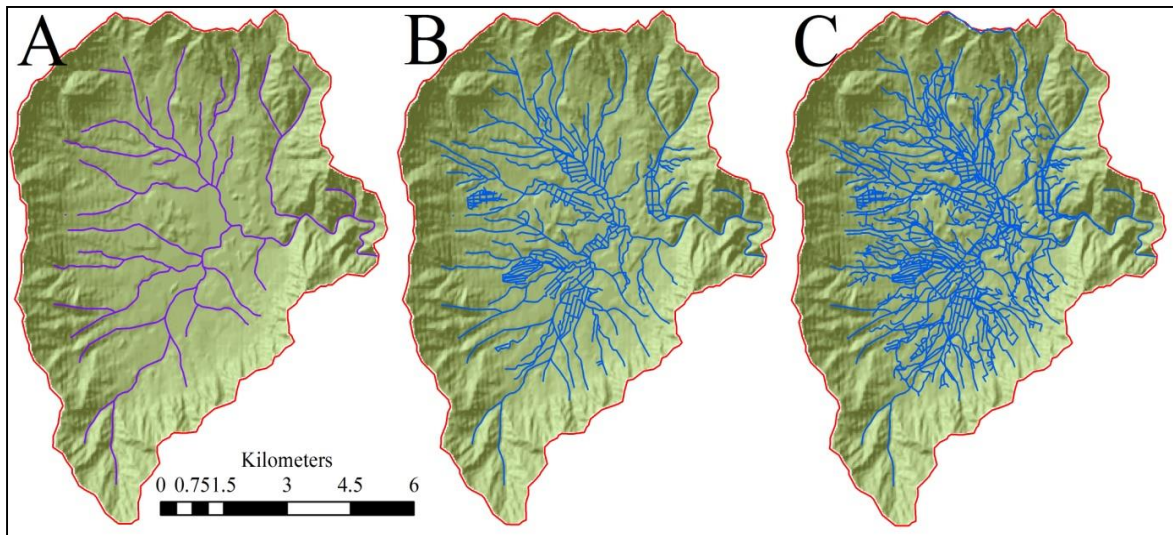


Figure 3.2 Multiple river system and infrastructure model configurations within the Haeon catchment which, contribute to surface discharge accumulation and flow routing. The panels display the configuration for (A) solely the Haeon river network; (B) the river network and engineered culvert drainage system; and (C) the river network, the culvert system, and the road infrastructure

3.3.3.2 Soils

Regional soil information was obtained from the Rural Development Administration (RDA) (1:25000) and based on a single surficial soil layer. The Haeon spatial soil data set (TERRECO) coupled the RDA soil data, LULC, and extensive field-based soil profiles to develop a spatial distribution of multiple soil horizons to a depth of 3 m. Our results found that Haeon soils are intensively managed and modified and highly dependent on land use (Tenhunen et al., 2011). Soil properties, including the hydrologic soil group, texture class, the percentage content of rock, sand, silt, and clay content, and the hydraulic conductivity, were derived from a 2009 catchment-wide field survey that was aggregated into 6 unique soil types (Table 3.2). The hydrologic group and texture for each of the soils is (1) very

steep forest soil (C, loam-sand), (2) forest soil (C, loam-sand), (3) moderately steep dry soil (D, sand-silt), (4) flat dryland soil (D, sand-silt), (5) rice paddy soil (C, sand), and (6) sealed ground (D, clay).

3.3.3.3 Land use and land cover (LULC)

Intensive field-based, plot-scale LULC observations for each of the years 2009 through 2011 resulted in up to 126 individual LULC classes. For the purposes of this study, the 2009 ground survey data have been distilled to 15 different LULC classes (Table 3.2). Haeon is a mixed land use catchment, which contains 54 % agricultural land, and fields are typically less than 0.40 km². The remainder of the catchment area is upland forest at higher elevations, predominately composed of 30 to 40 yr old mixed deciduous forest. Major species include Mongolian oak (*Quercus mongolica*), Daimyo oak (*Quercus dentata*), and Korean ash (*Fraxinus rhynchophylla*). While this agriculture dependent catchment has exhibited LULC increases up to 37 % through forest encroachment (Kim et al., 2011), the LULC distribution throughout the study period between 2009 and 2011 remained relatively stable (± 1.2 %, Yanggu County Office, 2012).

3.3.4 Management inputs and crop parameterization

3.3.4.1 Management parameter estimation

Agricultural management practices within the Haeon catchment were surveyed between 2009 through 2011 through a combination of on-site stakeholder interviews, empirical field observations (Tenhunen et al., 2011), published literature (i.e., Nguyen et al., 2012), and regulatory reports from the Research Institute of Gangwon (RIG), the Ministry of Environment, the National Institute of Agricultural Science, and Technology and the Korean Forest Research Institute. More than 300 interviews of stakeholders and farmers were completed under the TERRECO project to quantify fertilization and pesticide application quantities and timing, irrigation practices, planting and harvesting activities, and tillage methodologies. TERRECO managed plots were also used to obtain comprehensive temperature-based planting, fertilizer, tillage, mulching, development, and harvest information (J. Tenhunen, unpublished data). An example of the land use and crop management schedule, application rate, and application frequency is provided in Table 3.3. Fertilizer application parameters within the SWAT database were varied for each crop and subbasin for spatially distributed management. The simulated timing of management actions (i.e., fertilization, tillage, planting, irrigation, harvesting) was implemented in SWAT through daily heat unit summations because traditional planting and harvest methods are dependent on climatic observations closely correlated to heat units.

Table 3.3 Agricultural crop management schedule including planting and harvest dates, fertilization dates, amounts, and type of fertilizer, tilling dates and method, SCS curve number for each crop, and the heat units required to reach maturity

LULC/ crop	PHU ^b			Tillage type	Fertilizer			Planting (leaf out) ^e	Harvest (cessation) ^e	Age (yr)	Initial LAI (-)	Planting Biomass (kg ha ⁻¹)
	CN ^a	(°C)	JD		JD	type ^c	Amnt ^d	JD	JD			
General Bean	70.3	1710	121	Rotary hoe	133	Chem	345	135	224			
			133	Furrow out	133	Org	120					
General cabbage	71	2159	126	Rotary hoe	138	Chem	360	140	201			
			138	Furrow out	138	Org	150					
			171	Chem	0.72							
Potato	71.8	2381	101	Rotary hoe	113	Chem	330	115	243			
			113	Furrow out	113	Org	100					
Radish	71.3	1631	136	Rotary hoe	150	Chem	340	152	232			
			150	Furrow out	150	Org	150					
			182	Chem	150							
Rice	78	2736	124	Rotary hoe	136	Chem	230	138	288	0	0.2	50
			136	Rice roller	156	Chem	0.2					
					169	Chem	0.2					
					181	Chem	0.5					
					193	Chem	0.5					
Ginseng	71.5	3065	109	Rotary hoe	121	Chem	468	123	298			
			121	Furrow out	121	Org	120					
Maize	69.7	2999	111	Rotary hoe	123	Chem	316	125	295			
			123	Furrow out	123	Org	100					
General Orchard	58.6	3163	106	Rotary hoe	118	Chem	287	120	303	10	0	100
			118	Furrow out	118	Org	100					
Timothy	72	2912						135	304			
Codonopsis	40.7	2833			120	Chem	320	120	307			
					120	Org	150					
					166	Chem	0.5					
Forest	50.5	2896						112	307	40	0	342

^a CN is the SCS curve number. ^b PHU is the cumulative heat units above 0.0 °C required for the LULC/crop to reach maturity. ^c Fertilizer type is classified as Chem (inorganic chemical) not explicitly described or Org (organic manure).

^d Fertilizer amount (kg ha⁻¹). ^e Leaf out and cessation define the beginning and end of season for forest and orchard land use

3.3.4.2 Biomass sampling, analysis, and plant growth

Biomass analysis was completed by collecting and sampling 5 to 10 entire plants, representative of each crop type (Table 3.2) from a 2009 catchment-wide sample set of TERRECO harvest plots (J. Tenhunen, unpublished data). Each of the plants was field separated and subsequently weighed for fresh weight. The leaf area was individually measured using a portable leaf area meter (Opti-Sciences, Inc., AM 300). The samples were then separated and dried at 80 °C for more than 1 week, prior to measuring the sample dry weight.

To differentiate between crop types particular to South Korea (i.e., ginseng), several modified land use classes were created in the SWAT crop database. Nine representative field plots along an elevation transect were analyzed and crop parameters were varied to minimize the simulated and observed residuals for leaf area index (LAI), biomass, and crop yield. The crop parameters were altered based on observed measurements, plant physiology modeling results from the PIXGRO model (i.e., Adiku et al., 2006), and published literature. The crop parameters that were varied are presented in Tables 3.3 and 3.4. Intensive cultivation was also present in agricultural areas not serviced by irrigation canals and therefore, groundwater abstraction was estimated from the PIXGRO model as the quantity required for optimal plant growth. Typical to many Asian catchments, Haean can be considered a highly managed catchment with increased uncertainty due to insufficient spatiotemporal water management data.

Table 3.4 Example SWAT model crop parameter database variations in the Haeen model

LULC	Heat ^a units	HUSC ^b	BLAI ^c	DLAI ^d	FRGRW1 ^e	LAIMX1 ^f	FRGRW2 ^e	LAIMX2 ^f	GSI ^g	T_BASE ^h	ALAI ⁱ MIN	HVSTI ^j	CHTMX ^k	BIO_E ^l	BIO_ ^m LEAF	BM ⁿ DIE-OFF
Rice	1250	0.15	4	0.95	0.1	0.1	0.5	0.95	0.005	10	0	0.5	0.6	22	0	0.1
Radish	3300	0.01	5	0.9	0.1	0.1	0.3	0.95	0.3	0	0	2	0.6	30	0	0.1
Potato	3000	0.01	4	0.9	0.1	0.1	0.5	0.95	0.003	0	0	0.95	0.6	25	0	0.1
General beans	1050	0.15	5.4	1	0.1	0.1	0.5	0.95	0.003	10	0	0.31	0.6	25	0	0.1
General cabbage	900	0.2	3.5	0.9	0.1	0.1	0.5	0.95	0.003	0	0	0.8	0.5	19	0	0.1
Deciduous forest	300	0.01	7	1	0.1	0.1	0.5	0.95	0.0005	0	0	0.76	10	15	0.15	0.1
Coniferous forest	800	0.01	7	0.97	0.1	0.1	0.5	0.95	0.0005	0	0.06	0.76	10	15	0.15	0.1

^a Heat Units is the total base zero annual heat units for the plant cover/land use to reach maturity. ^b HUSC is the fraction of the total base zero annual heat units at which the management operation occurs. ^c BLAI is the maximum potential leaf area index. ^d DLAI is the fraction of the growing season when the leaf area begins to decline. ^e FRGRW1,2 represent the fraction of the plant growing season corresponding to the 1st and 2nd point on the optimal leaf area development curve. ^f LAIMX 1,2 represent the fraction of the maximum leaf area index corresponding to the 1st and 2nd point on the optimal leaf area development curve. ^g GSI is the maximum stomatal conductance at high solar radiation and low vapor pressure deficit (m s^{-1}). ^h T_BASE is the minimum or base temperature for plant growth ($^{\circ}\text{C}$). ⁱ ALAI_MIN is the minimum leaf area index for the plant during the dormant period ($\text{m}^2 \text{m}^{-2}$). ^j HVSTI is the fraction of aboveground biomass removed during a harvest operation and lost from the system. ^k CHTMX is the maximum canopy height (m). ^l BIO_E is the radiation use efficiency or biomass energy ratio ($(\text{kg ha}^{-1})/(\text{MJ m}^{-2})$).

^m BIO_LEAF is the fraction of tree biomass accumulated each year that is converted to residue during dormancy. ⁿ BMDIEOFF is the biomass die-off fraction.

3.3.4.3 Rice paddies, potholes, and water abstraction

The quantity and timing of river and groundwater abstractions is uncontrolled and local estimates were inadequate for model inclusion. Depending on the HRU location, irrigation water was extracted from an adjacent river reach or from shallow groundwater. Groundwater-derived irrigation practices were limited to orchards and rice paddies and were accounted for in the simulations through water availability based auto-irrigation at the HRU level and defined by the soil water deficit. Haean rice paddies were simulated in SWAT as potholes, which are hydrologically similar to ponded areas. Rice paddies are typically characterized by multiple cascading-elevation plots separated by embankments. The rice paddies had low infiltration and typically saturated soil conditions and therefore, infiltration as a function of water content rather than flow routing was used for estimation of subsurface losses. The HRUs within each subbasin were developed using 0 % land use and 0 % slope threshold for reach subbasins resulting in maximum number of HRUs. Since a subbasin can have multiple HRUs but only have a single pothole, we limited the rice paddies in each subbasin to a single HRU. We accomplished this by varying the soil threshold until only a single rice paddy HRU was in each of the subbasins.

3.4 Results and discussion

3.4.1 Meteorological drivers and the effects of interpolation

Meteorological time series data, particularly precipitation is a highly sensitive driver in hydrologic modeling applications (Strauch et al., 2012). Spatial monitoring distributions are typically limited and do not capture heterogeneous meteorological conditions that can be interpolated by wide-meshed monitoring networks (Notter et al., 2007). Large variations in elevation throughout the Haean catchment influence the precipitation volume, soil moisture, and plant growth. They can also influence the peak flow and the time of concentration to peak discharge of the simulated hydrograph (Khakbaz et al., 2012; Wilson et al., 1979). Our weather analysis revealed heterogeneous meteorological conditions throughout the Haean catchment that are dependent on elevation and aspect and largely focused in subregions (Choi et al., 2010; Shope et al., 2013). These meteorological variations have a direct influence on the relative humidity and therefore, the spatial variability of plant growth parameters between subbasins was significant (Figure 3.3).

We examined the model sensitivity to alternative precipitation interpolation methods (IDW, Spline, nearest neighbor, and kriging), both through spatially explicit plant growth response and river discharge to assess the robustness of interpolation in our domain. We found that total river discharge between interpolation methods varied less than 0.1 % at the integrated catchment outlet (S7) and the discharge differences at multiple locations throughout the catchment (S1, S4, S5, and S6) were negligible. The IDW univariate interpolation technique for precipitation did result in slightly improved plant growth response for selected crops and locations than other methods. Similar to results obtained by Notter et al. (2012), the IDW method was invoked to develop a continuous grid of meteorological drivers that were subsequently assigned to individual subbasins.

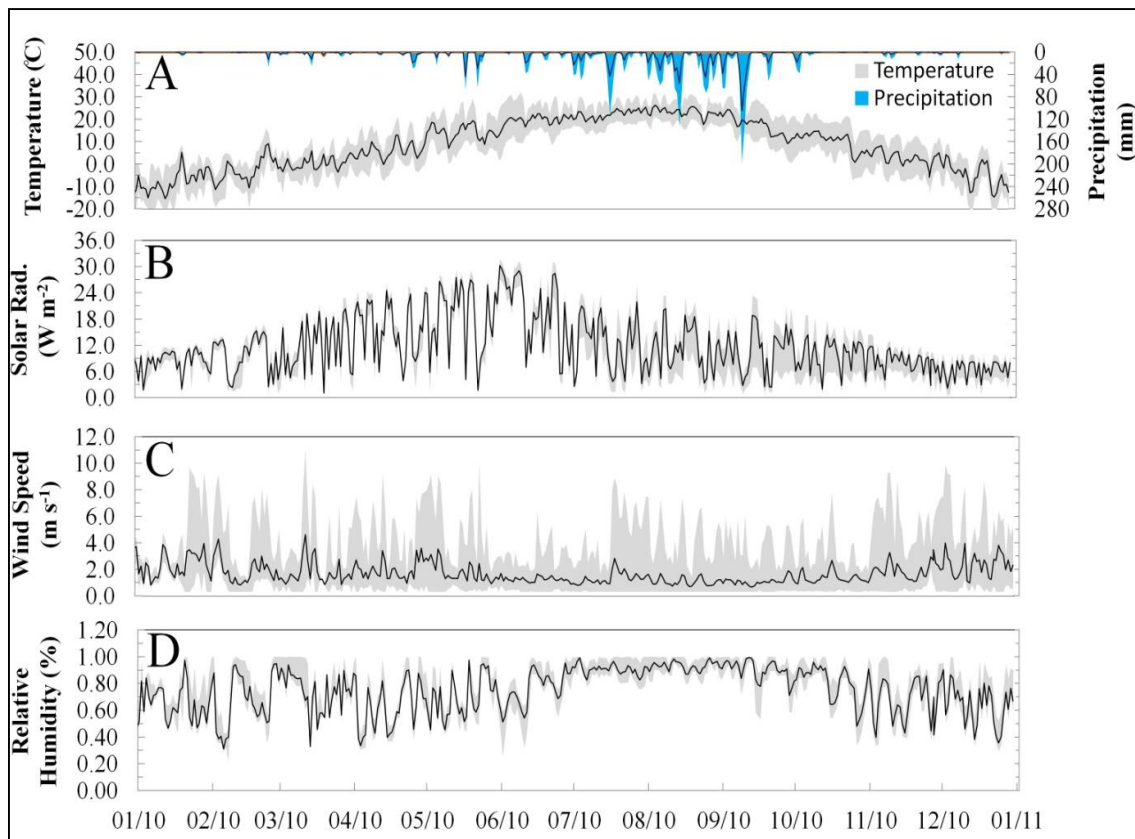


Figure 3.3 Meteorologic variability and average daily value of each variable throughout the Haeon catchment for 2010. (A) describes the daily precipitation and temperature variability, (B) is the range in solar radiation and the average value between all of the locations, (C) is the wind speed variability, and (D) is the relative humidity range

3.4.2 Model calibration, validation, and uncertainty assessment

3.4.2.1 Sensitivity and model parameterization

The model sensitivity was addressed with respect to spatial distribution (number and location of meteorological stations, LULC distribution), observational record (LULC coverages, meteorological stations), resolution (soil coverage, subbasin discretization), and hydrologic stimulus (rainfall runoff). The Haeon catchment model configuration resulted in 142 topographically based subbasins and 2532 individual HRUs. Previous investigations have shown that the number of subbasins has little influence on runoff (Jha et al., 2004; Tripathi et al., 2006; Xu et al., 2012a, b). Alternatively, other studies have found that HRU discretization can have a substantial effect depending on the physical catchment conditions, data quality, and investigative scale (i.e., Setegn et al., 2008; Haverkamp et al., 2002). We assessed the effect of subbasin size and HRU definition on surface water discharge and found no appreciable difference between model results. However, our results show that elevation-based plant parameters and convective precipitation captured through increased subbasin discretization can be important. Subbasins with steep slopes and extensive vertical gradients must account for elevation-based climate conditions, which contribute to highly variable ET conditions. The sensitivity analysis of discharge related model parameters was achieved by sequentially varying an individual parameter

while maintaining the remaining parameters for each monitoring location. Between eight and eleven parameters from the original 15 discharge-related parameters were found to be sensitive to catchment-wide flow partitioning (Figure 3.4). Subsequently, the range of each of the parameters was minimized during calibration procedures.

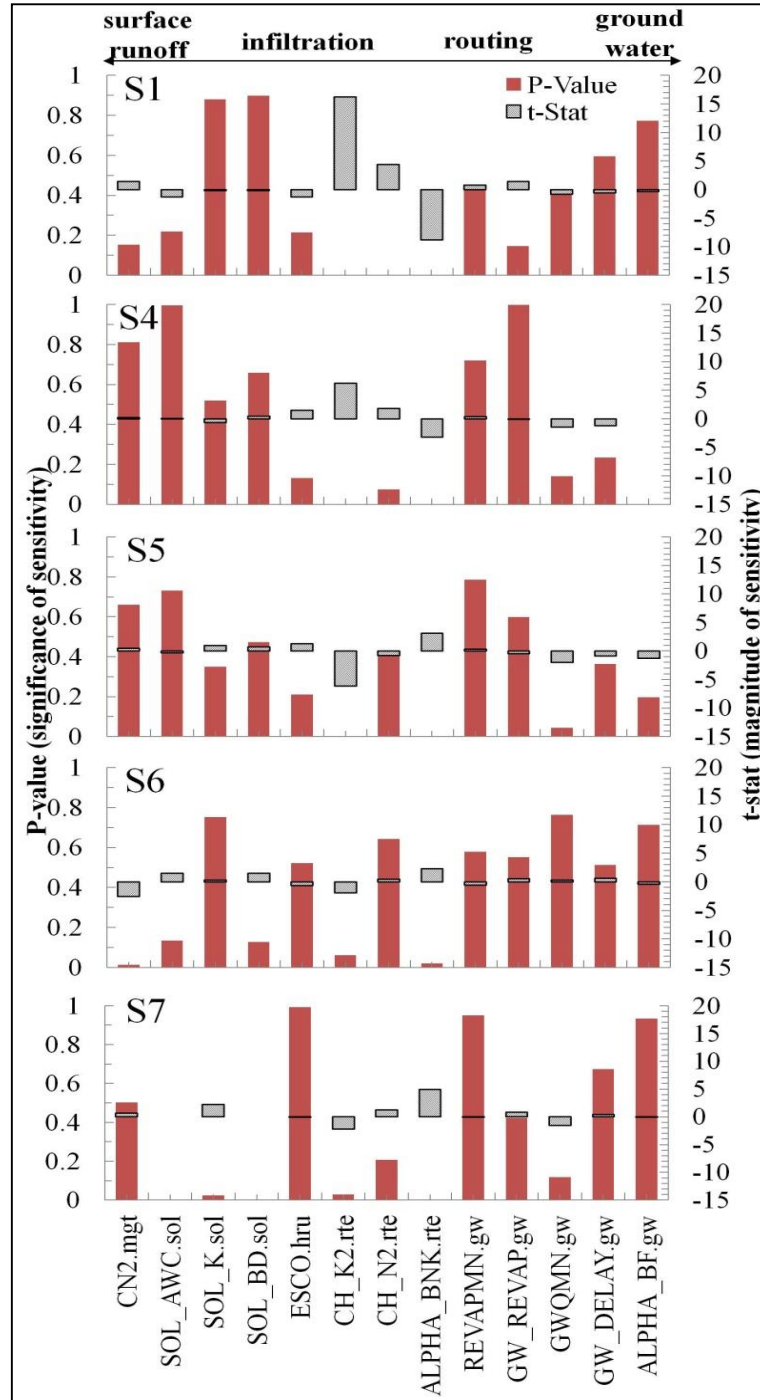


Figure 3.4 SWAT simulated parameter sensitivity (p value) and model significance (t test) for the Haeon catchment for monitoring locations S1, S4, S5, S6, and S7 along the elevation transect

Chapter 3-Hydrologic process modeling and discharge partitioning

Table 3.5 SWAT parameter sensitivity and significance between discharge parameters throughout the Haeen catchment (Figure 3.4). Calibrated SWAT parameters for the Haeen catchment, including the individual ranking along the elevation-based transect, the minimum and maximum parameter values for all subbasins accounted for by each monitoring location, and the average calibrated parameter value. Because of the distributed nature of the Haeen model, individual parameters varied depending on crop type, elevation, aspect and therefore, a specific parameter value is not available

Parameter (distribution)	Parameter ranking						P value (sensitivity of significance)						t stat (significance magnitude)						Minimum-Maximum Parameter value [Final Average Parameter Value]				
	S1a	S1	S4W	S5	S6	S7	S1a	S1	S4w	S5	S6	S7	S1a	S1	S4w	S5	S6	S7	S1	S4W	S5	S6	S7
<i>CH_K2.rte</i> (subbasin)	13	13	12	13	12	10	0.00	0.00	0.00	0.00	0.06	0.03	16.23	6.01	6.21	-6.18	-1.89	-2.21	81-139 [94]	43-139 [83]	-51-70 [9.2]	24-117 [71]	51-143 [97]
<i>ALPHA_BNK.rte</i> (subbasin)	12	12	8	12	13	11	0.00	0.00	0.00	0.00	0.02	0	-8.77	-3.68	-3.18	3.1	2.34	4.94	0.01-0.35 [0.34]	0.05-0.80 [0.22]	0.15-0.87 [0.51]	0.28-0.92 [0.60]	0.42-1.25 [0.83]
<i>CH_N2.rte</i> (subbasin)	11	9	11	11	9	9	0.00	0.39	0.07	0.43	0.64	0.21	4.44	0.87	1.79	-0.79	0.46	1.27	0.13-0.39 [0.26]	0.08-0.31 [0.17]	0.03-0.22 [0.12]	0.08-0.30 [0.19]	0.06-0.29 [0.17]
<i>CN2.mgt</i> (land use, subbasin)	10	11	10	9	5	4	0.15	0.11	0.81	0.66	0.01	0.5	1.43	1.62	0.24	0.44	-2.51	0.67	-0.62-0.23 [-0.58]	-0.55-0.36 [-0.05]	-0.32-0.54 [0.11]	-0.33-0.60 [0.14]	-0.38-0.52 [0.07]
<i>ESCO.hru</i> (land use, subbasin)	9	7	6	5	3	2	0.21	0.42	0.13	0.21	0.52	0.99	-1.24	0.81	1.51	1.26	-0.64	-0.01	0.19-0.89 [0.39]	0.16-0.91 [0.55]	0.25-1.01 [0.63]	0.13-0.89 [0.51]	0.21-0.97 [0.59]
<i>GW_REVAP.gw</i> (soil type, subbasin)	8	6	1	1	2	5	0.15	0.3	1.00	0.6	0.55	0.42	1.45	1.05	0	-0.53	0.6	0.8	0.06-0.16 [0.09]	0.05-0.18 [0.09]	0.03-0.15 [0.09]	0.02-0.16 [0.09]	0.03-0.16 [0.10]
<i>GWQMN.gw</i> (soil type, subbasin)	7	2	5	4	4	7	0.41	0.6	0.14	0.04	0.76	0.12	-0.82	0.52	-1.48	-2.02	0.3	-1.57	32-4151 [475]	1370-4800 [2675]	512-3596 [2054]	323-3894 [2108]	1133-4890 [3011]
<i>ALPHA_BF.gw</i> (soil type, subbasin)	6	1		6	6	8	0.77	0.81		0.20	0.71	0.93	-0.29	0.24		-1.29	-0.37	-0.08	0.12-0.46 [0.20]	0.11-0.52 [0.22]	0.02-0.39 [0.21]	0.00-0.38 [0.19]	0.08-0.46 [0.27]
<i>SOL_K(1).sol</i> (subbasin)	5	3	9	10	1	6	0.88	0.61	0.52	0.35	0.75	0.03	-0.15	0.51	-0.65	0.94	0.32	2.25	-1.46-0.22 [-0.78]	-0.56-0.71 [0.10]	-0.64-0.85 [0.10]	-0.90-0.42 [-0.24]	-0.85-0.56 [-0.15]
<i>SOL_AWC(1).sol</i> (subbasin)	4	10	4	3	10		0.22	0.43	1.00	0.73	0.13		-1.23	-0.79	0	-0.35	1.51		-0.20-0.39 [0.30]	-0.41-0.47 [0.02]	-0.56-0.21 [-0.17]	-0.49-0.48 [-0.01]	-0.67-0.18 [-0.25]
<i>REVAPMN.gw</i> (soil type, subbasin)	3	4	7	7	7	1	0.43	0.69	0.72	0.79	0.58	0.95	0.8	-0.41	0.36	0.27	-0.56	-0.06	2.73-6.74 [4.72]	1.98-9.53 [6.14]	0.41-8.62 [4.51]	1.42-8.36 [4.89]	1.62-9.13 [5.38]
<i>GW_DELAY.gw</i> (soil type, subbasin)	2	5	3	8	8	3	0.59	0.39	0.23	0.36	0.51	0.67	-0.53	0.88	-1.19	-0.91	0.66	0.42	138-453 [398]	16-334 [202]	73-412 [242]	-28-322 [147]	31-362 [197]
<i>SOL_BD(1).sol</i> (subbasin)	1	8	2	2	11		0.9	0.07	0.66	0.47	0.13		-0.13	1.85	0.44	0.72	1.53		-0.36-0.44 [-0.25]	-0.43-0.30 [-0.05]	-0.62-0.13 [-0.25]	-0.34-0.36 [0.01]	-0.34-0.35 [0.01]

The use of lumped, semi-distributed, and fully distributed model parameterization was also investigated through sensitivity analysis. We assigned the same parameter magnitudes by crop type for the lumped distributed parameters, by crop type and subbasin for semi-distributed, and by HRU in the fully distributed construction. We found that fully distributed parameters between subbasin, soil, and LULC were negligibly better than semi-distributed parameters based on aggregated LULC within individual subbasins. We also found that the use of a lumped parameter assignment did not perform as well as either the fully or semi-distributed parameterization. Therefore, for computational efficiency, a semi-distributed approach was taken throughout the catchment utilizing the most sensitive parameters at each monitoring location for parameterization in adjacent areas.

While we did not explicitly quantify the optimal parameterization, through a series of iterations we weighted the objective functions (R^2 , NSE, PBIAS, and baseflow percentage) in decreasing order as we compared individual locations throughout the catchment. In effect, we used a multi-criteria decision making process to determine the relative priority of each alternative when all of the criteria were considered simultaneously. Because our results indicated that the sensitivity analysis was significantly based on the monitoring location, we calibrated multiple locations along an elevation transect. In Figure 3.4, the “t stat” provides a measure of parameter sensitivity where larger absolute values are more sensitive and the “p value” determines the significance of sensitivity with higher significance as values approach zero (Abbaspour,2011).

Our results generally indicate surface runoff and routing parameters are more sensitive at higher elevations with increasing sensitivity to infiltration and groundwater parameters at lower elevations (Figure 3.4). The REVAPMN groundwater parameter was a sensitive parameter at each location; however, the magnitude was relatively small. CH_K(2) was the least sensitive parameter, although included in the analysis for comparison. Table 3.6 provides a summary of the SWAT parameters. The infiltration parameters suggest significant baseflow response at higher elevations. At mid-elevations, surface runoff and routing parameters become more sensitive. At lower catchment elevations, infiltration, routing, and groundwater parameters dominate. Since the upper elevation locations are composed of shallow, highly permeable (S. Arnhold, unpublished results) soils over bedrock; we conceptualize high infiltration rates that contribute to increased baseflow and streamflow accumulation. At mid- to low- elevation locations, higher land management, and soil amendments lead to runoff and less infiltration. These results identify the importance of and differences between model sensitivities as a function of the model equations, model sensitivity, and observational dynamics. Therefore, caution should be exercised in rainfall–runoff process simulations in relatively ungauged basins.

Table 3.6 Calibration and validation statistics for each of the monitoring locations throughout the Haeen Catchment. The data includes the subbasin demarcation of the monitoring locations, the total number of observations, the observed and simulated water balance, the NSE, R^2 , and PBIAS statistics, and the percent baseflow contribution

Monitoring location	Drainage area (km ²)	No. of observ.	NSE	R^2	PBIAS (%)	Percent baseflow
<i>2010 calibration period</i>						
S1	0.35	283	0.83	0.84	9.61	0.49
SD	1.54	33	0.9	0.91	-8.78	0.16
S4	1.66	202	0.95	0.96	8.86	0.42
S5	2.09	259	0.85	0.89	1.27	0.16
SN	3.12	34	0.95	0.96	-1.08	0.13
SS	6.55	36	0.85	0.95	-72.38	0.21
SW	6.65	35	0.97	0.98	-10.60	0.13
SK	7.28	35	0.95	0.97	-6.93	0.2
S6	22.15	267	0.64	0.7	41.33	0.06
S7	52.08	207	0.73	0.93	29.39	0.13
<i>2009 validation period</i>						
S1	0.35	66	0.92	0.83	-6.85	0.54
SD	1.54	20	0.98	0.97	-9.05	0.15
S4	1.66	0	-	-	-	-
S5	2.09	65	0.88	0.9	-3.18	0.18
SN	3.12	22	0.91	0.94	-14.47	0.14
SS	6.55	22	0.76	0.87	-33.31	0.2
SW	6.65	22	0.94	0.95	-3.59	0.1
SK	7.28	22	0.62	0.71	19.76	0.26
S6	22.15	0	-	-	-	-
S7	52.08	22	0.74	0.97	26.3	0.13

3.4.2.2 Metrics of model performance for calibration procedures

Model performance was assessed by several metrics at each location including the simulated and observed water balance, the coefficient of determination (R^2), Nash–Sutcliffe efficiency (NSE), percentage bias (PBIAS), and the baseflow contribution. The R^2 was used to evaluate time and space dependent cross-correlations and indicate if system behavior is accurately represented by the model (Bennett et al., 2012). The Nash–Sutcliffe efficiency (NSE) is a normalized correlation related statistic used to compare observational variance to the residual variance, particularly during peak events (Nash and Sutcliffe, 1970). The percentage bias (PBIAS) is a quantitative measure of simulated versus observed river discharge for the entire simulation period and defines the total volume differences between the simulated and observed fluxes. In addition, the baseflow statistic compares the simulated baseflow contribution to the calculated estimate at each location to alleviate hydrologic partitioning from alternative sources. This metric provides an independent check on a specific component of the water budget. Finally, measured plant growth dynamics were compared with simulated results.

3.4.2.3 Manual and automated model calibration

Due to the complexity of large-scale multi-objective analyses, watershed models are typically highly parameterized and manual calibration can be virtually impossible (Schuol and Abbaspour, 2006)

although multi-site, multi-objective inverse calibration and uncertainty analysis can aid in understanding the system (Abbaspour et al., 2004; Duan et al., 2003). Model calibration was separated into two components, (1) manual catchment-scale calibration to estimate system processes and variability, and (2) automated calibration to quantify model uncertainty.

The SWAT model was simulated from 2006 through 2011 with the first 3 yr excluded for model initialization. The calibration and validation of river discharge was performed at a daily time step from 2009 through 2011, with 2010 as the calibration period and 2009 as the validation period. For locations S4 and S6, we did not have observational records for the 2009 validation period and instead used the concept of self-similarity for validation results. Since the transect followed an elevation gradient in a limited portion of the catchment, we conceptualized that similar hydrologic processes were occurring for similar elevation and drainage areas in other parts of the catchment. For example, location S4 was calibrated to the 2010 observational data, although there was limited data to validate for 2009. Because SD and SK had similar topography, elevation, drainage area, and land use patterning as S4 and S6, respectively, they were used to validate the S4 calibration parameters. Intensive manual calibration was performed at each of the subbasins routed to a monitoring station and used to minimize the acceptable parameter range at each site. The difficulty is that manual calibration sensitivity suffers from the linearity assumption by not accounting for correlations between individual parameters.

After manual calibration was optimized through the weighted, multi-criteria metrics previously discussed, automated model calibration, validation, and uncertainty analysis was completed using the Sequential Uncertainty Fitting Algorithm (SUFI-2) (Abbaspour et al., 2004, 2007). The manual calibration results provided distributed, physically based parameter ranges that were incorporated into the SUFI-2 auto-calibration routine, starting with the catchment outlet and following a top to bottom approach. Model uncertainty in auto-calibration is quantified by the 95 % prediction uncertainty (95PPU) at the 2.5 and 97.5 % cumulative distribution, which is obtained through Latin hypercube sampling procedure (Abbaspour et al., 2004). Because the model varies multiple parameters at the same time, two indices are used to assess the stochastic calibration performance. The “*p* factor” describes the percentage of data bracketed by the 95 % prediction uncertainty and the “*r* factor” describes the average width of the prediction band divided by the standard deviation of the measured data (Faramarzi et al., 2009). Since the uncertainty in field-based river discharge measurements was typically < 5 % (Shope et al., 2013), a conservative 10 % measurement error was included in the “*p* and *r* factor” calculations (Abbaspour et al., 2009; Andersson et al., 2009; Butts et al., 2004; Schuol et al., 2008). Yang et al. (2008) found that reasonable prediction uncertainty ranges were achieved with 1500 model simulation iterations, while, (Güngör and Göncü, 2012) showed that 300 iterations provided similar results to 1500 iterations. In Haean, at least 300 simulation iterations at each location were performed throughout the auto-calibration routine (Table 3.5).

As described, the calibration parameters were selected to optimize the PBIAS, R^2 , and NSE test statistics, the estimated groundwater baseflow, and the plant growth dynamics. The main SWAT parameters controlling baseflow processes in Haeon include GW_REVAP, GWQMN, GW_DELAY, ALPHA_BF, and ESCO (Table 3.6). The primary parameters that affected surface runoff throughout the Haeon catchment are CN2 and SOL_AWC. During model calibration procedures, the ESCO and GW_REVAP parameters were typically adjusted to minimize the PBIAS and improve the annual discharge and water balance trends. The GWQMN parameter was then adjusted to simulate the seasonal discharge trends assessed by maximizing the monthly R^2 and NSE statistics. Finally, the CN2, CH_N(2), and GWDELAY parameters were calibrated to account for daily trends by maximizing the NSE. When the Muskingum routing method was utilized, the channel parameters CH_N(2) and CH_K(2) were ranked 2 and 3 in the sensitivity analysis. However, the relative change in NSE between outlet results was negligible (~ 0.01) compared to the default variable storage routing method, and the addition of more parameters was substantial. Therefore, variable storage routing within the SWAT model was chosen to limit the model parameterization.

The explanation for the deviations in runoff at the low elevation locations (S6 and S7) is not known or reflected in the SWAT input data. However, by examining a combination of optimized calibrated data, process-based comparisons, and field observations, the overall calibration metrics indicated increased flow routing directly from high elevation locations to lower elevation river locations. A possible explanation is the density of surface water collection and sedimentation ponds within the catchment, which may have impacted the observed runoff characteristics of the watershed (Cho et al., 2012). Using a multi-criteria optimization approach, we identified that engineered flow routing and infrastructure construction such as roads and culverts, contributed to increased discharge at lower elevations. These catchment-wide landscape engineering results are further discussed in Sect. 3.4.5.

3.4.3 Spatiotemporal flow partitioning with respect to river discharge

The calibration and validation of the Haeon catchment daily discharge yielded good results given the scarcity and the temporal longevity of the available data. The modeling results indicated that SWAT performance at the Haeon catchment relied heavily on the quality and more importantly abundance of discharge data, similar to the results of Dessu and Melesse (2012). The NSE score for monitoring locations S1, S4, S5, S6, and S7 ranged between 0.64 and 0.95 with an average score of 0.76 for the 2010 calibration period and between 0.40 and 0.98 for the validation period (Figure 3.5). Satisfactory NSE scores of > 0.5 (Moriassi et al., 2007) were achieved at all 14 gauge locations in the calibration period and at 12 of 14 in the validation period. The R^2 value was also reasonable for each of the monitoring locations, ranging from 0.70 to 0.96 with an average value of 0.81 for the calibration period and between 0.71 and 0.97 for the validation period (Figure 3.5). The fact that similar performance measures were reached in both validation and calibration periods indicate that there was minimal “overfitting” of the distributed parameters.

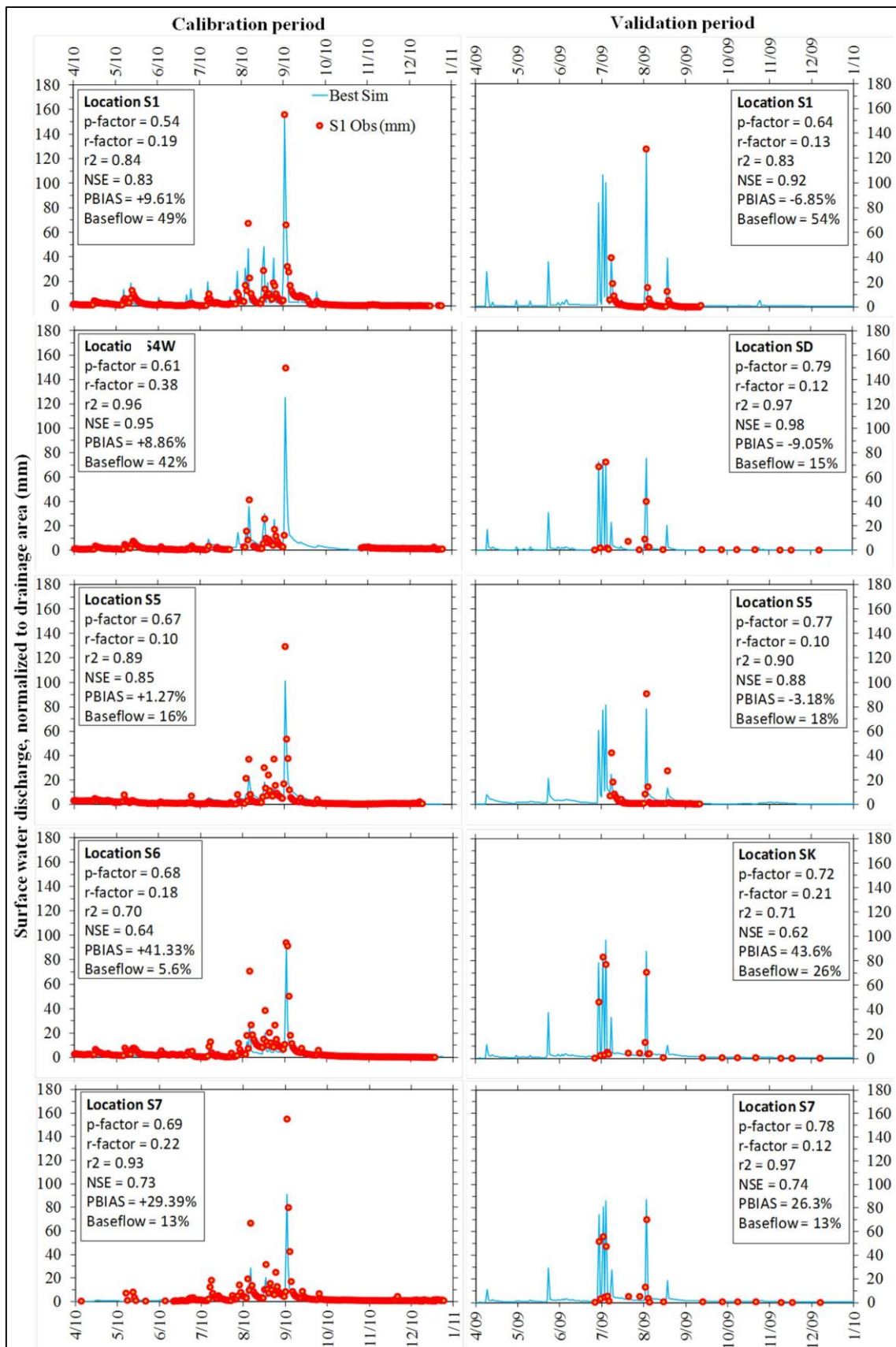


Figure 3.5 Calibrated and validated daily comparison of drainage area normalized observed and simulated river discharge along the elevation transect of monitoring locations S1, S4, S5, S6, and the catchment outlet S7. Included on each panel are the objective function and optimization statistics

The baseflow contribution estimated at monitoring location S4 using a digital filter hydrograph separation technique was 26 %, although the calibrated estimate was 42 %. The hydrograph separation magnitude varied significantly, depending on the data quality, the length of the analysis, and the time step investigated. However, the digital filter methodology for estimation of the hydrograph separation is not process-based and may have significant uncertainty. The calibrated baseflow of 42 % at S4 is similar to the estimate at the upstream location S1 and nearly twice as high as all of the downstream locations, indicating that this mid-elevation area may be transition zone between baseflow and runoff dominated streamflow. This suggests that high elevation locations have increased baseflow contributions, relative to low elevation locations, regardless of the observational data period.

We found increased differences between the simulated and observed water balance as measured through PBIAS statistics at locations S6 and S7, which were 41 and 29 %, respectively. These PBIAS estimates are unsatisfactory according to Morasi et al. (2007), regardless of the very good R^2 and NSE metrics and acceptable baseflow estimates. The increase in water balance was hypothesized to be a function of rapid and large flow contributions from high elevation locations that were routed through culverts, drainages, and road systems to lower catchment locations. Essentially, the effect of the anthropogenic routing not only creates a large disparity in simulated discharge, but limits the subsurface infiltration at the plot-scale for higher elevation locations and surreptitiously develops a misleading flashy flow system with reduced landscape water storage.

The lower NSE score and R^2 values could be attributed to the low magnitude relative variability of discharge at higher elevation monitoring locations, which contributes to increased deviations of NSE scores during event conditions, particularly monsoonal extreme events. At location SK, there is scarce observation data and because the NSE statistics weight extreme events higher, limited but high deviations have a much larger impact than minor deviations. In addition, the difficulty in accurately simulating the river discharge at monitoring location SK was hypothesized to be a function of high elevation flow contributions that bypassed the monitoring gage as hyporheic flow (Shope et al., 2013). The hydrological response throughout East Asia and within the Haeen catchment in particular, is typically flashy and erratic, further attributing to event-based deviations in the objective functions. At monitoring location S5, a higher temporal density of observations was obtained and the model performance metrics are generally better than for other locations.

Overall, the calibration and validation results were good and the percentage of baseflow contribution at each location was reasonable in terms of the hydrograph separation estimates. The auto calibration metrics of p -value and r value are both reasonable, while the R^2 and NSE statistics were consistently above satisfactory and predominately considered very good. The average p factor throughout the calibration period at all stations was 0.64 (0.54 to 0.69) and the r factor was 0.21 (0.10 to 0.38). The average p factor and r factor from the validation period was 0.74 (0.64 to 0.79) and 0.14 (0.10 to 0.21), respectively (Figure 3.5). This indicates that the majority of the simulated results were within the 95 %

confidence interval and that the standard deviation was adequately minimized. As shown in Figure 3.5 and Table 3.7, the validation results at these locations were good and consistent with the results estimated at the calibration locations.

Table 3.7 Biomass production and crop yield statistics for South Korea and specifically, for the Haean catchment.

	Area S korea cultivation			2009 Haean	2009 LULC area		2009 Haean
	Area (ha)	Production (metric tn)	Yield (tn ha ⁻¹)	Plot Yield (tn ha ⁻¹)	Plot (ha)	Haean (ha)	Crop Yield (tn)
Rice	936 766	6 869 305	7.33	11.26	13.32	87 312	73 796
Cabbage	34 321	2 542 000	74.07	4.81	10.35	32 742	15 226
Potato	26 804	600 000	22.38	22.94	1.17	25,038	490 895
Radish	23 780	1 223 000	51.43	35.24	1.26	21 828	610 422
Soybean	80 505	137 000	1.70	14.66	0.09	16 692	2 719 127
Deciduous forest	-	-	-	42.03	103.05	359 520	146 620

Sources: Ministry for Food, Agriculture, Forestry & Fisheries (MIFAFF), Korea Rural Economic Institute, Korean Statistical Information Service (KOSIS), Korea Agro-Fisheries Trade Corp. (aT), Yanggu statistical year-book 2003–2011 from the Yanggu County Office, FAOSTAT 2008, World Bank 2009

Each of the objective functions, hydrologic partitioning quantified by PBIAS, and the baseflow percentages were calibrated simultaneously, which while optimizing the values of some parameters, were at the detriment of other parameters. For example, the NSE at S5 was initially 0.89; however, parameter adjustments were made to minimize the water balance, which resulted in a lower NSE value. The event on 1 September 2010 had a major influence on the magnitude of the NSE and R^2 objective function. This is primarily due to the paucity of observation points and therefore, the weight of individual points on the overall relationship, particularly during peak events.

The simulation results were very good in terms of adequately simulating baseflow contributions, the majority of moderate events, and most extreme events for each location. In addition, the other statistical objective functions were typically good to very good. The quality of input data, such as the estimated river discharge (Shope et al., 2013) or the short duration of observational data, significantly affected the model performance. For example, extensive observational data was collected at S5 but more limited at S4 and S6, resulting in decreased statistics at the latter location, even after calibration. The relatively large 95 PPU band “*r* factor” necessary to bracket the observed data indicates that the uncertainty in the conceptual model is also very important for the Haean catchment.

3.4.4 Agricultural management and production

The heat sum methodology used to estimate time variable management and planting actions, provides the flexibility to account for unseasonable variations in meteorological drivers between years (Figure 3.3). Heat sums are calculated as the cumulative daily temperature greater than the base temperature of 0.0 °C initiated on the planting date and completed at the maximum growth. The HUSC is the percentage of the total heat units necessary for optimal growth of an individual crop and is prescribed for each management activity. The minimum heat sum over the period of record was 4246 °C during 2009, the maximum was 5783 °C during 2003, and the average annual heat sum is 5222 °C (Figure

3.6). The 12 yr linear trend line of maximum cumulative annual heat sum values indicates a general decrease of nearly 74.8 °C per year. When the potentially extreme years of 2003, 2008, and 2009 were excluded, a decrease of 15.3 °C per year was estimated. While precipitation trends suggest more extreme events occurring over a shorter time, these results indicate a decreasing trend in annual heat output necessary for optimal plant growth.

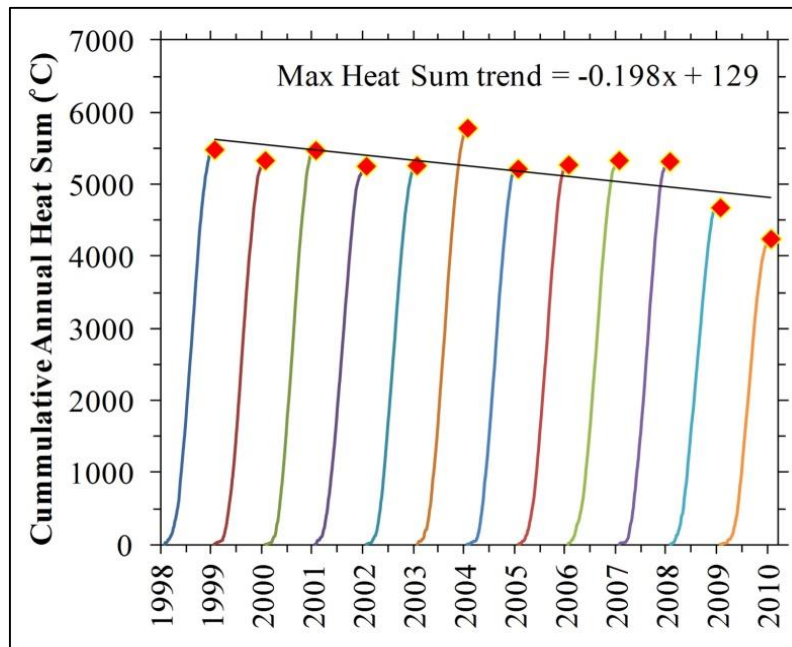


Figure 3.6 Daily heat sum estimate between 1998 and 2010 for the S1forest boundary monitoring location within the Haeon watershed (Figure 3.1)

To evaluate the SWAT simulation results on the ecohydrologic response, we also analyzed the simulation results in terms of agricultural growth dynamics at selected plot locations throughout the catchment. While calibrating spatiotemporal discharge as previously described, we also investigated the effect of crop dynamics through temporal leaf area index (LAI) as a proxy for crop growth and development (Figure 3.7). Individual crop growth and development parameters were adjusted for a comparison between observed and simulated LAI (Table 3.4). Results indicate a generally reasonable approximation of simulated LAI where the R^2 for each of the crop types ranged from 0.51 to 0.76 (Figure 3.7). More importantly, the results provide a consistent estimate of temporal trends in simulated biomass or agricultural production.

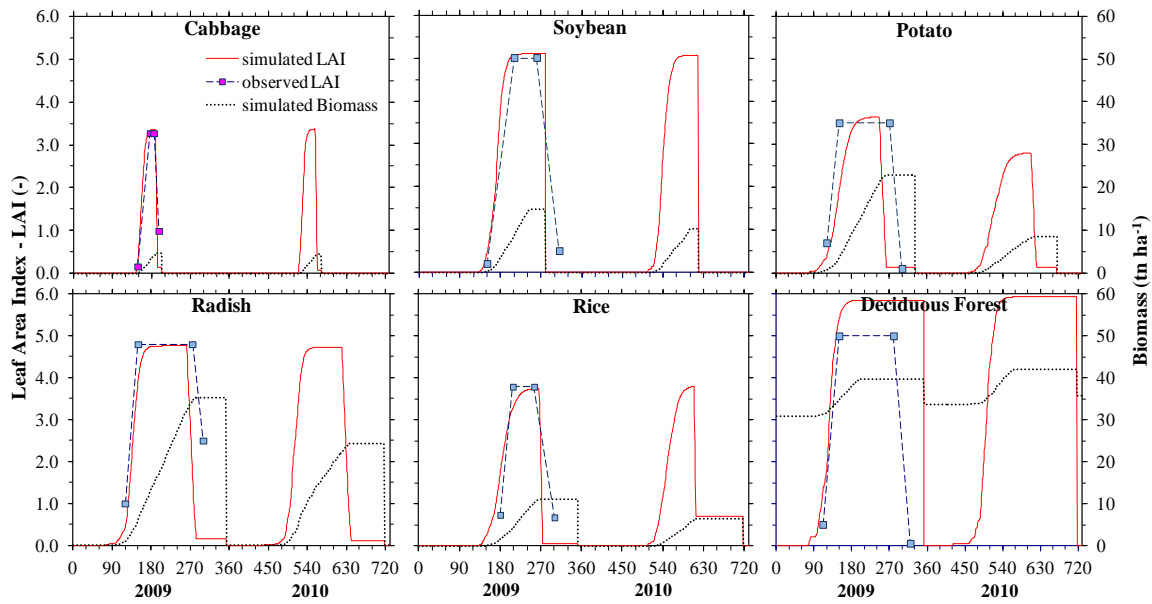


Figure 3.7 Comparison of simulated versus observed leaf area index (LAI) for five of the primary crops grown in Haean and the deciduous forest.

3.4.5 Influence of engineered landscape structure

Both the calibration and validation indicate successful spatial results with very good metrics, although a point of concern between observed and simulated results was at monitoring locations S6 and S7. The river discharge discrepancies between simulated and observed results were realized through PBIAS, which accounts for observed and simulated water balance differences. Field-based observations showed that catchment-wide surface runoff near the high elevation crops is routed to culverts immediately adjacent to the individual fields and road networks that discharge to low elevation river network reaches. As indicated in Figure 3.2, many of these long, extensive features traverse from high elevation plots near the forest boundary down to the lower portions of the catchment. To test the impact of these anthropogenic engineered structures on catchment-wide hydrologic partitioning, we compared several different surficial flow routing configurations. The routing configurations utilized in the model simulations were (1) with rivers only, (2) with both rivers and culverts, and (3) a combination of rivers, culverts, and roads (Figure 3.2). As previously described in Sect. 3.4.3, the model performance in terms of PBIAS decreased toward the catchment outlet, particularly near S6 and S7. As the transect continues to the catchment outlet, the p factor decreases from 71 to 11 %, indicating that less data is bracketed by the 95 % confidence interval, while the r factor describing the standard deviation of the observed discharge increases from 0.20 to 0.36.

When the model was reconfigured to account for both the river drainage network and the culverts, a better calibration was obtained where the PBIAS at monitoring locations S6 and S7 decreased from 41 and 29 % to 8 and 9 %, respectively. The dramatic difference in PBIAS was not extended by including the roads into the river and culvert drainage network with a negligible increase in PBIAS observed at S6 and S7. Therefore, inclusion of the field-based drainage culverts was effective in moderating the

difference in observed and model computed river discharge at lower elevation monitoring points and consistent with field-based observations of event-peak flow routing through the Haean watershed. However, it is surprising that the road network had minimal influence. During peak event conditions, substantial overland flow and sediment transport was observed throughout the Haean catchment. Since the poured concrete culverts are immediately adjacent to many of the plots, reduced landscape-scale infiltration required to maintain local soil moisture storage and rapidly transported excessive nutrients from fertilizer applications into the lower parts of the catchment is prevalent. This results in a rapid transport of elevated nutrient and sediment loads into the river. Therefore, while there is a significant influence on landscape-scale surface runoff, river discharge, and effectively hydrologic partitioning, a potentially greater issue is the impact expected from the rapid and large-scale alteration in water quality.

3.5 Conclusions

To provide a high accuracy estimate of spatiotemporal meteorological conditions, we used a unique high-frequency, quality control, and gap-filling algorithm to develop a detailed interpolation of weather patterns. The interpolated meteorological conditions were then discretized throughout the catchment and the conditions were prescribed at the centroid of each of the subbasins. This novel technique provided a better estimate of the dynamic variability due to convective storm events than the default SWAT application of prescribing the nearest weather station to the subbasin centroid.

We demonstrate that the use of a novel catchment-wide, multi-location, multi-objective function approach can drastically improve process-based estimates of catchment-wide hydrologic partitioning. By calibrating the model to many locations distributed throughout the catchment, landscape controls on hydrologic partitioning can be estimated as opposed to the integrated effect simulated at the catchment outlet. Because the catchment is essentially a bowl-shaped topographic feature, the concept of symmetry enabled the results from a single elevation-based transect of monitoring locations to be utilized in a catchment-wide model calibration and validation. Our results showed that a combination of statistical, hydrologic, and plant growth objective functions as modeling metrics provide a more comprehensive understanding of system interactions. We included not only classical statistical metrics to calibrate our model, but we also calibrated the model to independent baseflow contribution estimates and plant growth dynamics. These novel calibration metric additions enabled us to improve the simulated hydrologic partitioning distributed throughout the catchment.

Our goal of simulating high-frequency monsoonal events in an area of complex physiographic topography provided substantial reliability in the use of the SWAT model in similar mountainous areas, particularly throughout East Asia. To enhance the calibration of the SWAT model, simulation of daily spatiotemporal stream discharge was improved through the incorporation of additional modeling metrics. Spatial variations of baseflow contributions and spatiotemporal plant growth dynamics through LAI helped to better constrain catchment-wide hydrologic partitioning. Our results show that

fundamental shifts between surficial and baseflow driven hydrologic flow partitioning occur within the catchment. High elevation steep sloping regions were found to be generally baseflow dominated while lower elevation locations were predominately influenced by surface runoff.

The influences of engineered infrastructure systems (roads and culverts) were significant in hydrologic flow partitioning. Our results indicate that multiple calibration metrics and hydrologic characteristics (R^2 , NSE, PBIAS, baseflow percentage, and plant growth) were influential in quantifying scale-dependent watershed processes. By not including the culverts into the simulations, we demonstrate that the model simulations adequately represented observed spatiotemporal discharge. However, by including PBIAS as a calibration metric, we improved flow partitioning on the landscape scale by up to 33 %, particularly at the low elevation locations while minimal variations were observed at upper elevations. To optimize PBIAS, we explicitly included the culverts and the culverts and roads into the modeled drainage system to demonstrate that the spatially extensive irrigation culverts adjacent to most fields and the road network play an important role in flow routing.

However, there were limitations in the reliability of modeling in similar regions, particularly with respect to field estimates, data collection, and the conceptual model. In relatively ungauged locations, it can be difficult to adequately distribute a monitoring network with high-frequency temporal resolution. Data gaps due to equipment malfunction and instrument sensitivity to ice can be prevalent in locations with complex topography and meteorological variability. Another significant source of uncertainty is irrigation and consumptive use water withdrawal quantification. However, limited detailed data is typically available on the quantity, timing, or location of water withdraws and care should be taken to incorporate into model construction.

Overall, the results of this study show that unique modeling methodologies can be employed to decrease modeling uncertainty including accurate meteorological boundary conditions, spatially distributed monitoring locations, and additional physically based modeling metrics. Our results further elucidate the effect of catchment-scale engineered structures on discharge and the potential influence on nutrient loading and contaminant transport. Care must be taken during model construction to avoid overlooking valuable hydrologic information and complex relationships that may be deciphered through additional objective function metrics. This study shows the challenges of applying the SWAT model to complex terrain and meteorological extreme environments and the means to overcome these difficulties.

3.6 Acknowledgements.

The authors thank S. Bartsch for the invaluable technical assistance and hydrologic data collection, monitoring and analysis. We also thank Y. Kim for nutrient, fertilization, gas exchange analysis, and DNDC modeling simulations. We appreciate the interview data collected by P. Poppenborg, .Nguyen, and S. Trabert. This manuscript was significantly improved through the critical reviews of M. Volk and K. Bieger. Support from the International Research Training Group TERRECO (GRK 1565/1) funded through the Deutsche Forschungsgemeinschaft (DFG) at the University of Bayreuth is greatly acknowledged.

3.7 References

- Abbaspour, K.C., 2011 SWAT-CUP4: SWAT Calibration and Uncertainty Programs – A User Manual. EAWAG Swiss Federal Institute of Aquatic Science and Technology. **2011**: 103 pp.
- Abbaspour, K.C., M. Faramarzi, S.S. Ghasemi, H. Yang, 2009 Assessing the impact of climate change on water resources in Iran C8 - W10434. *Water Resources Research*. **45**: W10434.
- Abbaspour, K.C., C.A. Johnson, M.T. van Genuchten, 2004 Estimating Uncertain Flow and Transport Parameters Using a Sequential Uncertainty Fitting Procedure. *Vadose Zone Journal*. **3**: 1340-1352.
- Abbaspour, K.C., J. Yang, I. Maximov, R. Siber, K. Bogner, J. Mieleitner, J. Zobrist, R. Srinivasan, 2007 Modelling hydrology and water quality in the pre-alpine/alpine Thur watershed using SWAT. *Journal of Hydrology*. **333**: 413-430.
- Adiku, S.G.K., M. Reichstein, A. Lohila, N.Q. Dinh, M. Aurela, T. Laurila, J. Lueers, J.D. Tenhunen, 2006 PIXGRO: A model for simulating the ecosystem CO₂ exchange and growth of spring barley. *Ecological Modelling*. **190**: 260-276.
- Allen, R.G., L.S. Pereira, D. Raes, M. Smith, 1988 Crop Evapotranspiration – Guidelines for Computing Crop Water Requirements. FAO – Food and Agriculture Organization of the United Nations, Rome, Italy, FAO Irrigation and Drainage Paper. **56**.
- Andersson, J.C.M., A.J.B. Zehnder, G.P.W. Jewitt, H. Yang, 2009 Water availability, demand and reliability of in situ water harvesting in smallholder rain-fed agriculture in the Thukela River Basin, South Africa. *Hydrol. Earth Syst. Sci.* **13**: 2329-2347.
- Arnhold, S., M. Ruidisch, S. Bartsch, C.L. Shope, B. Huwe, 2013 Simulation of runoff patterns and soil erosion on mountainous farmland with and without plastic-covered ridge-furrow cultivation in South Korea. *Trans. ASABE*. **56**.
- Arnold, J.G., R. Srinivasan, R.S. Muttiah, J.R. Williams, 1998 Large area hydrologic modeling and assessment – Part 1: Model development. *JAWRA Journal of the American Water Resources Association*. **34**: 73-89.
- Bartsch, S., S. Frei, M. Ruidisch, C.L. Shope, S. Peiffer, B. Kim, J.H. Fleckenstein, 2014 River-aquifer exchange fluxes under monsoonal climate conditions. *Journal of Hydrology*. **509**: 601-614.
- Bennett, N.D., B.F.W. Croke, G. Guariso, J.H.A. Guillaume, S.H. Hamilton, A.J. Jakeman, S. Marsili-Libelli, L.T.H. Newham, J.P. Norton, C. Perrin, S.A. Pierce, B. Robson, R. Seppelt, A.A. Voinov, B.D. Fath, V. Andreassian, 2012 Characterising performance of environmental models. *Environmental Modelling & Software*. **40**: 20pp.
- Berka, C., H. Schreier, K. Hall, 2001 Linking Water Quality with Agricultural Intensification in a Rural Watershed. *Water, Air, and Soil Pollution*. **127**: 389-401.
- Butts, M.B., J.T. Payne, M. Kristensen, H. Madsen, 2004 An evaluation of the impact of model structure on hydrological modelling uncertainty for streamflow simulation. *Journal of Hydrology*. **298**: 242-266.
- Calder, I.R., 1992 Hydrologic effects of land use change, in: *Handbook of Hydrology*. Edited by: Maidment, D. R., McGraw Hill, Inc., New York, NY.
- Cho, J., D. Bosch, G. Vellidis, R. Lowrance, T. Strickland, 2012 Multi-site evaluation of hydrology component of SWAT in the coastal plain of southwest Georgia. *Hydrological Processes*. **27**: 1691-1700.
- Choi, G., B. Lee, S. Kang, J. Tenhunen, 2010 Variations of Summertime Temperature Lapse Rate within a Mountainous Basin in the Republic of Korea – A case study of Punch Bowl. *Yanggu in 2009*.

- Dessu, S.B., A.M. Melesse, 2012 Modelling the rainfall–runoff process of the Mara River basin using the Soil and Water Assessment Tool. *Hydrological Processes*. **26**: 4038-4049.
- Duan, Q., S. Sorooshian, V. Gupta, A.N. Rousseau, R. Turcotte, 2003 Calibration of watershed models. American Geophysical Union, Washington D.C.
- Eckhardt, K., 2005 How to construct recursive digital filters for baseflow separation. *Hydrological Processes*. **19**: 507-515.
- Faramarzi, M., K.C. Abbaspour, R. Schulin, H. Yang, 2009 Modelling blue and green water resources availability in Iran. *Hydrological Processes*. **23**: 486-501.
- Forti, M.C., C. Neal, A. Jenkins, 1995 Modeling perspective of the deforestation impact in stream water quality of small preserved forested areas in the amazonian rainforest. *Water, Air, and Soil Pollution*. **79**: 325-337.
- Gassman, P.W., M.R. Reyes, C.H. Green, J.G. Arnold, 2007 The soil and water assessment tool: Historical development, applications, and future research directions. *Trans. ASABE*. **50**: 1211–1250.
- Green, H., G.A. Ampt, 1912 Studies on Soil Physics: Part II – The Permeability of an Ideal Soil to Air and Water. *The Journal of Agricultural Science*. **5**: 1-26.
- Güngör, Ö., S. Göncü, 2012 Application of the soil and water assessment tool model on the Lower Porsuk Stream Watershed. *Hydrological Processes*. **27**: 453-466.
- Hargreaves, G.H., Z.A. Samani, 1985 Reference crop evapotranspiration from temperature. *Appl. Eng. Agr.* **1**: 96-99.
- Haverkamp, S., R. Srinivasan, H.G. Frede, C. Santhi, 2002 Subwatershed spatial analysis tool: discretization of a distributed hydrologic model by statistical criteria. *JAWRA Journal of the American Water Resources Association*. **38**: 1723-1733.
- Jha, M., P.W. Gassman, S. Secchi, R. Gu, J. Arnold, 2004 Effect of watershed subdivision on swat flow, sediment, and nutrient predictions. *JAWRA Journal of the American Water Resources Association*. **40**: 811-825.
- Jo, K.-W., J.-H. Park, 2010 Rapid Release and Changing Sources of Pb in a Mountainous Watershed during Extreme Rainfall Events. *Environmental Science & Technology*. **44**: 9324-9329.
- Jun, M., 2009 Device for Reducing Muddy Water in the Watershed of Soyang Dam. Regional Institute of Gangwon, South Korea.
- Jung, B.-J., H.-J. Lee, J.-J. Jeong, J. Owen, B. Kim, K. Meusburger, C. Alewell, G. Gebauer, C. Shope, J.-H. Park, 2012 Storm pulses and varying sources of hydrologic carbon export from a mountainous watershed. *Journal of Hydrology*. **440-441**: 90-101.
- Khakbaz, B., B. Imam, K. Hsu, S. Sorooshian, 2012 From lumped to distributed via semi-distributed: Calibration strategies for semi-distributed hydrologic models. *Journal of Hydrology*. **418-419**: 61-77.
- Kim, I., G.Y. Jeong, S. Park, J. Tenhunen, 2011 Predicted Land Use Change in the Soyang River Basin, South Korea. TERRECO Science Conference, Karlsruhe Institute of Technology, Garmisch-Partenkirchen, Germany, October 2–7, 2011.
- Kwon, Y.S., H.H. Lee, U. Han, W.H. Kim, D.J. Kim, D.I. Kim, S.J. Youm, 1990 Terrain analysis of Haean Basin in terms of earth science. *J. Korean Earth Sci. Soc.* **11**: 236-241.
- Lam, Q.D., B. Schmalz, N. Fohrer, 2012 Assessing the spatial and temporal variations of water quality in lowland areas, Northern Germany. *Journal of Hydrology*. **438-439**: 137-147.

- Lee, H.J., K.W. Chun, C.L. Shope, J.H. Park, 2014 Detecting rapid changes in stream water quality in mountainous forested watersheds during the monsoon period – The importance of highfrequency monitoring. *J. Hydrol.*, in review.
- Lee, J.M., J.C. Ryu, H.W. Kang, H.S. Kang, D.H. Kum, C.H. Jang, J.D. Choi, K.J. Lim, 2012 Evaluation of SWAT Flow and Sediment Estimation and Effects of Soil Erosion Best Management Practices. *J. Korean Soc. Agr. Eng.* **54**: 99–108.
- Lee, J.W., J.S. Eum, B. Kim, W.S. Jang, J.C. Ryu, H.W. Kang, K.S. Kim, K.J. Lim, 2011 Water Quality Prediction at Mandae Watershed using SWAT and Water Quality Improvement with Vegetated Filter Strip. *J. Korean Soc. Agr. Eng.* **53**: 37–45.
- Mekonnen, M.A., A. Wörman, B. Dargahi, A. Gebeyehu, 2009 Hydrological modelling of Ethiopian catchments using limited data. *Hydrological Processes.* **23**: 3401-3408.
- Monteith, J.L., 2009 1965 Evaporation and the Environment, in: *The state and movement of water in living organisms.* Edited by: Fogg, G. E., Cambridge University Press: 205–234.
- Moriassi, D.N., J.G. Arnold, M.W.V. Liew, R.L. Bingner, R.D. Harmel, T.L. Veith, 2007 Model Evaluation Guidelines for Systematic Quantification of Accuracy in Watershed Simulations. *Trans. ASABE.* **50**: 885–900.
- Nash, J.E., J.V. Sutcliffe, 1970 River Flow Forecasting through Conceptual Models Part 1 – A Discussion of Principles. *J. Hydrol. (Amsterdam).* **10**: 282-290.
- Neitsch, S.L., J.G. Arnold, J.R. Kiniry, R. Srinivasan, J.R. Williams, 2010 Soil and Water Assessment Tool Input/Output File Documentation Version 2009. Grassland, Soil and Water Research Laboratory, Agricultural Research Service and Blackland Research Center, Texas Agricultural Experiment Station, College Station, Texas.
- Neitsch, S.L., J.G. Arnold, J.R. Kiniry, J.R. Williams, 2011 Soil and Water Assessment Tool Theoretical Documentation Version 2009. Grassland, Soil and Water Research Laboratory, Agricultural Research Service and Blackland Research Center, Texas Agricultural Experiment Station, College Station, Texas, 2011.
- Nguyen, T.T., V.-N. Hoang, B. Seo, 2012 Cost and environmental efficiency of rice farms in South Korea. *Agricultural Economics.* **43**: 369-378.
- Notter, B., H. Hurni, U. Wiesmann, K.C. Abbaspour, 2012 Modelling water provision as an ecosystem service in a large East African river basin. *Hydrol. Earth Syst. Sci.* **16**: 69-86.
- Notter, B., L. MacMillan, D. Viviroli, R. Weingartner, H.-P. Liniger, 2007 Impacts of environmental change on water resources in the Mt. Kenya region. *Journal of Hydrology.* **343**: 266-278.
- Penman, H.L., 1948 Natural Evaporation from Open Water, Bare Soil and Grass. *Proceedings of the Royal Society of London A: Mathematical, Physical and Engineering Sciences.* **193**: 120-145.
- Priestley, C.H.B., R.J. Taylor, 1972 On the Assessment of Surface Heat Flux and Evaporation Using Large-Scale Parameters. *Mon. Weather Rev.* **100**: 81–92.
- Ruidisch, M., J. Kettering, S. Arnhold, B. Huwe, 2013 Modeling water flow in a plastic mulched ridge cultivation system on hillslopes affected by South Korean summer monsoon. *Agricultural Water Management.* **116**: 204-217.
- Schuol, J., K.C. Abbaspour, 2006 Calibration and uncertainty issues of a hydrological model (SWAT) applied to West Africa. *Adv. Geosci.* **9**: 137-143.
- Schuol, J., K.C. Abbaspour, R. Srinivasan, H. Yang, 2008 Estimation of freshwater availability in the West African sub-continent using the SWAT hydrologic model. *Journal of Hydrology.* **352**: 30-49.
- Setegn, S., G.R. Srinivasan, B. Dargahi, 2008 modelling in the Lake Tana Basin, Ethiopia using SWAT model. *The Open Hydrol. J.* **2**: 49-62.

- Shope, C.L., S. Bartsch, K. Kim, B. Kim, J. Tenhunen, S. Peiffer, J.-H. Park, Y.S. Ok, J. Fleckenstein, T. Koellner, 2013 A weighted, multi-method approach for accurate basin-wide streamflow estimation in an ungauged watershed. *Journal of Hydrology*. **494**: 72-82.
- Stehr, A., P. Debels, F. Romero, H. Alcayaga, 2008 Hydrological modelling with SWAT under conditions of limited data availability: evaluation of results from a Chilean case study. *Hydrological Sciences Journal*. **53**: 588-601.
- Strauch, M., C. Bernhofer, S. Koide, M. Volk, C. Lorz, F. Makeschin, 2012 Using precipitation data ensemble for uncertainty analysis in SWAT streamflow simulation. *Journal of Hydrology*. **414**: 413-424.
- Strauch, M., J.E.F.W. Lima, M. Volk, C. Lorz, F. Makeschin, 2013 The impact of Best Management Practices on simulated streamflow and sediment load in a Central Brazilian catchment. *Journal of Environmental Management*. **127**: S24-S36.
- Tenhunen, J., B. Seo, B. Lee, 2011 Spatial setting of the TERRECO project in the Haean catchment of Yanggu-gun and the Soyang watershed in Gangwan-do, AsiaFlux Training Course on Flux Monitoring: From Theory to Application, Seoul, South Korea.
- Tilman, D., K.G. Cassman, P.A. Matson, R. Naylor, S. Polasky, 2002 Agricultural sustainability and intensive production practices. *Nature*. **418**: 671-677.
- Tripathi, M.P., N.S. Raghuvanshi, G.P. Rao, 2006 Effect of watershed subdivision on simulation of water balance components. *Hydrological Processes*. **20**: 1137-1156.
- U.S.D.A., 1972 Soil Conservation Survey SCS, National Engineering Hand Book, Section 4, in: *Hydrology*, edited by: U.S.D.A, Washington, DC.
- Volk, M., S. Liersch, G. Schmidt, 2009 Towards the implementation of the European Water Framework Directive?: Lessons learned from water quality simulations in an agricultural watershed. *Land Use Policy*. **26**: 580-588.
- Wilson, C.B., J.B. Valdes, I. Rodriguez-Iturbe, 1979 On the influence of the spatial distribution of rainfall on storm runoff. *Water Resources Research*. **15**: 321-328.
- Xu, N., J.E. Sayers, H.F. Wilson, P.A. Raymond, 2012a Simulating streamflow and dissolved organic matter export from a forested watershed C8 - W05519. *Water Resources Research*. **48**: W05519.
- Xu, Y.D., B.J. Fu, C.S. He, G.Y. Gao, 2012b Watershed discretization based on multiple factors and its application in the Chinese Loess Plateau. *Hydrol. Earth Syst. Sci*. **16**: 59-68.
- Yang, J., P. Reichert, K.C. Abbaspour, J. Xia, H. Yang, 2008 Comparing uncertainty analysis techniques for a SWAT application to the Chaohe Basin in China. *Journal of Hydrology*. **358**: 1-23.
- Yanggu County Office, 2012 Yanggu statistical year-book, 2002–2011, Yanggu, Gangwon, Republic of Korea.

Chapter 4 Identifying scenario-based optimal land use systems and assessing trade-offs between farm income and environment: Haean catchment, South Korea

Ganga Ram Maharjan¹, Christopher L. Shope², Trung Thanh Nguyen³, Thomas Koellner⁴, Bernd Huwe¹, Seong Joon Kim⁵, John Tenhunen⁶, Sebastian Arnhold^{1,4}

¹University of Bayreuth, Dept. of Soil Physics, Universitatstrasse 30, 95440 Bayreuth, Germany

²US Geological Survey, 2329 Orton Circle, Salt Lake City, UT, USA

³University of Hannover, Institute for Environmental Economics and World Trade, Koenigsworther Platz 1, 30167-Hannover, Germany

⁴University of Bayreuth, Professorship of Ecological Services, Universitatstrasse 30, 95440 Bayreuth, Germany

⁵Konkuk University, Dept. of Civil & Environmental System Engineering, Seoul 143-701, Korea

⁶University of Bayreuth, Dept. of Plant Ecology, Universitatstrasse 30, 95440 Bayreuth, Germany

Abstract

Intensive agriculture and high economic activity based land use systems of major dryland crops (cabbage, potato, radish, and soybean) in the Haean catchment, South Korea produce extensive sediment and nutrient exports to Soyang Lake. The SWAT model was primarily implemented for scenario analysis of base line land use systems with dryland monoculture to determine the corresponding ecological and economical outputs. The novelty of this study is to present a simple and transparent methodological approach to reallocate crops from different monoculture and base line land use systems and derive optimal land use systems under different ecological and economic objectives. We derived four optimal land uses systems based on the objectives of: a) minimum surface runoff, b) minimum sediment, c) maximum crop yield, and d) maximum income for each field. Each optimal land use system was analyzed to identify the associated ecological and economical trade-offs with respect to surface runoff, sediment loss, crop yield, and farm income. The optimal land use system which produces the minimum sediment loss (10.19 tons ha⁻¹) has the trade-offs of reduced economic performance by producing 16 % lower income compared to the land use system optimized for maximum income. The optimal land use system for maximum income (67.40 million won ha⁻¹) has trade-offs of producing 46 % higher sediment loss compared to that optimized for minimum sediment loss. The presented methodological approach to derive an optimal land use system and to quantify the associated trade-offs aids farmers, stakeholders, and policy makers in the identification of land use systems for sustainable agriculture.

Keywords: *Soil and Water Assessment Tool (SWAT), crop reallocation, ecology, economy, land use systems, catchment*

4.1 Introduction

The worldwide population growth has put more stress on watershed resources (land, forest, water) to secure additional food, shelter, and high quality water (Arnell, 2004). The stress due to population growth leads to intensive agriculture production through a variety of land management practices and changes in land use including urbanization and deforestation (Rasul, 2009). These anthropogenic influences affect the watershed characteristics by producing the negative environmental impact of sediment and nutrient export to streams, which further exacerbates degradation of lake and reservoir water quality. Sustainable management activities that reduce the negative environmental impact of soil erosion and water quality deterioration while securing crop yield and farm income from the agricultural production within watersheds are of growing concern (Stoorvogel et al., 2004). The assurance of good water quality with decreased nutrient and sediment transport depends on an optimal land use system consistent with local and regional policy decisions and the socio-economic condition (Kruseman et al., 1995). The optimal land use systems are further constrained by local management requirements and climatic conditions. Consequently, the estimation of farm income from the specified land use system is a function of a farmer's willingness to adopt the land use system. The prediction of environmental impact and the associated income under different land use scenarios assists policy makers in the identification of trade-offs between environmental changes and farm income. The quantified trade-offs help to modify the land use system with recommendations of specific land uses to secure both environmental quality and farm income. The spatial and temporal variability of agricultural land use biophysical processes lead to complex interactions that produce a range of ecosystem services (crop yield and water quality). The resulting complexity necessitates a modeling approach to quantitatively determine the resulting ecosystem services. Biophysical process modeling in combination with Geographic Information Systems has been widely used to simulate and predict processes that are dependent on spatial variables such as topography, soil, land use and land cover characteristics throughout a watershed. In addition, several bio-economic models have been implemented that explore environmental and economic impacts resulting from the intervention of adaptive policy and technology changes in agricultural systems (Okumu et al., 2004; Shiferaw and Holden, 2000).

In this study, we used the Soil and Water Assessment Tool (SWAT) as a biophysical model to quantify crop yield/biomass, stream discharge, and sediment from a variety of land use system scenarios within the catchment. SWAT incorporates a suite of algorithms for the impact assessment of various land management and land use systems on non-point pollution sources (Amon-Armah et al., 2013; Cerro et al., 2014b; Ullrich and Volk, 2009). However, the economic income impact associated with the crop/land use system is not explicitly integrated within the SWAT model. Limited studies have used SWAT to link farm income/economics with management practices and land use changes in an effort to control non-point pollution sources (Attwood et al., 2000; Bhattarai et al., 2008). We developed a post-processing tool for the SWAT model using the R code (R software version 2.15.2)

for the prediction of farm income as a function of simulated crop yield, price, and total production cost.

The farm income associated with high economic activity in relation to this particular study area is based on the land use system of four major dryland crops (cabbage, potato, radish, and soybean). The farmer's attitude towards crop yield security by using excess fertilizer and cultivation in high elevations degrades environmental conditions through sedimentation and deterioration of the water quality. Several methods to increase soil stability (Choi et al., 2012) and best management practices (BMPs) such as vegetated filter strips (VFS) (Lee et al., 2011) and rice straw mats (Lee et al., 2012) have been implemented in similar highland agriculture locations throughout South Korea to control soil erosion. Multi-dimensional analysis (discharge, sediment, and crop yield/income) from different land use systems coupled with specific land management to reduce surface runoff and sediment and to secure crop yield and farm income is a major focus of this study. The novelty of this study is to present a simple and transparent methodological approach to derive optimal land use systems for different objectives. Four different land use systems optimized for maximum income, maximum crop yield, minimum sediment, and minimum surface runoff. The objectives of our study are to analyze economic and ecological trade-offs associated with each land use system. Our methodological approach can be implemented for similar studies to develop an understanding of land use systems under different objectives and quantify the associated trade-offs. This study helps farmers, policy makers, and other stakeholders to identify the effects on agricultural economics and ecosystem services as a function of optimized land use scenarios.

4.2 Methodology

4.2.1 Study area

This study was conducted in the Haeon catchment (62.7 km²) of South Korea, which is characterized by intensive agricultural practices and excessive fertilizer application. The catchment has been used for several field experiments to study sediment and nutrient transport under different management practices (Tenhunen et al., 2011). The study area (128°5' to 128°11' E, 38°13' to 38°20' N) is located in the Gangwon Province in the northeastern part of South Korea near the Demilitarized Zone (DMZ) between South and North Korea (Figure 4.1). The study catchment is near the headwaters of the Soyang Lake watershed which drains into the Soyang reservoir. The topography of the study catchment is a bowl-shaped valley surrounded by steep mountains mostly covered by deciduous forest. The percentage of land use coverage and the abbreviations for each spatially distributed land use system in Figure 4.1 is presented in Table 4.1. The elevation ranges from 340 m in the valley to 1320 m in the mountain highlands with an average slope of 28 % and a maximum slope of 84 %. The catchment was instrumented with several monitoring locations (Figure 4.1) along selected rivers from upstream to downstream including the main outlet of the watershed to record time series data on discharge, sediment, and nutrients. The yearly maximum and minimum average temperature were 12.5

°C and 2.5 °C, respectively and the average annual precipitation is 1658 mm, based on a 13 year meteorological record in the Haeon catchment (1999-2011). Nearly 70% of the annual precipitation is concentrated within June to September. The average monthly variations in precipitation and the maximum and minimum temperature are depicted in Figure 4.2.

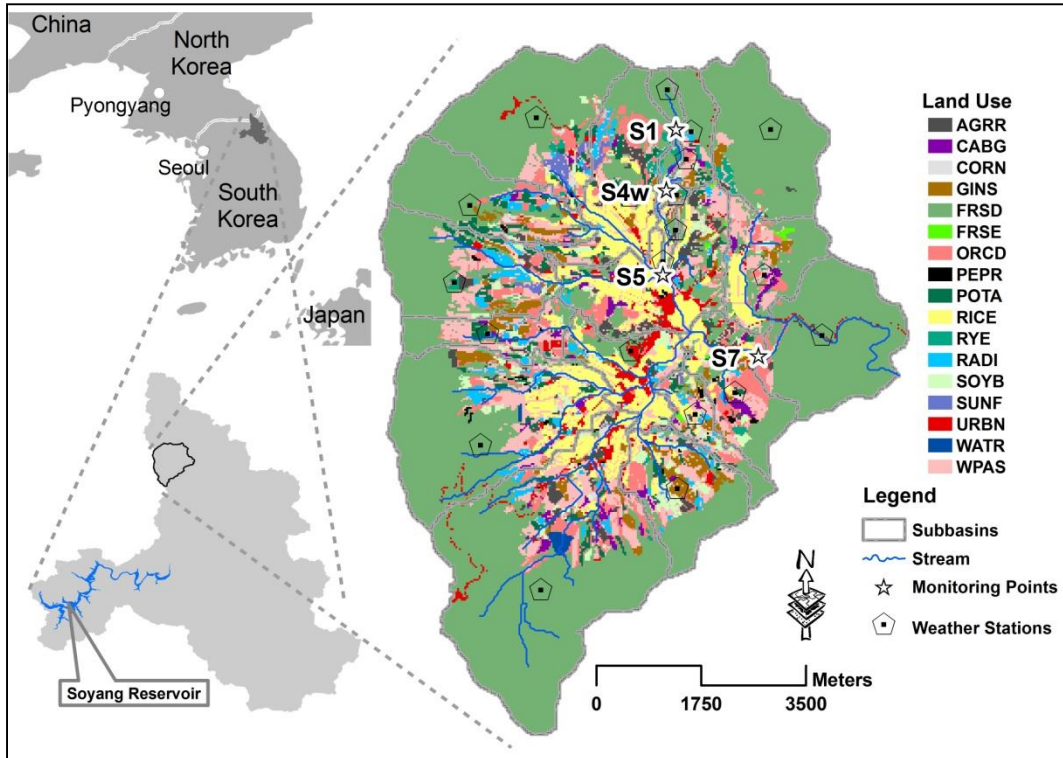


Figure 4.1 Location of the study area on the Korean peninsula and within the Soyang Lake watershed. In addition, the land use distribution of the Haeon catchment is depicted. Land use abbreviations are provided in Table 4.1. The Haeon catchment is a hot spot for sediment and nutrients transport to the Soyang Reservoir

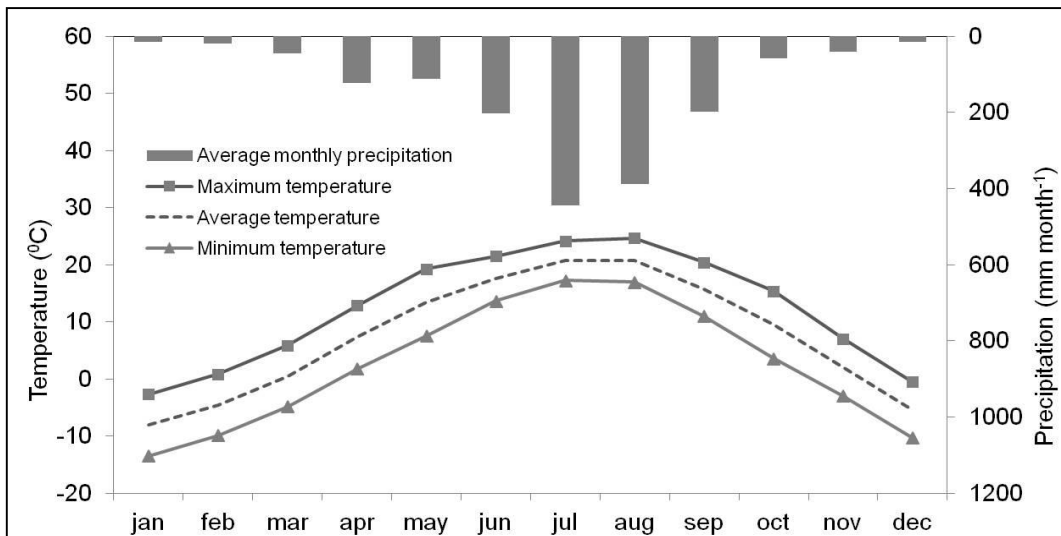


Figure 4.2 Average monthly temperature and precipitation in the Haeon catchment for the period of 1999 - 2011 from all weather stations (Figure 4.1) throughout the entire catchment.

Table 4.1 Land use distribution in the Haean catchment.

Land use	LULC Identification	Area (km ²)	Percentage catchment
Agricultural row crop	AGRR	1.46	2.33
Cabbage	CABG	0.70	1.12
Maize	CORN	0.18	0.29
Deciduous forest	FRSD	35.56	56.71
Coniferous forest	FRSE	0.07	0.11
Orchard	ORCD	3.55	5.66
Pepper	PEPR	0.15	0.24
Potato	POTA	1.56	2.49
Rice	RICE	5.17	8.24
Rye	RYE	0.50	0.80
Radish	RADI	1.21	1.93
Soybean	SOYB	1.42	2.26
Sunflower	SUNF	0.30	0.48
Ginseng	GINS	1.61	2.57
Residential area	URBN	1.56	2.49
Inland water	WATR	0.15	0.24
Winter pasture	WPAS	7.56	12.06

4.2.2 Data collection and model setup

This study used SWAT as a biophysical model to mimic the ecological condition of the Haean catchment and simulate discharge, sediment, and crop yield. Shope et al. (2014) described the methodological details necessary to provide and parameterize the input data into the SWAT model for the Haean catchment. The major input data sets for the SWAT model are spatiotemporal meteorological observations, the digital elevation model (DEM), the land use/land cover (LULC) characterization, and the soil distribution. The model input data and associated sources are provided in Table 4.2.

Table 4.2 Sources and scale of each of the input data sets for the SWAT model construction and daily meteorological inputs

Spatial data sets	Data set type	Scale
Catchment DEM	Clipped DEM from Soyang Lake contour map	1:25000
Stream network	Surveyed river channels in study area	1:10000
LULC map	Validated map for year 2010 (Seo et al., 2014)	1:5000
Soil map	Field based soil profile (1.2 m) from 2009-2011	1:10000
Daily solar radiation	Chuncheon network weather station (1998-2011)	point
Daily precipitation, temperature	Haean network weather station (1998-2011)	point
Daily relative humidity, wind speed	Yanguu network weather station (1998-2011)	point
Daily discharge and sediment	Used for model calibration/validation field-measurement	point

The agricultural land use is typically composed of small patches of agricultural fields that are spatially distributed throughout the catchment, where 32.3 % include annual dryland crops (such as cabbage, potato, radish, soybean etc) and perennial crops (orchard) and 8.2 % wet land crop (rice). Additional land use distributions include residential area (2.5 %), water bodies (0.3 %), and the dominant land cover of deciduous and coniferous forest (56.7 %), predominantly located in the elevated portions of the catchment (Figure 4.1, Table 4.1). Arnhold et al. (2013, 2014) described the sediment runoff from

several measurement plots with soil information throughout the catchment and Shope et al. (2014) synthesized this information with additional soil parameters based on a 2009 field survey and adapted the soil database of the SWAT model. The unique soil types and their relative spatial percentage within the catchment are presented in Table 4.3.

Table 4.3 Soil type distribution throughout the Haean catchment

Soil Type	Texture	Hydrologic group	Area (km ²)	Percentage catchment
Flat dryland soil	Sand – Silt	D	8.01	12.76
Forest soil	Loam – Sand	C	32.54	51.88
Moderate to steep dryland soil	Sand – Silt	D	9.22	14.69
Rice paddy soil	Sand	C	6.57	10.47
Sealed ground	Clay	D	1.72	2.74
Very steep forest soil	Loam – Sand	C	4.67	7.45

4.2.3 The SWAT model

The SWAT model is a catchment to river basin-scale model, which was developed by Arnold et al. (1993) to predict the impact of land management practices on water, sediment, and agricultural chemicals applied in watersheds under varying soil, land use, and management conditions over an extended period of time. The SWAT model uses the concept of hydrologic response units (HRUs). After division of the catchment into topographical sub-basins, the model combines the soil distribution with the land use and land cover discretization and the slope characteristics to form spatially distributed HRUs (Neitsch et al., 2011). The output variables of the model such as surface runoff and sediment accumulation and degradation are estimated at the HRU level which are aggregated from individual HRUs into the sub-basin level and then routed (the variable storage method is used in this study) through the stream network. The Manning equation is used to estimate the velocity and flow rate through the stream channels.

The fundamental hydrological equation, which is integrated into the SWAT model to quantify the stream discharge, is

$$SW_t = SW_0 + \sum_{i=1}^t [(R_{day})_i - (Q_{surf})_i - (E_a)_i - (W_{seep})_i - (Q_{GW})_i] \quad (4.1)$$

where, SW_i is the final soil water content (mm H₂O), SW_0 is the initial soil water content on day i (mm H₂O), R_{day} is the amount of precipitation on day i (mm H₂O), Q_{surf} is the amount of surface runoff on day i (mm H₂O), E_a is the amount of evapotranspiration on day i (mm H₂O), W_{seep} is the amount of percolation and bypass flow exiting the bottom of the soil profile on day i (mm H₂O), and Q_{GW} is the amount of return flow on day i (mm H₂O).

Sediment generation in the catchment is due to natural erosion processes and includes the detachment, transport, and deposition of soil particles by the erosive forces of raindrops and surface flow of water. The SWAT model estimates the sediment yield based on the Modified Universal Soil Loss Equation (MUSLE), which contains several parameters related to topography, soil properties, rainfall, as well as

the crop and management practices applied throughout the catchment (Swallow et al., 2009). Sediment loss is calculated as

$$sed = 11.8 \cdot (Q_{surf} \cdot q_{peak} \cdot area_{hru})^{0.56} \cdot K_{USLE} \cdot C_{USLE} \cdot P_{USLE} \cdot LS_{USLE} \cdot CFRG \quad (4.2)$$

where, sed is the sediment yield on a given day (metric tons), Q_{surf} is the surface runoff volume (mm H₂O ha⁻¹), q_{peak} is the peak runoff rate (m³ s⁻¹), $area_{hru}$ is the area of the HRU (ha), K_{USLE} is the USLE soil erodibility factor (0.013 metric ton m² hr (m³ metric ton cm)⁻¹), C_{USLE} is the USLE cover and management factor, P_{USLE} is the USLE support practice factor, LS_{USLE} is the USLE topographic factor, and $CFRG$ is the coarse fragment factor.

Several experimental plots were analyzed for the crop physiological parameters (LAI, leaf area index) of cabbage, potato, radish, soybean, and rice. In addition, the observed yield from each respective crop was used to determine the harvest index in the SWAT model. The plant growth component of the SWAT model is a simplified version of the EPIC model and based on daily accumulated heat units. The harvest index from the measured field harvest data is used to compare and optimize the crop yield from the simulated accumulated biomass. The maximum increase in biomass on a given day that will result from the intercepted photosynthetically active radiation is estimated from Monteith and Moss (1977) as,

$$\Delta bio = RUE \cdot H_{phosyn} \quad (4.3)$$

where, Δbio is the potential increase in total biomass on a given day (kg ha⁻¹), RUE is the radiation-use efficiency of the plant (kg ha⁻¹ · (MJ (m²)⁻¹)⁻¹ or 0.1g MJ⁻¹). H_{phosyn} is the amount of intercepted photosynthetically active radiation on a given day (MJ m⁻²). Further details on the crop growth component are provided in the SWAT Theoretical Documentation (Neitsch et al., 2011).

4.2.4 Model parameterization, calibration, and validation

The study area was delineated to incorporate 21 sub-basins based on the digital elevation model, which were further divided into 792 individual HRUs formed by combining the soil map and the land use and land cover map, as described previously. The model was simulated for the years 2007-2011 on a daily time step, in which the first two years of the simulation were considered as a warm up period to exclude the effects of initial conditions set by the user during the calibration. The model was separately calibrated and validated for stream discharge and sediment. The calibration was performed at multiple monitoring sites (S1, S4W, S5, and S7) (Figure 4.1). The calibration period was 2009-2010 and the validation period was 2011.

Following Shope et al. (2014), the multi-site calibration was performed initially for the entire catchment outlet (S7); subsequently, the model was calibrated for the remaining sites beginning with the highest elevation location and ending with a final calibration again at the catchment outlet. The

model calibration procedure was automated by using the Sequential Uncertainty Fitting Algorithm (SUFI2) in SWAT- CUP (Abbaspour et al., 2004; Abbaspour et al., 2007). Initially, the discharge parameters were varied within the absolute range defined as default conditions in SUFI2 while calibrating the individual sites (Appendix 4A). In the final calibration at the main outlet of the catchment (S7), the parameters for individual sites were varied based on the respective reach and the parameter ranges were modified to include the best fit value from the individual site calibrations. Further details on model calibration, validation, and uncertainty for discharge are presented in Shope et al. (2014).

The sediment calibration for site S1 was performed manually by adjusting the parameter value of USLE_K (0.07) (Eq.4.2, soil erodibility factor), USLE_P (0.37) (Equation-4.2, support practice factor), CANMX (21.76 mm) (amount of water that can be trapped in canopy), CN2 (66) (SCS curve number for moisture condition II) within their respective absolute values for sub-basin 1. The sediment calibration for S4W and S5 were based on automatic calibration and performed individually for each location using a similar methodology. The model performance was evaluated using the Nash-Sutcliffe efficiency (NSE) and the coefficient of determination (R^2). NSE values range from negative infinity to 1, where higher values represent a better goodness of fit with the measured variable. R^2 values range from 0 to 1, where values close to 1 represent that the simulated time series closely approximates the observed values. Once sediment calibration was performed for site S1, S4W, and S5, the model performance at the main outlet of the catchment (S7) was evaluated, resulting in NSE and R^2 values of 0.57 and 0.82, respectively.

Discharge and sediment calibration were followed by manual calibration of the leaf area index (LAI) development and crop yield for the major crops (cabbage, radish, soybean, potato, corn, and rice), deciduous forest, and orchard while controlling the outputs for discharge and sediment. LAI and biomass development affect discharge and sediment due to variation of evapotranspiration and USLE_C (crop coverage). The model performance for discharge and sediment is therefore directly related to a realistic representation of plant development in the catchment. Since crop development and yield were of major concern for the trade-off analysis in this study, the simulation required a simultaneous calibration of discharge, sediment loss, and crop yield (through LAI) to achieve reasonable model performance for both water quality and plant growth. The parameter values that were determined by the calibration of discharge, sediment, and LAI are presented in Appendix 4A and Appendix 4B. The stream discharge and sediment transport performance statistics of the model (NSE and R^2) for each monitoring location are presented in Table 4.4, both for the calibration and validation periods.

Table 4.4 Statistical performance of the model during calibration and validation

Stream sites	Stream discharge						Sediment					
	Calibration (2009-2010)			Validation (2011)			Calibration (2009-2010)			Validation (2011)		
	R ²	NSE	PBIAS (%)	R ²	NSE	PBIAS (%)	R ²	NSE	PBIAS (%)	R ²	NSE	PBIAS (%)
S1	0.76	0.72	5.4	0.75	0.54	46.3	0.98	0.87	8.8	0.71	0.62	-37.8
S4W*	0.82	0.64	3.7	0.7	0.03	46.8	0.32	0.23	11.2	0.77	0.31	126.9
S5	0.89	0.87	-1.8	0.74	0.48	75.5	0.94	0.94	33.6	0.83	0.62	68.1
S7	0.82	0.75	-38.4	0.85	0.73	-31.8	0.82	0.57	-46.7	0.92	0.90	11.3

*Calibration period for stream site S4W was only 2010

The calibration of monitoring sites S1, S5, and S7 produced NSE and R² values that were higher than 0.5 and typically greater than 0.7. However, calibration and validation results for both discharge and sediment transport from monitoring location S4W were less robust. The validations of discharge at S4W resulted in a NSE value of 0.03. In addition, the R² and NSE values for sediment calibration were as low as 0.23. According to previous analyses of SWAT-based calibration techniques, model performance can be considered acceptable when NSE and R² are greater than 0.5 and the model can be used for further scenario analysis (Gassman et al., 2007; Moriasi et al., 2007; Santhi et al., 2001). In addition to the NSE and R², the percentage bias (PBIAS) metric is considered to evaluate the model performance. Low-magnitude PBIAS values indicate reduced deviations between simulated and observed values and suggest accurate model simulation. Positive values indicate an overestimation bias, whereas negative values indicated a model underestimation bias. The overall PBIAS values during the calibration and validation for both discharge and sediment at the individual monitoring locations are presented in Table 4.4. The graphical inspection of the time series (simulated vs. observed data) for the calibrated and validated model are presented in Figure 4.3 and Figure 4.4, for discharge and sediment, respectively.

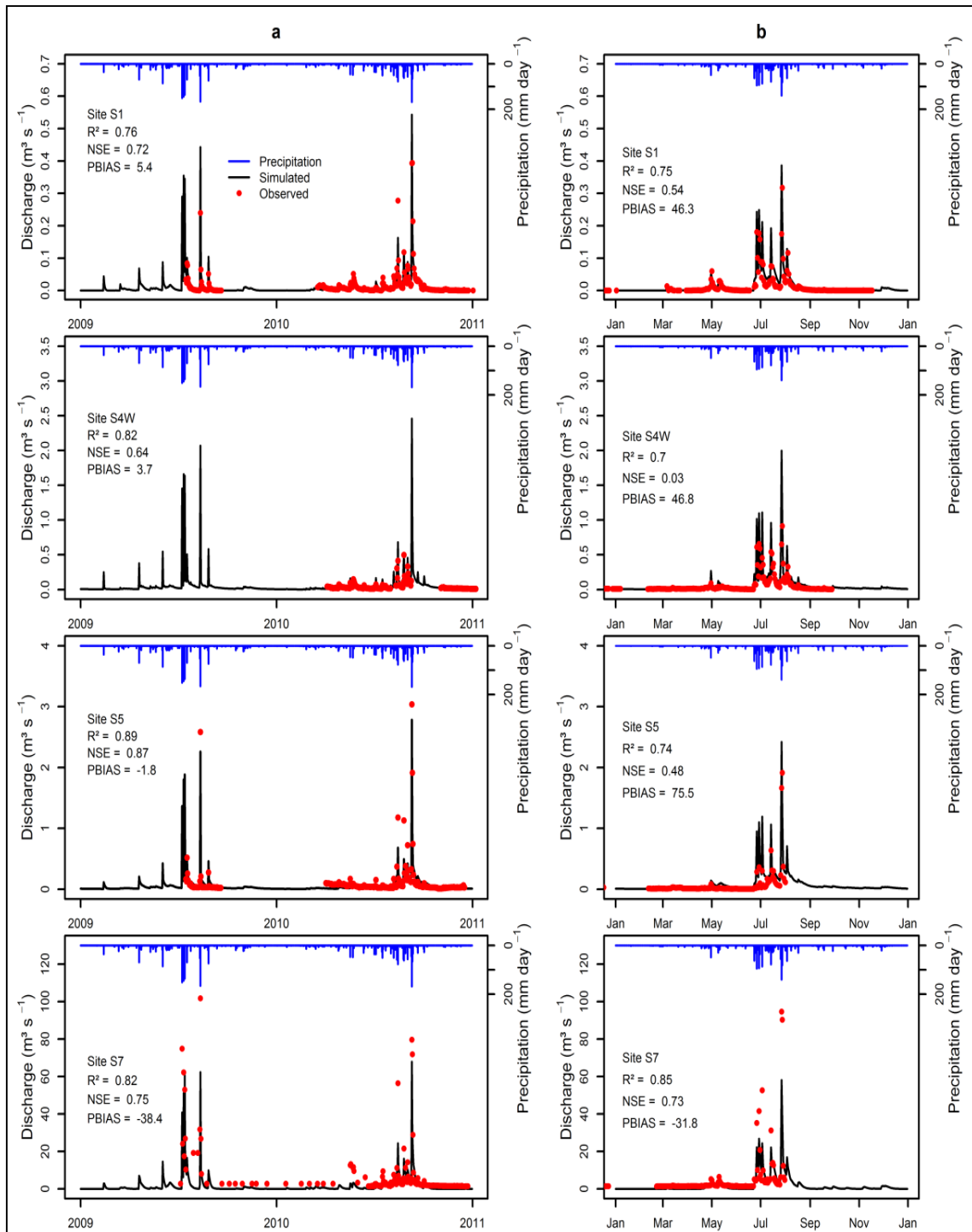


Figure 4.3 Observed and simulated discharge for the calibration (2009-2010) (a) and validation (2011) (b) periods at each of the different monitoring locations. The inverted secondary y-axis represents precipitation

From Figure 4.3, the peak discharge during the calibration period at monitoring locations S1 and S4W are both slightly overestimated, which are also indicated by the positive PBIAS values of 5.4 and 3.7 (Table 4.4), whereas low flows are well captured. However, during the validation period for monitoring locations S1 and S4W, peak discharge was highly overestimated as indicated by the high positive PBIAS values of 46.3 and 46.8, respectively. The PBIAS value for S5 during the calibration of discharge is -1.8 , which depicts a slight underestimation of peak flows, whereas during the

validation period, the model simulates an overestimation of several peaks (Figure 4.3 for site S5) with a positive PBIAS value of 75.5. In both calibration and validation of stream discharge for the catchment outlet (S7), the peak flows and low flows are under-predicted (Figure 4.3) indicated by negative PBIAS values (-38.4 and -31.8).

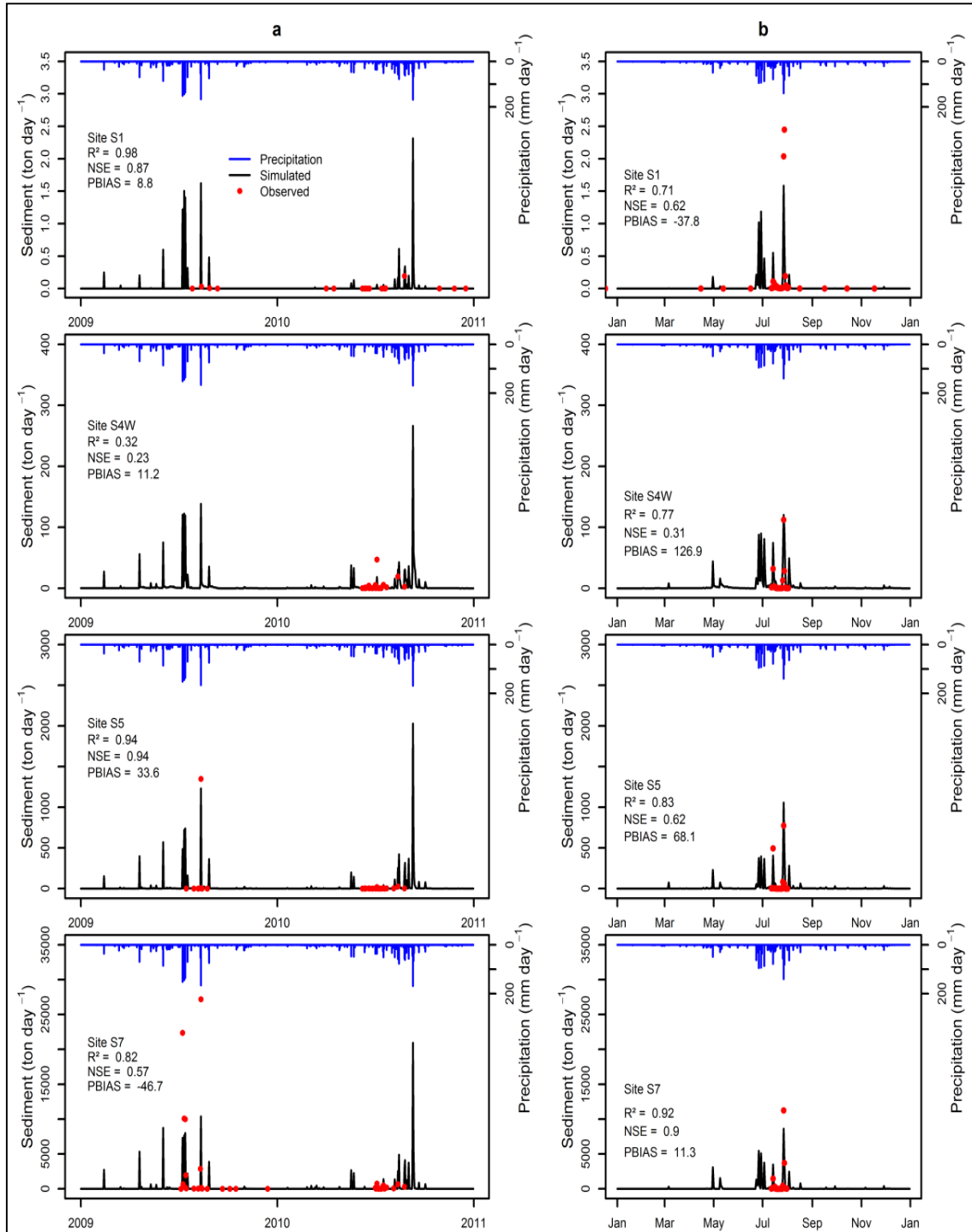


Figure 4.4 Observed and simulated sediment for the calibration (2009-2010) (a) and validation (2011) (b) at each of the different monitoring locations. The inverted secondary y-axis represents precipitation

The observed sediment data were not continuously measured for the whole period of 2010 and 2011 for all sites. Hence the observed sediment data points for all stream sites were limited and ranged from

a minimum of 20 data points for site S1 to a maximum of 34 for S7 during the calibration period. Despite the limited sediment observation record, the model was calibrated and validated for sediment yield at each monitoring location. The observed sediment loss for each of the monitoring locations (S1, S4W, and S5) during the calibration period is overestimated (Figure 4.4) and indicated by PBIAS values of 8.8, 11.2, and 33.6, respectively (Table 4.4). However, simulated sediment loss is underestimated at the catchment outlet S7, as indicated by a negative PBIAS of -46.7 during the sediment calibration. During the sediment validation, only location S1 was underestimated (PBIAS = -37.8). The PBIAS values for the other monitoring locations during sediment validation are 126.9, 68.1, and 11.3 for S4W, S5, and S7, respectively, depicting overestimation (Figure 4.4).

The development of the LAI and biomass for the individual HRUs are shown to evaluate minimum, maximum, and mean LAI and biomass with measured values for the individual crops within the experimental plots in the Haean catchment (Figure 4.5).

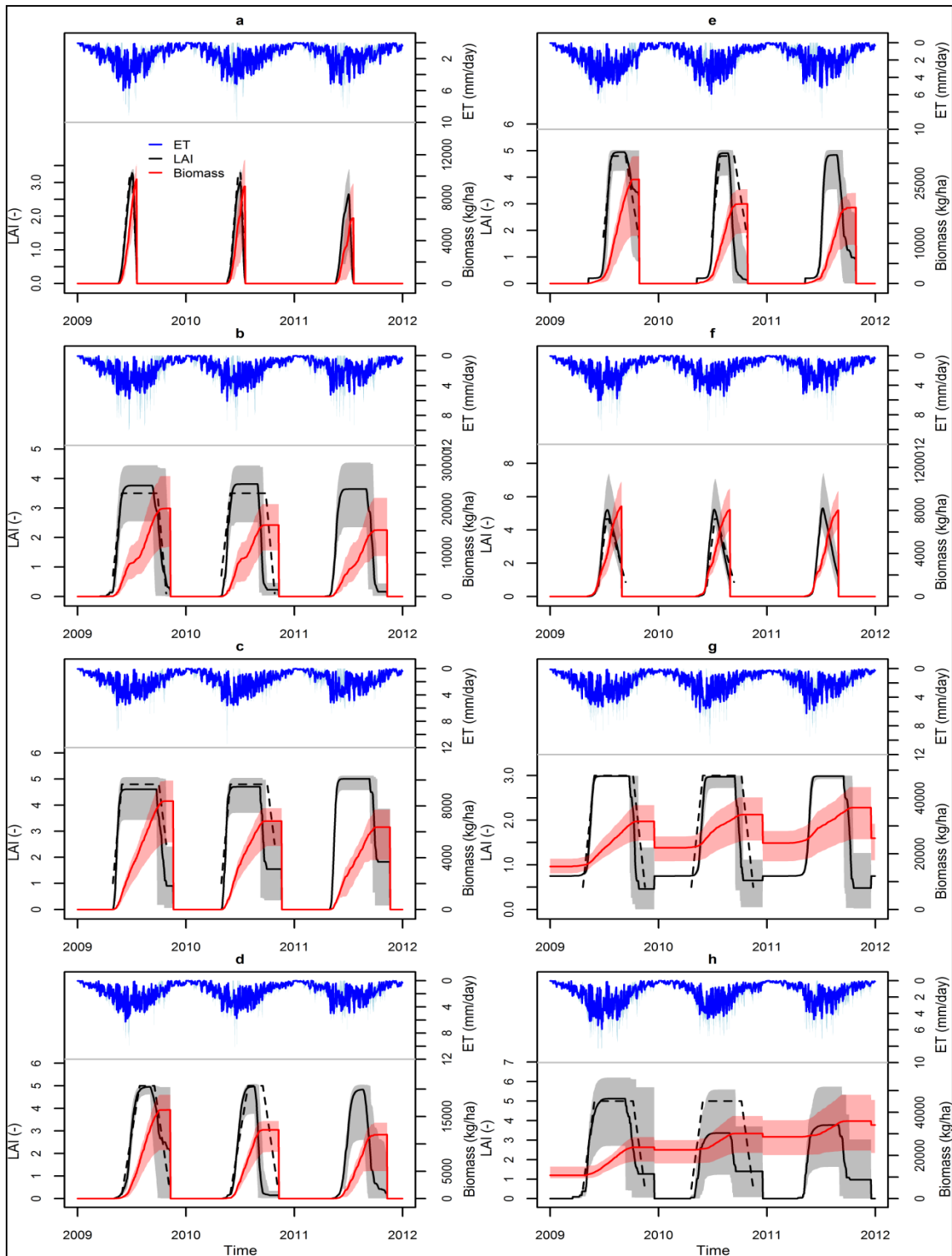


Figure 4.5 Observed (black dash line) and simulated mean leaf area index (LAI) (black solid line) during each growing season for 7 of the major agricultural crops (a-g: cabbage, potato, radish, soybean, rice, corn and orchard) and (h) deciduous forest in the Haean catchment. Gray shaded band: maximum and minimum LAI simulated from respective land use type HRUs. In addition, the mean simulated biomass production (red solid line) and range (pink shaded band: maximum and minimum biomass simulated from respective land use type HRUs) are depicted. For comparative purposes, the estimated evapotranspiration time series is included by blue lines.

Figure 4.5 shows that the observed LAI development curves and yields for the different crops were fairly well represented by the model, which was critical for the farm income and trade-off analysis.

4.2.5 Determination of crop allocation

The study area was dominated by small patches of various agricultural crops that were aggregated into 17 land use and land cover types to construct the base line scenario (Table 4.1). High elevation agriculture locations in South Korea, such as the Haeon catchment, are typically intensively used to produce high value, dryland vegetable crops such as cabbage, radish, potato, and soybeans (Kettering et al., 2012; Lee et al., 2010) In Haeon, dryland vegetable crops shown in the base line land use map (Figure 4.7) are spatially allocated in soil types of flat, moderate to steep, dryland soils with a soil texture of sand-silt. In addition such high value crops are typically grown in intensive monoculture systems (Kim et al., 2007). The change or choice of particular crops, and more importantly crop expansion and contraction, depends on policy intervention, market price, and environmental conditions. Poppenborg and Koellner (2013) argue that these changes are a function of the farmer's attitude and behavior towards ecosystem services of biomass production, soil erosion and water quality that aid their decision to choose specific agricultural land use systems. This study bolstered their argument through implementation of land use/crop allocation that was subjected to expansion of dryland crops one at a time (cabbage, potato, radish, and soybean) at the expense of other dryland agriculture crops such as maize, pepper, rye, and sunflower (Table 4.4). Other land use types, such as deciduous forest (FRSD), coniferous forest (FRSE), residential area (URBN), rice (RICE), inland water (WATR), and orchard (ORCD) (Table 4.1) were left unchanged. Moreover, only a single crop farming system (monoculture) is implemented in all of the combined agricultural HRUs of the SWAT model to produce surface runoff, sediment transport, crop yield, and estimated income. In other words, the model was parameterized with a single annual crop for each growing season, rather than multiple crops for an individual land use. We repeated the process of implementing a monoculture system for each of the four crops; cabbage, potato, radish and soybean. Such an extreme land use/crop allocation with catchment-wide monoculture systems has not and is not expected to be realized in the Haeon catchment; however, the scenarios provide a first step simulation of potential end-member effects on runoff, sediment, and crop yield. In general the production would change the market price of the commodity. In contrast, the farmers in the study area are price receivers and therefore, such monoculture systems and the associated increased production would not change the market price. We used previously generated data (simulated data: surface runoff, sediment, crop yield and income) for monoculture and base line land use systems to reallocate all of the dryland crops based on comparing the individual HRUs and selecting the HRUs with corresponding land use having individual functional attribute to produce minimum surface runoff, minimum sediment, maximum crop yield, and maximum income. The reallocation of all dryland crops assist the development of optimal land use systems, which are implemented for individual SWAT scenarios to analyze trade-offs that exist between other non-functional variables of the respective optimal land use system. The hierarchical line diagram of

individual SWAT scenarios for different monoculture crop types and the base line scenario to derive optimal land use considering the different output variables and the associated trade-offs is presented in Figure 4.6.

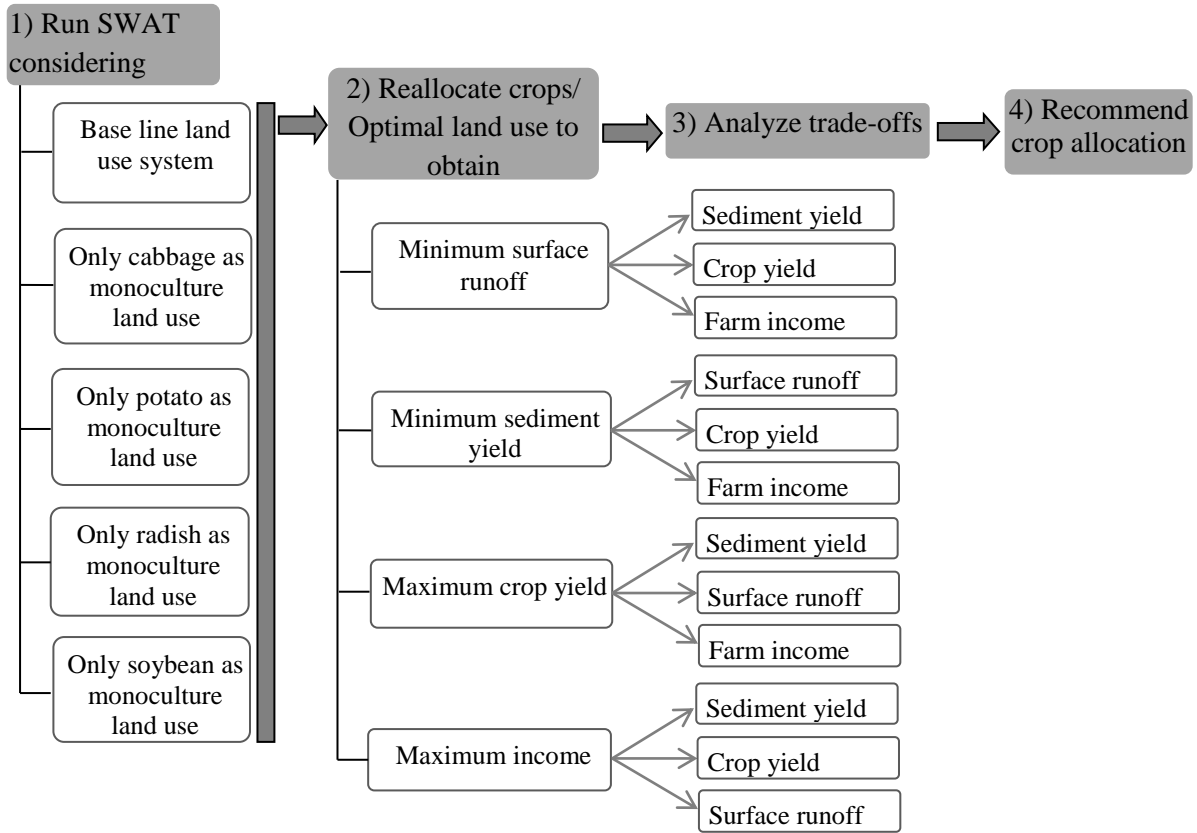


Figure 4.6 Hierarchical line diagram of the conceptual development of individual SWAT scenarios under different land use systems and crop reallocation to derive the optimal land use and associated trade-offs

4.2.6 Cost benefit analysis

The purpose of the cost benefit analysis was to link the output variable (crop yield) of the SWAT model with an economic evaluation to identify the economic viability of different land use systems. For the cost benefit analysis, the production cost and revenue from the crop yield were estimated based on the market price of agricultural commodities. We computed the net farm income (profit) from all monoculture and derived optimal land use systems. The net income generated due to crop yield from the land use systems were then compared with sediment transport and surface runoff at the catchment level to identify the trade-offs between net farm income and the associated crop yield, sediment transport, and surface runoff in ecological and economic terms. The income estimation from the land use system at the catchment level is derived by the following algorithm.

$$Farm\ Income\ (FI) = \sum_{i=1}^N [(1000 \cdot Y_{crop} \cdot P_r) - TCP_{crop}] \quad (4.4)$$

where, i is the field HRU for a respective crop type, Y_{crop} represents the crop yield (ton ha^{-1}), P_r represents the price of 1 kg of the respective crop (won ha^{-1}), and TCP_{crop} represents the total cost of

production for the respective crop. The crop yield simulated by the model was dry biomass, which was converted to fresh biomass by multiplying a conversion factor (cabbage: 12.9, potato: 3.6, radish: 22.9, soybean: 3.9) for each of the respective crops. The conversion factor was estimated based on field measurements and laboratory analysis after drying, as the ratio of fresh weight to dry weight, which enabled us to determine the marketable yield. Crops such as cabbage, potato, radish, and soybean for each land use system were considered in the income generation evaluation.

The market price for the respective crops was generated from an intensive interview surveys of more than 300 stakeholders and farmers throughout the Haeon catchment (Nguyen et al., 2014). We disaggregated the crop market price for cabbage, potato, radish, and soybean from the initial interview dataset, where the respective crop real market price was calculated as the three year average (2009-2011). Depending on farmers owning various crop fields, the interviews were aimed to identify the specific crop production cost. The production costs include labor cost for planting, harvesting, land rent and cost for other input (tillage and fertilizer). The total production cost for considered crop where averaged for similar crop types (Table 4.5) based on interview of farmers cultivating specific crops (cabbage, potato radish and soybean).

Table 4.5 Total production cost estimates for potato, cabbage, radish, and soybean in the Haeon catchment

Crop	Price (won*/kg)	Production cost (won */ha)
Radish	516	784,444
Cabbage	263	711,327
Potato	790	916,201
Soybean	4770	585,945

*Average price between 2009-2011 with average exchange rate of 1USD=1179 won

4.3 Results

4.3.1 SWAT simulation for monoculture land use system

After the SWAT model was successfully calibrated and validated for discharge and sediment loss as described, the model was used for scenario analyses of the individual monoculture land use systems for potato, cabbage, radish, and soybean. In each of the monoculture land use system scenarios, the land use types of deciduous forest (FRSD), coniferous forest (FRSE), residential area (URBN), water bodies (WATR), and rice (RICE) were not modified. Out of the total initial 792 HRUs from the base line scenario, 505 of the HRUs represented agricultural land use types and were adjusted for the respective monoculture system. The catchment level outputs simulated from the calibrated model for surface runoff (mm), sediment (ton ha⁻¹), crop yield (ton ha⁻¹), and farm income for each of the monoculture systems are shown in Table 4.6.

Table 4.6 Catchment level model output for the monoculture system and base line scenarios

Cropping system	Surface runoff (mm)	Sediment (tons ha ⁻¹)	Crop Yield (tons ha ⁻¹)	Farm income (Million won ha ⁻¹)
Base line (multiple crops)	553.92	10.70	1.60	50.30
Cabbage monoculture system	565.49	19.01	2.00	16.90
Potato monoculture system	552.88	15.00	4.80	43.00
Radish monoculture system	546.40	14.22	2.00	59.10
Soybean monoculture system	563.24	14.94	1.60	67.40

The average annual surface runoff and sediment yield were highest for the cabbage monoculture scenario with 565.49 mm and 19 tons ha⁻¹, respectively. Cabbage had the shortest growing period among all crops, resulting in the highest surface runoff and sediment yield relative to the other monoculture land use systems. The lowest surface runoff was simulated for the radish monoculture scenario at 546.40 mm. The lowest sediment yield was simulated for the base line land use system consisting of multiple crops through the entire catchment (Figure 4.7). The farm income estimated from the soybean monoculture scenario amounts to 67.40 Million won ha⁻¹ even with lowest crop yield of 1.6 tons ha⁻¹, which is due to soybean at the highest crop price (Table 4.5). Based on the high potential farm income, comprehensive soybean cultivation might be more attractive to farmers but produces relatively high sediment yields (14.94 tons ha⁻¹). However, the potato monoculture scenario revealed the highest crop yield of 4.8 tons ha⁻¹ but produced a relatively lower farm income of 43.00 million won ha⁻¹ and an estimated sediment yield of 15.00 tons ha⁻¹, which is higher than the values for monoculture system of radish (14.22 tons ha⁻¹), soybean (14.94 tons ha⁻¹), and the base line (10.70 tons ha⁻¹) scenarios. The spatial distributions of different crops within the associated land use classifications for the monoculture and the base line scenarios are presented in Figure 4.7.

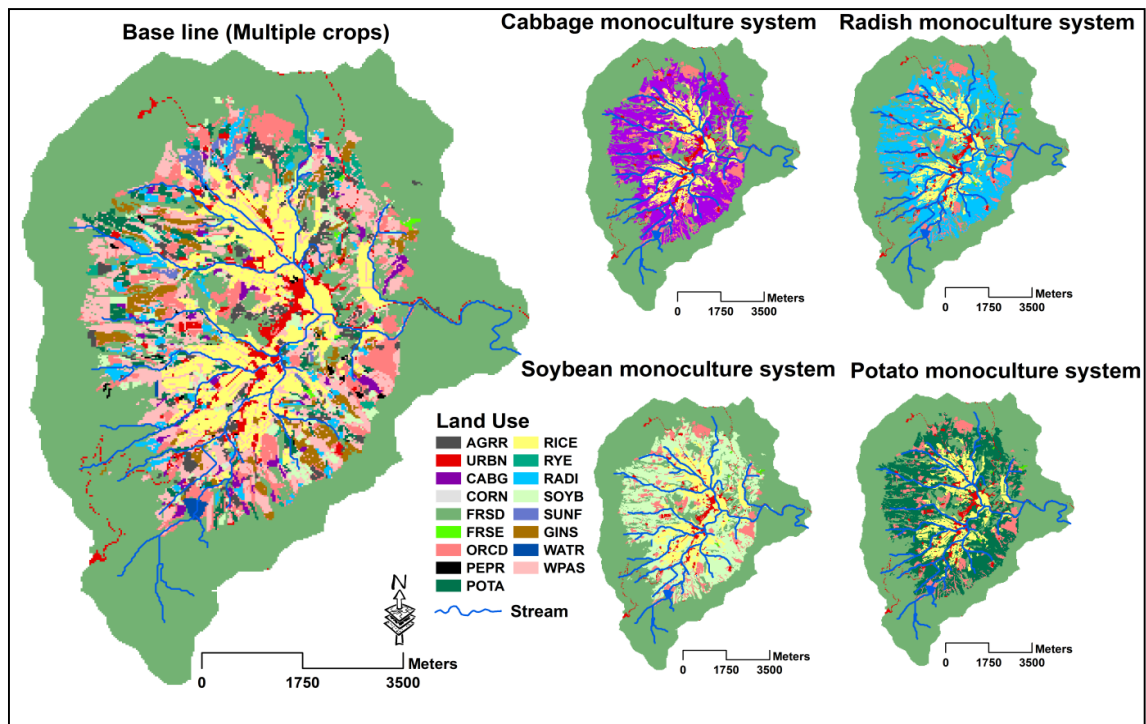


Figure 4.7 Land use discretization for the base line scenario and each of the four monoculture system scenarios. For the monoculture systems, HRUs representing agricultural crops were adjusted to the individual monoculture crop type throughout the entire catchment

4.3.2 SWAT simulation for the optimal land use system

Based on the aforementioned SWAT simulations for monoculture and base line scenarios, the land use/crops were reallocated to derive optimal land use for minimum surface runoff, minimum sediment loss, maximum yield, and maximum income. The model output for surface runoff, sediment loss, crop yield, and respective farm income for the monoculture and base line scenarios were analyzed for every HRU. The simulated results for every single agricultural crop HRU throughout the catchment from all monoculture and base line scenarios (Figure 4.7) were compared and land use/crops were individually reallocated by selecting the crop types that produced the minimum surface runoff, minimum sediment, maximum yield, and maximum income. Based on this procedure, four potential land use distributions for the Haean catchment were created which represented the optimal land use system to obtain each of the following functional attributes; minimum surface runoff, minimum sediment loss, maximum crop yield, and maximum farm income as shown in Figure 4.8 and Table 4.7.

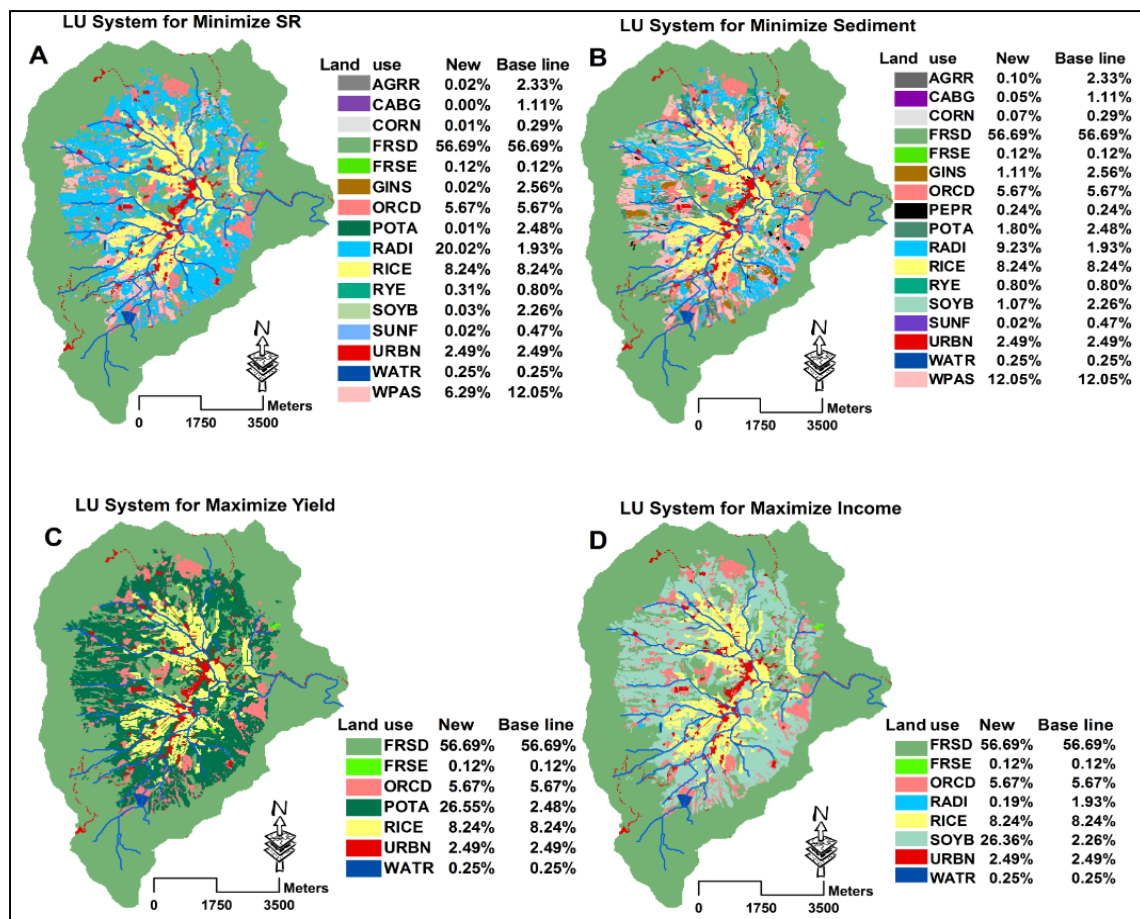


Figure 4.8 Optimal Land Use /Land Classification (LULC) systems derived by comparing individual HRUs to obtain A. Minimum surface runoff (SR), B. Minimum sediment, C. Maximum yield, and D. Maximum income. Note: “New” refers to the percent area corresponding to the optimal land use and “Base line” refers to the percent area in the base line scenario

Table 4.7 Land use distribution as a percentage of the catchment for the different derived optimal land use systems and the base line scenario.

Land use type	Base line scenario		Optimal land use to obtain for							
	Km ²	%	MinSRF*		MinSED**		MaxYLD***		MaxIC****	
			Km ²	%	Km ²	%	Km ²	%	Km ²	%
AGRR	1.46	2.33 %	0.01	0.02 %	0.06	0.10 %	-	-	-	-
CABG	0.70	1.11 %	0.00	0.00 %	0.03	0.05 %	-	-	-	-
CORN	0.18	0.29 %	0.00	0.01 %	0.04	0.07 %	-	-	-	-
FRSD	35.56	56.69 %	35.56	56.69 %	35.56	56.69 %	35.56	56.69 %	35.56	56.69 %
FRSE	0.07	0.12 %	0.07	0.12 %	0.08	0.12 %	0.07	0.12 %	0.07	0.12 %
GINS	1.61	2.56 %	0.01	0.02 %	0.70	1.11 %	-	-	-	-
ORCD	3.55	5.67 %	3.55	5.67 %	3.55	5.67 %	3.55	5.67 %	3.55	5.67 %
PEPR	0.15	0.24 %	-	-	0.15	0.24 %	-	-	-	-
POTA	1.56	2.48 %	0.00	0.01 %	1.13	1.80 %	16.65	26.55 %	-	-
RADI	1.21	1.93 %	12.56	20.02 %	5.79	9.23 %	-	-	0.12	0.19 %
RICE	5.17	8.24 %	5.17	8.24 %	5.17	8.24 %	5.17	8.24 %	5.17	8.24 %
RYE	0.50	0.80 %	0.08	0.13 %	0.05	0.80 %	-	-	-	-
SOYB	1.42	2.26 %	0.02	0.03 %	0.67	1.07 %	-	-	16.53	26.36 %
SUNF	0.30	0.47 %	0.01	0.02 %	0.01	0.02 %	-	-	-	-
URBN	1.56	2.49 %	1.56	2.49 %	1.56	2.49 %	1.56	2.49 %	1.56	2.49 %
WATR	0.15	0.25 %	0.15	0.25 %	0.15	0.25 %	0.15	0.25 %	0.15	0.25 %
WPAS	7.56	12.05 %	3.95	6.29 %	7.56	12.05 %	-	-	-	-

MinSRF*: Minimum surface runoff, MinSED** : Minimum sediment, MaxYLD***: Maximum Yield,

MaxIC****: Maximum Income

The optimal land use system derived to obtain the minimum surface runoff (Figure 4.8A) revealed a significant increase of radish (RADI) from 2 % of the surface area of the catchment to nearly 20 %. Radish was more likely to be selected in higher frequency than other crops in the derivation of the land use system, which is optimal to minimize the surface runoff. This is because a monoculture land use for radish revealed the least surface runoff among other monoculture land use scenarios (Table 4.6). However, the least surface runoff was also attributed to spatially variable characteristics of the individual HRUs including the soil moisture that defines the Curve Number (the SWAT model was constructed utilizing the soil moisture CN methods), the development of crops, and the respective evapotranspiration demands. The variability of surface runoff and evapotranspiration for the different crops exhibited in the monoculture and base line scenarios are provided in Appendix 4C and Appendix 4D, respectively. The variability of surface runoff and evapotranspiration for cabbage, potato, soybean, and radish were due to the respective monoculture land use system, whereas the variability for other remaining crops (AGRR, CORN, PEPR, RYE, SUNF, TOBC, and WPAS) originates from the base line land use system.

The derived optimal land use for minimum sediment loss (Figure 4.8B) is also dominated by radish (RADI) with an increase in spatial coverage from 1.93 % to 9.62 %. The sediment yield from the individual HRUs depends on the spatial variability of soil erodibility, slope length, and management practices as described in the Modified Universal Soil Loss Equation. However, the length of the growing period, crop coverage, and the biomass leftover after harvest also had significant effects on

the sediment loss. All management operations (planting, harvest, tillage) were kept constant throughout all scenario analyses (Appendix 4E). The variability in sediment loss for each of the different crops from the monoculture and base line scenarios is shown in Appendix 4F. The variability in sediment yield from the cabbage HRUs were the highest followed by potato, soybean, and radish. The least variability in sediment loss was found for the pepper HRUs followed by sunflower HRUs (Appendix 4F).

The optimal land use derived to obtain the maximum crop yield (Figure 4.8C) was the same as the land use developed for the monoculture land use system for potato. During the crop yield measurement in several fields, potato accounted for a very high harvest biomass (Lindner et al., 2015). The SWAT model estimates crop yield from biomass using a harvest index, which is the ratio of harvested biomass to above ground biomass. Due to the high harvested biomass, potato received the highest harvest index of more than 1 (Lindner et al., 2015) and, therefore, produced the highest yield during the model simulation. For this reason, when reallocating the land use/crops to determine the optimal land use/crop for maximum yield, it is always likely that HRUs of the potato monoculture are selected more frequently than from other land use types. Under this condition, the spatial distribution of the potato LULC was significantly increased from 2.5 % (base line scenario) to 26.5 % (optimized land use scenario for maximum yield) (Table 4.7) of the total catchment area. The yield variation of the different crops between the monoculture and base line scenarios is shown in Appendix 4G, from which the land use system optimized for maximum crop yield is identified. The average annual crop yield for the potato HRUs varies from 8.56 to 22.61 tons ha⁻¹, in which even the minimum crop yield from the potato HRUs is higher than any other crop (Appendix 4G). This depicts the reason to select potato for all HRUs, which always satisfies the objective of maximum crop yield.

The SWAT model does not produce farm income as an output variable. Therefore, in this study, the income was calculated based on the crop yield (SWAT output), crop price, and total production costs for particular crops. The land use system derived for maximum income is shown in Figure 4.8D. Soybean dominated the spatial distribution at 26.36 %, which increased from the base line scenario of 2.26 %. In contrast, the land use of radish decreased to 0.19 % from 1.93 % in the base line scenario. The reason for soybean domination in this scenario was that it maintained the highest crop price among all of the other crops.

The optimal land use systems for minimum surface runoff, minimum sediment loss, maximum crop yield, and maximum income were separately implemented in the model to identify the impact of other non-optimum variables. The catchment level output (surface runoff, sediment loss, crop yield, and farm income) for the optimal land use systems are presented in Table 4.8. The selection of individual optimal land use systems for specific objectives of pursuing minima of surface runoff and sediment, and maxima in crop yield and income have trade-offs. The trade-offs associated with particular optimized land use scenarios are further explained in the next section.

Table 4.8 Model output at the catchment level for derived optimal land use system and base line land use system

Derived optimal land use system to obtain	Surface runoff (mm)	Sediment (tons ha ⁻¹)	Crop yield (tons ha ⁻¹)	GMP (million won ha ⁻¹)
Minimum surface runoff	545.15	11.74	1.8	59.88
Minimum sediment yield	548.30	10.19	1.7	56.67
Maximum crop yield	552.88	14.94	4.8	43.01
Maximum income	563.11	14.87	1.6	67.40
Baseline	553.92	10.70	1.6	50.30

4.3.3 Trade-off analysis

The trade-off analysis was performed at the entire catchment level rather than the HRU or sub-basin levels in order to observe the impact of the spatially distributed land use system. The derived optimal land use systems were simulated with the SWAT model and the differences in the model outputs (surface runoff, sediment, crop yield, and total income) were evaluated at the catchment level (Table 4.8). The model outputs were compared with the economic benefits drawn from each of the optimal land use systems. As previously described, each optimum land use system was identified with an objective of minimizing surface runoff, minimizing sediment loss, maximizing yield, or maximizing total income. But at the same time, those derived optimized land use systems also produced other non-optimum model outputs that generated trade-offs. The average annual surface runoff at the catchment level for all optimal land use systems ranged between 545.15 and 563.11 mm, sediment loss ranged between 10.19 and 14.94 tons ha⁻¹, crop yield ranged between 1.6 and 4.8 ton ha⁻¹, and the total income was calculated to range between 43 and 67 million won ha⁻¹.

The economically and ecologically best scenario among the optimized land use scenarios would be the scenario which produces the minimum surface runoff, minimum sediment loss, maximum crop yield, and maximum income at the same time. However, any of the optimal land use scenarios in this study showed a combination of maximum yield and maximum income with minimum sediment and minimum surface runoff. From an economic point of view, the implementation of the optimal land use scenario for maximum income would be the most beneficial, producing an average income of 67.40 million won ha⁻¹. From the view point of soil conservation, the adoption of the optimal land use system exhibiting minimum sediment loss would be the most beneficial, with a relatively small sediment loss of 10.19 tons ha⁻¹. Maximum crop yield was nearly 4.8 tons ha⁻¹ from the optimal land use for maximum yield. However, the optimal land use scenario for maximum crop yield does not satisfy minimum surface runoff, minimum sediment loss, or maximum income requirements. Therefore, it is not the ideal land use system to fulfill the multi-objective function of maximizing crop yield and income while minimizing surface runoff and sediment loss. We do realize that none of the derived land use systems were economically and ecologically superior because none of the optimized scenarios revealed a definitive combination of high crop yield and income with low sediment loss and surface runoff in a single optimal land use system. However, it should be noted that a definitive and superior optimization scheme is elusive and highly subjective depending on the needs of the particular stakeholder. This is where trade-offs become useful in the decision making process and the

stakeholder can define the suitability of particular outcomes. The selection of the optimal land use for maximum income (67 million won ha⁻¹) would be associated with a sediment yield of 14.87 tons ha⁻¹, which is a 46 % higher sediment loss than the sediment loss (10.19 tons ha⁻¹) generated by the optimal land use system derived for minimum sediment loss. Similarly, a net crop yield of 1.6 tons ha⁻¹ and surface runoff of 563.11 mm were simulated with the optimal land use system derived for the maximum income, which represents a 67 % lower crop yield and 3 % more surface runoff compared to the derived optimal land use systems for maximum crop yield and minimum surface runoff, respectively. In contrast, the optimal land use system for maximum income produced potentially 19, 13, and 56 % higher farm income in comparison to income generated by the derived optimal land use systems for minimum sediment loss, minimum surface runoff, and maximum crop yield, respectively.

The optimal land use system, which was derived to generate maximum crop yield produced an average yield of 4.8 tons ha⁻¹. This is more than a 100 % increase in crop yield from any other optimal land use system (182, 166, and 200 % higher in comparison to the derived optimal land use systems to obtain minimum sediment, minimum surface runoff, and maximum income, respectively). The derived optimal land use system to obtain the maximum crop yield showed significant environmental trade-offs in producing the maximum sediment yield (14.94 tons ha⁻¹), which was 47 % higher than the sediment generated by the optimal land use system objectively defined to produce the minimum sediment loss possible (10.19 tons ha⁻¹). An interesting result of the optimal land use system derived to obtain the maximum crop yield is that this land use system revealed the smallest potential farm income of about 43 million won ha⁻¹ (36 % less than the maximum income scenario of 67.40 million won ha⁻¹). The surface runoff generated by this land use system was about 552.88 mm, 1.4 % higher than the optimal land use system which has the functional ability to generate minimum surface runoff (545.23 mm).

The land use system derived to obtain the minimum surface runoff resulted in 545.15 mm of runoff, 0.5, 1.4, and 3.3 % lower than the surface runoff simulated from the optimal land use systems which were derived to generate minimum sediment loss, maximum crop yield, and maximum income, respectively. The simulated sediment loss, crop yield, and calculated income from the optimal land use system designed to produce the minimum surface runoff was 11.74 tons ha⁻¹ (18 % increase above the optimal land use system designed for minimum sediment loss), 1.8 tons ha⁻¹ (66 % less crop yield than the optimal land use system derived for maximum crop yield), and 59.88 million won ha⁻¹ (11 % less income than the income generated by the land use system developed to obtain the maximum income), respectively.

Based on the specific objectives of all derived optimal land use systems, trade-offs were found with the other model output variables. As previously described, the land use system that would produce the maximum farm income of 67.40 million won ha⁻¹ was associated with a strong environmental impact due to the generation of the second highest sediment yield (14.87 tons ha⁻¹). Similar trade-offs could

be found through comparison of the other model output variables and implementation of any particular derived optimal land use system. The spider plot presented in Figure 4.9 visually supports the interpretation of different output variables resulting from the model simulations for different optimal land use systems.

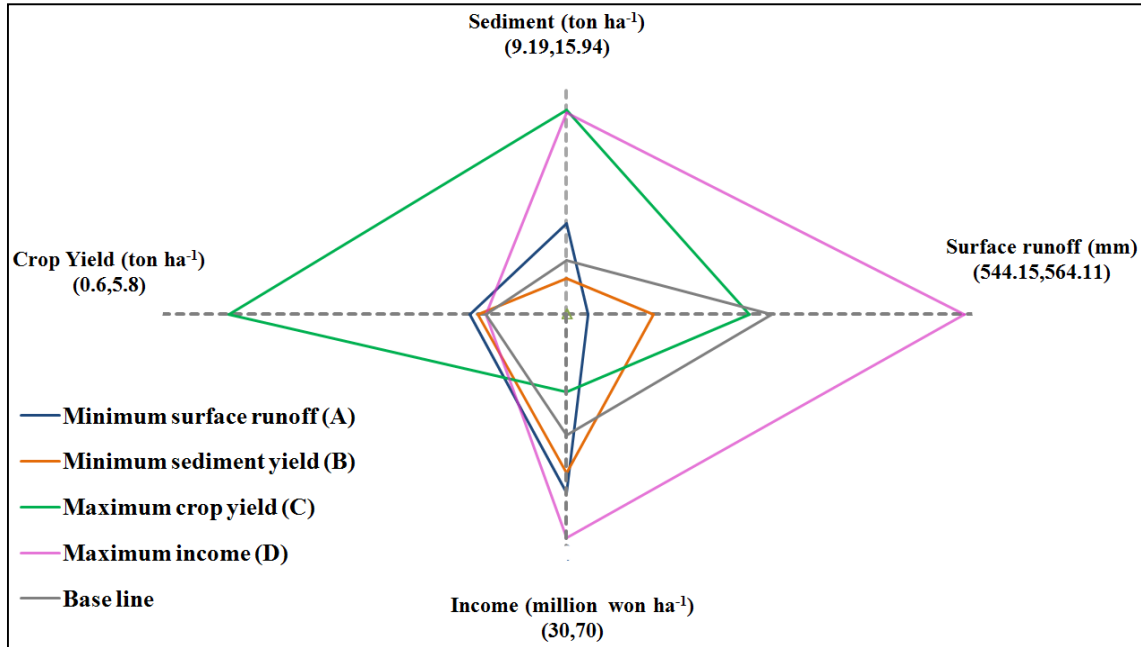


Figure 4.9 Spider plot showing the outputs from the different optimal land use and base line scenarios. Detailed spatial representation of the optimized land use systems (A, B, C and D) and "base line" scenarios are provided in Figure 4.8 and Figure 4.7. The four axes represent different scales for respective output variables. The numerical pairs at the four corners represent minimum (at crossing of the axes) and maximum (at the end point of the corner) for respective output variables

4.4 Discussion

The SWAT model was used as a primary tool to simulate the major biophysical processes in the study catchment by quantifying multiple ecosystem functions such as surface runoff generation, sediment loss, and crop yield. The analysis of model outputs associated with different monoculture land use systems and the derived optimal land use systems were based on a calibrated and validated SWAT model for stream flow and sediment loss. The model was calibrated and validated with limited observation data and the reliability and performance in simulating stream discharge and sediment load were tested with several statistical indicators (NSE, R^2 , and PBIAS). Overall, the model reliability and performance based on statistical indicators for discharge and sediment load can be improved at the expense of not representing the proper observed development of LAI and biomass for different crop types in the model. Therefore, the proper simulation of crop growth for different crop types, we compared the simulated LAI and biomass with measured LAI and biomass from plot experiment. In addition to the model performance measured by the NSE, R^2 , and PBIAS metrics, we also check the overall water balance (ET, surface runoff/baseflow ratios, plant yield, and biomass) and sediment

components (sediment source: terrestrial, stream deposition or degradation) by using the SWAT Check software (White et al., 2012) during the calibration process to verify if that reasonable estimates were produced.

The calibrated and validated model was considered as a base line scenario, from which different dryland crops were replaced by alternative crops in order to generate the respective monoculture land use system. The average annual outputs of the base line scenario at the catchment level were 554 mm of surface runoff, 10.7 tons ha⁻¹ of sediment, and 1.6 tons ha⁻¹ of crop yield, while producing 50.3 million won ha⁻¹ of farm income. The average annual sediment yield for the base line scenario from the major dryland crops (cabbage, soybean, potato, and radish) was 48 tons ha⁻¹. Arnhold et al. (2014) simulated the sediment yield from several plots of similar crops and estimated between 30.6 and 54.8 tons ha⁻¹ yr⁻¹, suggesting that our simulated results were reasonable. However, the sediment yield at the catchment level was only 10.7 tons ha⁻¹ yr⁻¹ due to the combined effect of other land use types (including perennial crops and forest) and reduced gradients in the central portion of the catchment. Overall, we found that the sediment yield from the dryland fields in this study agree well with previous erosion studies in the region (Arnhold et al., 2014; Arnhold et al., 2013).

Several studies have been conducted in the past to explore the impact of different best management practices to control sediment and nutrient exports. This study focused on reallocating land use/crops to derive an optimal land use system contributing to minimum surface runoff, minimum sediment loss, maximum crop yield, and maximum income. There are several approaches to derive the optimal land use system in combination with best management practices to satisfy multiple economic and environmental objectives. Arabi et al. (2006) and later Maringanti et al. (2011; 2009) each used genetic algorithms to define a spatial reallocation approach for best management practices in an economically efficient manner. Mayer et al. (2009) and Darradi et al. (2012) used a Global Programming (GP) approach to optimize multi-objective land use distributions and maximize the environmental performance of agricultural activities. Besides the large computational infrastructure and complexity in developing these algorithm for multi-objective optimization, a single tool cannot be guaranteed to find the optimal solution (Lautenbach et al., 2013). Difficulties in defining the weighting factors or prescribing equal weighting factors for competing objectives (Global Programming) can bias the optimal solution (Darradi et al., 2012). The multi-objective optimal solution by Global Programming is typically associated with higher trade-offs among the competing objectives. It is worth mentioning that the methodological approach we developed to reallocate different land use/crop types to obtain an optimal land use which satisfies a single objective (minimum surface runoff, minimum sediment loss, maximum crop yield, or maximum income) is based on a database generated by the SWAT model simulation for different land use scenarios (base line and monoculture land use system). Identifying an optimal land use system scenario for a single objective that is distributed throughout a catchment is very simple and transparent to stakeholders. The simplistic approach in this

study is used to derive the optimal land use system for several individual outputs; a) minimum surface runoff, b) minimum sediment, d) maximum crop yield, and e) maximum income. These functional attributes were based on the development of an empirical data set from a series of SWAT model simulations of the base line scenario with an existing land use distribution and simulated monoculture land use systems of potato, cabbage, radish, and soybean. The income estimation was based on an econometric approach of crop price and production cost. The selection of the optimum land use for every distributed HRU was based on satisfying the objective of the output variable within the empirical data set from the model simulation and its corresponding land use type.

Based on implementation of several optimal land use systems, the optimal land use representing maximum crop yield and income is favorable in terms of economic gain to a farmer that cultivates a field contributing to environmental loss due to the production of high sediment loss. On the other hand, the optimized land use representing minimum surface runoff and sediment loss is environmentally sound and favorable to a conservationist, but at the detriment of economic loss to a farmer through less crop yield and income. The derived optimal land use systems were individually implemented to assess their impact on other output variables. For example, the land use system derived to obtain minimum sediment loss can obviously produce the least sediment ($10.19 \text{ tons ha}^{-1} \text{ yr}^{-1}$) among other optimal land use systems (derived optimal land use systems for maximum crop yield and income). But at the same time, it also produces detrimental effects such as a) surface runoff of 548 mm yr^{-1} , which is higher than minimum surface runoff (545.15 mm), b) crop yield of $1.7 \text{ tons ha}^{-1} \text{ yr}^{-1}$ which is less than maximum crop yield ($4.8 \text{ tons ha}^{-1} \text{ yr}^{-1}$), and c) $56.67 \text{ million won ha}^{-1} \text{ yr}^{-1}$ of income, which is also less than the maximum possible income ($67.40 \text{ million won ha}^{-1} \text{ yr}^{-1}$). Hence, the focus of the optimal the land use system in targeting reduction of only sediment has to bear losses in crop yield and income. The implementations of other optimal land use systems were also assessed in a similar manner.

The land use characterized by the optimization of several outputs at one time is also possible for every single land use system. The HRU of different land use were access to identify the HRUs of land use satisfying the constrains imposed by minimum of sediment and runoff while maximum of crop yield and income. There exists very few HRUs satisfying all imposed constrains. The study objective was to identify different land use systems which satisfy the multi-objective function of minimum sediment loss, minimum surface runoff, maximum crop yield and maximum income. However, there are very few or any land use systems that can fully satisfy the previously mentioned multi-objective functions. Moreover, optimization of the land use system was separately determined for minimum surface runoff, minimum sediment loss, maximum crop yield, and maximum income rather than the production of a single optimum land use that satisfies all the functional criteria. This is primarily due to the fact that optimization of the functional attributes is highly subjective with a ranking system individualized for

specific stakeholders. In addition, typical catchments require a trade-off analysis of the benefits and drawbacks developed from these scenario analyses.

4.5 Conclusions

Agriculture is the main sector of economic activity in the Haeon catchment. Agriculture is associated with complex land use types of different crops and management practices. The crop yield relating income generation and other services of surface runoff and sediment retention were analyzed in this study for different land use systems. This study also separately identified different optimal land use systems with the objective of producing a) minimum surface runoff, b) minimum sediment loss, c) maximum crop yield, and d) maximum income. The implementation of certain optimal land use systems is possible based on the deterministic objective of a) through d). The choice of a particular optimal land use objective has to bear the deteriorative status of other objectives. Thus, there exist trade-offs between the different optimal land use systems. The optimal land use system that produces the maximum income also yields higher amounts of sediment loss and surface runoff and the land use system that has the capability to produce the minimum sediment loss and surface runoff has to bear a lower crop yield and income. The derived optimal land use to obtain the highest income was dominated by soybean cultivation, which increased from 2.26 % to 26.36 % areal catchment coverage compared to the base line land use system. The dominance of soybean coverage was due to the highest crop price among all other crops (cabbage, radish, and potato). In economic terms, soybean expansion would be more beneficial for farmers, but it had negative impacts from the ecological point of view, producing higher amounts of surface runoff and sediment loss. This study found that there is an existence of trade-offs between ecology and economy in every optimal land use system. None of the optimized land use systems evaluated in this study showed a total synergy between economic and environmental benefits, such as maximization of income with minimization of sediment loss and runoff. The land use system optimized for higher crop yield produces the highest sediment loss and the lowest income, which is not an attractive option for farmers nor for the environment. Instead of a higher yield option, the farmer could benefit more by the land use system that optimizes surface runoff reduction and produces the second highest income with the second lowest sediment loss. When compared to the maximum income scenario, the economic loss by adoption of the optimum land use system for minimum surface runoff can be neutralized by the ecological gain produced by the lowest surface runoff and decreased sediment loss. The option of an optimized land use system for minimum sediment produced the third highest income and the lowest sediment loss among all of the optimal land use systems, which is also ecologically sound with less loss in income. In brief, Figure 4.9 depicts the optimized land use system for maximum crop yield and maximum income, which are associated with higher levels of sediment loss and surface runoff. However, the optimal land use systems for minimum surface runoff and minimum sediment loss scenarios attributed significantly lower levels of crop yield and higher levels of income than the optimized crop yield scenario. The compensation to economic loss that would have been gained from implementation of the maximized income scenario

would encourage farmers in the Haean catchment to implement those land use systems that are optimal for minimum surface runoff and sediment losses. Implementation of these study findings should be taken with care based on current crop price fluctuations and the market demands of the commodity, particularly when the optimized land use system is dominated by a single crop type. However, the findings of this study assess the trade-offs between economy and ecology for different land use systems, which help farmers and policy makers in supporting the decision of implementing a particular land use system.

4.6 Acknowledgements

The authors highly acknowledge Jong-Yoon Park, Rim Ha and Sora Ahn from the Department of Civil and Environmental System Engineering, Kunkuk University for their valuable suggestions during the early stages of model setup and simulation. We also thank Kwanghun Choi for his assistance in developing the R-code for data file manipulation. Field measurements and analysis of the raw data by Svenja Bartsch is also highly appreciated. This research work, supported by the International Research Training Group TERRECO (GRK 1565/1) funded through the Deutsche Forschungsgemeinschaft (DFG) at the University of Bayreuth, is greatly acknowledged.

4.7 Appendix (4A–4G)

Appendix 4A. Fit parameter values for discharge and sediment during calibration

Discharge Parameter	Description	Initial value	Fit value	Range	
				Minimum bound	Maximum bound
v__GW_DELAY.gw	Groundwater delay time (days)	31	3.89	0	500
v__GW_DELAY.gw_1	Groundwater delay time (days)	31	27	24	30
v__GW_DELAY.gw_2	Groundwater delay time (days)	31	25	24	30
v__GW_DELAY.gw_3	Groundwater delay time (days)	31	0.97	0.2	1
v__GW_DELAY.gw_6	Groundwater delay time (days)	31	27	24	30
v__GW_DELAY.gw_10	Groundwater delay time (days)	31	26	24	30
v__ESCO.hru	Soil evaporation compensation coefficient	0	0.15	0.01	0.2
v__ESCO.hru_1	Soil evaporation compensation coefficient	0	0.20695	0.18	0.26
v__ESCO.hru_2	Soil evaporation compensation coefficient	0	0.24265	0.18	0.26
v__ESCO.hru_6	Soil evaporation compensation coefficient	0	0.23935	0.18	0.26
v__ESCO.hru_10	Soil evaporation compensation coefficient	0	0.18435	0.18	0.26
v__LAT_TTIME.hru	Lateral flow travel time (days)	0	1.64	0	5
v__LAT_TTIME.hru_1	Lateral flow travel time (days)	0	5.234375	5	10
v__LAT_TTIME.hru_2	Lateral flow travel time (days)	0	9.471875	5	10
v__LAT_TTIME.hru_6	Lateral flow travel time (days)	0	9.253125	5	10
v__LAT_TTIME.hru_10	Lateral flow travel time (days)	0	9.715625	5	10
v__GWQMN.gw	Threshold water level in shallow aquifer for base flow (mm H ₂ O)	0	6.61	0	13
v__GWQMN.gw_1	Threshold water level in shallow aquifer for base flow (mm H ₂ O)	0	45.33125	20	50
v__GWQMN.gw_2	Threshold water level in shallow aquifer for base flow (mm H ₂ O)	0	49.00625	20	50
v__GWQMN.gw_3	Threshold water level in shallow aquifer for base flow (mm H ₂ O)	0	0.206875	0.2	0.4
v__GWQMN.gw_6	Threshold water level in shallow aquifer for base flow (mm H ₂ O)	0	47.73125	20	50
v__GWQMN.gw_10	Threshold water level in shallow aquifer for base flow (mm H ₂ O)	0	20.09375	20	50
r__SOL_K().sol	Saturated hydraulic conductivity (mm/hr)	different	-0.49	-0.2	-0.5
r__SOL_K(1).sol_1	Saturated hydraulic conductivity (mm/hr)		1.054388	0.98	1.2
r__SOL_K(1).sol_2	Saturated hydraulic conductivity (mm/hr)		1.063187	0.98	1.2
r__SOL_K(1).sol_6	Saturated hydraulic conductivity (mm/hr)		1.096187	0.98	1.2
r__SOL_K(1).sol_10	Saturated hydraulic conductivity (mm/hr)		1.095913	0.98	1.2

Chapter 4-Derive optimal land use and trade-offs quantification

Discharge Parameter	Description	Initial value	Fit value	Minimum bound	Maximum bound
r__SOL_AWC().sol	Available water capacity of the soil (mm H ₂ O/mm soil)	different	-0.1	-0.3	-0.05
r__SOL_AWC(1).sol_1	Available water capacity of the soil (mm H ₂ O/mm soil)		2.5925	2	2.8
r__SOL_AWC(1).sol_2	Available water capacity of the soil (mm H ₂ O/mm soil)		2.7455	2	2.8
r__SOL_AWC(1).sol_6	Available water capacity of the soil (mm H ₂ O/mm soil)		2.7875	2	2.8
r__SOL_AWC(1).sol_10	Available water capacity of the soil (mm H ₂ O/mm soil)		2.2515	2	2.8
a__CN2.mgt	SCS curve number for moisture condition II	different	-7.55	-10	4
a__CN2.mgt_1	SCS curve number for moisture condition II		-11.809063	-12	-11.5
a__CN2.mgt_2	SCS curve number for moisture condition II		-11.877188	-12	-11.5
a__CN2.mgt_6	SCS curve number for moisture condition II		-11.784062	-12	-11.5
a__CN2.mgt_10	SCS curve number for moisture condition II		-11.837188	-12	-11.5
v__CANMX.hru	maximum canopy storage	25	28.35	0	30
v__CANMX.hru_1	maximum canopy storage	25	21.765625	0	25
v__CANMX.hru_2	maximum canopy storage	25	8.015625	0	25
v__CANMX.hru_6	maximum canopy storage	25	24.734375	0	25
v__CANMX.hru_10	maximum canopy storage	25	0.265625	0	25
v__REVAPMN.gw	Threshold water level in shallow aquifer for evaporation to occur (mm H ₂ O)	0	11.45	0	30
v__REVAPMN.gw_1	Threshold water level in shallow aquifer for evaporation to occur (mm H ₂ O)	0	23.813126	23	24
v__REVAPMN.gw_2	Threshold water level in shallow aquifer for evaporation to occur (mm H ₂ O)	0	23.766874	23	24
v__REVAPMN.gw_6	Threshold water level in shallow aquifer for evaporation to occur (mm H ₂ O)	0	23.156876	23	24
v__REVAPMN.gw_10	Threshold water level in shallow aquifer for evaporation to occur (mm H ₂ O)	0	23.190624	23	24
v__GW_REVAP.gw	Groundwater "revap" coefficient	0.02	0.13	0.02	0.2
v__GW_REVAP.gw_1	Groundwater "revap" coefficient	0.02	0.188356	0.17	0.2
v__GW_REVAP.gw_2	Groundwater "revap" coefficient	0.02	0.173844	0.17	0.2
v__GW_REVAP.gw_6	Groundwater "revap" coefficient	0.02	0.195744	0.17	0.2
v__GW_REVAP.gw_10	Groundwater "revap" coefficient	0.02	0.171669	0.17	0.2
v__OV_N.hru	Manning's "n" value for overland flow	0.14	0.79	0	0.8
v__OV_N.hru_1	Manning's "n" value for overland flow		0.4	0.6	6
v__OV_N.hru_2	Manning's "n" value for overland flow		0.4	0.6	21
v__OV_N.hru_6	Manning's "n" value for overland flow		0.4	0.6	39
v__OV_N.hru_10	Manning's "n" value for overland flow		0.4	0.6	54

Chapter 4-Derive optimal land use and trade-offs quantification

Discharge Parameter	Description	Initial value	Fit value	Minimum bound	Maximum bound
v__CH_N2.rte	Manning's n value for main channel	0.05	0.02	0	0.3
v__CH_N2.rte_1	Manning's n value for main channel	0.05	0.227763	0.19	0.25
v__CH_N2.rte_2	Manning's n value for main channel	0.05	0.231513	0.19	0.25
v__CH_N2.rte_6	Manning's n value for main channel	0.05	0.197987	0.19	0.25
v__CH_N2.rte_10	Manning's n value for main channel	0.05	0.212612	0.19	0.25
v__CH_K2.rte	Eff. hydraulic conductivity in main channel alluvium (mm/hr)	0	95.25	0	150
v__CH_K2.rte_1	Eff. hydraulic conductivity in main channel alluvium (mm/hr)	0	106.67687	106	109
v__CH_K2.rte_2	Eff. hydraulic conductivity in main channel alluvium (mm/hr)	0	107.12688	106	109
v__CH_K2.rte_6	Eff. hydraulic conductivity in main channel alluvium (mm/hr)	0	106.83063	106	109
v__CH_K2.rte_10	Eff. hydraulic conductivity in main channel alluvium (mm/hr)	0	108.79188	106	109
v__ALPHA_BF.gw	Baseflow alpha factor (days)	0.05	0.99	0	1
v__ALPHA_BF.gw_1	Baseflow alpha factor (days)	0.05	0.62475	0.54	0.78
v__ALPHA_BF.gw_2	Baseflow alpha factor (days)	0.05	0.59805	0.54	0.78
v__ALPHA_BF.gw_3	Baseflow alpha factor (days)	0.05	0.015469	0	0.75
v__ALPHA_BF.gw_6	Baseflow alpha factor (days)	0.05	0.74775	0.54	0.78
v__ALPHA_BF.gw_10	Baseflow alpha factor (days)	0.05	0.54795	0.54	0.78
v__EPCO.hru	Plant uptake compensation factor	0	0.7	0	1
v__EPCO.hru_1	Plant uptake compensation factor	0	0.792844	0.65	1
v__EPCO.hru_2	Plant uptake compensation factor	0	0.709281	0.65	1
v__EPCO.hru_6	Plant uptake compensation factor	0	0.741219	0.65	1
v__EPCO.hru_10	Plant uptake compensation factor	0	0.811656	0.65	1
v__SURLAG.bsn	Surface runoff lag coefficient	4	5.59	4	10
Sediment parameter	Description	Initial value	Fit value	Minimum bound	Maximum bound
v__SPCON.bsn	Linear parameter for calculating the maximum amount of sediment that can be reentrained during channel sediment routing	0	0.001688	0	0.01
v__SPEXP.bsn	Exponent parameter for calculating sediment reentrained in channel sediment routing	1	1.9084	1.04	1.35
v__PRF.bsn	Peak rate adjustment factor for sediment routing in the main channel	1	0.748	0	2
v__CH_EROD.rte	Channel erodibility factor	0	0	0	0.44
v__CH_COV.rte	Channel cover factor	0	0	0	1

Chapter 4-Derive optimal land use and trade-offs quantification

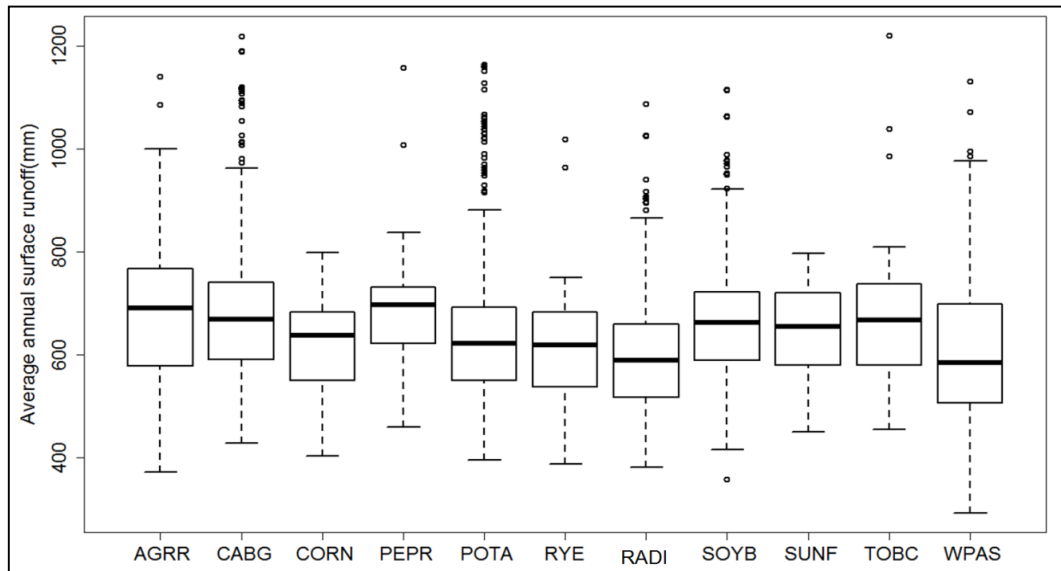
v__LAT_SED.hru	Sediment concentration in lateral flow and groundwater flow [mg/l]	0	0	0	50
v__LAT_SED.hru_3	Sediment concentration in lateral flow and groundwater flow [mg/l]	0	137.38019	0	2000
v__LAT_SED.hru_4	Sediment concentration in lateral flow and groundwater flow [mg/l]	0	4665.4951	2000	5000
v__LAT_SED.hru_6	Sediment concentration in lateral flow and groundwater flow [mg/l]		4634	0	5000
v__LAT_SED.hru_10	Sediment concentration in lateral flow and groundwater flow [mg/l]		1762	0	5000
v__HRU_SLP.hru_4	Average Slope steepness (m/m)	different	0.575655	0	0.6
v__HRU_SLP.hru_3	Average Slope steepness (m/m)	different	0.119042	0	0.6
v__HRU_SLP.hru_6	Average Slope steepness (m/m)	different	0.49512	0	0.6
v__HRU_SLP.hru_10	Average Slope steepness (m/m)	different	0.4716	0	0.6
v__SLSUBBSN.hru_3	Average Slope Length (m)	different	90.741211	40	100
v__SLSUBBSN.hru_4	Average Slope Length (m)	different	118.8147	100	130
v__SLSUBBSN.hru_6	Average Slope Length (m)		83.864006	10	150
v__SLSUBBSN.hru_10	Average Slope Length (m)		24.84	10	150
v__CANMX.hru_3	Maximum canopy storage	25	7.891374	0	100
v__CANMX.hru_4	Maximum canopy storage	25	21.054314	0	100
v__CANMX.hru_6	Maximum canopy storage		92.839996	0	100
v__CANMX.hru_10	Maximum canopy storage		73.559998	0	100
v__CH_COV1.rte_3	Channel erodibility factor	0	0.551757	0	1
v__CH_COV1.rte_4	Channel erodibility factor	0	0.48722	0	1
v__CH_COV1.rte_10	Channel erodibility factor		0.3004	0	1
v__CH_COV2.rte_3	Channel cover factor	0	0.180511	0	1
v__CH_COV2.rte_6	Channel cover factor		0.5508	0	1
v__CH_COV2.rte_4	Channel cover factor	0	0.795847	0	1
v__USLE_P.mgt	USLE support practice factor	1	0.14	0.1	1
v__USLE_P.mgt_1	USLE support practice factor	1	0.37	0.37	0.37
v__USLE_P.mgt_2	USLE support practice factor	1	0.65	0.65	0.65
v__USLE_P.mgt_3	Soil erosivity	1	0.1594	0.1594	0.1594
r__USLE_K().sol	Soil erosivity	different	0.55	0.29	0.88
v__USLE_K(1).sol_1	Soil erosivity	different		0.07	0.07
v__USLE_K(1).sol_2	Soil erosivity	different		0.06	0.06
r__USLE_K(1).sol_3	Soil erosivity	different		-0.25	0.25
r__USLE_K().sol_3	Soil erosivity	different	0.514201	-0.008	0.85
r__USLE_K().sol_4	Soil erosivity	different	0.724178	-0.008	0.85
r__USLE_K(1).sol_6	Soil erosivity	different	0.649914	-0.008	0.85
r__USLE_K(1).sol_10	Soil erosivity	different	0.108345	-0.008	0.85

"v__,a__,r__parameters Name" Given value in between the range is replaced, added and multiplied operation with existing value, "Parameters_1,2,3,4,6,10" values assigned to respective sub-basins, Parameter with initial value "different" mean values depends on different soil type and soil layer. ".ext " is defined for parameters in respective file in SWAT project

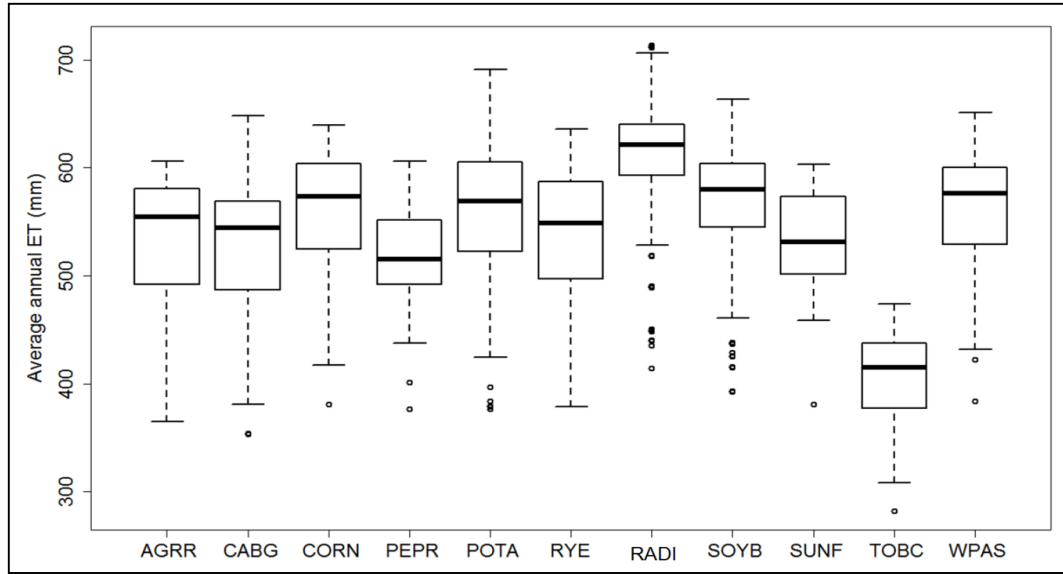
Appendix 4B. Plant parameter with fit value obtain in manual calibration

Parameters	Description	Potato	Cabbage	Radish	Soybean	Rice	Corn	Frstd	Orchard
BLAI.DAT	Potential maximum leaf area index for the plant	5	3.7	5.3	5.3	5.1	10	8.7	3
DLAI.DAT	Fraction of growing season at which senescence becomes the dominant growth process	0.95	0.75	0.99	0.87	0.85	0.4	0.99	0.99
LAIMX1.DAT	Fraction of the maximum plant leaf area index corresponding to the 1 st point on the optimal leaf area development curve	0.01	0.3	0.02	0.05	0.01	0.05	0.05	0.15
LAIMX2.DAT	Fraction of the maximum plant leaf area index corresponding to the 2 nd point on the optimal leaf area development curve	0.95	0.95	0.95	0.95	0.95	0.95	0.95	0.75
FRGRW1.DAT	Fraction of the growing season corresponding to the 1 st point on the optimal leaf area development curve	0.01	0.25	0.01	0.1	0.15	0.15	0.01	0.12
FRGRW2.DAT	Fraction of the growing season corresponding to the 2 nd point on the optimal leaf area development curve	0.18	0.4	0.12	0.48	0.45	0.38	0.2	0.2
PHU.MGT	potential heat unit for plant growing at beginning of simulation (heat units)	1720	1050	2150	1270	1300	1500	1500	2700
RUE.DAT	Radiation use efficiency	25	32	7	23	47	39	15	15

Appendix 4C. Variability of surface runoff for different crops from which optimize land use for minimum surface runoff is identified



Appendix 4D. Variability of evapotranspiration (ET) for different crops

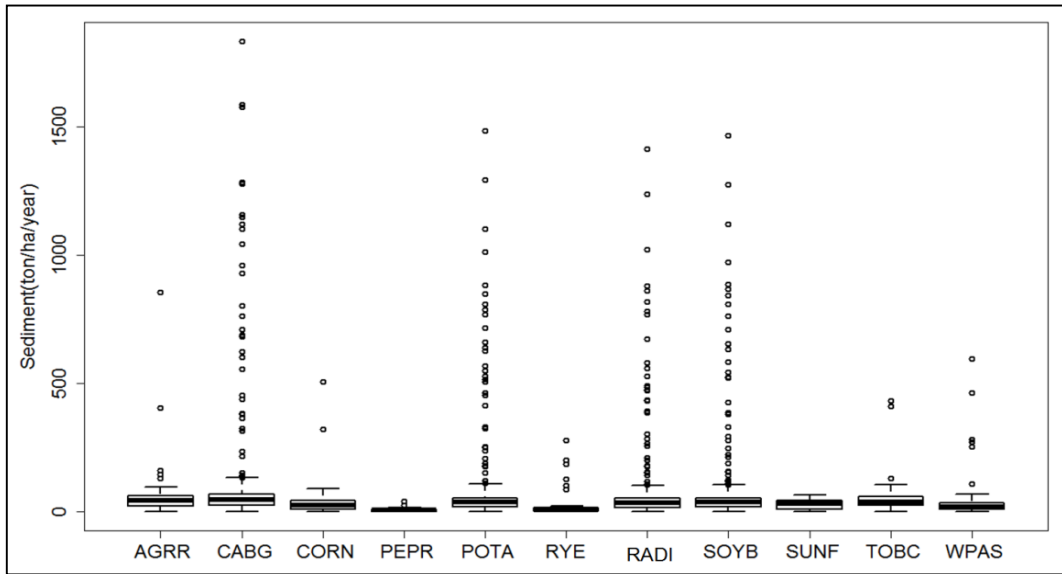


Appendix 4E. Management operation

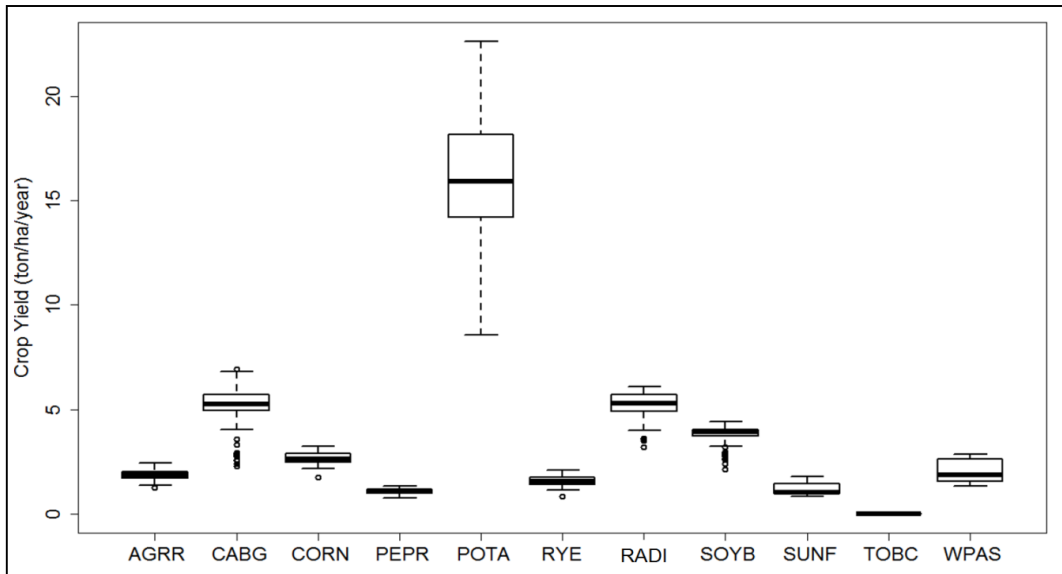
Land use	Potato Expansion	Cabbage Expansion	Radish Expansion	Soybean Expansion	Operational date	Operational material
Area (ha)	1993.69	1993.69	1993.69	1993.69		
Tillage	Rotary Hoe				1-Mar	Tractor
Fertilizer (kg/ha)	330				13-Mar	*(13-13-13)
Tillage	*Furrow-O-C				13-Mar	Tractor
Fertilizer (kg/ha)	100				13-Mar	Dairy-Fresh Manure
Plant/Begin growing season	1720 PHU				15-Mar	Potato
Harvest/kill operation					10-Nov	Potato
Tillage		Rotary Hoe			6-May	Tractor
Fertilizer (kg/ha)		360			18-May	*(08-08-00)
Fertilizer (kg/ha)		150			18-May	Dairy-Fresh Manure
Tillage		Furrow-O-C			18-May	Tractor
Plant/Begin growing season		1050 PHU			20-May	Cabbage
Fertilizer (kg/ha)		0.72			20-Jun	(15-15-00)
Harvest/kill operation					20-Jul	Cabbage
Tillage			Rotary Hoe		15-Apr	Tractor
Tillage			Furrow-O-C		30-Apr	Tractor
Fertilizer (kg/ha)			340		30-Apr	(08-08-00)
Fertilizer (kg/ha)			150		30-Apr	Dairy-Fresh Manure
Plant/Begin growing season			2150 PHU		1-May	Sugar Beet
Fertilizer (kg/ha)			150		1-May	*(18-04-00)
Harvest/kill operation					20-Nov	Sugar Beet
Tillage				Rotary Hoe	1-Apr	Tractor
Fertilizer (kg/ha)				120	15-Apr	Dairy-Fresh Manure
Tillage				Furrow-O-C	15-Apr	Tractor
Fertilizer (kg/ha)				345	15-Apr	*(03-06-00)
Plant/Begin growing season				1270 PHU	1-May	Soybean
Harvest/kill operation					10-Nov	Soybean

*Furrow-O-C: Furrow out cultivator, *(13-13-13), *(08-08-00), *(18-04-00): Fertilizer Codes in Swat model data base in Fertilizer.dat,PHU:Potential Heat Unit

Appendix 4F. Sediment variability for different crops from which optimize land use system for minimum sediment is identified.



Appendix 4G. Crop yield variability for different crops from which optimize land use system for maximum crop yield is identified



4.8 References

- Abbaspour, K.C., C.A. Johnson, M.T. van Genuchten, 2004 Estimating uncertain flow and transport parameters using a sequential uncertainty fitting procedure. *Vadose Zone Journal* **3**: 1340-1352.
- Abbaspour, K.C., J. Yang, I. Maximov, R. Siber, K. Bogner, J. Mieleitner, J. Zobrist, R. Srinivasan, 2007 Modelling hydrology and water quality in the pre-alpine/alpine Thur watershed using SWAT. *Journal of Hydrology*. **333**: 413-430.
- Amon-Armah, F., E. Yiridoe, N.M. Ahmad, D. Hebb, R. Jamieson, D. Burton, A. Madani, 2013 Effect of nutrient management planning on crop yield, nitrate leaching and sediment loading in thomas brook watershed. *Environmental Management*. **52**: 1177-1191.
- Arabi, M., R.S. Govindaraju, M.M. Hantush, 2006 Cost-effective allocation of watershed management practices using a genetic algorithm. *Water Resources Research*. **42**: W10429.
- Arnell, N.W., 2004 Climate change and global water resources: SRES emissions and socio-economic scenarios. *Global Environmental Change*. **14**: 31-52.
- Arnhold, S., S. Lindner, B. Lee, E. Martin, J. Kettering, T.T. Nguyen, T. Koellner, Y.S. Ok, B. Huwe, 2014 Conventional and organic farming: soil erosion and conservation potential for row crop cultivation. *Geoderma*. **219-220**: 89-105.
- Arnhold, S., M. Ruidisch, S. Bartsch, C.L. Shope, B. Huwe, 2013 Simulation of runoff patterns and soil erosion on mountainous farmland with and without plastic-covered ridge-furrow cultivation in South Korea. *Transactions of the ASABE*. **56**: 667-679.
- Arnold, J.G., P.M. Allen, G. Bernhardt, 1993 A comprehensive surface-groundwater flow model. *Journal of Hydrology*. **142**: 47-69.
- Attwood, J.D., B. McCarl, C.-C. Chen, B.R. Eddleman, B. Nayda, R. Srinivasan, 2000 Assessing regional impacts of change: linking economic and environmental models. *Agricultural Systems*. **63**: 147-159.
- Bhattacharai, G., P. Srivastava, L. Marzen, D. Hite, U. Hatch, 2008 Assessment of economic and water quality impacts of land use change using a simple bioeconomic model. *Environmental Management*. **42**: 122-131.
- Cerro, I., Antigüedad, I., Srinivasan, R., Sauvage, S., Volk, M., Sanchez-Perez, J.M., 2014 Simulating land management options to reduce nitrate pollution in an agricultural watershed dominated by an alluvial aquifer. *Journal of Environmental Quality*. **43**, 67-74.
- Choi, J., Lee, H., Park, S., Won, C., Choi, Y., Lim, K., 2010 Sediment control practices in sloping highland fields in Korea. In: Gilkes, R. J., Prakongkep, N. (Eds.), *Proceedings of the 19th World Congress of Soil Science. Soil solutions for a changing world*. International Union of Soil Sciences, pp. 132-135.
- Choi, Y.B., S.S. Lee, S.W. Kim, Y.S. Ok, 2012 Changes of runoff, soil loss, and radish growth (*Raphanus sativus*) in soil treated with polymeric soil amendments. *Journal of Agricultural, Life and Environmental Sciences*. **24**: 50-57.
- Darradi, Y.s., E. Saur, R. Laplana, J.-M. Lescot, V. Kuentz, B.C. Meyer, 2012 Optimizing the environmental performance of agricultural activities: A case study in La Boulouze watershed. *Ecological Indicators*. **22**: 27-37.
- Gassman, P.W., M.R. Reyes, C.H. Green, J.G. Arnold, 2007 The Soil and Water Assessment Tool: historical development, applications, and future directions. *Transactions ASABE*. **50**: 1211-1250.
- Kettering, J., J.-H. Park, S. Lindner, B. Lee, J. Tenhunen, Y. Kuzyakov, 2012 N fluxes in an agricultural catchment under monsoon climate: a budget approach at different scales. *Agriculture, Ecosystems & Environment*. **161**: 101-111.

- Kim, S., Yang, J., Park, C., Jung, Y., Cho, B., 2007 Effects of winter cover crop of ryegrass (*Lolium multiflorum*) and soil conservation practices on soil erosion and quality in the sloping uplands. *Journal of applied biological chemistry*. **55**: 22–28.
- Kruseman, G., Ruben, R., Hengsdijk, H., Van Ittersum, M.K., 1995 Farm household modelling for estimating the effectiveness of price instruments in land use policy. *Netherlands Journal of Agricultural Science*. **43**: 111-123.
- Lautenbach, S., M. Volk, M. Strauch, G. Whittaker, R. Seppelt, 2013 Optimization-based trade-off analysis of biodiesel crop production for managing an agricultural catchment. *Environmental Modelling & Software*. **48**: 98-112.
- Lee, G.J., J.T. Lee, J.S. Ryu, S.W. Hwang, J.E. Yang, J.H. Joo, Y.S. Jung, 2010 Status and soil management problems of highland agriculture of the main mountainous region in the South Korea. In: Gilkes, R. J., Prakongkep, N. (Eds.), *Proceedings of the 19th World Congress of Soil Science. Soil solutions for a changing world*. International Union of Soil Sciences, pp. 78-81.
- Lee, J., J.S. Eom, S. Jae, B. Kim, W.S. Jang, J.C. Ryu, H. Kang, K. Kim, K.J. Lim, 2011 Water quality prediction at mandae watershed using swat and water quality improvement with vegetated filter strip. *Journal of the Korean Society of Agricultural Engineers*. **53**: 37-45.
- Lee, J.M., Ryu, J., Kang, H., Kang, H., Kum, D., Jang, C.H., Choi, J.D., Lim, K.J., 2012. Evaluation of SWAT flow and sediment estimation and effects of soil erosion best management practices. *Journal of the Korean Society of Agricultural Engineers* **54**: 99-108.
- Lindner, S., D. Otieno, B. Lee, W. Xue, S. Arnhold, H. Kwon, B. Huwe, J. Tenhunen, 2015 Carbon dioxide exchange and its regulation in the main agro-ecosystems of Haean catchment in South Korea. *Agriculture, Ecosystems & Environment*. **199**: 132-145.
- Maringanti, C., I. Chaubey, M. Arabi, B. Engel, 2011 Application of a multi-objective optimization method to provide least cost alternatives for NPS pollution control. *Environmental Management*. **48**: 448-461.
- Maringanti, C., I. Chaubey, J. Popp, 2009 Development of a multiobjective optimization tool for the selection and placement of best management practices for nonpoint source pollution control. *Water Resources Research*. **45**: W06406.
- Meyer, B., J.-M. Lescot, R. Laplana, 2009 Comparison of two spatial optimization techniques: a framework to solve multiobjective land use distribution problems. *Environmental Management*. **43**: 264-281.
- Monteith, J.L., C.J. Moss, 1977 Climate and the Efficiency of Crop Production in Britain [and Discussion]. *Philosophical Transactions of the Royal Society of London. B, Biological Sciences*. **281**: 277-294.
- Moriyas, D.N., J.G. Arnold, M.W. Van Liew, R.L. Binger, R.D. Harmel, T.L. Veith, 2007 Model evaluation guidelines for systematic quantification of accuracy in watershed simulations. *Transactions of the ASABE*. **50**: 885-900.
- Neitsch, S.L., J.G. Arnold, J.R. Kiniry, J.R. Williams, 2011 Soil and Water Assessment Tool Theoretical documentation version 2009. Grassland, Soil and water research laboratory, Agricultural research service and Blackland research center, Texas agricultural experiment station, College station, Texas
- Nguyen, T.T., M. Ruidisch, T. Koellner, J. Tenhunen, 2014 Synergies and tradeoffs between nitrate leaching and net farm income: The case of nitrogen best management practices in South Korea. *Agriculture, Ecosystems & Environment*. **186**: 160-169.
- Okumu, B.N., N. Russell, M.A. Jabbar, D. Colman, M.A.M. Saleem, J. Pender, 2004 Economic impacts of technology, population growth and soil erosion at watershed level: the case of the ginchi in ethiopia. *Journal of Agricultural Economics*. **55**: 503-523.

- Poppenborg, P., T. Koellner, 2013 Do attitudes toward ecosystem services determine agricultural land use practices? An analysis of farmers' decision-making in a South Korean watershed. *Land Use Policy*. **31**: 422-429.
- Rasul, G., 2009 Ecosystem services and agricultural land-use practices: a case study of the Chittagong Hill Tracts of Bangladesh. *Sustainability: Science, Practice, & Policy*. **5**: 15-27.
- Santhi, C., J.G. Arnold, J.R. Williams, W.A. Dugas, R. Srinivasan, L.M. Hauck, 2001 Validation of the swat model on a large river basin with point and nonpoint sources. *JAWRA Journal of the American Water Resources Association*. **37**: 1169-1188.
- Seo, B., C. Bogner, P. Poppenborg, E. Martin, M. Hoffmeister, M. Jun, T. Koellner, B. Reineking, C.L. Shope, J. Tenhunen, 2014 Deriving a per-field land use and land cover map in an agricultural mosaic catchment. *Earth System Science Data*. **7**: 339-352.
- Shiferaw, B., S.T. Holden, 2000 Policy instruments for sustainable land management: the case of highland smallholders in Ethiopia. *Agricultural Economics*. **22**: 217-232.
- Shope, C.L., G.R. Maharjan, J. Tenhunen, B. Seo, K. Kim, J. Riley, S. Arnhold, T. Koellner, Y.S. Ok, S. Peiffer, B. Kim, J.H. Park, B. Huwe, 2014 Using the SWAT model to improve process descriptions and define hydrologic partitioning in South Korea. *Hydrology and Earth System Sciences* **18**: 539-557.
- Stoorvogel, J.J., J.M. Antle, C.C. Crissman, W. Bowen, 2004 The tradeoff analysis model: integrated bio-physical and economic modeling of agricultural production systems. *Agricultural Systems*. **80**: 43-66.
- Swallow, B.M., J.K. Sang, M. Nyabenge, D.K. Bundotich, A.K. Duraiappah, T.B. Yatich, 2009 Tradeoffs, synergies and traps among ecosystem services in the Lake Victoria basin of East Africa. *Environmental Science & Policy*. **12**: 504-519.
- Tenhunen, J., B. Seo, B. Lee, 2011 Spatial setting of the TERRECO project in the Haean catchment of Yanggu-gun and the Soyang watershed in Gangwan-do. *AsiaFlux Training Course on Flux Monitoring: From Theory to Application*, Seoul, South Korea.
- Ullrich, A., M. Volk, 2009 Application of the Soil and Water Assessment Tool (SWAT) to predict the impact of alternative management practices on water quality and quantity. *Agricultural Water Management*. **96**: 1207-1217.
- Valdivia, R.O., J.M. Antle, J.J. Stoorvogel, 2012 Coupling the Tradeoff Analysis Model with a market equilibrium model to analyze economic and environmental outcomes of agricultural production systems. *Agricultural Systems*. **110**: 17-29.
- White, M.J., R.D. Harmel, J.G. Arnold, J.R. Williams, 2012 SWAT Check: A Screening Tool to Assist Users in the Identification of Potential Model Application Problems. *Journal of Environmental Quality*. **43**: 208-214.

Chapter 5 Assessing effectiveness of split fertilization and cover crop cultivation to conserve soil and water resources and improve crop productivity

Ganga Ram Maharjan^{1*}, Marianne Ruidisch², Christopher L. Shope³, Kwanghun Choi⁴, Bernd Huwe¹, Seong Joon Kim⁵, John Tenhunen², Sebastian Arnhold^{1,6}

¹University of Bayreuth, Dept. of Soil Physics, Universitatstrasse 30, 95440 Bayreuth, Germany

²University of Bayreuth, Dept. of Plant Ecology, Universitatstrasse 30, 95440 Bayreuth, Germany

³US Geological Survey, 2329 Orton Circle, Salt Lake City, UT, USA

⁴University of Bayreuth, Dept. of Biogeographical Modelling, Universitatstrasse 30, 95440 Bayreuth, Germany

⁵Konkuk University, Dept. of Civil & Environmental System Engineering, Seoul 143-701, Korea

⁶University of Bayreuth, Professorship of Ecological Services, Universitatstrasse 30, 95440 Bayreuth, Germany

Abstract

Intensive agricultural practices to secure crop yields have negative environmental effects due to generation of sediment and nutrients from agricultural fields. The monsoon climate and current agricultural practices on hillslopes in the Haean catchment in South Korea aggravates water quality by transporting sediment and nutrients to downstream water bodies. The aim of this study is the permanent reduction of sediment and nitrate from this catchment through an efficient application of best management practices (BMPs). We applied two BMPs, i.e., split fertilizer application (SF) and winter cover crop cultivation (CC) and both in combination (SFCC) to major dryland crops (cabbage, potato, radish and soybean) in order to investigate their effectiveness at the catchment scale by using the Soil and Water Assessment Tool (SWAT) model. We found that the SF scenario reduced nitrate pollution while sediment and crop yield did not change relative to the base line (BL) scenario. The application of CC scenario reduces both sediment and nitrate load while crop yields increased. The combination of split fertilization and cover cropping (SFCC) showed the highest positive effect on reducing sediment and nitrate and increasing crop yields compared to its single application. We determined the variation of the effectiveness of BMPs for major crop types and could demonstrate that specific sites and crop types such as soybean were less supportive in reducing sediment and nitrate loads. Those sites and crops could be considered for additional BMP measures to mitigate water deterioration by target pollutants. Recommendations for BMP applications should also consider minor crops and other land use types in order to reduce water pollution and improve crop yields efficiently in this catchment.

Keywords: *BMP, cover crop, crop yield, intensive agriculture, monsoon, nitrate loss, sediment loss, split fertilization*

5.1 Introduction

In recent decades, agricultural production has been intensified to meet the food demand of a growing population. Worldwide, the intensification of agricultural production is consistent with negative environmental impacts, including deterioration of water and soil resources (Lal, 2008; Matson et al., 1997; Tilman et al., 2002). Agricultural mismanagement such as over-fertilization, inappropriate pesticide application, over-tillage as well as over-grazing trigger nutrient leaching and soil erosion which can turn agricultural ecosystems into non-productive areas (Scherr and Yadav, 1996). Land degradation and soil losses are threats not only to economic and social welfare by decreasing yields and farmers income, but also ecosystem services as soil resources, water yield and water quality. From a regional perspective, absolute agricultural land degradation was found to be highest in Asia, accounting for 206 million hectares (Oldeman et al., (1994) cited in Scherr and Yadav, (1996)). Meanwhile, the world wide degradation of productive farmland was recognized and a trend reversal by achieving global zero net land degradation until 2030 was postulated by the UN Convention to Combat Desertification (Stavi and Lal, 2015; UNCCD, 2012). Instead of focusing solely on productivity and profits, sustainable agricultural production should comprehensively integrate biological, chemical, physical, ecological, economic, and social aspects to secure food supply and human welfare as well as environmental resources (Lichtfouse et al., 2009). Generally, soil loss rates are up to ten-fold higher ranging from 10 to 100 tons ha⁻¹ yr⁻¹ in comparison to soil formation rates on cultivated land (Pimentel et al., 1987). However, the extent of soil erosion does not only depend on management practices but also on natural factors such as climate and topography. The amount and intensity of rainfall events, water infiltration capacity of soils and thus the magnitude of surface runoff formation also determine the vulnerability of soils to water erosion. Cultivated and bare soils on slopes in monsoon-driven regions therefore constitute risk areas for erosion (Morgan, 2005). In some areas, the total amount and the intensity of monsoonal events are predicted to increase under changing climate (Park et al., 2010). Thus, the vulnerability of soils and the need for management practices to ensure conservation of agricultural farmland is especially important in monsoon driven areas.

Moreover, in these regions over-fertilization causes high levels of nitrate and phosphorus leaching through surface flow and percolation into aquatic systems thus deteriorating fresh water resources. Tilman et al. (2002) reported that only 30 - 50 % of the applied nitrogen fertilizer and ~45 % of phosphorus fertilizer is taken up by crops. A significant amount of the applied nitrogen and a slightly smaller portion of the applied phosphorus are lost from agricultural fields. The mountainous agriculture in South Korea is characterized by a very high level of chemical fertilization which continuously increased from 230 kg ha⁻¹ in 1980 to 450 kg ha⁻¹ in the mid 1990s (Shim, 1998). The current management practices in vegetable dryland agriculture amplify soil erosion and nutrient leaching under the influence of the East-Asian summer monsoon in South Korea (Arnhold et al., 2013; Kettering et al., 2012; Ruidisch et al., 2013a; Ruidisch et al., 2013b).

In order to reduce non-point source pollution, the adaptation of agriculture best management practices (BMPs) have been promoted and encouraged by subsidies in many places worldwide. However, in some areas, policies and incentives to encourage farmers to adapt BMPs are still missing. To maintain productive farmland and to prevent soil and nutrient loss is not only the responsibility of local farmers but also of governmental institutions and local communities. To pave the way for a sustainable agriculture, which ensures appropriate yields as well as environmental benefits, policy makers, watershed managers and farmers need evidence of the effectiveness of such BMPs under local conditions. Hence, to cope this cross-functional task and to assist water resource managers in assessing the impact of management and climate on water supplies and non-point source pollution in watersheds and large river basins, the SWAT model (Soil and Water Assessment Tool) was developed in the early 1990 (Arnold and Fohrer, 2005). Worldwide, this model serves as a basis for land use decision making.

Using the SWAT model, the effectiveness of BMPs such as filter strips, spring litter application, optimal grazing management, terraces, fertilizer and manure management have been analyzed by several researchers worldwide (Chiang et al., 2012; Lam et al., 2011; Santhi et al., 2006; Tuppad et al., 2010). Chiang et al. (2012) compared 171 BMP combinations and recommended combinations of spring litter application, optimum grazing management, and vegetative filter strips to improve water quality performance. The BMP of field buffer strips along the main channel was assessed in a lowland watershed by Lam et al. (2011) who found considerable reduction in annual loads for flow, sediment and nutrients. The pre and post BMPs impact on sediment and nutrient were compared by Santhi et al. (2006) and several BMP combinations in relation to nutrient management (reduced fertilizer), residue management, grade stabilization structure, contour farming reduce sediment at farm level that varied from 5 to 99 % and nitrogen loading reductions varied from 5 to 90 %. The BMPs impact in this study showed less than 1 and 2 % reduction in sediment and nutrient load at watershed level because of BMPs implementation were limited to less than 1 % of the watershed area. Depending on various BMPs, Tuppad et al. (2010) reported a reduction of 3 to 37 % and 1 to 24 % for sediment and total nitrate, respectively.

Many studies on BMP applications are limited in order to evaluate the effectiveness to reduce nonpoint source pollution at field and watershed levels. Very few BMP applications (Amon-Armah et al., 2013) include impacts on both crop yield and water quality pollutants (sediment, nitrate). In addition, the effectiveness of BMP considering different crop types are missing from the literature. In the Haeon catchment of South Korea, BMPs with regard to tillage and fertilization were proposed based on field measurements and plot scale modeling results (Arnhold et al., 2013; Kettering et al., 2013; Ruidisch et al., 2013a; 2013b). These studies assumed that the most effective BMPs in dryland vegetable production would be fertilizer best management practices and cover crop cultivation in the winter to reduce sediment and nutrient loss. We thus hypothesize that the implementation of a cover

crop and split fertilizer application reduces the sediment and nitrate level significantly in comparison to conventional agricultural management. In order to evaluate how these recommendations apply to different crops in decreasing sediment and nutrient loss at the catchment level, we use the SWAT model. In our study we aim to:

- (i) estimate *crop yields* from the dominant dryland agricultural crops including cabbage, radish, soybean and potato under current management practices
- (ii) quantify *sediment loss* and *nitrate loss* from the area of these specific dryland agricultural crops as well as for the entire catchment area under current management practices
- (iii) estimate *crop yields* and quantify *sediment loss* and *nitrate loss* for the individual crop types and the whole catchment when applying BMPs. In our study BMP scenarios include the implementation of (a) cover crop cultivation after the main growing season and (b) split fertilization as well as (c) the combination of both.
- (iv) provide useful *recommendations for farmers and policy makers*, those who could redesign agriculture management in order to meet both higher crop yields and thus higher farm income as well as environmental benefits by conservation of soil and water resources.

5.2 Materials and methods

5.2.1 Study area

The Haean catchment (62.7 km²) is located in the Kangwon Province of South Korea between 38°13' to 38°20'N and 128°5' to 128°11' E (Figure. 5.1). The mountainous catchment is dominated by intensive agriculture, where large amounts of sediment and nutrients are released during monsoonal rainfall and transported downstream into the Soyang reservoir. The Soyang reservoir is the largest reservoir in the country and was constructed in 1973 for multiple purposes including drinking water provision for the inhabitants of Seoul (Kim et al., 2000). The elevation of the Haean catchment ranges from 340 to 1320 m with an average slope of 28% and a maximum slope of 84 %. The high mountains surrounding the catchment are covered by deciduous and coniferous forests (56.7 %). The hill slopes near the forest edges are dominated by cultivation of annual cash crops, primarily cabbage, potato, radish, and soybean (7.8 %), perennial crops such as orchards and ginseng (8.3 %), and other dryland crops including maize, pepper, rye, and sunflowers (4.1 %). The flat areas in the catchment center are dominated by rice paddies (8.2 %). The remaining area is covered by field margins, residential, and fallow lands (14.9 %). The soils of the Haean catchment are dominated by *Cambisols* formed from weathered granite. The dominant soil texture class is *loamy sand* which accounts for 59.4 % of the catchment area, followed by *Sand silt* with 27.5 % and *sand* and *clay* with 10.5 and 2.7 %, respectively. The yearly maximum and minimum average temperatures were 12.5 and 2.5°C, respectively, and the annual precipitation is 1658 mm, based on 13 years weather station records in the

Hae-an catchment (1999-2011). Almost 70% of the annual precipitation is concentrated in the monsoon season between June and September.

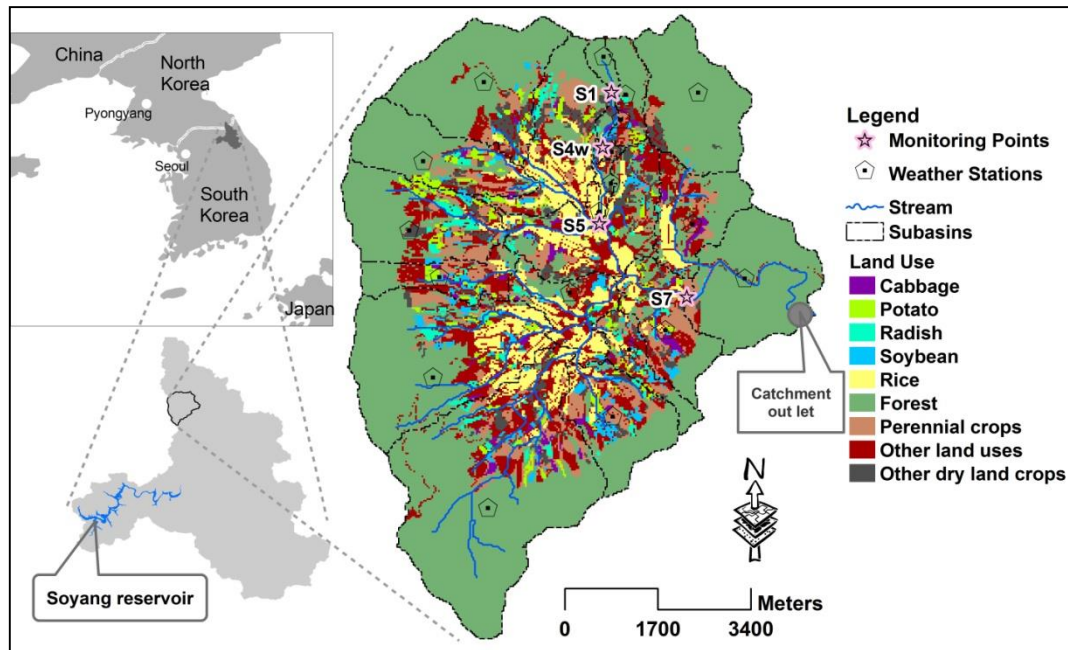


Figure 5.1 Location and land use distribution of the Hae-an catchment including sub-basins, weather stations, and stream monitoring points used for this study. The Hae-an catchment is one of the hotspots for sediment and nutrients transport into the Soyang reservoir

5.2.2 Model application

We used the Soil and Water Assessment Tool (SWAT) (Arnold and Fohrer, 2005) to simulate the impacts of BMP scenarios on sediment, nitrate, and crop yields within the Hae-an catchment. The SWAT model was developed by the USDA-ARS as an integrated process based watershed model which includes water flow, sediment and nutrient transport, and plant growth. In SWAT, the catchment is delineated into sub-basins which are further subdivided into hydrological response unit (HRUs). HRUs are land units of homogenous land use, soil type, and slope within the sub-basins and represent the spatial landscape heterogeneity of the catchment (Neitsch et al., 2011). The heterogeneity significantly alters the model outputs including surface runoff, nutrient leaching and associated pollution, as well as crop biomass and yield. The output variables of SWAT are simulated at the HRU level which are aggregated from every HRU to the sub-basin level and then routed through the stream network toward the catchment outlet. Detailed model descriptions for the simulation of discharge, sediment, nutrients, and crop yield are given in (Arnold et al., 1998) and (Neitsch et al., 2011).

5.2.3 Model parameterization

The main input data for the SWAT model are shown in Table 5.1. The intrinsic characteristics and spatial landscape variability of the catchment were represented through superimposition of three spatial data sets: digital elevation model (DEM, topographical variability), land use and land cover map (LULC, crop variability), and soil map (soil properties variability). The land use map for the

Haeon catchment was created based on a comprehensive field survey in 2010 (Seo et al., 2014). The soil map was developed from soil pit surveys conducted in 2009 and 2010 (Shope et al., 2014). With the above data sets, the SWAT model configuration for the Haeon catchment consisted of 21 sub-basins and 792 HRUs. The climate data sets required for SWAT (temperature, solar radiation, precipitation, relative humidity, and wind speed) were obtained from a network of automatic weather station distributed in the Haeon catchment to account for the spatial and temporal microclimate variability (Figure 5.1). Point measurements of discharge, sediment, and nitrate concentration at different stream sites (Figure 5.1) were used to calibrate and validate the SWAT model. Management schedules (tillage, plantation, harvest, and fertilization) for the major dryland crops cabbage, potato, radish, and soybean were defined based on interviews with farmers within the Haeon catchment (Table 5.2). In addition, data from plot level experiments for LAI and biomass development (Lindner et al., 2015) were used to calibrate the crop growth parameters in the model for the four major crops.

Table 5.1 Input data set for SWAT model of the Haeon catchment

Spatial data set	Data set type	Scale
Catchment DEM	Clipped DEM from Soyang Lake contour map	1:25000
Stream network	Surveyed river channels in study area	1:10000
LULC map	Validated map for year 2010 (Seo <i>et al.</i> , 2014)	1:5000
Soil map	Field based soil profile (1.2 m) from 2009-2011	1:10000
Daily solar radiation	Chuncheon network weather station (2007-2010)	Point
Daily precipitation, temperature	Haeon network weather station (2007–2010)	Point
Daily relative humidity, wind speed	Yanggu network weather station (2007–2010)	Point
Daily discharge, sediment, and nutrients (NO ₃ ⁻)	Used for model calibration/validation obtained from field-measurement	Point
LAI/Biomass-Yield	Field measurement (cabbage, potato, radish and soybean)	Field

Table 5.2 Management schedules for the cultivation of the four major dryland crops in the Haeon catchment

Crop	Tillage date	Tillage type	Fertilizer date	Fertilizer* amount	Planting date	Harvest date
Cabbage	6-May	Rotary hoe	11-May	360	15-May	15-Jul
	10-May	Furrow out cultivator				
Potato	1-Apr	Rotary hoe	17-Apr	330	29-Apr	29-Aug
	12-Apr	Furrow out cultivator				
Radish	25-May	Rotary hoe	27-Apr	490	1-Jun	5-Sep
	30-May	Furrow out cultivator				
Soybean	10-May	Rotary hoe	25-May	345	29-May	20-Oct
	15-May	Furrow out cultivator				

*Mineral fertilizer in kg ha⁻¹

5.2.4 Model calibration and validation

The SWAT model was calibrated and validated for three daily output variables: discharge, sediment, and nitrate (NO₃⁻). The calibration period for all three output variables was 2009-2010, while 2011 was used for validation. Multiple monitoring locations (S1, S4W, S5, and S7) (Figure 5.1) are located along an elevation transect were used for calibration and validation of discharge and sediment. The downstream monitoring location S7 was used for calibration and validation of nitrate (NO₃⁻). Proper simulation of LAI and biomass is important as they affect the overall water balance and water quality due to changes of evapotranspiration and crop cover (i.e., USLE_C). Therefore, we used measured

LAI and biomass/yield data to adjust the model's LAI and biomass development during the growing season for the four major crops while calibrating discharge, sediment, and nitrate. The fitted parameter values for the crop growth simulation for the different crops/land covers are presented in the supplementary Table ST1. The calibration of hydrology and water quality was performed in sequential order of discharge, sediment, and nitrate (Shrestha et al., 2013) using the automatic calibration procedure of SWAT-CUP (Abbaspour et al., 2004). We used the sequential uncertainty fitting (SUFI-2) algorithm (Abbaspour et al., 2004) incorporated in SWAT-CUP to optimize the parameter values and the Nash-Sutcliffe efficiency (NSE) and coefficient of determination (R^2) as objective functions. Additional to NSE and R^2 , we used the percent bias (PBIAS) to evaluate the model performance for calibration and validation (Moriassi et al., 2007). In addition to the statistical indicators, the overall water and sediment balances were checked to assure a realistic representation of evapotranspiration, baseflow/total flow and surface runoff/total flow ratios, as well as crop yields and sediment components (sediment source: terrestrial, stream deposition or degradation). The sensitive parameters and ranges for different output variables required for SUFI-2 were identified by iterative simulations for each parameter while maintaining default values for the remaining parameters. Several previous studies were referenced to identify sensitive parameters (Arnold et al., 2011; Cao et al., 2006; White and Chaubey, 2005; Zhang et al., 2009), including a previous study at the same study area (Shope et al., 2014). The parameter values were allowed to change by replacement, addition, and relative change to the initial values based on different crop types and sub-basins. The detailed automatic calibration procedures are reported in Abbaspour et al. (2007). The supplementary Table ST2 provides the ranking of the sensitive parameters and best fit values of the calibrated model. The calibrated and validated model was considered our baseline scenario (BL, described in section 5.2.5). The output variables of sediment, nitrate, and crop yield were then compared for scenarios representing the different BMPs (section 5.2.5).

5.2.5 BMP scenarios

The model configuration of the catchment contained a total of 200 HRUs that represented the four major crops (38 for cabbage, 48 for potato, 50 for radish, and 64 for soybean). After model calibration, BMP scenarios including split fertilizer application and cover crop cultivation were implemented to those 200 HRUs. The simulation period was set from January 2007 to December 2010 with a 3 year warm up period (2007-2008). However, based on availability of land use data for other years, the model output could be considered for entire period of the simulation. The model output for the simulation year 2010 was used to compare the different BMP scenarios because the land use map used in the model was based on 2010.

Scenario BL refers to the base line scenario with single fertilizer application at the beginning of the growing season. The application of split fertilization corresponds to SF. Cover crop cultivation is represented by CC, and the combination of split fertilization and cover crop cultivation is abbreviated

as SFCC scenario. As cover crop we selected rye grass because of its low base temperature which allows growth during cold seasons (Yeo et al., 2014) and ensures high ground cover (Rice et al., 2007). In the simulations, a cover crop was planted after harvest of the main crops and was removed before field preparation for the main crops were performed in the following year. Detailed operation schedules including tillage, fertilization, planting and harvesting are presented in Table ST3 in the supplementary material.

5.3 Results

5.3.1 SWAT model performance

The SWAT model for the Haean catchment showed good performance for discharge, sediment, and nitrate for most of the monitoring sites. The performance statistics (NSE, R^2 , and PBIAS, Moriasi et al., 2007) for the calibration and validation periods are presented in Table 5.3. Times series plots with observed vs. simulated discharge, sediment, and nitrate are given in supplementary Figures SPF1, SPF2 and SPF3 in the supplementary material. The average NSE scores for discharge were 0.74 and 0.45 for calibration and validation, respectively. The average values for R^2 were 0.82 and 0.76 and for PBIAS -10.95 and 30.18 , for calibration and validation respectively. NSE values for sediment calibration ranged from 0.58 to 0.87 with an average value of 0.78 and for validation from 0.35 to 0.90 with average value of 0.60. The average R^2 for sediment were 0.90 and 0.80 respectively during calibration and validation. The average PBIAS values for sediment calibration and validation were -2.90 and 42.65 , respectively. NSE and R^2 for nitrate calibration were 0.48 and 0.62 and for validation 0.52 and 0.61, for NSE and R^2 respectively. The PBIAS for nitrate calibration and validation were -40.1 and 34.1 , respectively. According to the SWAT literature (Gassman et al., 2007; Moriasi et al., 2007; Santhi et al., 2001), the model performance can be considered acceptable when NSE and R^2 are greater than 0.5 and the model can be used for further scenario analysis. Except for site S4W, which showed low NSE values for the validation of discharge (0.02) and sediment (0.33), the model performed well for all output variables.

Table 5.3 Model performance for different output variables at different stream sites

Variable	Stream site	Calibration (2009-2010)			Validation (2011)		
		R^2	NSE	PBIAS(%)	R^2	NSE	PBIAS(%)
Discharge	S1	0.76	0.72	2.7	0.75	0.56	43.8
	S4W*	0.8	0.6	-1.9	0.68	0.02	43.4
	S5	0.89	0.88	-5.7	0.74	0.5	66.7
	S7	0.82	0.75	-38.9	0.85	0.73	-33.2
Average		0.82	0.74	-10.95	0.76	0.45	30.18
Sediment	S1	0.98	0.82	13.0	0.64	0.56	-38.9
	S4W*	0.87	0.86	6.8	0.78	0.35	125.7
	S5	0.92	0.87	15.6	0.84	0.60	72.2
	S7	0.82	0.58	-47	0.92	0.90	11.6
Average		0.90	0.78	-2.9	0.80	0.60	42.65
Nitrate**	S7	0.62	0.48	-40.10	0.61	0.52	34.1

*Calibration period for stream site S4W was only 2010, **Nitrate calibrated and validated only for downstream site at S7

5.3.2 BMP impact on sediments

The simulated weighted mean of sediment generation for the BL scenario for cabbage, potato, radish, and soybean fields were 48, 53, 52, and 35 tons ha⁻¹, respectively. The simulated sediment amounts showed high variations for the different BMP scenarios between individual HRUs (Figure. 5.2) due to the strong spatial heterogeneity in topography and soil properties in the catchment. For all crops, the scenarios CC and SFCC decreased sediment generation from all HRUs which highlights the effectiveness of cover crops for soil protection beyond the growing season. SF had no impact on sediment loss. Among the four major crops, cabbage showed the strongest reduction in sediment loss for the CC and SFCC scenarios compared to the BL scenario, with 81 and 80 % reduction, respectively. The sediment reduction for the CC and SFCC scenarios were smallest for soybean with only 20 % reduction compared to the BL scenario. Scenarios CC and SFCC for potato reduced the sediment generation by 64 % and for radish by 52 %. Both scenarios CC and SFCC had almost equal capabilities to reduce sediment in comparison to the BL scenario for individual crops.

We performed a Kruskal-Wallis Test to identify significant differences between the scenarios. We found that the SF scenario did not show a significant difference in sediment loss from the BL scenario (indicated in Figure. 5.2 with "a" for both BL and SF). The scenarios CC and SFCC (indicated with "b" in Figure. 5.2) showed significant differences in reducing sediment compared to BL and SF scenarios for all crops except soybean. On the other hand, the scenarios CC and SFCC scenarios did not show significant differences between these two scenarios for the respective crop type. Soybean did not show any significant differences between the four scenarios (indicated with "a" for all scenarios in Figure 5.2D) which suggests that BMP implementations on soybean fields are not efficient in reducing sediment.

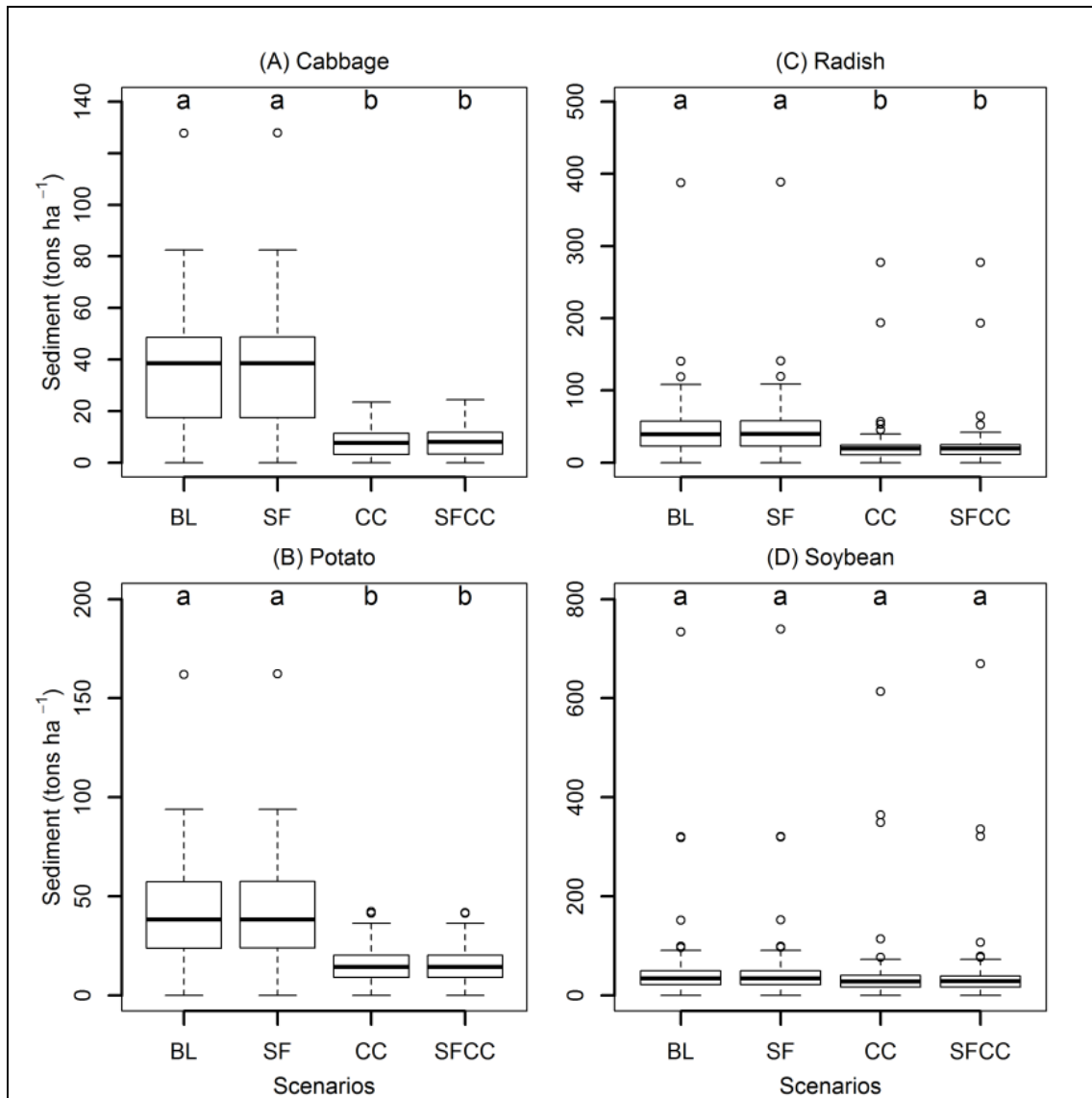


Figure 5.2 Variation of sediment loss from the respective crop HRUs simulated for the different scenarios. Small letters "a" and "b" are used to indicate statistical significance between the scenarios. Presence of same letter indicates no significance while different letter indicates significant differences between scenarios

The total sediment generated from the four major dryland crops for the different BMP scenarios is presented in Figure 5.3. The total sediment loss in the BL and SL scenario showed almost equal amounts of 23000 tons. The highest proportion of sediment was produced from potato fields (8260 tons), followed by radish (6356 tons), soybean (5038 tons), and cabbage (3347 tons). In the CC scenario, the total sediment was reduced to 10607 tons which represents a 54 % reduction compared to the BL scenario. The combination scenario SFCC reduced sediment loss to 10704 tons which also amounts to 54 % reduction compared to BL. The individual sediment contribution from the four crops in both scenarios CC and SFCC were almost similar (Figure. 5.3) and were highest for soybean (4071 tons), followed by radish (3019 tons), potato (2944 tons), and cabbage (643 tons) compared to CC scenario. Although, CC and SFCC scenarios were not significantly different, the SFCC scenario showed in total 1 % (97 tons) higher sediment loss than the CC scenario. Total simulated sediment

loss from all land use types in the catchment was 63973 tons for the BL scenario from which 36 % originates from the four major dryland crops. The CC and SFCC scenarios reduced the total sediment amount to 51446 tons which represents a 19 % reduction compared to the BL scenario. The summary of the BMP scenarios and their impacts on sediment loss for the four major crops are presented in Table 5.4.

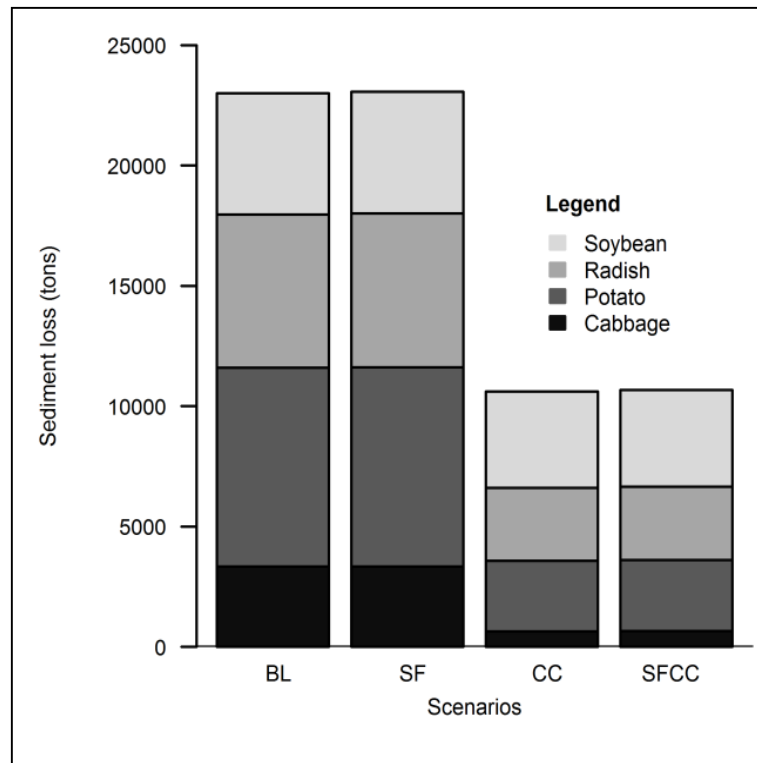


Figure 5.3 Total sediment loss from four major dryland crops estimated for different BMP scenarios

Table 5.4 Scenario impact on sediment loss from different crop types: ton ha⁻¹ (% difference compared to BL scenario)

Crop types	Area (ha)	BL	SF	CC	SFCC
Cabbage	69.84	47.9	47.9(0%)	9.2(-81 %)	9.5(-80 %)
Potato	155.79	53.0	53.1(0%)	18.9(-64 %)	18.9(-64 %)
Radish	121.23	52.4	52.7(0%)	24.9(-52 %)	25.1(-52 %)
Soybean	141.93	35.5	35.6(0%)	28.3(-20 %)	28.4(-20 %)
*Average	488.79	47.1	47.2(0%)	21.7(-54 %)	21.9(-54 %)
**Catchment average	6273.9	10.2	10.2(0%)	8.2(-19 %)	8.2(-19 %)

*Sediment calculated at field level is due to weighted mean for major dry land crops: cabbage, potato, radish, and soybean, **Sediment simulated at catchment level is weighted mean for all land use type within the entire catchment

5.3.3 BMP impact on nitrate

The impact of BMP scenarios on total nitrate loss from the different crop cultivations is shown in Figure 5.4. The amount of total nitrate loss via the different pathways (surface runoff, lateral flow, and leaching) for the four major dryland crops in different BMP scenarios are presented in supplementary Figure. SPF 5.4 - SPF 5.6 in the supplementary material. Here after, total nitrate and nitrate are

ambiguously same unless indicated. The yearly weighted mean of nitrate loss simulated for the BL scenario ranged from 95 kg ha⁻¹ from soybean to 315 kg ha⁻¹ from radish fields. Total nitrate loss for all scenarios was highest for radish, followed by cabbage and potato. The lowest loss of total nitrate was simulated for soybean regardless of the BMP scenario. The SF scenario reduced total nitrate loss from 8 to 13 % compared to the BL scenario for cabbage and radish fields, whereas nitrate loss increased by 1 % for soybean fields. The highest reduction of nitrate loss by the SF scenario of 13 % was simulated for radish, primarily driven by reduction of nitrate losses in surface runoff and lateral flow (45 % nitrate losses reduction in surface runoff, 6 % in lateral flow and no (0 %) reduction in leaching). The SFCC scenario reduced total nitrate loss by 43 % from potato fields with 50 % reduction in nitrate from surface runoff, 21 % from lateral flow and 41 % from leaching. The SFCC scenario showed the smallest effect for soybean with 3 % reduction of total nitrate loss, which was attributed to 11 % reduction in surface runoff and 7 % in lateral flow, whereas the nitrate lost via leaching increased by 29 %. Generally, we found that the SF scenario had a higher capability to reduce nitrate loss in surface runoff than the CC scenario, whereas CC had a higher capability to reduce nitrate loss via lateral flow and leaching. The SFCC scenario showed mutual benefits of reducing nitrate loss via all pathways independently of the crop type (see supplementary Tables ST 5.4-ST 5.6).

We applied the Kruskal-Wallis test to identify significant differences between the scenarios for nitrate. The SF and CC scenarios for cabbage and radish did not show significant differences compared to the BL scenario. The scenarios SF and CC were also not significantly different (Figure 5.4). Soybean did not show significant differences in nitrate loss between the BMP scenarios. The scenario SFCC showed significant difference in reducing nitrate from cabbage, potato, and radish cultivations compared to the BL scenario. For all crops the SF scenario did not show significant nitrate reduction compared to BL.

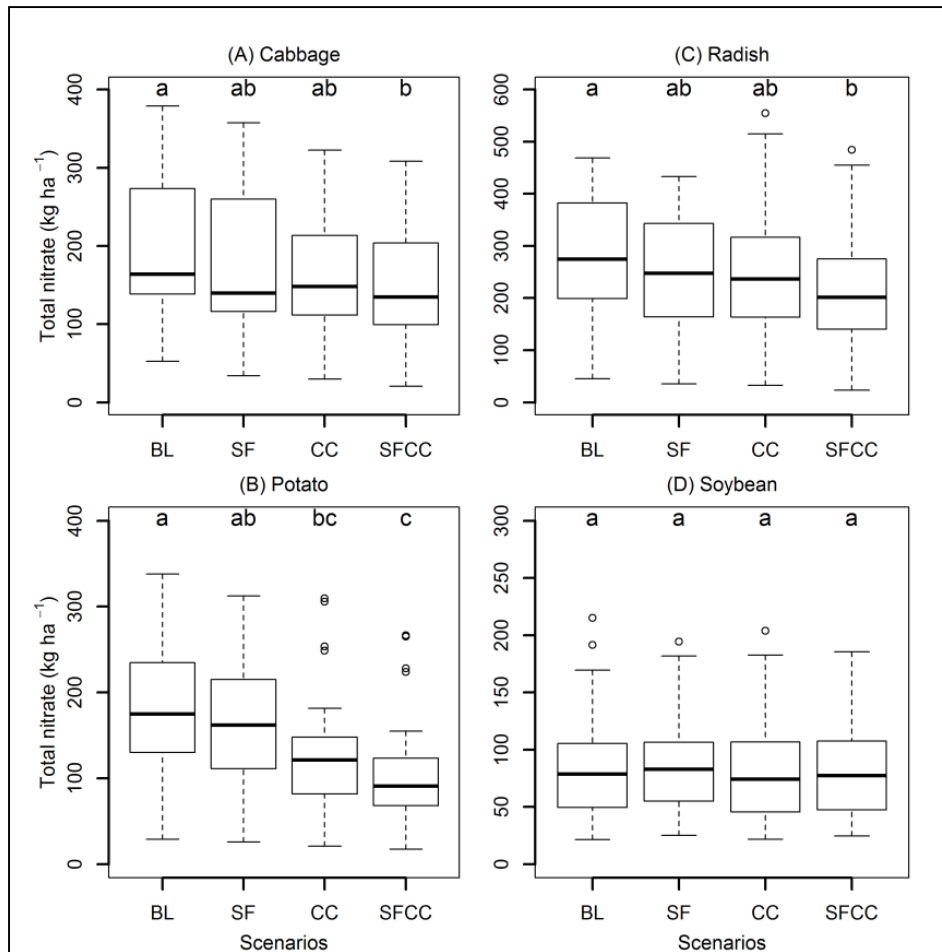


Figure 5.4 Variation of total nitrate from the respective crop HRUs simulated in different scenarios

The total nitrate lost from cabbage, potato, radish, and soybean fields for the different scenarios is shown in Figure 5.5. Total nitrate loss from all crop fields amounts to 97835 kg with the largest contribution from radish (38129 kg), followed by potato (30041 kg), cabbage (16218 kg), and soybean (13447 kg). As indicated in Figure 5.5, total nitrate loss decreased for the BMP scenarios to 88471, 79673, and 70386 kg for SF, CC, and SFCC, respectively, which represent reductions of 9, 18, and 28 % compared to the BL scenario. The total nitrate for the BL scenario from all land use types in the catchment was 245993 kg, from which 40 % were produced by the four major dryland crops. The BMP scenarios reduced total nitrate loss to 238408, 225860, and 219587 kg for SF, CC, and SFCC, respectively, which represents a reduction of 4, 7, and 11 % compared to BL. The summary of the BMP scenarios and their impacts on nitrate loss is presented in Table 5.5.

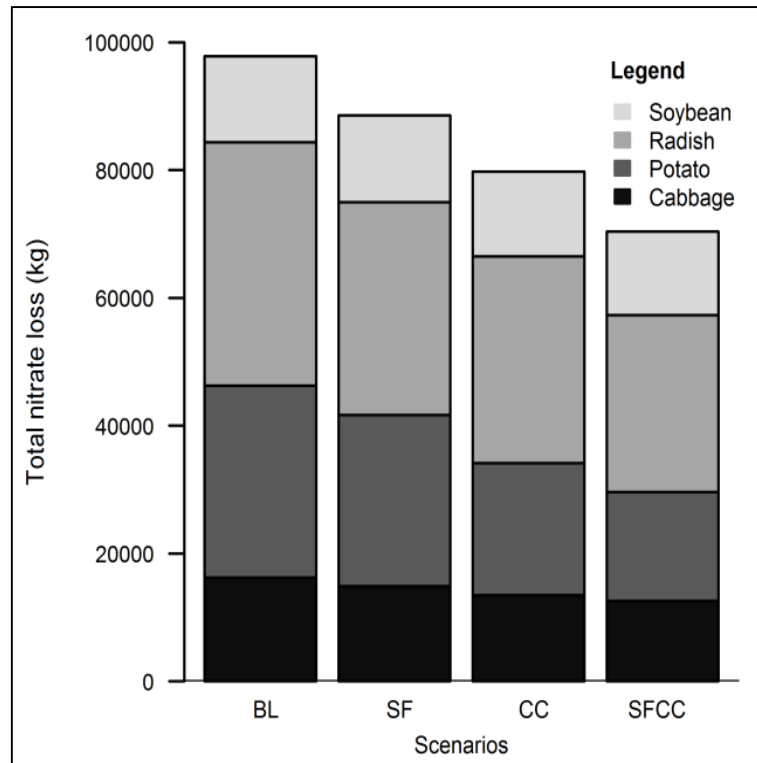


Figure 5.5 Total nitrate loss from four major dryland crops estimated for different BMP scenarios

Table 5.5 Scenario impact for total nitrate loss for the different crops: kg ha⁻¹ (% difference from BL scenario)

Crop types	Area (ha)	BL	SF	CC	SFCC
Cabbage	69.84	232	213(-8 %)	193(-17 %)	181(-22 %)
Potato	155.79	193	172(-11 %)	132(-31 %)	109(-43 %)
Radish	121.23	315	275(-13 %)	267(-15 %)	228(-27 %)
Soybean	141.93	95	96(1 %)	93(-2 %)	92(-3 %)
*Average	488.79	200	181(-9 %)	163(-18 %)	144(-28 %)
**Catchment average	6273.9	39	38(-4 %)	36(-7 %)	35(-11 %)

*Total nitrate calculated as average is due to weighted mean for major dry land crops: cabbage, potato, radish and soybean, **Total nitrate simulated at catchment level is weighted mean for all land use type within the whole study catchment

5.3.4 BMP impact on crop yield

The variation of the simulated crop yields for the different scenarios and crop types are shown in Figure 5.6. Except for soybean, we found increasing trends in crop yield for the scenarios SF, CC and SFCC. For the BL scenario, crop yield ranged from 3 to 12.6 tons ha⁻¹ for radish and potato, respectively. The SF scenario did not have any impact on crop yield for all crop types (Figure 5.6), whereas the CC and SFCC scenarios showed increasing crop yields for all crops except soybean. The maximum level of crop yield was simulated for the SFCC scenario for potato which showed about 39% more yield compared to the BL scenario. A similar effect of SFCC was observed for cabbage and radish with increasing crop yield by 17 % and 27 %, respectively. The crop yield for soybean was observed to be constant throughout all scenarios (SF, CC, and SFCC) with only minor changes (1 % decrease) in the CC and SFCC scenarios. The Kruskal-Wallis test showed that the SF scenario did not show significant differences in crop yield compared to the BL scenario for all crops, while the CC and SFCC scenarios resulted in significantly higher yields than BL for all crops except soybean.

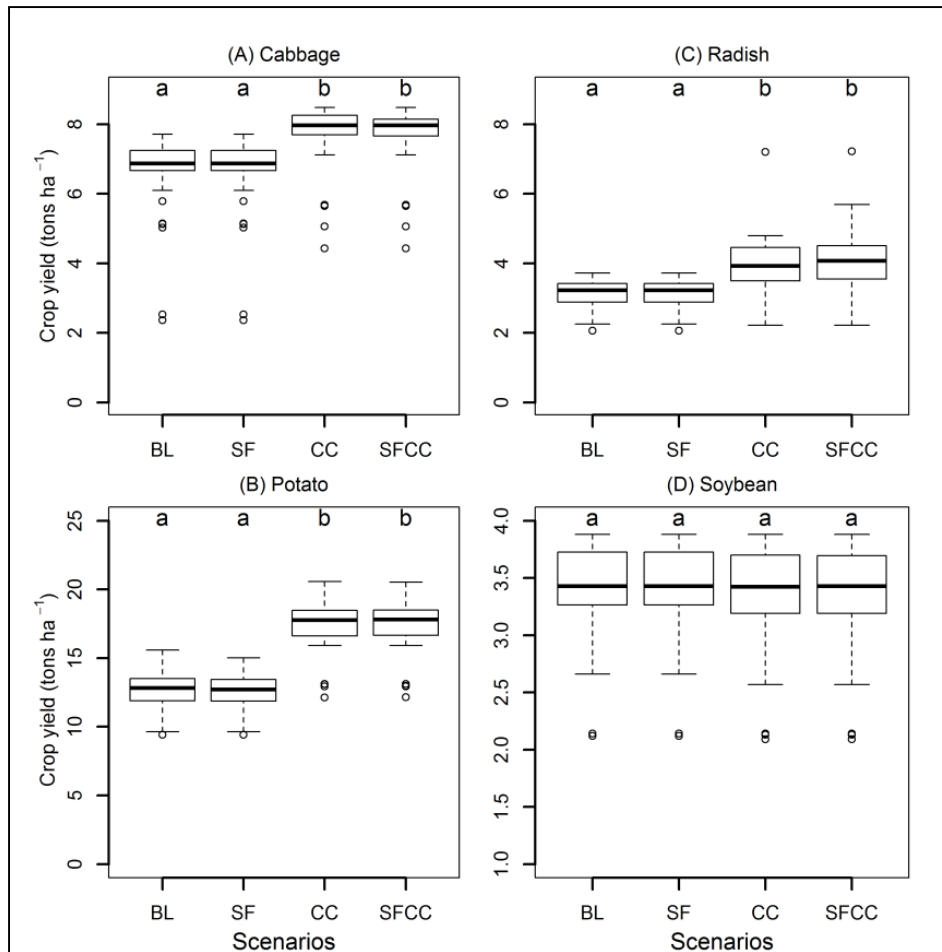


Figure 5.6 Variation of crop yield from the respective crops HRUs simulated for different scenarios

The total crop yields of the four major crop types in the different BMP scenarios are presented in Figure 5.7. The total amount of harvested yield simulated for the BL scenario was 3247 tons with the highest contribution from potato (1956 tons), followed by soybean (477 tons), cabbage (447 tons), and radish (366 tons). The SF scenario did not affect total crop yield, whereas the CC and SFCC scenarios increased the yield to 4204 tons which is 29 % higher than BL. The crop yield produced by other land use types in the catchment was not evaluated as they were not considered during the biomass calibration. The summary of crop yields for the different BMP scenarios is shown in Table 5.6.

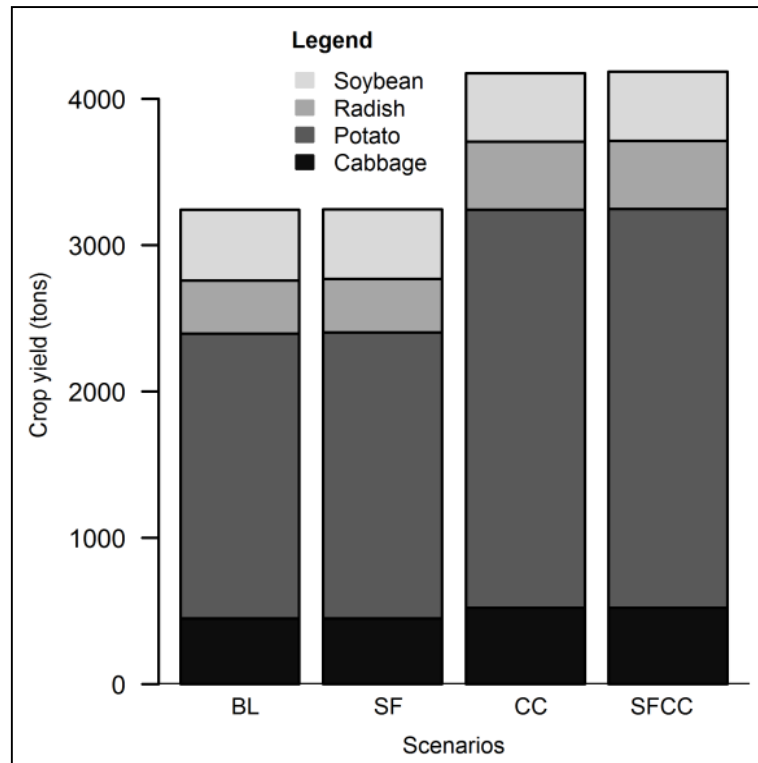


Figure 5.7 Total crop yield from four major dryland crops estimated for different BMP scenarios.

Table 5.6 Scenario impact on crop yield for the different crops: ton ha⁻¹ (% difference from BL scenario)

Crop type	Area (ha)	BL	SF	CC	SFCC
Cabbage	69.84	6.4	6.4(0 %)	7.5(+17 %)	7.5(+17 %)
Potato	155.79	12.6	12.5(0 %)	17.5(+39 %)	17.5(+39 %)
Radish	121.23	3.0	3.0(0 %)	3.8(+27 %)	3.8(+27 %)
Soybean	141.93	3.4	3.4(0 %)	3.3(-1 %)	3.3(-1 %)
*Average	488.79	6.6	6.6(0 %)	8.6(+29 %)	8.6(+29 %)
**Catchment average	6273.9	1.7	1.7(0 %)	1.9(+12 %)	1.9(+12 %)

*Crop yield calculate at field level is due to weighted mean for major dry land crops:

cabbage, potato, radish and soybean, **Crop yield simulated at catchment level is

weighted mean for all land use type within the whole study catchment

5.3.5 BMP impact on water quality at catchment outlet

The simulated daily nitrate concentration at the catchment outlet for 2010 is presented in Figure 5.8(A) and cumulative total nitrate for the different BMP scenarios is shown in Figure 5.8(B). The cumulative total nitrate loss for the BL scenario at the end of the year was about 181977 kg, which could be reduced by 3, 12, and 15 % due to the implementation of SF, CC, and SFCC, respectively. Sharp increases in total nitrate load were simulated for all scenarios between July and October. The cumulative total nitrate for BL at the downstream monitoring site S7 was 149352 kg at the end of the year, which was reduced by 4, 13, and 17 % for the SF, CC, and SFCC scenarios, respectively. For the midstream monitoring site S5, total nitrate loss was about 2264 kg for BL, which was reduced by 4, 9, and 13 % for the SF, CC, and SFCC scenarios, respectively. Nitrate loss at the upstream monitoring site S4W was 1650 kg for the BL scenario, which could be reduced by 3, 10, and 14 % due to the implementation of SF, CC, and SFCC, respectively. We observed that the contribution of total cumulative nitrate increases from upstream to the main catchment outlet along the elevation transect.

The impacts of the BMP scenarios in reducing nitrate losses to the stream were relatively similar when moving from upstream sub-basins to the catchment outlet.

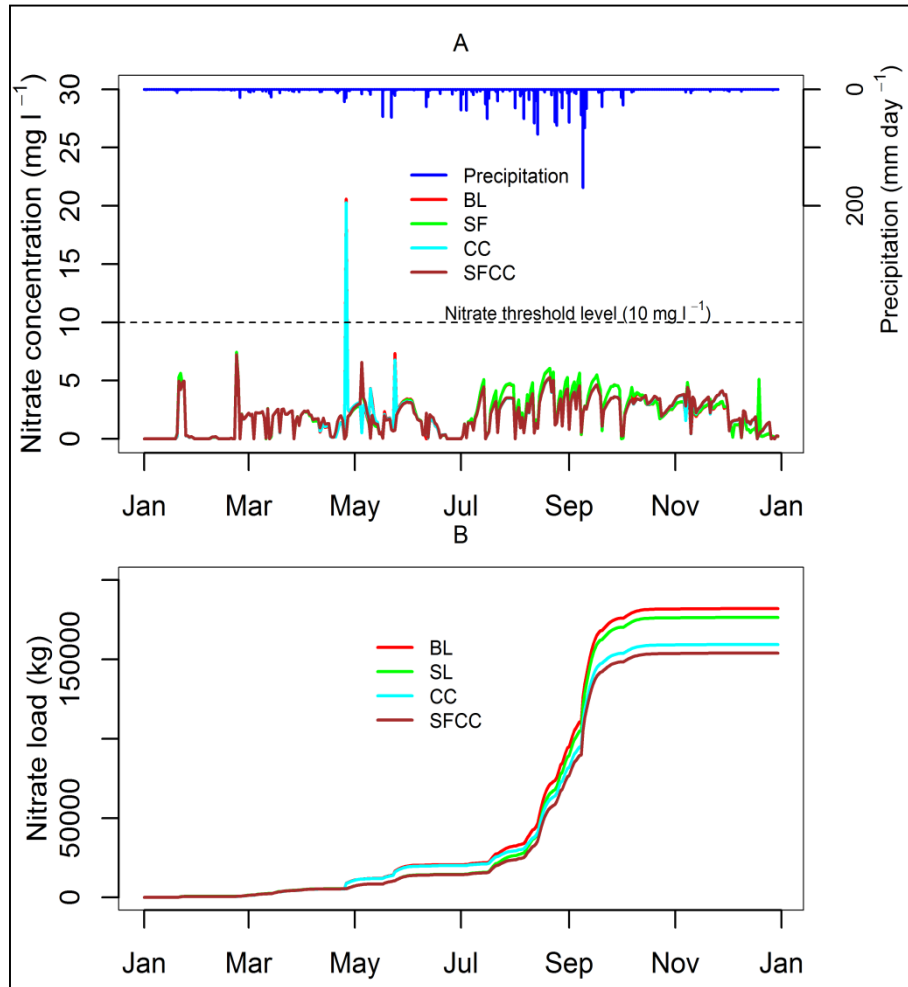


Figure 5.8 Simulated daily nitrate concentration (A) and cumulative daily total nitrate load (B) at the catchment outlet for different scenarios

The daily sediment concentration for the year 2010 and cumulative sediment load at the catchment outlet simulated for the different BMP scenarios are presented in Figure 5.9 (A and B). Sediment concentration could be considerably reduced through the implementation of the CC and SFCC scenarios, whereas the SF scenario did not show a reduction in the sediment concentration. The cumulative sediment load at the catchment outlet for the BL scenario was about 61546 tons per year. The SF scenario did not affect total sediment load, whereas both CC and SFCC showed a 18 % reduction of sediment load to 50205 tons at the end of the year. In the BL scenario the total cumulative sediment load at the downstream outlet (S7) was 55323 tons. The implementation of CC and SFCC scenarios had equal impact to reduce sediment load by 19 % whereas the SF scenario did not show any impact to reduce total sediment load. For the midstream outlet at S5 the cumulative sediment load was estimated to be 5458 tons in BL scenario and was reduced by 7 % by implementation of CC and SFCC scenarios. The lowest cumulative sediment load (1081 tons) among other outlets (S5 and S7) was

simulated at the upstream outlet (S4W) in the BL scenario which was reduced by 13 % due to implementation of CC and SFCC scenario. The SF scenario did not show any impact on sediment reduction at all monitoring outlets. The upstream (S4W) and midstream (S5) monitoring sites in the catchment showed maximum sediment concentrations of 250000 and 60000 mg l⁻¹ in the BL scenario. The maximum sediment concentration decreased when moving downstream to S7 and to the catchment outlet to 25000 mg l⁻¹ for BL. Total cumulative sediment load, however, increased from upstream sub-basin to the catchment outlet.

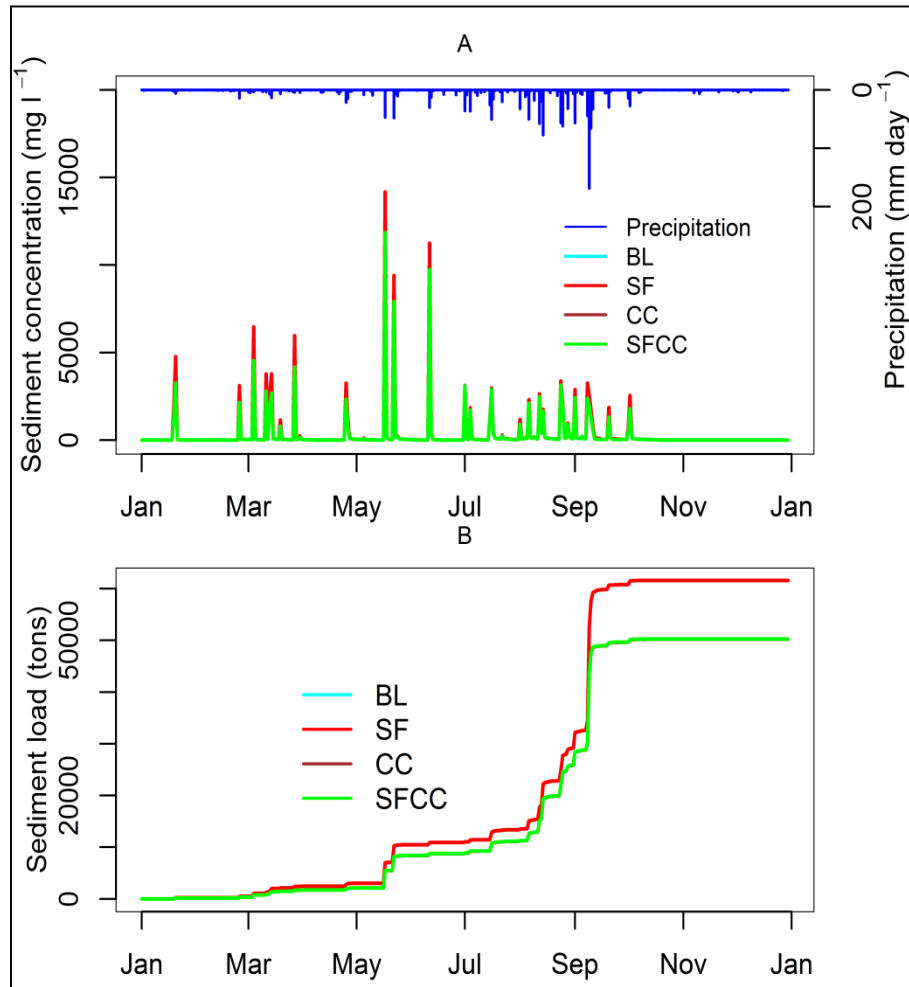


Figure 5.9 Simulated sediment concentration (A) and cumulative total sediment load (B) at catchment outlet for different scenarios

5.4 Discussion

Our results revealed a considerable variability in the effectiveness of the BMP scenarios among different crop types and with respect to different target variables. The SF scenario showed a reduction in total nitrate loss, while it had no impact on sediment and yield for all four dryland crops. The positive impact of split fertilizer application to reduce nitrate by 20 % has been also approved by Yuan et al. (2011). However, split fertilizer application is also expected to increase crop yields (Kettering et al., 2013) due to fertilizer application according to the plant's needs, which could not be confirmed in

our study. The reason for similar crop yields under the BL and SF scenarios may be due to the timing of the split fertilizer application and therefore limited availability of nitrogen for the plants. The management schedules of the farmers including dates and fertilizer application rates were based on interviews among stakeholders within the study catchment. We additionally analyzed small shifts in fertilizer application dates using the same amounts of fertilizer and found that application dates coinciding with rainfall events could induce high nitrate losses contributing to the stream. Similar effects were also reported by Sanchez and Blackmer, (1988) who found between 49 and 64 % of the applied N fertilizer that was lost and transported to the streams. Hence, we slightly modified fertilizer application dates in the management schedule in order to avoid heavy rainfall events coinciding with application days. However, as our study area is highly affected by monsoonal climate, fertilizer N could still be removed rapidly from the soil by subsequent rain events after split application, which limits the N availability even for SF and reduced impact on biomass development. In SWAT, plant biomass development is directly related to erosion, and thus, we did not observe considerable differences in sediment loss between BL and SF. Similar results have been also found in the work of Amon-Armah et al. (2013) who reported only minimal or no effects of split fertilization on sediment reduction which could be indirectly related to insufficient changes on crop yields. The positive impact of split fertilizer application on nitrate leaching is also supported by Cerro et al. (2014a) and Ruidisch et al. (2013b). Cerro et al. (2014a) reported a reduction of only 3 % in nitrate leaching while Ruidisch et al. (2013b) found 59 % lower nitrate losses through leaching for split fertilizer application. However, in our study, the efficiency of SF to reduce nitrate loss was higher for surface runoff than for lateral flow and leaching for all crops. In the simulations, fertilizers were applied primarily to the topsoil (85 % in the top 10 mm) and were readily available to be transported by surface runoff. For BL, the majority of fertilizer N in the topsoil was removed through surface runoff during the first rain events. For SF, less fertilizer N was present during those first storms and the remainder was made available for plant uptake and denitrification through the successive application. Therefore, a smaller proportion of the total applied fertilizer was available for transport via surface runoff compared to the lateral flow and leaching pathways in the SF scenario.

The cultivation of cover crops (CC and SFCC scenarios) showed considerably lower sediment loss for all crop types, which has been approved also by Dabney, (1998) and Kaspar et al. (2001). In addition, both scenarios revealed reductions in nitrate loss for cabbage, potato, and radish, although only small reductions was simulated for soybean. The reason for the lower level of nitrate reduction for soybean may be due to decomposition and mineralization of crop residues after harvest which contributed additional nitrate to the soils N pool that was subsequently released to the stream.

Additionally to the above BMP scenarios, we simulated the impact of no fertilizer application to all crops (not included in the analysis) and found a considerable reduction in nitrate loss (34-86 %) compared to the other scenarios. Similar reductions of up to 72 % have been also reported by Aouissi

et al. (2014) if no fertilizer was applied to crop fields. However, in consequence of the absence of fertilizers, we found a large increase in sediment levels due to a strongly reduced crop biomass. Although reduced mineral fertilizer applications, such as in organic farming systems, have the potential to considerably reduce nitrate pollution, they carry the risk of low yields and higher erosion rates (Arnhold et al., 2014; Nguyen et al., 2014).

We observed that both the SF and CC scenarios independently showed the highest effectiveness to reduce nitrate and sediment loss contributing to the stream network of the catchment. In addition, the combination of both scenarios (SFCC) showed mutual benefits for reducing sediment and nitrate loss while increasing crop yields simultaneously. Because of the ability of the cover crop to take up residual nitrogen and release it again in the following season, it substantially contributes to the reduction of nitrate loss and increasing crop yields (Saleh et al., 2007). In addition, cover crops support year-round soil cover, transpire water, increase infiltration, and decrease surface runoff and overland flow velocity in the absence of the main crop, which assist to protect soils from erosion and sediment generation (Hoorman, 2009).

The comparison of the scenario impacts between individual crops, agricultural fields, and the entire catchment generally revealed lower efficiencies of the BMPs for the catchment than for the field and crop levels. The BMPs were only implemented for the four major dryland crops, because they comprise the main source of agricultural pollution in the water bodies of the catchment. However, other land use types and minor crops can, in sum, contribute considerably to sediment and nitrate loads in the stream although of low individual importance. Arabi et al. (2006) evaluated several BMPs including terracing and field borders and found high effectiveness for reducing sediment at field levels (50 % reduction) but only small effects (2 % reduction) at the catchment level. The efficiency of BMPs at large scales can therefore be limited, if only applied to the most apparent “hotspots” and less obvious land use and management types are ignored. The efficiency assessment of BMPs at the catchment outlet is therefore of major importance to quantify total offsite damages related to certain management systems applied in an agricultural landscape. The applicability of BMPs for other land use types including minor crops, but also adjacent field margin and forest slopes should be considered in order to evaluate catchment wide water quality protection measures.

5.5 Conclusions

We analyzed the efficiency of three BMP scenarios (split fertilization, cover crop cultivation, and both in combination) for reducing sediment and nitrate loss as well as increasing yields of four major dryland crops (cabbage, potato, radish, and soybean). We found lower nitrate loss for split fertilization, but the expected synchronizing behavior of split application and plant uptake and associated higher crop yields could not be observed. The cultivation of cover crops showed significant reductions of sediment and nitrate loss compared to the conventional practice leaving the dryland fields fallow after harvesting of the main crop, which constitutes a main source of agricultural water

pollution in the catchment. The combination of split fertilization and cover crop cultivation showed a synergy effect on reducing sediment and nitrate loss while increasing crop yields. However, the efficiencies of the BMPs varied among the different crops. Our study helps to identify specific field sites and crop types that require special consideration through implementation of additional BMPs, such as soybean which showed only small responses to the applied BMP scenarios. Generally, the evaluation of BMPs in this study revealed that split fertilization and cover crop cultivation are capable of significantly reducing sediment and nitrate loads in the streams and can therefore contribute to water quality improvements of the Soyang reservoir. However, we also found that the effectiveness of the BMPs in reducing total catchment loads is limited when focusing solely on dominant agricultural areas as major sources of water pollution. Minor crops and other land use types can also considerably contribute to water quality degradation and must be considered in catchment wide management plans.

5.6 Acknowledgements

The authors highly acknowledge Jong Yoon Park, Rim Ha, and Sora Ahn from the Dept. of Civil and Environmental System Engineering, Kunkuk University, for their valuable suggestions during the early stage of the model setup and simulation. The provision of field measurement data by Svenja Bartsch for model calibration and validation is also highly appreciated. The research work supported by the International Research Training Group TERRECO (GRK 1565/1) funded through the Deutsche Forschungsgemeinschaft (DFG) at the University of Bayreuth is greatly acknowledged.

5.7 Supplementary material (Supplementary Table: ST 5.1-ST 5.6 & Figures SPF1-SPF6)

ST 5.1 Plant parameter with fit value obtained in manual calibration

Parameters	Description	Potato	Cabbage	Radish	Soybean	Rice	Corn	Forest	Perennial crops
BLAI.DAT	Potential maximum leaf area index for the plant	5	3.7	5.3	5.3	5.1	10	8.7	3
DLAI.DAT	Fraction of growing season at which senescence becomes the dominant growth process	0.95	0.75	0.99	0.87	0.85	0.4	0.99	0.99
LAIMX1.DAT	Fraction of the maximum plant leaf area index corresponding to the 1 st point on the optimal leaf area development curve	0.01	0.3	0.02	0.05	0.01	0.05	0.05	0.15
LAIMX2.DAT	Fraction of the maximum plant leaf area index corresponding to the 2 nd point on the optimal leaf area development curve	0.95	0.95	0.95	0.95	0.95	0.95	0.95	0.75
FRGRW1.DAT	Fraction of the growing season corresponding to the 1 st point on the optimal leaf area development curve	0.01	0.25	0.01	0.1	0.15	0.15	0.01	0.12
FRGRW2.DAT	Fraction of the growing season corresponding to the 2 nd point on the optimal leaf area development curve	0.18	0.4	0.12	0.48	0.45	0.38	0.2	0.2
PHU.MGT	potential heat unit for plant growing at beginning of simulation (heat units)	1720	1050	2150	1270	1300	1500	1500	2700
RUE.DAT	Radiation use efficiency	25	32	7	23	47	39	15	15

Chapter 5-Modeling of split fertilization and cover crop cultivation

ST 5.2 The fitted parameter values, ranges, and sensitivity ranking related to discharge, sediment, and nitrate

Variable	Parameter Name	Description and units	Initial value	Fit value	Minimum bound	Maximum bound	Ranking
Discharge	v__LAT_TTIME.hru	Lateral flow travel time (days)	0	1.64 - 9.7	0 - 5	5 - 10	1
	v__CANMX.hru	maximum canopy storage (mm)	25	0.26 - 28.35	0 - 0	25 - 30	2
	a__CN2.mgt	SCS curve number for moisture condition II (-)	different	-7.55 - -11.87	-10 - -12	-11.5 - 4	3
	v__ALPHA_BF.gw	Baseflow alpha factor (days)	0.05	0 - 0.99	0 - 0.78	1 - 51	4
	v__CH_N2.rte	Manning's n value for main channel (-)	0.05	0.02 - 0.23	0 - 0.19	0.3 - 0.25	5
	v__CH_K2.rte	Effective hydraulic conductivity in main channel alluvium (mm/hr)	0	95.25 - 108.79	0 - 106	109 - 150	6
	r__SOL_AWC().sol	Available water capacity of the soil (mm H ₂ O/mm soil)	different	0.1 - 2.78	-0.3 - 2	-0.05 - 2.8	7
	v__GWQMN.gw	Threshold water level in shallow aquifer for base flow (mm H ₂ O)	0	0.2 - 20	0 - 50	13 - 62	8
	r__SOL_K().sol	Saturated hydraulic conductivity (mm/hr)	different	-0.49 - 0.98	-0.2 - 0.98	-0.5 - 1.2	9
	v__ESCO.hru	Soil evaporation compensation coefficient (-)	0	0.15 - 0.24	0.01 - 0.18	0.2 - 0.26	10
	v__GW_DELAY.gw	Groundwater delay time (days)	31	0.97 - 27	0 - 24	1 - 500	11
	v__OV_N.hru	Manning's "n" value for overland flow (-)	0.14	0.4 - 0.79	0 - 0.6	0.8 - 54	12
	v__REVAPMN.gw	Threshold water level in shallow aquifer for evaporation to occur (mm H ₂ O)	0	11.45 - 23.8	0 - 23	24 - 30	13
	v__EPCO.hru	Plant uptake compensation factor (-)	0	0.7 - 0.81	0 - 0.65	1 - 1	14
	v__GW_REVAP.gw	Groundwater "revap" coefficient (-)	0.02	0.13 - 0.19	0.02 - 0.17	0.2 - 0.2	15
Sediment	v__PRF.bsn	Peak rate adjustment factor for sediment routing in the main channel (-)	1	0.748	0	2	1
	v__LAT_SED.hru	Sediment concentration in lateral flow and groundwater flow (mg/l)	0	0 - 4665	0 - 2000	50 - 5000	2
	r__USLE_K().sol	Soil erosivity (-)	different	0.108 - 0.72	-0.008 - 0.29	-0.25-0.85	3
	v__SPCON.bsn	Linear parameter for calculating the maximum amount of sediment that can be reentrained during channel sediment routing (-)	0	0.001688	0	0.01	4
	v__SPEXP.bsn	Exponent parameter for calculating sediment reentrained in channel sediment routing (-)	1	1.9084	1.04	1.35	5
	v__CH_EROD.rte	Channel erodibility factor (-)	0	0	0	0.44	6
	v__CH_COV.rte	Channel cover factor (-)	0	0	0	1	7
Nitrate	v__NPERCO.bsn	Nitrogen percolation coefficient (-)	0.2	0.591	0	0.7	1
	v__ANION_EXCL.sol	Fraction of porosity from which anions are excluded (-)	0.5	0.733	0	0.75	2
	r__SOL_BD().sol	Moist bulk density (Mg/m ³ or g/cm ³)	different	-0.139	-0.15	0.15	3
	v__CMN.bsn	Rate factor for humus mineralization of active organic nutrients (-)	0.0003	0.002	0.002	0.003	4
	v__N_UPDIS.bsn	Nitrogen uptake distribution parameter (-)	20	42.726	0	60	5
	r__SOL_CBN().sol	Organic carbon content (% soil weight)	different	0.089	-0.02	0.15	6

"v__,a__,r__parameters Name" Given value in between the range is replaced, added and multiplied operation with existing value "different" mean values depends on different soil type and soil layer for .sol parameter and crop type in .mgt parameter. ".ext" is defined for parameters in respective file in SWAT project depends on different soil type and soil layer. The range in fit values refers to values to the parameters are different for different HRUs. Single value in fit value refers to same value for all HRUs

Chapter 5-Modeling of split fertilization and cover crop cultivation

ST 5.3 Field management schedule for tillage, fertilizer and fertilizer amount, planting and harvest applied to major dryland crops in different scenarios

Baseline (BL) scenario

Management schedule for BL scenario for cabbage

Month	Day	Operation	Operation type	Amount (kg ha ⁻¹)
May	6	Tillage	Rotary hoe	
May	10	Tillage	Furrow out cultivator	
May	11	Fertilizer	Elemental nitrogen	360
May	15	Planting (main crop)	Cabbage	Main crop
July	15	Harvest and kill (main crop)		

Management schedule for BL scenario for potato

Month	Day	Operation	Operation type	Amount (kg ha ⁻¹)
April	1	Tillage	Rotary hoe	
April	13	Tillage	Furrow out cultivator	
April	17	Fertilizer	Elemental nitrogen	330
April	29	Planting (main crop)	Potato	Main crop
August	29	Harvest and kill (main crop)		

Management schedule for BL scenario for radish

Month	Day	Operation	Operation type	Amount (kg ha ⁻¹)
April	27	Fertilizer	Elemental nitrogen	490
May	25	Tillage	Rotary hoe	
May	30	Tillage	Furrow out cultivator	
June	1	Planting	Radish	
September	5	Harvest and Kill		

Management schedule for BL scenario for soybean

Month	Day	Operation	Operation type	Amount (kg ha ⁻¹)
May	10	Tillage	Rotary hoe	
May	15	Tillage	Furrow out cultivator	
May	25	Fertilizer	Elemental nitrogen	345
May	29	Planting	Soybean	
October	20	Harvest and Kill		

Split fertilizer (SF) scenario

Management schedule for SF scenario for cabbage

Month	Day	Operation	Operation type	Amount (kg ha ⁻¹)
April	14	Fertilizer	Elemental nitrogen	200
May	6	Tillage	Rotary hoe	
May	10	Tillage	Furrow out cultivator	
May	15	Planting	Cabbage	Main Crop
May	27	Fertilizer	Elemental nitrogen	100
July	15	Harvest and kill		
October	4	Fertilizer	Elemental nitrogen	60

Management schedule for SF scenario for potato

Month	Day	Operation	Operation type	Amount (kg ha ⁻¹)
April	1	Tillage	Rotary hoe	
April	13	Tillage	Furrow out cultivator	
April	15	Fertilizer	Elemental nitrogen	200
April	29	Planting	Potato	Main Crop
May	27	Fertilizer	Elemental nitrogen	100
August	29	Harvest and kill		
October	4	Fertilizer	Elemental nitrogen	30

Management schedule for SF scenario radish

Month	Day	Operation	Operation type	Amount (kg ha ⁻¹)
April	2	Fertilizer	Mineral fertilizer	250
May	25	Tillage	Rotary hoe	
May	27	Fertilizer	Mineral fertilizer	100
May	30	Tillage	Furrow out cultivator	
June	1	Planting	Radish	
September	5	Harvest and kill		
October	4	Tillage	Mineral fertilizer	140

Cont..Table ST 5.3

Management schedule for SF scenario for soybean				
Month	Day	Operation	Operation type	Amount (kg ha ⁻¹)
May	2	Fertilizer	Elemental nitrogen	200
May	10	Tillage	Rotary hoe	
May	15	Tillage	Furrow out cultivator	
May	29	Planting (main crop)	Soybean	
June	1	Fertilizer	Elemental nitrogen	100
October	20	Harvest and kill (main crop)		
October	27	Fertilizer	Elemental nitrogen	45

Cover crop (CC) scenario				
Management schedule for CC scenario for cabbage				
Month	Day	Operation	Operation type	Amount (kg ha ⁻¹)
May	3	Kill (cover crop)		
May	6	Tillage	Rotary hoe	
May	11	Fertilizer	Elemental nitrogen	360
May	18	Tillage	Furrow out cultivator	
May	15	Planting (main crop)	Cabbage	
July	15	Harvest and kill (main crop)		
July	18	Planting (cover crop)	Rye	

Management schedule for CC scenario for potato				
Month	Day	Operation	Operation type	Amount (kg ha ⁻¹)
April	1	Tillage	Rotary hoe	
April	13	Tillage	Furrow out cultivator	
April	17	Fertilizer	Elemental nitrogen	330
April	29	Planting (main crop)	Potato	
August	29	Harvest and kill		
September	1	Planting (cover crop)	Rye	
March	29	Kill (cover crop)		

Management schedule for CC scenario for radish				
Month	Day	Operation	Operation type	Amount (kg ha ⁻¹)
April	27	Fertilizer	Elemental nitrogen	490
May	20	Kill (cover crop)		
May	25	Tillage	Rotary hoe	
May	30	Tillage	Furrow out cultivator	
June	1	Planting (main crop)	Radish	
September	5	Harvest and kill (main crop)		
September	7	Planting (cover crop)	Rye	

Management schedule for CC scenario for soybean				
Month	Day	Operation	Operation type	Amount (kg ha ⁻¹)
May	5	Kill (cover crop)		
May	10	Tillage	Rotary hoe	
May	15	Tillage	Furrow out cultivator	
May	25	Fertilizer	Elemental nitrogen	345
May	29	Planting (main crop)	Soybean	
October	20	Harvest and kill (main crop)		
October	23	Planting (Cover Crop)	Rye	

Split fertilizer and cover crop (SFCC) scenario				
Management schedule for SFCC scenario for cabbage				
Month	Day	Operation	Operation type	Amount (kg ha ⁻¹)
April	14	Fertilizer	Elemental nitrogen	200
May	3	Kill (cover crop)		
May	6	Tillage	Rotary hoe	
May	10	Tillage	Furrow out cultivator	
May	15	Planting (main crop)	Cabbage	
May	27	Fertilizer	Elemental nitrogen	100
July	15	Harvest and kill (main crop)		
July	18	Planting (cover crop)	Rye	
October	4	Fertilizer	Elemental nitrogen	60

Cont..Table ST 5.3

Management schedule for SFCC scenario for potato				
Month	Day	Operation	Operation type	Amount (kg ha ⁻¹)
April	1	Tillage	Rotary hoe	
April	13	Tillage	Furrow out cultivator	
April	15	Fertilizer	Elemental nitrogen	200
April	29	Planting(main crop)	Potato	
May	27	Fertilizer	Elemental nitrogen	100
August	29	Harvest and kill (main crop)		
September	1	Planting (cover crop)	Rye	
October	4	Fertilizer	Elemental nitrogen	30
March	29	Kill (cover crop)		

Management schedule for SFCC scenario for radish				
Month	Day	Operation	Operation type	Amount (kg ha ⁻¹)
April	2	Fertilizer	Elemental nitrogen	250
May	20	Kill (cover crop)		
May	25	Tillage	Rotary hoe	
May	27	Fertilizer	Elemental nitrogen	100
May	30	Tillage	Furrow out cultivator	
June	1	Planting (main crop)	Radish	
September	5	Harvest and kill (main crop)		
September	7	Planting (cover crop)	Rye	
October	4	Fertilizer	Elemental nitrogen	140

Management schedule for SFCC scenario for soybean				
Month	Day	Operation	Operation type	Amount (kg ha ⁻¹)
May	5	Kill (cover crop)		
May	2	Fertilizer	Elemental nitrogen	200
May	10	Tillage	Rotary hoe	
May	15	Tillage	Furrow out cultivator	
May	29	Planting (main crop)	Soybean	
June	1	Fertilizer	Elemental nitrogen	100
October	20	Harvest and kill (main crop)		
October	23	Planting (cover crop)	Rye	
October	27	Fertilizer	Elemental nitrogen	45

ST 5.4 Scenario impact for nitrate in surface runoff for different crops: ton ha⁻¹ (% difference from baseline BL)

Crop types	Area (ha)	BL	SF	CC	SFCC
Cabbage	69.84	71.6	52.8(-26 %)	53.9(-25 %)	44.4(-38 %)
Potato	155.79	59.5	36.0(-40 %)	43.3(-9 %)	29.6(-50 %)
Radish	121.23	86.4	47.8(-45 %)	89.6(4 %)	49.9(-42 %)
Soybean	141.93	72.5	74.0(2 %)	65.7(-9 %)	64.4(-11 %)
Field*	488.79	71.7	52.4(-27 %)	66.3(-8 %)	46.9(-35 %)
Catchment**	6273.90	21.4	19.9(-7 %)	20.9(-2 %)	19.4(-9 %)

*Sediment calculated at field level is due to weighted mean for major dryland crops: cabbage, potato, radish and soybean, **Sediment simulated at catchment level is weighted mean for all land use type within the whole study catchment

ST 5.5. Scenario impact for nitrate in lateral flow for different crops: ton ha⁻¹ (% difference from baseline BL)

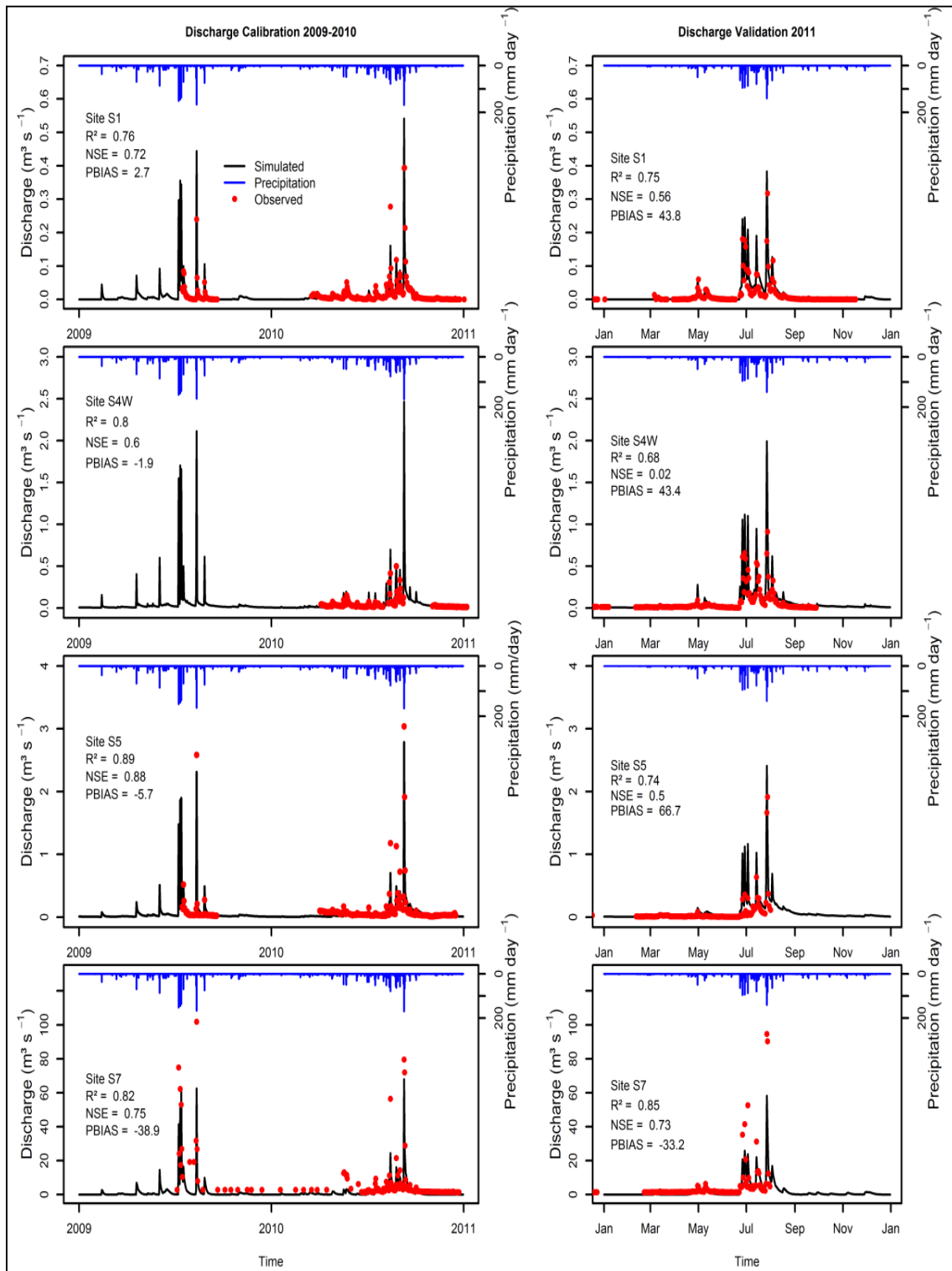
Crop types	Area (ha)	BL	SF	CC	SFCC
Cabbage	69.84	4.3	4.2(-2 %)	3.5(-19 %)	3.4(-21 %)
Potato	155.79	3.3	3.3(-2 %)	2.7(-21 %)	2.6(-21 %)
Radish	121.23	4.9	4.6(-6 %)	4.6(-16 %)	4.2(-16 %)
Soybean	141.93	2.2	2.2(-1 %)	2.2(-7 %)	2.1(-7 %)
Field*	488.79	3.5	3.4(-3 %)	3.1(-17 %)	3.0(-17 %)
Catchment**	6273.90	2.7	2.7(0 %)	2.7(-2 %)	2.7(-2 %)

*Sediment calculated at field level is due to weighted mean for major dryland crops: cabbage, potato, radish and soybean, **Sediment simulated at catchment level is weighted mean for all land use type within the whole study catchment

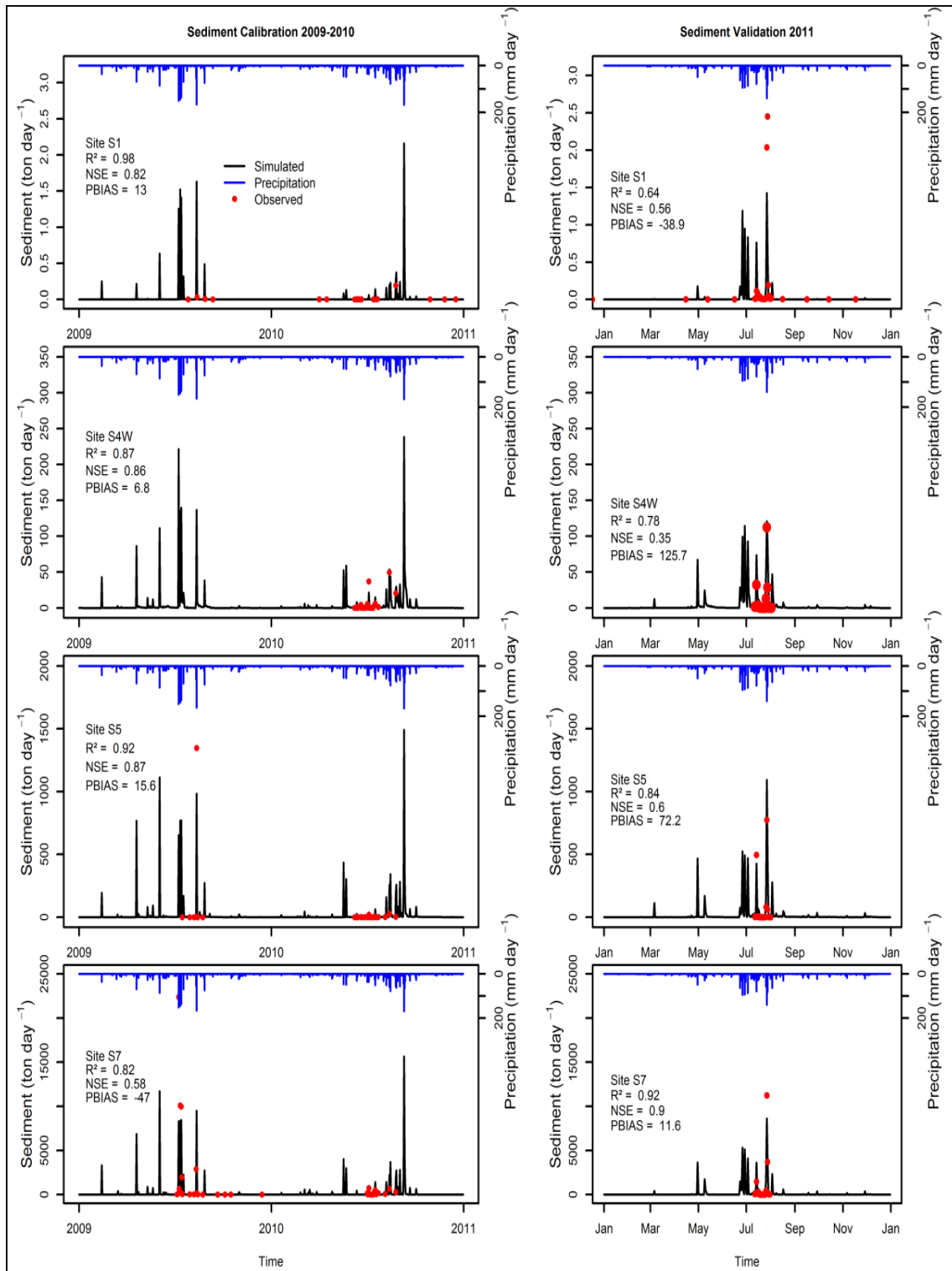
ST 5.6. Scenario impact for nitrate in leaching for different crops: ton ha⁻¹ (% difference from baseline BL)

Crop types	Area (ha)	BL	SF	CC	SFCC
Cabbage	69.84	156.3	156.3(0%)	135.8(-13 %)	132.9(-15 %)
Potato	155.79	130.0	132.5(2%)	75.4(-42 %)	76.9(-41 %)
Radish	121.23	223.2	222.6(0%)	173.1(-22 %)	174.4(-22%)
Soybean	141.93	20.0	20.0(0%)	25.3(+26 %)	25.8(+29 %)
Field*	488.79	124.9	124.9(0%)	93.7(-25 %)	94.2(-25 %)
Catchment**	6273.90	15.1	15.1(0%)	12.7(-16 %)	12.8(-16 %)

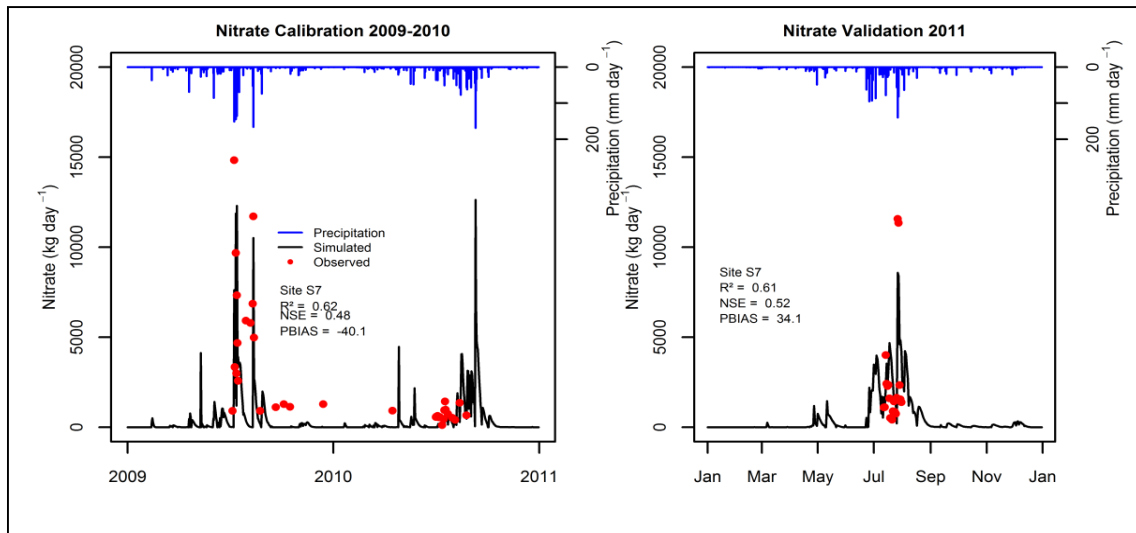
*Sediment calculated at field level is due to weighted mean for major dryland crops: cabbage, potato, radish and soybean, **Sediment simulated at catchment level is weighted mean for all land use type within the whole study catchment



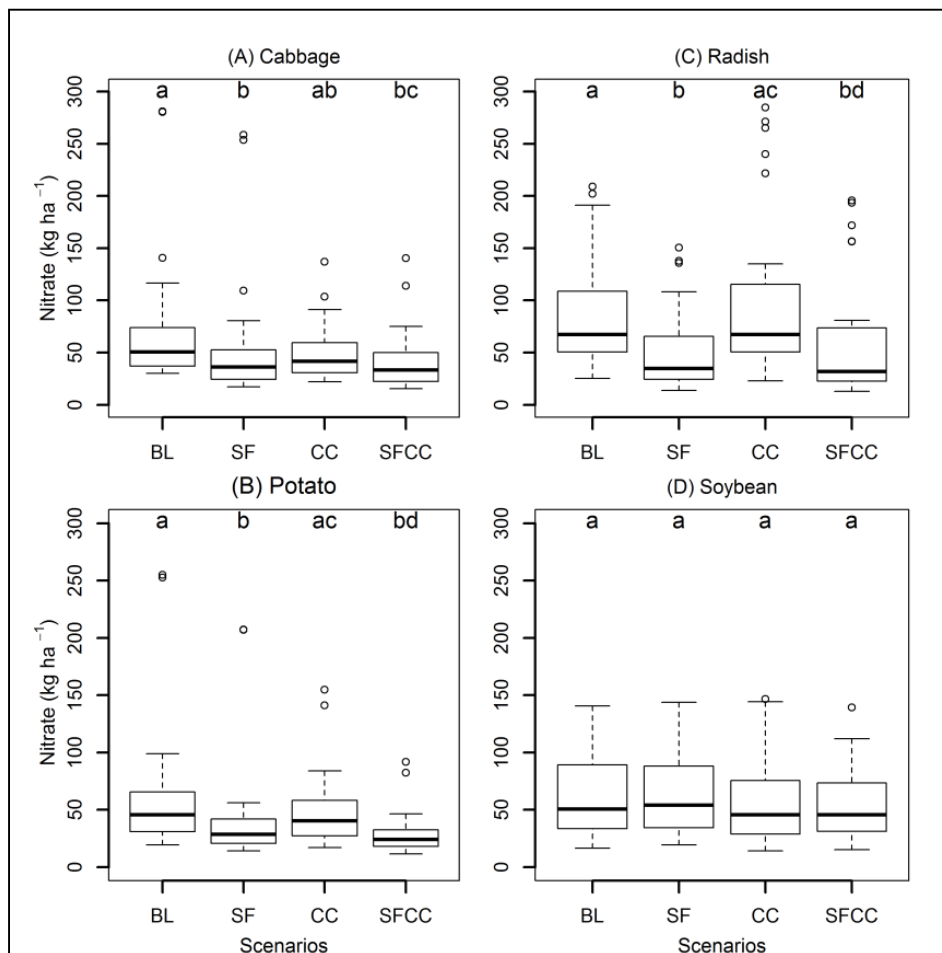
SPF 5.1 Daily simulated and measured discharge during A) calibration B) validation at different outlet as S1, S4W, S5 and S7



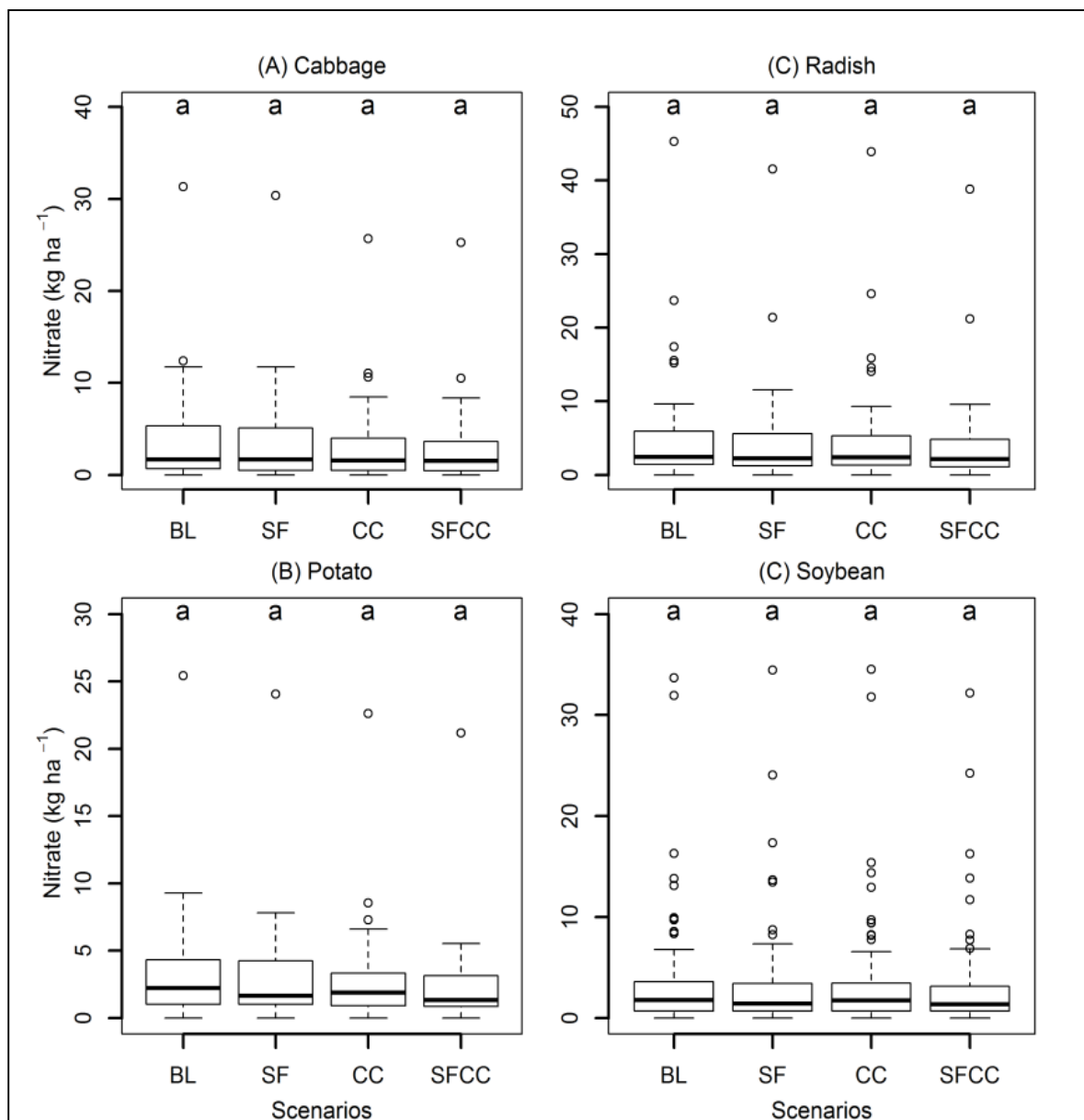
SPF 5.2. Daily simulated and measured sediment during A) calibration and B) validation at different out let as S1, S4W, S5 and S7



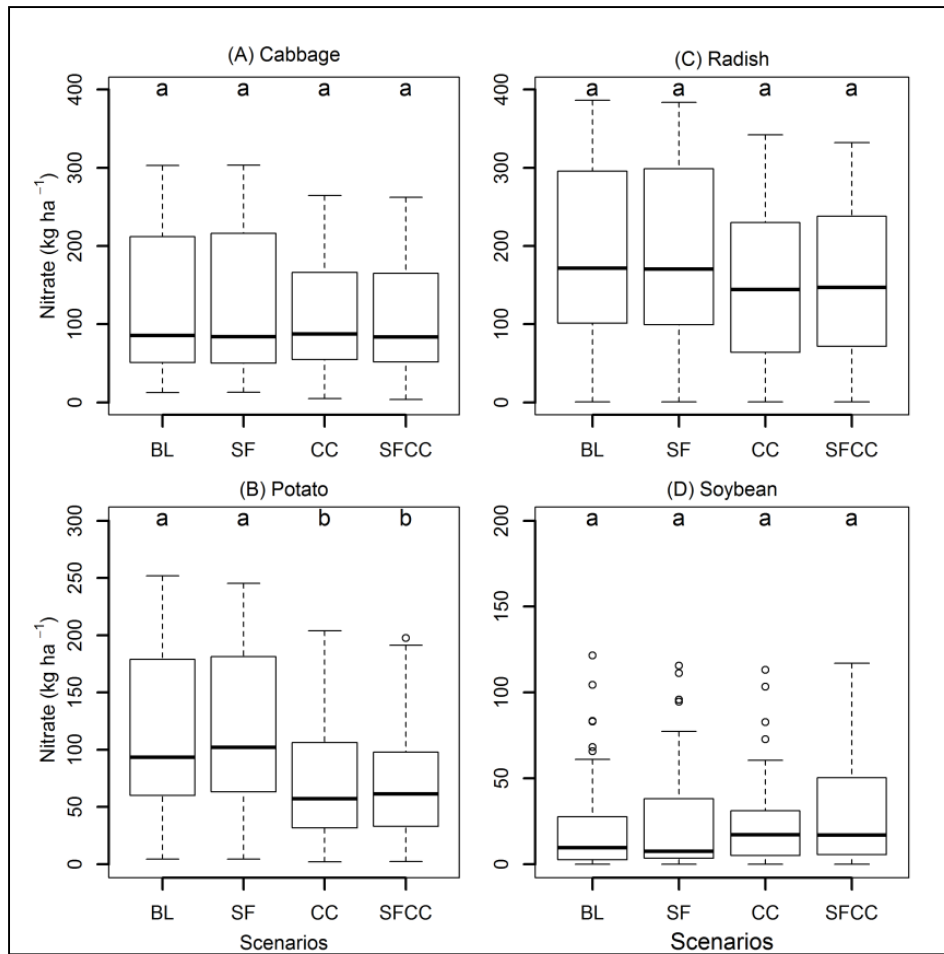
SPF 5.3. Daily simulated and measured nitrate during A) calibration and B) validation at outlet S7.



SPF 5.4. Nitrate in y-axis: Nitrate in surface runoff. Variation of nitrate in surface runoff simulated in different scenarios from respective crop HRUs. Small letters "a", "b", "c" and "d" are used to indicate statistical significance between the scenarios. Presence of similar smaller letter indicates no significance and different smaller letter indicates significance difference between scenarios.



SPF 5.5. Nitrate in y-axis: Nitrate in lateral flow. Variation of nitrate in lateral flow simulated in different scenarios from respective crop HRUs. Small letters "a" is used to indicate statistical significance between the scenarios. Presence of similar smaller letter indicates no significance and different smaller letter indicates significance difference between scenarios



SPF 5.6. Nitrate in y-axis: Nitrate in leaching. Variation of nitrate in leaching simulated in different scenarios from respective crop HRUs. Small letters "a" and "b" are used to indicate statistical significance between the scenarios. Presence of similar smaller letter indicates no significance and different smaller letter indicates significance difference between scenarios

5.8 References

- Abbaspour, K.C., C.A. Johnson, M.T. van Genuchten, 2004 Estimating uncertain flow and transport parameters using a sequential uncertainty fitting procedure. *Vadose Zone Journal* **3**: 1340-1352.
- Abbaspour, K.C., J. Yang, I. Maximov, R. Siber, K. Bogner, J. Mieleitner, J. Zobrist, R. Srinivasan, 2007 Modelling hydrology and water quality in the pre-alpine/alpine Thur watershed using SWAT. *Journal of Hydrology*. **333**: 413-430.
- Amon-Armah, F., E. Yiridoe, N.M. Ahmad, D. Hebb, R. Jamieson, D. Burton, A. Madani, 2013 Effect of nutrient management planning on crop yield, nitrate leaching and sediment loading in thomas brook watershed. *Environmental Management*. **52**: 1177-1191.
- Aouissi, J., S. Benabdallah, Z.L. Chabaâne, C. Cudennec, 2014 Modeling water quality to improve agricultural practices and land management in a Tunisian catchment using the Soil and Water Assessment Tool. *J. Environ. Qual.* **43**: 18-25.
- Arabi, M., R.S. Govindaraju, M.M. Hantush, 2006 Cost-effective allocation of watershed management practices using a genetic algorithm. *Water Resources Research*. **42**: W10429.
- Arnhold, S., S. Lindner, B. Lee, E. Martin, J. Kettering, T.T. Nguyen, T. Koellner, Y.S. Ok, B. Huwe, 2014 Conventional and organic farming: soil erosion and conservation potential for row crop cultivation. *Geoderma*. **219-220**: 89-105.
- Arnhold, S., M. Ruidisch, S. Bartsch, C.L. Shope, B. Huwe, 2013 Simulation of runoff patterns and soil erosion on mountainous farmland with and without plastic-covered ridge-furrow cultivation in South Korea. *Trans. ASABE*. **56**: 667-679.
- Arnold, J.G., N. Fohrer, 2005 SWAT2000: current capabilities and research opportunities in applied watershed modelling. *Hydrological Processes*. **19**: 563-572.
- Arnold, J.G., D.N. Moriasi, P.W. Gassman, K.C. Abbaspour, M.J. White, R. Srinivasan, C. Santhi, R.D. Harmel, A. van Griensven, M.W. Van Liew, N. Kannan, M.K. Jha, 2011 SWAT: Model use, calibration, and validation. *Transactions of the ASABE*. **55**: 1491-1508.
- Arnold, J.G., R. Srinivasan, R.S. Muttiah, J.R. Williams, 1998 large area hydrologic modeling and assessment part i: model development. *JAWRA Journal of the American Water Resources Association*. **34**: 73-89.
- Cao, W., W.B. Bowden, T. Davie, A. Fenemor, 2006 Multi-variable and multi-site calibration and validation of SWAT in a large mountainous catchment with high spatial variability. *Hydrological Processes*. **20**: 1057-1073.
- Cerro, I., I. Antigüedad, R. Srinivasan, S. Sauvage, M. Volk, J.M. Sanchez-Perez, 2014 Simulating land management options to reduce nitrate pollution in an agricultural watershed dominated by an alluvial aquifer. *J. Environ. Qual.* **43**: 67-74.
- Chiang, L.-C., I. Chaubey, N.-M. Hong, Y.-P. Lin, T. Huang, 2012 Implementation of BMP Strategies for Adaptation to Climate Change and Land Use Change in a Pasture-Dominated Watershed. *International Journal of Environmental Research and Public Health*. **9**: 3654-3684.
- Dabney, S.M., 1998 Cover crop impacts on watershed hydrology. *Journal of Soil and Water Conservation*. **53**: 207-213.
- Gassman, P.W., M.R. Reyes, C.H. Green, J.G. Arnold, 2007 The Soil and Water Assessment Tool: historical development, applications, and future directions. *Transactions ASABE*. **50**: 1211-1250.
- Hoorman, J., 2009 Using Cover Crops to Improve Soil and Water Quality. FACT SHEET, Agriculture and Natural Resources. The Ohio State University.
- Kaspar, T.C., J.K. Radke, J.M. Laflen, 2001 Small grain cover crops and wheel traffic effects on infiltration, runoff, and erosion. *Journal of Soil and Water Conservation*. **56**: 160-164.

- Kettering, J., J.-H. Park, S. Lindner, B. Lee, J. Tenhunen, Y. Kuzyakov, 2012 N fluxes in an agricultural catchment under monsoon climate: a budget approach at different scales. *Agriculture, Ecosystems & Environment*. **161**: 101-111.
- Kettering, J., M. Ruidisch, C. Gaviria, Y. Ok, Y. Kuzyakov, 2013 Fate of fertilizer 15N in intensive ridge cultivation with plastic mulching under a monsoon climate. *Nutrient Cycling in Agroecosystems*. **95**: 57-72.
- Kim, B., K. Choi, C. Kim, U.H. Lee, Y.-H. Kim, 2000 Effects of the summer monsoon on the distribution and loading of organic carbon in a deep reservoir, Lake Soyang, Korea. *Water Research*. **34**: 3495-3504.
- Lal, R., 2008 Soils and sustainable agriculture. A review. *Agronomy for Sustainable Development*. **28**: 57-64.
- Lam, Q.D., B. Schmalz, N. Fohrer, 2011 The impact of agricultural Best Management Practices on water quality in a North German lowland catchment. *Environmental Monitoring and Assessment*. **183**: 351-379.
- Lichtfouse, E., M. Navarrete, P. Debaeke, V. Souchère, C. Alberola, J. Ménessieu, 2009 Agronomy for sustainable agriculture. A review. *Agronomy for Sustainable Development*. **29**: 1-6.
- Lindner, S., D. Otieno, B. Lee, W. Xue, S. Arnhold, H. Kwon, B. Huwe, J. Tenhunen, 2015 Carbon dioxide exchange and its regulation in the main agro-ecosystems of Haean catchment in South Korea. *Agriculture, Ecosystems & Environment*. **199**: 132-145.
- Matson, P.A., W.J. Parton, A.G. Power, M.J. Swift, 1997 Agricultural Intensification and Ecosystem Properties. *Science*. **277**: 504-509.
- Morgan, R.P.C., 2005 Soil Erosion and Conservation. Third ed. Blackwell, Malden. Natural Resources Conservation Service (NRCS), 2007. Conservation Practice Standards. United States Department of Agriculture.
- Moriassi, D.N., J.G. Arnold, M.W. Van Liew, R.L. Binger, R.D. Harmel, T.L. Veith, 2007 Model evaluation guidelines for systematic quantification of accuracy in watershed simulations. *Transactions ASABE*. **50**: 885-900.
- Neitsch, S.L., J.G. Arnold, J.R. Kiniry, J.R. Williams, 2011 Soil and Water Assessment Tool Theoretical Documentation Version 2009. Texas Water Resources Institute Technical Report No. 406.
- Nguyen, T.T., M. Ruidisch, T. Koellner, J. Tenhunen, 2014 Synergies and tradeoffs between nitrate leaching and net farm income: The case of nitrogen best management practices in South Korea. *Agriculture, Ecosystems & Environment*. **186**: 160-169.
- Park, J.-H., L. Duan, B. Kim, M.J. Mitchell, H. Shibata, 2010 Potential effects of climate change and variability on watershed biogeochemical processes and water quality in Northeast Asia. *Environment International*. **36**: 212-225.
- Pimentel, D., J. Allen, A. Beers, L. Guinand, R. Linder, P. McLaughlin, B. Meer, D. Musonda, D. Perdue, S. Poisson, S. Siebert, K. Stoner, R. Salazar, A. Hawkins, 1987 World Agriculture and Soil Erosion. *BioScience*. **37**: 277-283.
- Rice, P.J., J.A. Harman-Fetcho, A.M. Sadeghi, L.L. McConnell, C.B. Coffman, J.R. Teasdale, A. Abdul-Baki, J.L. Starr, G.W. McCarty, R.R. Herbert, C.J. Hapeman, 2007 Reducing Insecticide and Fungicide Loads in Runoff from Plastic Mulch with Vegetative-Covered Furrows. *Journal of Agricultural and Food Chemistry*. **55**: 1377-1384.
- Ruidisch, M., S. Arnhold, B. Huwe, C. Bogner, 2013a Is Ridge Cultivation Sustainable? A Case Study from the Haean Catchment, South Korea. *Applied and Environmental Soil Science*. Article ID 679467. **2013**.

- Ruidisch, M., S. Bartsch, J. Kettering, B. Huwe, S. Frei, 2013b The effect of fertilizer best management practices on nitrate leaching in a plastic mulched ridge cultivation system. *Agriculture, Ecosystems & Environment*. **169**: 21-32.
- Saleh, A., E. Osei, D.B. Jaynes, B. Du, J.G. Arnold, 2007 Economic and environmental impacts of ISNT and cover crops for nitrate-nitrogen reduction in walnut creek watershed, Iowa, using FEM and enhanced SWAT models. *Transactions of the ASABE*. **50**: 1251-1259.
- Sanchez, C.A., A.M. Blackmer, 1988 Recovery of Anhydrous Ammonia-Derived Nitrogen-15 During Three Years of Corn Production in Iowa. 102-108.
- Santhi, C., J.G. Arnold, J.R. Williams, W.A. Dugas, R. Srinivasan, L.M. Hauck, 2001 Validation of the swat model on a large Rwer Basin with point and nonpoint sources. *JAWRA Journal of the American Water Resources Association*. **37**: 1169-1188.
- Santhi, C., R. Srinivasan, J.G. Arnold, J.R. Williams, 2006 A modeling approach to evaluate the impacts of water quality management plans implemented in a watershed in Texas. *Environmental Modelling & Software*. **21**: 1141-1157.
- Scherr, S.J., S.N. Yadav, 1996 Land Degradation in the Developing World: Implications for Food, Agriculture, and the Environment to 2020. *Food, Agriculture, and the Environment Discussion Paper*. **14**.
- Seo, B., C. Bogner, P. Poppenborg, E. Martin, M. Hoffmeister, M. Jun, T. Koellner, B. Reineking, C.L. Shope, J. Tenhunen, 2014 Deriving a per-field land use and land cover map in an agricultural mosaic catchment. *Earth Syst. Sci. Data Discuss*. **7**: 271-304.
- Shim, S., 1998 Discharge of Nitrogen and Phosphorus from Nonpoint Sources of Fertilizer and Animal Feed in Korea. Thesis MS, Chuncheon: Kangwon National University, in Korean with an English abstract.
- Shope, C.L., G.R. Maharjan, J. Tenhunen, B. Seo, K. Kim, J. Riley, S. Arnhold, T. Koellner, Y.S. Ok, S. Peiffer, B. Kim, J.H. Park, B. Huwe, 2014 Using the SWAT model to improve process descriptions and define hydrologic partitioning in South Korea. *Hydrol. Earth Syst. Sci*. **18**: 539-557.
- Shrestha, B., M.S. Babel, S. Maskey, A. van Griensven, S. Uhlenbrook, A. Green, I. Akkharath, 2013 Impact of climate change on sediment yield in the Mekong River basin: a case study of the Nam Ou basin, Lao PDR. *Hydrol. Earth Syst. Sci*. **17**: 1-20.
- Stavi, I., R. Lal, 2015 Achieving Zero Net Land Degradation: Challenges and opportunities. *Journal of Arid Environments*. **112, Part A**: 44-51.
- Tilman, D., K.G. Cassman, P.A. Matson, R. Naylor, S. Polasky, 2002 Agricultural sustainability and intensive production practices. *Nature*. **418**: 671-677.
- Tuppad, P., N. Kannan, R. Srinivasan, C. Rossi, J. Arnold, 2010 Simulation of Agricultural Management Alternatives for Watershed Protection. *Water Resources Management*. **24**: 3115-3144.
- UNCCD, 2012 Zero Net Land Degradation. A Sustainable Development Goal for Rio+20, UNCCD Secretariat policy brief.
- White, K.L., I. Chaubey, 2005 Sensitivity analysis, calibration, and validations for a multisite and multivariable swat model. *JAWRA Journal of the American Water Resources Association*. **41**: 1077-1089.
- Yeo, I.-Y., S. Lee, A.M. Sadeghi, P.C. Beeson, W.D. Hively, G.W. McCarty, M.W. Lang, 2014 Assessing winter cover crop nutrient uptake efficiency using a water quality simulation model. *Hydrology and Earth System Sciences Discussions*. **10**: 14229 - 14263.

Yuan, Y., M.H. Mehoff, R.D. Lopez, R.L. Bingner, R. Bruins, C. Erickson, M.A. Jackson, 2011 AnnAGNPS Model Application for Nitrogen Loading Assessment for the Future Midwest Landscape Study. *Water* **3**: 196-216.

Zhang, X., R. Srinivasan, K. Zhao, M.V. Liew, 2009 Evaluation of global optimization algorithms for parameter calibration of a computationally intensive hydrologic model. *Hydrological Processes*. **23**: 430-441.

Declaration / Erklärung

(§ 8 S. 2 Nr. 6 PromO)

Hiermit erkläre ich mich damit einverstanden, dass die elektronische Fassung meiner Dissertation unter Wahrung meiner Urheberrechte und des Datenschutzes einer gesonderten Überprüfung hinsichtlich der eigenständigen Anfertigung der Dissertation unterzogen werden kann.

(§ 8 S. 2 Nr. 8 PromO)

Hiermit erkläre ich eidesstattlich, dass ich die Dissertation selbständig verfasst und keine anderen als die von mir angegebenen Quellen und Hilfsmittel benutzt habe.

(§ 8 S. 2 Nr. 9 PromO)

Ich habe die Dissertation nicht bereits zur Erlangung eines akademischen Grades anderweitig eingereicht und habe auch nicht bereits diese oder eine gleichartige Doktorprüfung endgültig nicht bestanden.

(§ 8 S. 2 Nr. 10 PromO)

Hiermit erkläre ich, dass ich keine Hilfe von gewerblichen Promotionsberatern bzw. -vermittlern in Anspruch genommen habe und auch künftig nicht nehmen werde.

Bayreuth, 26 August 2015

.....

Ort, Datum, Unterschrift

Ganga Ram Maharjan